THE UNIVERSITY of ADELAIDE

Defining The Role of a Novel Gene "MyoD Family Inhibitor Domain Containing (MDFIC)" Important in Cardiovascular Development

---

SABA MONTAZARIBARFOROUSHI
The University of Adelaide

Thesis submitted for the degree of
Doctor of Philosophy
(Ph.D. In Medicine)

Faculty of Health and Medical Science

Adelaide Medical School
The University of Adelaide
November 2023

Table of Contents

List of Figures

List of Tables

Abstract

Central conducting lymphatic anomaly (CCLA), characterised by dysfunction of core collecting lymphatic vessels including the thoracic duct and cisterna chyli, often manifests *in utero* as non-immune hydrops fetalis (NIHF) (also known as foetal hydrops). Clinical presentation of CCLA may also include chylothorax, pleural effusions, chylous ascites or lymphoedema, and is a severe disease for which few effective treatments are available. The genetic aetiology of CCLA remains uncharacterised in the majority of cases. Here, by exploring the genetics underlying lymphatic vascular disorders, we identified seven affected individuals in six independent families with CCLA in whom biallelic variants in *MDFIC*, encoding the MyoD family inhibitor domain containing protein, were identified. Generation of a mouse model of a recurrent human MDFIC truncating variant (Met131Asnfs*3) revealed that $Mdfic^{M131fs*/M131fs*}$ homozygous mutant mice died perinatally exhibiting chylothorax with accumulation of lipid rich chyle in the thoracic cavity. The lymphatic vasculature of these mice was profoundly mis-patterned, particularly in the diaphragm and thoracic wall, and exhibited defects in lymphatic vessel valve development. This work is the first to identify pathogenic *MDFIC* variants underlying human lymphatic vascular disease and reveals that MDFIC plays a pivotal role in the development of lymphatic vessel valves. Mechanistically, we demonstrate that the cysteine-rich C-terminus of MDFIC, which is absent in the MDFIC p.Met131fs* truncated protein, is essential for interaction with GATA2, a transcription factor with an essential role in lymphatic vessel valve development. Alteration in GATA2 subcellular localisation and transcriptional activity within cells in a setting of MDFIC deficiency was detected. Our preliminary data also suggest that biallelic truncating *MDFIC* variants in patients exhibiting CCLA increases MAPK/ERK signalling activity, raising the question as to whether the dampening activity of this pathway might provide a therapeutic opportunity for the treatment of CCLA caused by *MDFIC* variants. Future work aims to characterise the mechanisms by which MDFIC controls the activity of GATA2 and RAS/MAPK signalling in the lymphatic vasculature and to investigate the efficacy of small molecule inhibitors of GATA2 and RAS/MAPK signalling in rescuing the symptoms and lethality of CCLA in our novel genetic mouse model of this disease.

Declaration

I certify that this work contains no material which has been accepted for the award of any other degree or diploma in my name, in any university or other tertiary institution and, to the best of my knowledge and belief, contains no material previously published or written by another person, except where due reference has been made in the text. In addition, I certify that no part of this work will, in the future, be used in a submission in my name, for any other degree or diploma in any university or other tertiary institution without the prior approval of the University of Adelaide and where applicable, any partner institution responsible for the joint award of this degree.

I acknowledge that the copyright of published works contained within this thesis resides with the copyright holder(s) of those works. I also give permission for the digital version of my thesis to be made available on the web, via the University's digital research repository, the Library Search and also through web search engines, unless permission has been granted by the University to restrict access for a period of time.

Saba Montazaribarforoushi

Student number: a1772340

Signed
DATE 23/November/2023

Acknowledgments

First and foremost, I would like to take this opportunity to extend my sincere gratitude to my PhD supervisors, Professor Hamish Scott and Professor Natasha Harvey for their intellectual input, guidance, patience, support, and encouragement over the past four years. I would like to thank Hamish for giving me the opportunity to study in his laboratory, giving me freedom, fatherly advice, and great support in my work and personal life. I would like to thank Natasha for her insightful advice and the opportunity to work in her laboratory, for supporting my attendance at multiple conferences and for providing the chance to learn and develop new skills.

I owe a deep sense of gratitude to Dr Chris Hahn for his never-ending support, help, his keen interest in my work at every stage of my research and his kindness.

I would also like to thank my fellow lab mates and colleagues (both past and present) in the Molecular Pathology Research Laboratory and Lymphatic Development Laboratory (Centre for Cancer Biology) for providing me with an enjoyable and collaborative environment to work and for invaluable friendships, support and debrief sessions (over coffee or in the pub) in both times of despair and celebration. I learnt a lot from you all.

Lastly, I would like to thank my family and friends for supporting me throughout my studies. Especially Mum and Dad, thanks for putting up with my grumpiness and always believing in me. Your love and support have made this thesis possible. I couldn't have done this without you.

Abbreviations

Standard Terms

+	Plus
-	Minus
%	Percentage
ºC	Degree Celsius
bp	Base pair
cDNA	Complementary DNA
DNA	Deoxyribonucleic Acid
E	Embryonic Day
g	Gram
gDNA	Genomic DNA
hr	Hours
kb	Kilobase
KO	Knockout
KD	Knockdown
L	Litre
M	Molar
µg	Microgram
µL	Microliter
µm	Micrometre
µM	Micromolar
mL	Millilitre
min	Minutes
mM	Millimolar
mRNA	Messenger RNA
ng	Nanograms
nM	Nanomolar
pH	Potential Hydrogen
rpm	Revolutions per minute

RNA	Ribonucleic Acid
siRNA	Small interfering RNA
UV	Ultraviolet
V	Volts
W	Watts
WT	Wild-type

Materials and Methods

ANOVA	Analysis of variance
BSA	Bovine serum albumin
DAPI	4',6-diamidino-2-phenylindole
DEPC	Diethlypyrocarbonate
DMEM	Dulbecco's modified eagle medium
DMSO	Dimethyl sulfoxide
EBM	Endothelial basal *medium*
ECF	Extracellular fluid
ECM	Extracellular matrix
EDTA	Ethylenediaminetetraacetic acid
EGF	Epidermal growth factor
FBS	*Foetal bovine serum*
FCS	Foetal calf serum
GAC	Genome analysis Centre
KCL	Potassium chloride
OCT	Optimal cutting temperature compound
PBS	Phosphate buffered saline
PBST	Phosphate buffered saline Tween20
PCR	Polymerase chain reaction
PFA	Paraformaldehyde
PVDF	Polyvinylidene fluoride or polyvinylidene difluoride
RT-qPCR	Quantitative real-time PCR
SAGE	SA Genome Editing
SD	Standard deviation
SDS	Sodium dodecyl-sulfate
SEM	Structural error of the mean
TBST	Tris Buffered Saline with Tween20
TE	Tris-EDTA
TRIS	Trisaminomethane
WES	Whole exome sequencing
WGS	Whole genome sequencing

Genes and Proteins

*Given most of the comparisons in this thesis are between human and mouse, to facilitate identification of the species, human proteins are all in upper case and mouse proteins will have an upper case first letter with the rest of the protein in lower case. Genes follow the same nomenclature but are italicised.

ACTB	Beta actin
ARAF	A-Raf proto-oncogene, serine/threonine kinase
BMP9	Bone morphogenetic protein 9
BRAF	B-Raf Proto-Oncogene, Serine/Threonine Kinase
CBL	Cbl Proto-Oncogene
CCBE1	Calcium-binding EGF domain-containing protein 1
CCL21	Chemokine (C-C motif) ligand 21
CDH5	Vascular endothelial cadherin 5
CEP76	Centrosomal Protein 76
CERS2	Ceramide Synthase 2
COUP-TFII	Chick ovalbumin upstream promoter-transcription factor 2
CYB5R3	Cytochrome B5 Reductase 3
FAM234A	Family With Sequence Similarity 234 Member A
FLI1	Fli-1 Proto-Oncogene, ETS Transcription Factor
FOXC2	Forkhead Box Protein C2
GATA2	GATA Binding Protein 2
HAND1	Heart And Neural Crest Derivatives Expressed 1
HHEX	Haematopoietically-expressed homeobox protein
HRAS	Hras Proto-Oncogene, GTPase
ITGA9	Integrin alpha 9
KRAS	Kirsten rat sarcoma virus
LAMA5	Laminin Subunit Alpha 5
LYVE-1	Lymphatic Vessel Endothelial Receptor 1
MAFB	Musculoaponeurotic fibrosarcoma oncogene homolog B
MAPK	Mitogen-activated protein kinase
MDFIC	MyoD Family Inhibitor Domain Containing
MLLT11	MLLT11 Transcription Factor 7 Cofactor

NDUFS2	NADH: Ubiquinone Oxidoreductase Core Subunit S2
NFATC1	Nuclear Factor of Activated T-Cells, Cytoplasmic 1
NRP2	Neuropilin 2
P3H4	Prolyl 3-Hydroxylase Family Member 4 (Inactive)
PDPN	Podoplanin
PECAM1	Platelet and endothelial cell adhesion molecule 1
PIEZO1	Piezo Type Mechanosensitive Ion Channel Component 1
PLPP3	Phospholipid Phosphatase 3
PROX1	Prospero-related homeobox domain 1
PTPN11	Protein Tyrosine Phosphatase Non-Receptor Type 11
RAF1	Raf-1 Proto-Oncogene, Serine/Threonine Kinase
RASA1	RAS P21 Protein Activator 1
RIT1	Ras Like Without CAAX 1
RRP1B	Ribosomal RNA Processing 1B
SOS1	SOS Ras/Rac Guanine Nucleotide Exchange Factor 1
SOX18	SRY-related HMG-box 18
VEGFC	Vascular endothelial growth factor C
VEGFD	Vascular Endothelial Growth Factor D
VEGFR3	Vascular endothelial growth factor receptor 3

Chapter 1: Introduction

1.1 Stillbirth

Stillbirth is a devastating life event and a personal tragedy for couples going through it. It is a serious public health issue that impacts parents, other families involved, society and the government. The short and long-term negative psychological consequences of losing a baby can last many years and affect subsequent pregnancies. Families going through stillbirth have a higher chance of experiencing perinatal death again. Therefore, the majority of women who decide to become pregnant again experience high levels of anxiety and depression (Burden et al., 2016). The development of improved clinical care for the prevention of stillbirth and improved bereavement care following the loss of a baby is essential in the healthcare system.

Stillbirth is distinguished from miscarriages and second trimester spontaneous abortion by the factors of gestational age and birth weight (Fretts, 2005). The definition of stillbirth has been registered differently in each country. For international comparison, however, stillbirth generally refers to the delivery of the foetus with no sign of life after a gestational age of 28 weeks or more, or birth body weight of 1000 grams. Although this definition is useful, many developed countries prefer to use the strategy of registering stillbirths at earlier weeks of gestation, some as early as 16 weeks, to improve the reliability of reporting stillbirth rates at later gestations (Frøen et al., 2011; Reddy et al., 2009).

Stillbirth comes with many downstream consequences, which are most significantly experienced by mothers. Women who go through this experience are at higher risk of anxiety, depression, somatisation disorders, posttraumatic stress disorders and family disorganisation. (Frøen et al., 2011).

1.1.1   Common causes of stillbirth

In the 1960s, the most common causes of stillbirth reported were intrapartum stillbirth, Rh diseases, and congenital anomalies (Spong, 2011; Bring et al., 2014). However, with the introduction of intrapartum monitoring, improvement of quality of care and availability of emergency caesarean, the proportion of stillbirths at intrapartum significantly dropped (Spong, 2011). Later with the introduction of Rhogam administration to Rh-positive

babies, Rh iso immunisation stillbirth also became a rare event (Bowe, 1970; Jennings et al., 1969). Rh disease is a condition caused by incompatibility between the blood of a mother and foetus. It occurs when antibodies in the mother's bloodstream produced by her immune system cross the placenta, reach the foetus and attack the foetus's blood cells (Bowe, 1970). Rh disease in babies can cause anaemia, jaundice, brain damage, heart failure and death. The rate of perinatal death due to congenital anomalies depends on factors such as environmental exposure, maternal nutrition, resources in the health system and availability of pregnancy termination. In utero screening has reduced death due to congenital anomalies notably, as termination of pregnancy due to this condition has become more liberal in various countries (Goldenberg et al., 2009; Reddy et al., 2009).

Nowadays, even though there are many controversies on how the causes of stillbirth have been classified and whether the underlying conditions are considered as causes or risk factors for stillbirth, most causes of stillbirth remain unknown (Bukowski et al., 2011). Unexplained losses are those pregnancies that have not been complicated by foetal, maternal, or placental conditions and occur in an appropriately grown baby without evidence of infection or antepartum bleeding. Basically, the cases where the death pathway is either not clear or uncertain (Coulam,1986; Saravelos and Regan, 2013).

The second and third most common causes of stillbirth are severe growth restriction and abruptio placenta, respectively. Severe growth restriction occurs as a gradual process where foetal growth falls off the expected growth, while abruptio placenta is a more acute process where there is antepartum bleeding and premature separation of the placenta that is severe enough to cause a foetal demise (Spong, 2011). Other causes of stillbirth are asphyxia and infection associated with pre-eclampsia, umbilical cord accidents, as well as foetal and maternal trauma (McClure et al., 2022).

1.1.2 Stillbirth, perinatal and neonatal deaths in Australia

According to the definition offered by the Australian Institute of Health and Welfare, "Perinatal deaths are those occurring prior to or during labour and/or birth (stillbirth) or up to 28 days after birth (neonatal death) where babies are of 20 or more completed weeks gestation or with a birthweight of at least 400 grams". This definition of stillbirth differs from the standard definition of the World Health Organisation (WHO). Reporting of neonatal deaths is however the same for both the Australian and WHO definitions (Stillbirths and Neonatal Deaths in Australia, 2017).

Based on the report published by the Australian Institute of Health and Welfare, even though Australia is among the safest places to give birth, and despite modern advances in healthcare and medical practices, the rate of stillbirth and neonatal death has not changed over the past two decades and a high proportion of stillbirths in Australia are unexplained (Stillbirths and Neonatal Deaths in Australia, 2017) (Figure.1).

Every day in Australia, 6 babies are stillborn and 2 die within 28 days of birth (neonatal death). Unfortunately, even though the rate of stillbirth has been almost 3 times higher than postnatal death in Australia (6.7% to 2.3%), the scope of the problem has been significantly overlooked by researchers. There are various limitations and barriers to studying stillbirth and performing perinatal autopsy which is essential in understanding the underlying causes and classification of stillbirth. Cultural and religious beliefs, stigma on speaking about stillbirth and autopsy, lack of experience in clinicians to discuss the matter with families and provide effective help, cost and access to active health services are some of the main issues that need to be addressed by implementing a systematic approach and providing an educational program for both families and clinicians. Providing a safe environment is vital for families to trust discussing their problems without fear of judgement, blame and confusion. Only recently in 2022, The Stillbirth Clinical Care Standard was developed by the Australian Commission on Safety and Quality in Health Care to guide on better care for women before and during pregnancy. The standard aims to reduce the stillbirth rate and provide a pathway to closing the equity gaps from cultural and geographic barriers. By implementing essential healthcare programs, families would feel more comfortable addressing their issues and encourage them to consent to an

autopsy, which eventually would minimise the limitations researchers face in investigating stillbirth (Sexton et al, 2021).
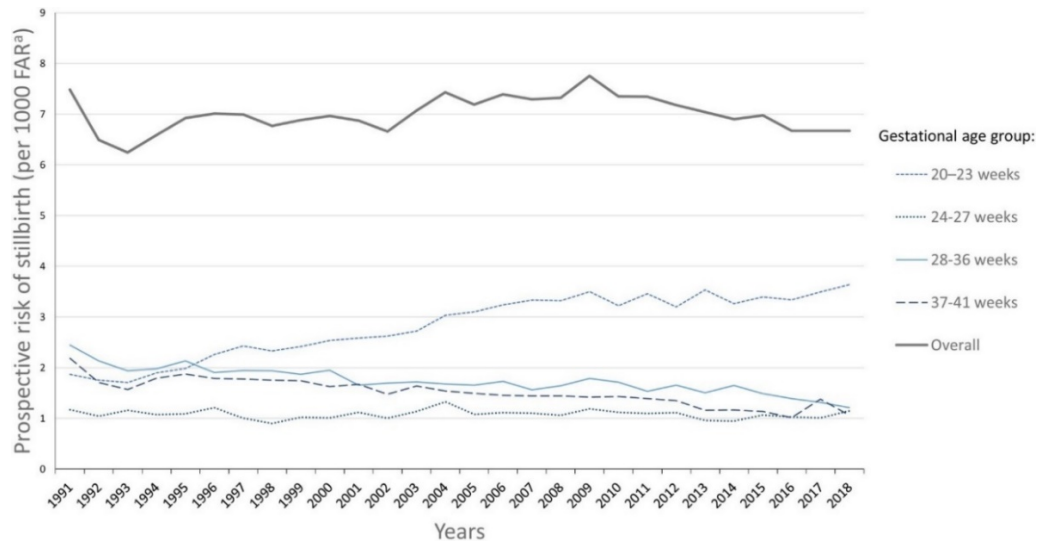
Figure 1. Stillbirth risk in Australia from 1991. Graph illustrates the rate of stillbirth at different gestational age groups in Australia, which has been unchanged over the past two decades. (Adapted from (Stillbirths and Neonatal Deaths in Australia, 2017)).

Reports have also demonstrated that the overall perinatal mortality rate in Australia has not changed significantly since 1999. For perinatal death, in 2004 and 2005 the highest rate of 10.5 perinatal deaths per 1,000 births was reported. This number reached its lowest rate of 9.1 perinatal deaths per 1,000 births in 2016. The rate of stillbirth from 1999 to 2018 was insignificant, however the reduction in neonatal deaths, however, was reported to be somewhat significant (from 3.2 to 2.4 per 1,000 live births) (Figure.2).
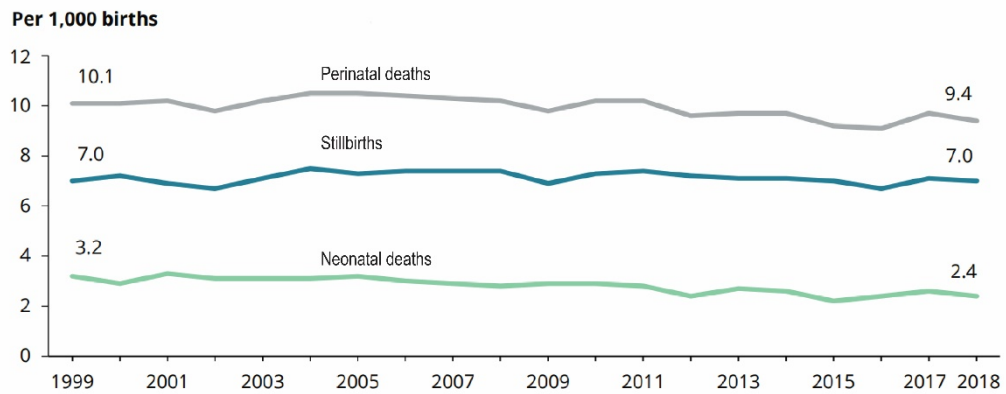
Figure 2. Rates of perinatal deaths in Australia, 1999–2018. Graph illustrates the rate of perinatal and neonatal death in Australia from 1999 to 2018, which has not changed significantly. (Adapted from (Stillbirths and Neonatal Deaths in Australia, 2017)).

1.1.3   Causes of perinatal death in Australia

Causes of perinatal death in Australia have been classified according to the Perinatal Society of Australia and New Zealand (PSANZ) Perinatal Mortality Classification System, version 2.2 (Flenady et al., 2009). This classification system includes a Perinatal Death Classification (PSANZ-PDC) and a Neonatal Death Classification (PSANZ-NDC). PSANZ-PDC is being used to classify all perinatal deaths including stillbirth and neonatal death based on the chain of events that results in the death. PSANZ-NDC however only being applied to neonatal death identifies the single most significant condition present in the neonatal period that caused the death in the baby (between birth and 28 days) (Au, 2009; *Stillbirths and Neonatal Deaths in Australia*, 2017; Vicki et al.,2020).

The "Stillbirth and Neonatal Deaths in Australia" report has summarised the main causes of perinatal and neonatal death according to the PSANZ-PDC and PSANZ-NDC classification group (Au, 2009) (Table.1 & Table.2).

6

Table 1. Causes of perinatal deaths based on PSANZ-PDC classification group. (Adapted from (Stillbirths and Neonatal Deaths in Australia, 2017)).

PSANZ-PDC primary classification groups:	
These are the 11 high-level groups used in reporting:	
1. **Congenital anomaly**	deaths in which a congenital anomaly in the baby (whether structural, functional, or chromosomal) is considered to have been of major importance in the cause of the death.
2. **Perinatal infection**	primary infections occurring in term and preterm neonatal and foetal deaths and secondary infections in term infants (such as Group B Streptococcus and Cytomegalovirus).
3. **Hypertension**	deaths where a hypertensive disorder, such as pre-eclampsia or pre-existing high blood pressure, is considered to have led to the death.
4. **Antepartum haemorrhage**	all perinatal deaths where the primary factor leading to the death was bleeding from the placental bed in the woman's uterus.
5. **Maternal conditions**	deaths where a medical condition (e.g., diabetes) or a surgical condition (e.g., appendicitis) or an injury in the mother (including complications or treatment of that condition) is the cause.
6. **Specific perinatal conditions**	deaths of normally formed, appropriately grown babies, in which a specific perinatal condition, such as cord entanglement or a blood group incompatibility, was the main underlying cause.
7. **Hypoxic peripartum deaths**	deaths from acute or chronic inadequate oxygen supply from the placenta of normally formed babies, typically of >24 weeks of gestation or >600grams birthweight.
8. **Foetal growth restriction**	deaths of babies that were significantly low birthweight for their gestational age or where repeated antenatal ultrasound measurements had shown poor or absent growth before death.
9. **Spontaneous preterm**	deaths of normally formed, appropriately grown preterm babies following spontaneous onset of preterm labour or spontaneous rupture of membranes, irrespective of whether labour was subsequently induced and mode of delivery.
10. **Unexplained antepartum death**	deaths of normally formed foetuses prior to the onset of labour where no predisposing factors are considered likely to have caused the death.
11. **No obstetric antecedent**	: Includes Sudden Infant Death Syndrome (SIDS), postnatally acquired infection (such as Newborn Intensive Care Unit-acquired septicaemia from an intravenous line), accidental asphyxiation and other accidents, poisoning, or violence.

Table 2. Causes of neonatal deaths based on PSANZ-NDC classification group (Adapted from (Stillbirths and Neonatal Deaths in Australia, 2017)).

PSANZ-NDC primary classification groups:	
The PSANZ-NDC classification system is applied only to neonatal deaths and classifies them by the most significant condition present in the baby, in the neonatal period, leading to the death.	
1. **Congenital anomaly**	deaths in which a congenital anomaly in the baby (whether structural, functional, or chromosomal) is considered to have been of major importance in the cause of the death.
2. **Extreme prematurity**	neonatal death in infants deemed too immature for resuscitation or continued life support beyond the delivery room (typically infants of gestational age ≤24 weeks or birthweight ≤600 grams).
3. **Cardio-respiratory disorders**	neonatal deaths in which a cardio-respiratory condition (such as respiratory distress syndrome or meconium aspiration syndrome) is considered to have been the major contributor to the death.
4. **Infection**	neonatal deaths in which infection is considered to have been the major contributor (such as early onset Group B Streptococcus sepsis, pneumonia).
5. **Neurological**	neonatal deaths in which asphyxial brain damage (hypoxic ischaemic encephalopathy) or intracranial haemorrhage was considered to have been the major contributor.
6. **Gastrointestinal**	Primarily includes neonatal deaths related to necrotizing enterocolitis (a medical condition where a portion of the bowel dies).
7. **Other**	Includes Sudden Infant Death Syndrome (SIDS), multisystem failure, trauma, and treatment complications.

Congenital anomaly, unexplained antepartum death, spontaneous preterm birth, maternal condition and spontaneous haemorrhage were demonstrated as the top main causes of perinatal and neonatal death in Australia in 2017 and 2018 (*Stillbirths and Neonatal Deaths in Australia*, 2017; Vicki et al., 2020) (Table.3).

Table 3. Main causes of perinatal death, stillbirths and neonatal death (PSANZ-PDC and PSANZ-NDC) in 2017 and 2018 (Adapted from (Stillbirths and Neonatal Deaths in Australia, 2017)). Congenital anomaly, unexplained antepartum death and spontaneous preterm birth were demonstrated as the main causes of perinatal death in Australia in 2017-2018. Congenital anomaly, unexplained antepartum death and maternal conditions were found to be the most significant causes of death in Stillbirth in Australia in 2017-2018. And Congenital anomaly, unexplained antepartum death and antepartum haemorrhage were the most significant causes of death in neonatal death in Australia in 2017-2018.

	Perinatal Deaths	Stillbirth	Neonatal Death
Cause of Death	Total (%)	Total (%)	Total (%)
Congenital Anomaly	30.80%	30.30%	32.40%
Unexplained Antepartum Death	16.20%	22%	26.60%
Spontaneous Preterm Birth	11.80%		
Maternal Conditions		12.20%	
Antepartum Haemorrhage			8.30%

1.2 Hydrops Fetalis

Hydrops fetalis is a serious condition that arises as a result of excess and abnormal fluid build-up in more than two body compartments and may be characterised by pleural effusion, skin oedema, ascites and pericardial effusion. Hydrops fetalis is an important cause of stillbirth associated with a high mortality rate, resulting in foetal or perinatal death in 1 out of every 1700-3000 pregnancies (Sparks et al., 2019).

Hydrops fetalis is classified as either immune hydrops or non-immune hydrops. Immune hydrops are less common and can occur as a result of severe Rh incompatibility between mother and foetus, where the mother's immune system attacks and destroys the foetus's red blood cells (Bellini & Hennekam, 2012). Non-immune hydrops (NIHF) however is responsible for 75-90% of all cases of hydrops and occurs when another condition or disease interferes with the baby's ability to regulate fluid homeostasis. The survival rate for affected foetuses, even with intervention, is very low. Only about 20% of the babies diagnosed with NIHF will survive after delivery and even after that, they may have underdeveloped lungs, a higher risk of seizures, brain damage, heart failure and hypoglycaemia (Hannah & Rowitch, 2016). Methods employed to treat hydrops include: antiarrhythmic medication to control foetal arrhythmias, intrauterine transfusions for genetic disorders causing foetal anaemia, drainage or shunt placement therapy to remove excess fluid from body compartments before or after birth, providing breathing

support after birth along with medication to control heart failure and help the kidneys remove the excess fluid (Cardwell, 1988; Chainarong et al., 2021; Gembruch et al., 1988; Kadyrberdieva et al., 2019).

Four main theories associated with the aetiology of foetal hydrops have been proposed (Bellini et al., 2009):

1. Cardiac dysfunction or obstruction to venous return, leads to increased pressure in the capillary bed and increased exit of fluid from the bloodstream.
2. Hepatic congestion, which leads to reduced albumin production that subsequently reduces the plasma oncotic pressure.
3. Obstruction of lymphatic flow.
4. Damage to peripheral capillary integrity.

The susceptibility of the foetus to interstitial fluid accumulation may be a result of their greater capillary permeability, compliant interstitial compartments that can accommodate extra fluid and/or their vulnerability to venous pressure on lymphatic return (Sekar, 2019).In addition, foetal hypoxia during pregnancy has been proposed to cause NIHF. Foetal hypoxia causes a reduction of blood flow to foetal gut and kidney and a redistribution of blood to vital organs such as the brain, heart, and adrenals. The renin angiotensin system subsequently gets activated as a result of reduced renal blood flow to enhance cardiac output. This also increases the venous pressure and therefore raises the accumulation of interstitial fluid in foetuses (Degani, 2008; Kurjak et al., 2007; Sekar, 2019).

Moreover, characteristics of capillaries in various tissues, which influence vascular integrity, have been suggested to contribute to interstitial oedema. The balance of fluid movement between interstitial and vascular spaces is regulated by the filtration of fluid across the capillary wall, which is governed by the Starling equation. The Starling equation is based on the four typical values of pressure: interstitial and capillary hydrostatic pressure, along with interstitial and capillary oncotic pressure. Normal foetal fluid balance can be affected by abnormal regulation of any of these forces and subsequently lead to hydrops (Apkon, 1995; Levick & Michel, 2010).

Ultrasound examination during the first and second trimester is the method by which hydrops are detected (Bellini et al., 2006). However, the aetiology of about half of NIHF cases remains unknown following standard evaluation.

To understand the causes behind the development of hydrops, studying the aetiology of NIHF is imperative, and will result in more effective management of pregnancies, the anticipation of neonatal care requirements and improved counselling of families regarding prognosis and recurrence risks. Recent studies have shown that NIHF can be identified prenatally in 65% of cases and up to 85% postnatally (Sekar, 2019).

The general pathophysiological pathway in identifying the various causes of NIHF classified as genetic or non-genetic aetiologies is illustrated in Figure 3 (Bellini et al., 2009). Among all the recognised aetiologies that lead to NIHF, chromosomal abnormalities and cardiovascular defects are reported to be the major causes of hydrops in patients diagnosed in early foetal life and second trimester, respectively (Luna, 1998) (Figure.3).
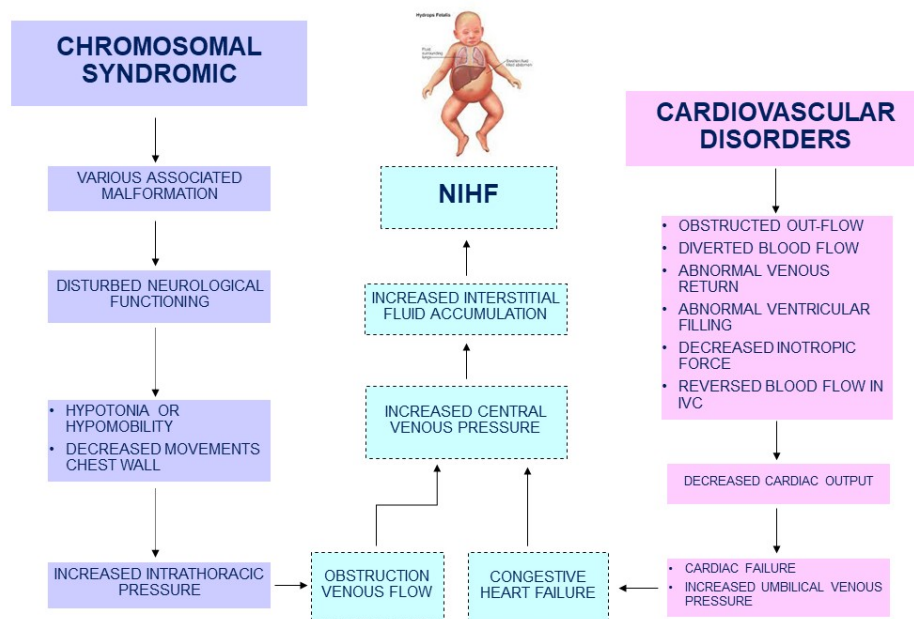
Figure 3. General pathophysiologic pathways in chromosomal syndromic and cardiovascular disorders causing non-immune hydrops fetalis. Cardiovascular disorders and chromosomal abnormalities leading to congestive heart failure and obstruction of venous flow respectively, which subsequently results in increased central venous pressure and interstitial fluid accumulation causing non-immune hydrops fetalis (Adapted from Bellini et al., 2009).
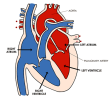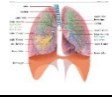
Lymphatic vessels are crucial components of the cardiovascular and immune systems. The failure of lymphatic vessels to develop and function *in utero* results in fluid accumulating to a level that can have profoundly damaging consequences for the foetus as a result of the constrained intrauterine environment (Miller & Gal, 2017). Several pathogenic mutations have been associated with developmental anomalies of the lymphatic system. Chromosomal abnormalities can result in various lymphatic complications which have been shown to cause non-immune hydrops fetalis (Dempsey et al., 2020). One of the early lymphatic conditions described in 1989 is Hennekam syndrome. Patients with Hennekam syndrome exhibit severe genital, limb and facial lymphedema. Mutations in various genes crucial to lymphangiogenesis, including *CCBE1*, *ADAMTS3* and *FAT4*, have been identified as a cause of this condition and recurrent foetal hydrops (Alders et al., 2014; Connell et al., 2010; Hogan et al., 2009; Melber et al., 2018). Lymphoedema-distichiasis, Milroy disease and generalised lymphatic dysplasia have been also reported as some of the known lymphatic malformations where patients exhibit foetal hydrops. Pathogenic mutations in the transcription factor *FOXC2* were identified to cause lymphoedema-distichiasis syndrome (Fang et al., 2000; Gulati et al., 2018). Heterozygous mutations in *FLT4* (*VEGFR3*) were found to cause Milroy disease. Foetuses affected by this condition present with ascites, oedema and pleural effusion (Brice et al., 2005; Ghalamkarpour et al., 2006; Gordon et al., 2013). Homozygous mutations in *PIEZO1* were demonstrated to cause generalised lymphatic dysplasia, where individuals affected with this syndrome showed effusions and pulmonary lymphangiectasia postnatally, in addition to widespread lymphoedema. Autosomal dominant mutations in *PIEZO1* were also found to cause severe foetal hydrops and oedema perinatally (Fotiou et al., 2015; Jones & Mansour, 2017). Mutations in several other genes essential in lymphatic vascular development have been identified to cause non-immune hydrops fetalis, including *EPHB4*, *GATA2*, *ITGA9* and *SOX18*, all of which are important for the development and/or maintenance of lymphatic vessels and lymphatic vessel valves during embryonic and neonatal life (Irrthum et al., 2003; Almedina et al., 2016; Ostergaard et al., 2011; Yang et al., 2012; Zhang et al., 2015).

Due to the difficulty of classifying genetic diseases and syndromes into one primary affected organ system, a practical approach was taken where different organ systems were reviewed separately and underlying genetic aetiologies were considered when
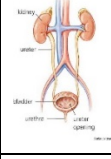
specific features were observed in addition to NIHF. Information about identified chromosomal abnormalities causing NIHF in different organs is summarised in Table.4. Mutations in several genes were identified resulting in lymphatic dysfunction which subsequently led to NIHF. However, this field of study is not well studied, and a more comprehensive investigation is required to identify lymphatic genes associated with NIHF, which has not been diagnosed yet.

Table 4. Summary of the genetic and chromosomal abnormalities with syndromes and their prevalence in various organs associated with NIHF. Causes of NIHF attributed to lymphatic dysfunction are bolded in this table.

Genetic disease or syndrome	Disorder	Gene or location	Prevalence	References
Aneuploidies	Monosomy X (Turner syndrome)	Chromosome X	1 in 2000 to 2500 female live births	(Papp et al., 2006)
	Trisomy 21 (Down syndrome)	Chromosome 21	1 in 800 live births	(Smith-Bindman et al., 2001)
	Trisomy 18 (Edwards syndrome)	Chromosome 18	1 in 5500 live births	(Bronsteen et al., 2004)
	Trisomy 13 (Patau syndrome)	Chromosome 13	1 in 5000 to 20 000 live births (but greater than 75% die in utero)	(Szigeti et al., 2006)
	Triploidy (partial mole)	69, XXX 69,XXY 69,XY	1% to 3% of clinically recognised pregnancies; 20% of spontaneous abortions	(Massalska et al., 2017)
Central nervous system	Meckel Gruber syndrome	*B9D1*, *B9D2*, *CC2D2A*, *CEP290*, *MKS1*, *RPGRIP1L*, *TMEM67*, and *TMEM216*	1 in 13 250-140 000	(Baala et al., 2007)
	Proliferative vasculopathy and hydranencephaly-hydrocephaly syndrome	*FLVCR2*	Unknown	(Petrovski et al., 2019)
	Smith Lemli Opitz	*DHCR7*	1 in 20 000 to 60 000 (higher in Caucasians)	(Maymon et al., 1999)
	Zellweger syndrome	*PEX1* (70%), *PEX2*, *PEX 3*, *PEX5*, *PEX6*, *PEX10*, *PEX11B*, *PEX12*, *PEX13*	1 in 50 000	(Dursun et al., 2009; Shen et al., 2016)

		, *PEX14*, *PEX16*, *PEX19*, and *PEX26*		
Cardiovascular 	22q11 microdeletion syndrome	22q11.2	1 in 4,000	(Machlitt et al., 2002)
	9q duplication	9q	Unknown	(Amarillo et al., 2015)
	ALPK3 related disorders	*ALPK3*	Unknown	(Almomani et al., 2016)
	Barth syndrome	*TAZ*	1 in 300 000 to 400 000	(Steward et al., 2010)
	Congenital long QT syndrome	*KCNQ1*, *KCNH2*, and *SCN5A*	1 in 2000 live births	(Anuwutnavin et al., 2013)
	GATA-5-related disorders	*GATA5*	Unknown	(Kassab et al., 2016)
	Kabuki syndrome	*KMT2D* and *KDM6A*	1 in 32 000	(Long et al., 2016)
	Klippel-Trenaunay-Weber syndrome	*PIK3CA*	1 in 100 000	(Tanaka et al., 2015)
	McKusick-Kaufman syndrome	*MKKS*	1 in 10 000 of Old Order Amish population	(Gaucherand et al., 2002; Tsai et al., 2014)
	Opitz G/BBB syndrome, X-linked	*MID1*	1 in 50 000 to 100 000 males	(Cho et al., 2006; Rasuli & Skandhan, 2018)
	PIK3CA-associated segmental overgrowth (including CLOVES and MCAP syndromes)	*PIK3CA*	Unknown	(Emrick et al., 2014; Mirzaa et al., 2021; Nyberg et al., 2005)
	Capillary malformation-arteriovenous malformation syndrome (*RASA1*-related disorders)	*RASA1*	1 in 100 000 people of northern European descent	(Overcash et al., 2015)
	Tuberous sclerosis	*TSC1* and *TSC2*	1 in 6000	(Pruksanusak et al., 2012)
	Williams syndrome	7q11.23	1 in 7500 to 10 000	(Morris et al., 1993)
	Wolff-Parkinson-White syndrome	Most unknown; *PRKAG2*	1 to 3 in 1000	(Hoeffler et al., 2016; Rudolph, 2010)
Pulmonary and thoracic 	Cornelia de Lange syndrome	*NIPBL*, *SMC1A*, *HDAC8*, *RAD21*, and *SMC3*	1 in 10 000 to 30 000	(Banait et al., 2015; Tayebi, 2008)
	Fraser syndrome	*FRAS1* (greater than 50%), *FREM2*, and *GRIP1*	1 in 200 000 live births; 1 in 10 000 foetal losses/ spontaneous abortions	(Tessier et al., 2016)

	Fryns syndrome	Unknown	Unknown; 1.3% to 10% of Congenital diaphragmic hernia cases	(Ramsing et al., 2000)
	Pallister-Killian syndrome	Tetrasomy 12p (usually with isochromosome 12p)	1 in 20 000 live births	(Doray et al., 2002)
	VACTERL association	Unknown	1 in 10 000 to 40 000 newborns	(Oral et al., 2012)
Gastrointestinal	Beckwith-Wiedemann syndrome	11p15.5	1 in 13 700 live births	(Hillstrom et al., 1995)
	Lysosomal storage disorders			(Futerman & Van Meer, 2004)
	Galactosialidosis	*CTSA*	Unknown (100 reported cases)	(Caciotti et al., 2013; Patel et al., 1999)
	Gaucher disease	*GBA*	1:855 in Ashkenazi Jewish, 1:57 000 to 1.16:100 000 in general	(Beaujot et al., 2013)
	Mucolipidosis I (Sialidosis)	*NEU1*	Unknown (1 to 4:200 000)	(Capobres et al., 2016)
	Mucolipidosis II (I-cell disease)	*GNPTAB*	1:640 000	(Capobres et al., 2016)
	Mucopolysaccharidosis IVa (Morquio syndrome)	*GALNS*	1:250 000	(Dũng et al., 2013)
	Mucopolysaccharidosis type IVB (GM1-gangliosidosis)	*GLB1*	1:100 000 to 1:200 000	(Caciotti et al., 2013) (Dũng et al., 2013)
	Mucopolysaccharidosis VII (Sly syndrome)	*GUSB*	1:250 000 to 1:<1 000 000	(Den Hollander et al., 2000; Dũng et al., 2013)
	Niemann-Pick A	*SMPD1*	1:40 000 in Ashkenazi Jewish, 1:250 000 in general populations	(Schoenfeld et al., 1985)
	Niemann-pick C	*NPC1* and *NPC2*	1:150 000	(Ples et al., 2018)
	Salla disease	*SLC17A5*	Unknown, less than 1:1 000 00	(Aula & Aula, 2006)
	Mevalonate kinase deficiency	*MVK*	Unknown (200 reported worldwide)	(Peciuliene et al., 2016)
	Wolman disease	*LIPA*	1:350 000	(Blitz et al., 2018)
Genitourinary and renal	Bartter syndrome	*SLC12A1*, *KCNJ1*, *CLCNKB*, *BSND*, *CLCNKA*, and *CLCNKB*	Unknown	(Maldergem et al., 1992)

	Autosomal recessive polycystic kidney disease	*PKHD1*	1 in 20 000 to 40 000	(Gunay-Aygun et al., 2006)
	Congenital nephrosis Pierson syndrome	*LAMB2*	Unknown	(Kagan et al., 2008)
	Finnish nephrosis	*NPHS1* and *NPHS2*	1 to 3 in 100 000 worldwide 1 in 10 000 in Finland	(Zenker et al., 2004)
Musculoskeletal	Skeletal dysplasias	*TRIP11, SLC26A2,* and *COL2A1*	Unknown	(Heinrich et al., 2015; Pretorius et al., 1986)
	Achondrogenesis	*FGFR3*	1 in 15 to 40 000	(Hatzaki et al., 2011)
	Asphyxiating thoracic dystrophy (Jeune syndrome)	*CEP120, CSPP1, DYNC 2H1, IFT80, IFT140, IFT 172, TTC21B, WDR19, WDR34, WDR35,* and *WDR60*	1 to 5 in 500 000 live births	(Tonni et al., 2013)
	Congenital disorders of glycosylation type 1	*PMM2, ALG1,* and *ALG9*	800 cases reported	(Kranz et al., 2007)
	Hydrops-ectopic calcification moth eaten (HEM) skeletal dysplasia (Greenberg dysplasia)	*LBR*	Unknown	(Konstantinidou et al., 2008)
	Osteogenesis imperfecta	*COL1A1, COL1A2, CRT AP,* and *P3H1*	6 to 7 in 100 000	(Steiner et al., 2021)
	Osteopetrosis congenita	*CLCN7* (75%), *CA2, IKB KG, ITGB3, OSTM1, PL EKHM1, TCIRG1, TNFR SF11A,* and *TNFSF11*	1 in 20 000	(El Khazen et al., 1986)
	Roberts syndrome	*ESCO2*	150 cases reported	(Dalal & Phadke, 2006)
	Schneckenbecken dysplasia	*SLC35D1*	Unknown	(Nikkels et al., 2001)
	Short rib polydactyly, type 1 (Saldino-Noonan)	*DYNC2H1*	1 in 200 000 live births	(Badiner et al., 2017; Kumru et al., 2005; Silveira et al., 2017)

	Short rib polydactyly, type 2 (Majewski)	*NEK1*		(El Hokayem et al., 2012)
	Short rib polydactyly, type 3 (Verma-Naumoff)	*DYNC2H1*		(Dagoneau et al., 2009)
	Short rib polydactyly, type IV (Beemer-Langer)	*IFT122*		(Silveira et al., 2017)
	Thanatophoric dysplasia	*FGFR3*	1 in 20 000 to 50 000 newborns	(Pretorius et al., 1986)
	Yunis-Varon syndrome	*FIGURE 4*	Unknown	(Basel-Vanagaite et al., 2008)
	Oral-facial-digital syndrome	*OFD1*	1 in 50 000 to 250 000 newborns	(Alby et al., 2018; Van Maldergem et al., 1992)
	Foetal akinesia			(Chen, 2012)
	Arthrogryposis multiplex congenita (Pena-Shokeir syndrome)	*DOK7, MUSK, RAPSN*	1 in 12 000	(Gupta et al., 2011)
	Lethal multiple pterygium syndrome	*CHRNG, CHRNA1, CHRND*, and *RAPSN*	Unknown	(Chen, 2012)
	Myotonic dystrophy	*DMPK*	1 in 8000	(Stratton & Patterson, 1993)
	Neu-Laxova syndrome	*PHGDH, PSATI1*, and *PSPH*	Unknown	(Mattos et al., 2015)
	IPEX syndrome	*FOXP3*	Unknown	(Reichert et al., 2016; Shehab et al., 2017)
Haematologic	Alpha thalassemia (HbH and Hb Barts)	*HBA1* and *HBA2*	1 in 200 to 2000 births in Southeast Asia	(Chui, 2009)
	Congenital dyserythropoietic anaemia	*CDAN1* and *SEC23B*	Unknown	(Tamary et al., 1996)
	Congenital erythropoietic porphyria	*CEP* and *UROS*	Unknown	(Pannier et al., 2003)
	Diamond Blackfan anaemia	*GATA1, RPL5, RPL11, RPL15, RPL26, RPL27, RPL31, RPL35A, RPL36, RPS7, RPS10, RPS15, RPS17, RPS19, RPS24,*	5 to 7 per 1 million	(Dunbar et al., 2003)

		RPS26, RPS27, RPS28, RPS29, and TSR2		
	εγδβ-thalassemia	HBB and locus control region of beta-globin locus on 11p	Unknown	(Makis et al., 2019)
	Glucose-6-phosphate dehydrogenase deficiency	G6PD	400 million people worldwide	(Arcasoy & Gallagher, 1995)
	Glucose phosphate isomerase deficiency	GPI	Unknown (~50 cases reported)	(Arcasoy & Gallagher, 1995)
	Pyruvate kinase deficiency	PKLR	1 in 20 000 people of European descent, especially Old Order Amish of Pennsylvania	(Arcasoy & Gallagher, 1995)
Lymphatic	RASopathies	RIT1, RRAS, RASA2, A 2ML1, SOS2 and LZTR1		(Aoki et al., 2015)
	Noonan syndrome	PTPN11, SOS1, RAF1, and RIT1	1:1000 to 1:2500	(Croonen et al., 2013)
	Costello syndrome	HRAS	1:300 000 to 1:1 230 000	(Lin et al., 2002, 2009)
	Cardiofaciocutaneous syndrome	MAP 2 K2	Unknown (200-300 worldwide)	(Gos et al., 2018)
	Casitas B-cell lymphoma syndrome	CBL	Unknown	(Bülow et al., 2015)
	Noonan-like syndrome with loose anagen hair	SHOC2	Unknown	(Lee & Yoo, 2019)
	Generalised lymphoedema			(Bartolomeis et al., 2008)
	ITGA9-associated foetal chylothorax	ITGA9	1 in 12 000	(Yeang et al., 2012)
	Generalised lymphatic dysplasia	PIEZO1	Unknown	(Fotiou et al., 2015a)
	Hennekam lymphangiectasia-lymphoedema syndrome	CCBE1 and FAT4	<1:1 000 000	(Mardy et al., 2019)
	Hereditary lymphoedema (nonne-Milroy disease)	VEGFR3	1 in 6000	(Gordon et al., 2013; Lev-Sagie et al., 2003)
	Hypotrichosis-lymphoedema-telangiectasia syndrome	SOX18	Unknown	(Irrthum et al., 2003)

	Lymphoedema-cholestasis syndrome (Aagenaes syndrome)	15q, gene unknown	<1:1 000 000	(Shah et al., 2013)
	Lymphoedema-distichiasis	*FOXC2*	Unknown	(Gulati et al., 2018)
	Primary lymphoedema (Emberger syndrome)	*GATA2*	<1:1 000 000	(Ostergaard et al., 2011)
	Yellow nail syndrome	Unknown	Unknown	(Nanda et al., 2010)
Skin	Sphingosine-1-phosphate lyase deficiency	*SGPL1*	Unknown	(Choi & Saba, 2019)

1.3 The lymphatic system

1.3.1 Structure and function of the lymphatic system

The lymphatic and blood-vascular circulatory systems are closely linked and have many structural and anatomical similarities. However, these two circulatory systems function quite differently (Choi et al., 2012). Over the last few years, new findings employing modern molecular, cellular and genetic techniques and advanced imaging technologies, have provided major new insight into the role and importance of the lymphatic vasculature (Choi et al., 2012). The interest in lymphatic research has increased by the growing evidence that lymphatics contribute to several diseases such as cancer metastasis, inflammatory disorders and lymphoedema (Cueni & Detmar, 2008). Therefore, understanding the function and development of the lymphatic system is essential to comprehend its association with related human diseases. The lymphatic system consists of lymphatic vessels (LVs) which are found in almost all vascularised organs and tissues. The lymphatic vascular network is a low-pressure and low-flow unidirectional circulatory system in the body essential for maintaining body fluid homeostasis by draining interstitial fluid (IF) from extracellular spaces of tissues and organs and returning it to the blood circulation. LVs are also crucial in immune cell trafficking, uptake and transport of dietary

lipids and reverse cholesterol transport (Alitalo et al., 2005). The lymphatic system comprises lymphoid tissue (leukocytes, bone marrow, thymus, spleen, and lymph nodes) and lymphatic vessels, which are organised into capillaries or initial lymphatics, pre-collectors and collecting vessels (Escobedo & Oliver, 2016). LVs are lined by lymphatic endothelial cells (LECs), a distinct endothelial cell (EC) lineage with specific transcriptional and metabolomic profiles that mediate fluid reabsorption from tissues into the lymph (Randolph et al., 2017). Distinct structural features of lymphatic vessels facilitate their specific role in the circulatory system. Lymphatic capillaries are thin-walled and blind-ended. 'Oak-leaf' shaped endothelial cells in capillaries are connected through loose intercellular junctions (button-like), which makes them highly permeable and equipped with anchoring filaments composed of emilin-1 and fibrillin that connect the basal surface of the LEC to the surrounding extracellular matrix (Baluk et al., 2007). Lymphatic capillaries also have very little or no basement membrane and lack supporting smooth muscle-like contractile cells (Alitalo et al., 2005; Mäkinen et al., 2007; Tammela & Alitalo, 2010). These unique features of lymphatic capillaries provide essential structures for the uptake of fluid, large molecules, and cells. The lymphatic fluid then drains into pre-collector and larger collecting lymphatic vessels. Collecting lymphatics have 'zipper-like' junctions and are equipped with intact, continuous basement membrane and surrounded by lymphatic muscle cells (Baluk et al., 2007). The presence of bi-leaflet valves in collecting vessels enables unidirectional movement of lymph and prevents lymph backflow (Bazigou & Makinen, 2013). Formation and maintenance of the lymphatic vasculature are essential for both embryonic development and adult haemostasis, aberrations in this contribute to the pathogenesis of various disorders including lymphoedema, transplant rejections, inflammatory conditions, psoriasis, cancer and tumour metastasis (Cueni & Detmar, 2008; Kerjaschki et al., 2004; Kunstfeld et al., 2004; Witte et al., 2001).

Recent evidence suggests that the lymphatic route can provide a better-targeting advantage over blood circulation for drug delivery. Lymphatics not only regulate tissue fluid balance; they serve as a major transport route for immune cells and dissemination of tumour cells along with interstitial macromolecules. Increased exposure during lymphatic delivery due to lower flow rates and smaller shear stresses when travelling in the lymphatic system and higher efficacy versus toxicity of lymphatic therapeutic

approaches shown that lymphatic delivery can be more beneficial (Trevaskis et al., 2015). Studies also provided evidence that lymphatic transport can be more effective in certain circumstances and depending on the delivery strategies in vaccination (injection of vaccine into lymph nodes or mucosal vaccination), immune therapy (delivery of small-molecule drugs to targets within the lymphatics), treatment of infection (targeting the delivery of drug to the lymphatic system where viruses reside or replicate within the lymphatics) and cancers (lymph node targeting therapies) (Dane et al., 2011; De Titta et al., 2013; Jewell et al., 2011; Lalanne et al., 2007; Li et al., 2012; Ling et al., 2008; Maloy et al., 2001; Pasetti et al., 2011; Senti et al., 2008; Sosnik et al., 2009; Yang et al., 2011). Targeting lymphatic routes can also result in avoiding dose-limiting systemic side effects, systemic dilution, and liver degradation (Khan et al., 2013; Z. Zhang et al., 2021).

An increase in understanding of lymphatic biology and the role of lymphatics in diseases surged the interest in studying and addressing the potential therapeutic approaches targeting the lymphatic system. However, it is also important to consider that many diseases also affect lymphatic function. Therefore, further work in targeting the lymphatic system in therapeutic approaches also needs to address the impact of disease-mediated changes in lymphatic structure and function (Trevaskis et al., 2015).

Pre-collectors then converge into collecting lymphatics, which are fully covered by BM and SMCs. The presence of lymphatic valves facilitates the unidirectional flow of lymph (Adapted form (Jiang et al., 2018)) (Figure. 4).
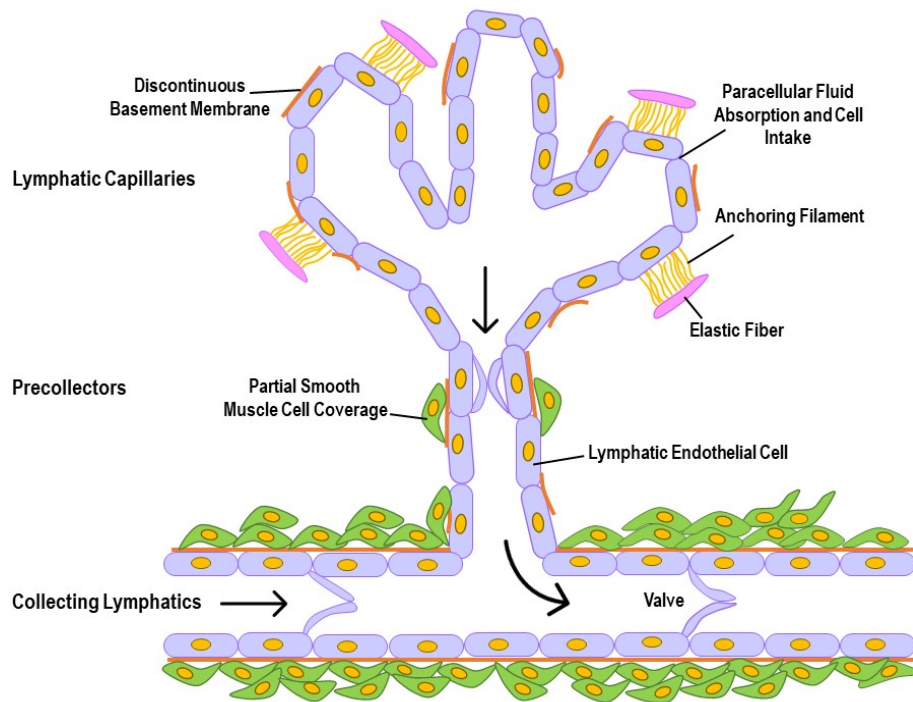
Figure 4. Schematic diagram of the lymphatic vasculature. The lymphatic vasculature consists of lymphatic capillaries, pre-collectors and collecting lymphatics. Lymphatic endothelial cells (LECs) in capillaries are covered by discontinuous basement membrane (BM). Anchoring filaments attached to LECs facilitates the entrance of interstitial fluid into capillaries. Pre-collector LECs are partially covered by BM and smooth muscle cells (SMCs).

1.3.2   Embryonic origin and development of the lymphatic system

A functional cardinal vein is present in mice at E8.5, which expresses vascular endothelial growth factor receptor 3 (VEGFR-3) (Kaipainen et al., 1995). At E9.0-9.5, few discrete venous endothelial cells (ECs) that line the anterior cardinal vein express lymphatic vessel endothelial hyaluronan receptor 1 (LYVE1). Following the expression of LYVE1 in these ECs, the development of the lymphatic vasculature initiates with the expression of Prospero-related homeobox 1 (Prox1) in a polarised population of cells in the anterior cardinal veins at E9.5. Studies have shown that SRY-box containing gene 18 (Sox18) is expressed in these LYVE1-positive cells approximately half a day prior to the onset of Prox1, which is required to induce the expression of *Prox1* in venous EC (François et al., 2008; Irrthum et al., 2000) (Figure.5 A and B). At the early stages of developmental

lymphangiogenesis, the function of Prox1 in LEC differentiation also requires heterodimerisation with chick ovalbumin upstream promoter-transcription factor 2 (COUP-TFII) (Aranguren et al., 2013; Yang et al., 2019). Vegfc-mediated activation of vegfr3 signalling is also essential in the maintenance of Prox1 expression in these LEC progenitors. Proteolytic processing of Vegfc by Ccbe1 and Adamts3 is required for lymphatic development to occur (Bos et al., 2011; Bui et al., 2016; Hägerling et al., 2013; Hogan et al., 2009; Jeltsch et al., 2014; Karkkainen et al., 2004; Guen et al., 2014) (Figure.5 C and D). These Prox1^{+} LEC progenitors ultimately bud off from the cardinal veins and start expressing differentiation markers such as podoplanin (Pdpn) and form a primary lymphatic plexus and subsequently form a lymph sac, from which the rest of the lymphatic networks form (Oliver, 2004; Oliver & Harvey, 2002). PROX1 expression is crucial in promoting LEC differentiation and directing endothelial cells toward a lymphatic fate (Kim et al., 2010) (Figure.5 E). Maturation of the lymphatic plexus includes the expression of a complete profile of lymphatic markers to form a hierarchical network of lymphatic capillaries and collecting vessels (Figure.5 F). The formation of collecting LVs is tissue-dependent and occurs at different timing. During collecting LV development, the expression level of capillary markers such as LYVE1 and CCL21 reduces in LECs, along with the reduction in VEGFR3 signalling suggesting a decrease in lymphangiogenic signalling. Collecting lymphatic vessel formation includes pruning of capillaries, intraluminal lymphatic valve development and lymphatic muscle cell coverage. The lymphatic vascular system continues to grow separately from the blood vascular system but maintains select connections to allow lymph to return to the blood circulation (Majesky, 2016; Okuda et al., 2012).
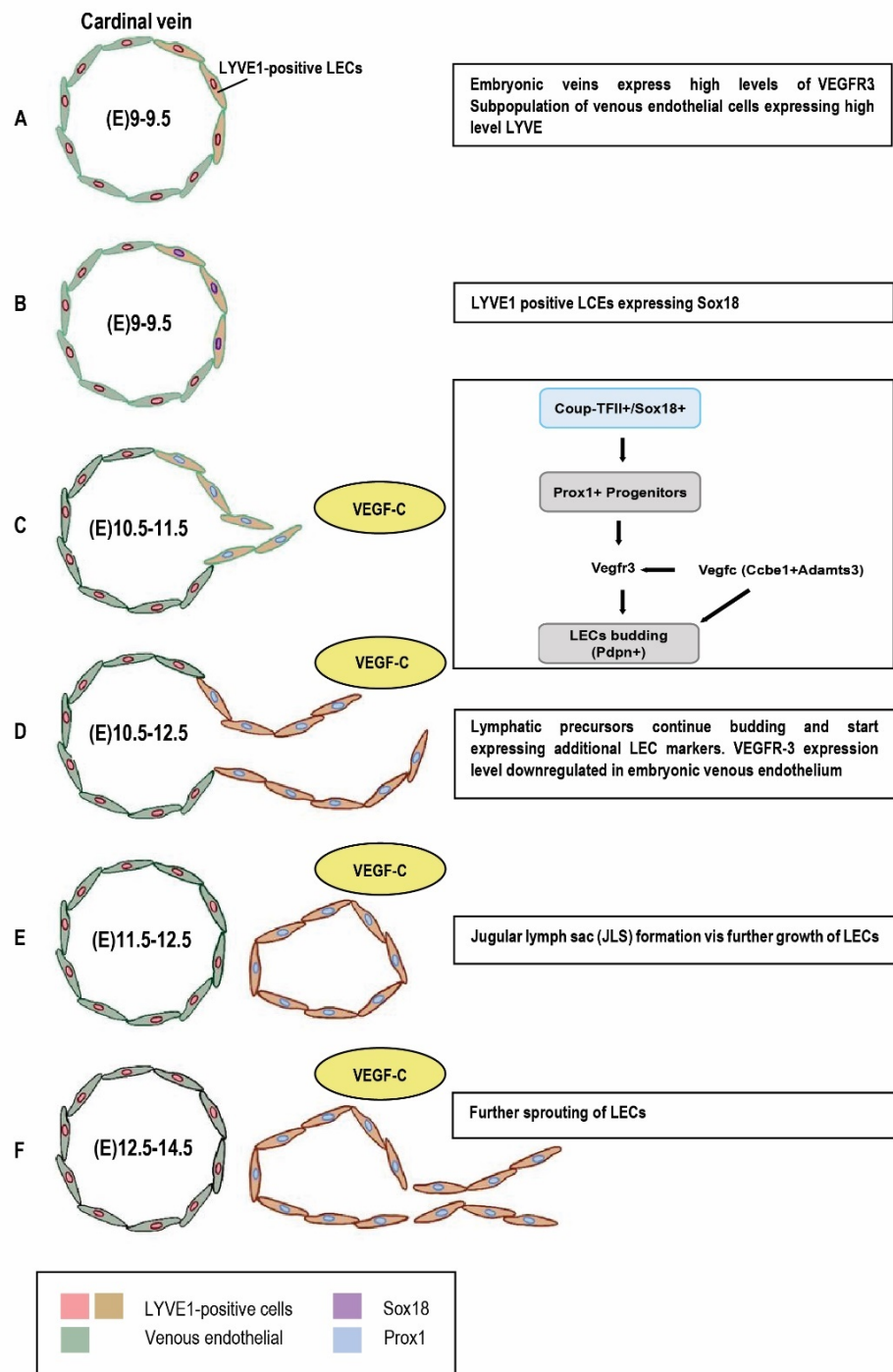
Figure 5. Origin of mammalian lymphatic vasculature. This figure illustrates the development of the lymphatic vasculature during early embryogenesis. (A) high expression of hyaluronan receptor 1 (LYVE1) at embryonic day (E)9.0-9.5 in specific subpopulation of LECs initiates the developmental process. (B) LYVE-1- positive LECs then start expressing SRY-box containing gene 18 (Sox18). (C) Expression of Sox18 induces the activation of Prox1, which subsequently initiates budding and migration of these LECs in response to vascular endothelial growth factor C (VEGFC). (D) Further budding of these lymphatic

precursors is facilitated by expression of additional lymphatic markers including Podoplanin, Neuropilin 2 (Nrp2) and chemokine (C-C motif) ligand 21 (CCL21). At this stage VEGFR3 expression downregulates in the embryonic venous endothelium. (E) At E11.5-12.5, continuous growth from cardinal vein results in formation of jugular lymph sacs (JLS). (F) Further sprouting, differentiation and maturation of LECs generates the entire lymphatic network (Figure adapted from (Oliver, 2004; Oliver & Harvey, 2002; Tammela & Alitalo, 2010)).

Lymphatic valve development includes collective migration of valve-forming cells, accumulation of ECM and formation of a bi-leaflet intraluminal structure capable of preventing lymph backflow. Various transcription factors regulating cell polarity, adhesion, migration, and cell-cell junctional communication have been identified to play important roles in lymphatic valve development. The formation of lymphatic valves was also found to be critically dependent on lymph flow. Genetic loss of endothelial junctional mechanosensitive complex PECAM1, the shear stress sensor Ca^{2+}-channel PIEZO1 and VE-cadherin results in impaired lymphatic valve development (Nonomura et al., 2018; Wang et al., 2016; Ying Yang et al., 2019). Expression of FOXC2, which is a forkhead transcription factor induced by oscillatory shear stress has been also shown to be vital in valve development. Inactivation of *Foxc2* totally prevents lymphatic valves and collecting vessel formation (Fotiou et al., 2015a; Sabine & Petrova, 2014; Wang et al., 2016).

At later stages of lymphatic valve development, gap junction communication via CX37 and Ca^{2+}-calcineurin/NFAT signalling plays an important role, which is also a downstream effector of FOXC2. In addition to an important role in the initial sprouting of LECs from the cardinal veins, GATA2 also plays a major role in lymphatic valve development, specifically in valve maintenance and morphogenesis (Kazenwadel et al., 2015). Like FOXC2, GATA2 expression is also regulated by oscillatory shear stress (Kanady et al., 2011; Kazenwadel et al., 2015) (Figure. 6).
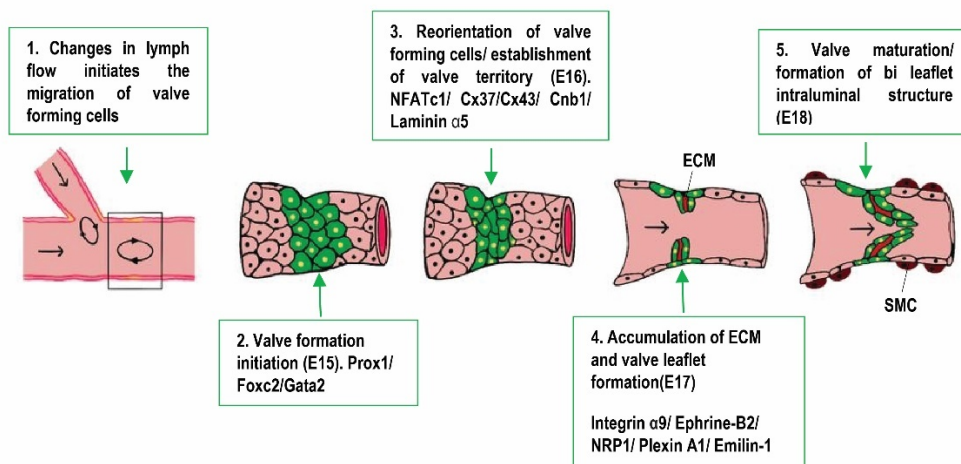
Figure 6. Schematic model of lymphatic valve development in collecting lymphatic vessels. Flow direction in lymphatic vessels initiates changes in the shape and polarity of valve forming cells. Expression of key regulators shown in the figure in lymphatic endothelial cells facilitates valve formation and establishment. Furthermore, accumulation of extracellular matrix components results in valve maturation and formation of a bi-leaflet intraluminal structure.

1.3.3   Non-venous derived origins of the lymphatic vasculature

The origin of embryonic lymphatic endothelial cells has been debated for over a century (Huntington & McClure, 1910; Sabin, 1902; Srinivasan et al., 2007; Ulvmar & Mäkinen, 2016). Venous-derived LECs were initially proposed to be the predominant source of lymphatic endothelial cells comprising the lymphatic vasculature (Sabin, 1902). Lineage tracing experiments performed by Srinivasan et al in the mouse embryo later demonstrated that most cells within the lymphatic vasculature originated from PROX1-positive progenitor cells residing in the cardinal and intersomitic veins (Srinivasan et al., 2007; Yang et al., 2012).

A few years later, a re-examination of an alternative cellular origin of lymphatic endothelial cells, first described by Huntington and McClure 1910, was prompted upon the discovery of a process observed in the mesentery of mice termed lymphvasculogenesis (Huntington & McClure, 1910). Huntington and McClure proposed a mesenchymal origin for lymphatic development. It was hypothesised that primary lymph sacs originate from mesenchyme-

derived endothelial precursors, independent of the veins and secondarily established venous connection (Huntington & McClure, 1910).

Additional, non-venous sources of lymphatic endothelial cells have been identified in recent years and include the contribution of blood capillary endothelial cells in the dermal lymphatics (Thievend et al., 2018) and hemogenic endothelium-derived cells to lymphatics in the heart and mesentery (Klotz et al., 2015; Stanczuk et al., 2015). It has been suggested that this diverse lymphatic origin may contribute to the structural and functional lymphatic heterogeneity in different organs in both health and disease (Jafree et al., 2019).

Lineage tracing experiments also facilitated the recent discovery of a contribution of paraxial mesoderm to the generation of venous-derived LECs in the mouse (Stone & Stainier, 2019). The paraxial mesoderm (PXM) is a transient cell population found between the neural tube and the intermediate mesoderm, giving rise to muscle lineages and limb endothelium. PXM was proposed to direct venous endothelial cells to the dorsolateral wall of the cardinal veins (Stone & Stainier, 2019).

In a recent study done by Lioux et al, the first random, lineage-unrestricted clonal analysis of the developing heart was performed. This study identified a new vasculogenic niche contributing to coronary lymphatic development and confirmed the heterogeneous origin and function of cardiac lymphatics. They demonstrated the contribution of second heart field (SHF), a progenitor pool of cells in the heart, to the lymphatic endothelium of the ventral heart and suggested that there is a direct contribution from SHF to lymphatics, independent of the CV-derived LECs (Lioux et al., 2020; Meilhac & Buckingham, 2018). The study of lymphatics in the brain meninges is novel and the source of progenitor cells giving rise to the meningeal lymphatic has not been fully established (Figure. 7).
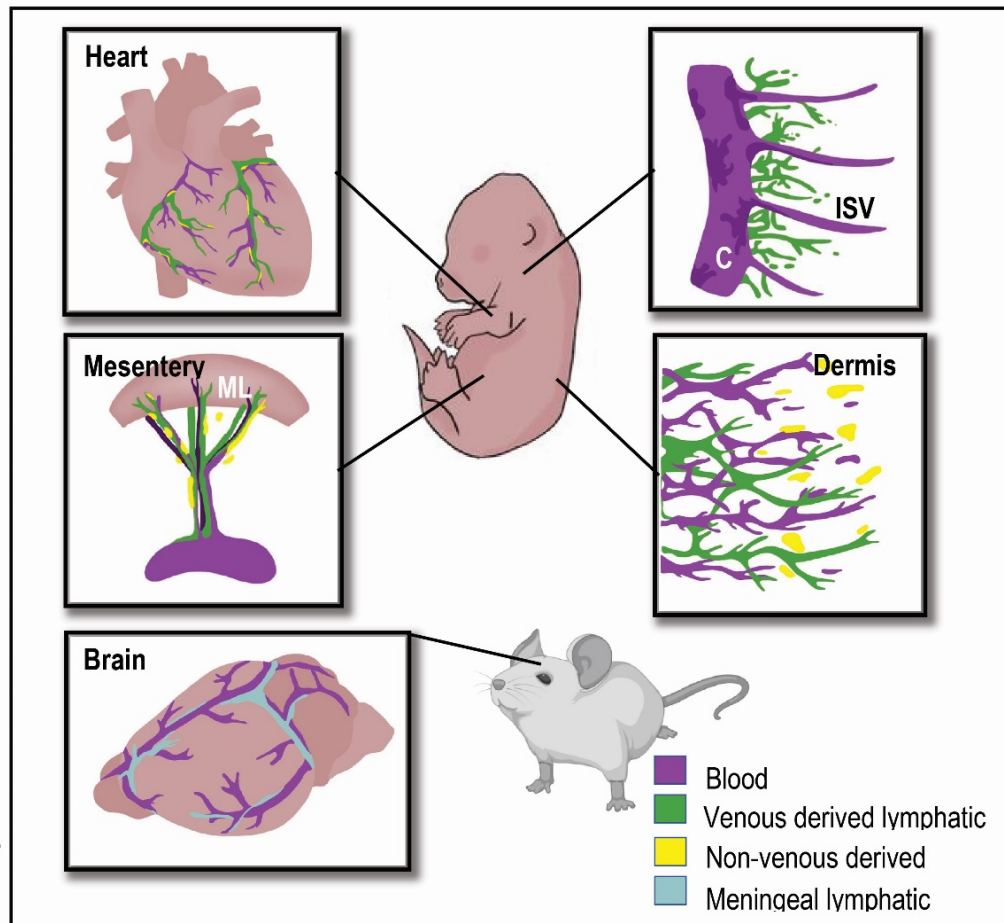
Figure 7. Schematic illustration of embryonic and postnatal origins of lymphatic vessels associated with specific organs in the mouse. Initial lymphatics (green) have venous origin. These lymphatics sprout from the cardinal veins (C) and intersomitic veins (ISV) to generate lymph sac and lymphatic plexus which extends throughout the embryo. A sub-population of lymphatic endothelial cells within the lymphatic vessels in the dermis originate from the blood vascular capillary plexus (yellow) rather than the veins. Lymphatic vessels in the heart originate from both venous (green) and non-venous (yellow) progenitors. Non-venous LEC in the heart have been proposed to originate from yolk-sac hemogenic endothelium and second heart field progenitor cells**.** In the mesenteric vessels, some lymphatic endothelial cells are derived from a non-venous, *c-KIT* positive hemogenic endothelial lineage (yellow) and others such as those that constitute the mesenteric lymph sac (MLS) are of venous origin (green). Meningeal lymphatic vessels start developing in the post-natal brain by sprouting from established vessels. Isolated clusters of LEC are also observed. The origins of these vessels have not yet been assessed by lineage tracing experiments (Adapted from (Kazenwadel & Harvey, 2018)).

1.3.4 Signalling pathways involved in lymphatic vascular development.

Several signalling pathways have been identified to play crucial roles during lymphatic vascular development. Mitogen-activated protein kinase/extracellular signal-regulated kinase (MAPK/ERK) signalling initiates the signal for LEC differentiation and activates SOX18, which subsequently induces the expression of PROX1 (Deng et al., 2013; Duong et al., 2014). Expansion of the lymphatic vasculature and migration of LECs is directed via VEGFC (Vascular Endothelial Growth Factor C) and its primary receptor tyrosine kinase VEGFR3, which is highly expressed in PROX1 positive cells. VEGFC is the most well-known lymphangiogenic growth factor, found to be vital in sprouting the first lymphatic vessels from cardinal veins in mouse embryos (Karkkainen et al., 2004). Interaction of VEGFC with VEGFR3 leads to activation of phosphatidylinositol 3-kinase (PI3K)/protein kinase B (PKB/AKT) and MAPK/ERK signalling, which subsequently promotes LEC proliferation, migration and survival (Mäkinen et al., 2001) (Figure. 8).
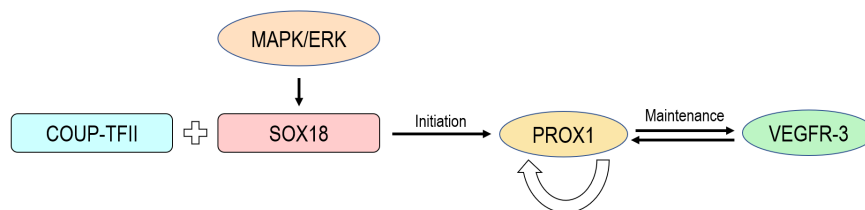
Figure 8. Involvement of signalling pathways in lymphangiogenesis. MAPK/ERK signalling initiates the signal for LEC differentiation and activation of SOX18 and PROX1 (Adapted from Ying Yang and Guillermo Oliver, 2014).

VEGF-C activity is controlled by collagen and calcium-binding EGF domain-containing protein 1 (CCBE1) and the metalloprotease ADAMTS3, which converts the inactive, full-length VEGFC into its active form making it capable of binding and activating VEGFR3 (Bos et al., 2011; Hogan et al., 2009; Jeltsch et al., 2014). Recently, VEGFC has been shown to regulate the expression of musculoaponeurotic fibrosarcoma oncogene homolog B (*MAFB*). *MAFB* is a transcription factor that controls the expression of *PROX1*, *SOX18*, and *NR2F2* (COUP-TFII) (Dieterich et al.,

2015; Koltowska et al., 2015). Another signalling pathway that plays a major role in regulating lymphatic development and postnatal lymphangiogenesis is the Delta-like 4 (Dll4)/Notch signalling pathway. The Notch signaling pathway is mediated by various factors such as 4 Notch receptors and 5 transmembrane ligands including Delta-like ligands (Dll1/3/4) and Jagged ligands (Jagged1/2) (Niessen et al., 2011; Min et al,2016). Notch receptors have been shown to be expressed in lymphatic tissues (Shawber et al.,2007). Receptor-ligand interaction between adjacent cells leads to proteolytic cleavage of the receptor. When the receptor is released in the intracellular domain, it translocates to the nucleus and regulates gene transcription through the binding of transcriptional regulators. Gene expression of several important lymphatic genes such as LYVE1, Prox1 and VEGFR3 was found to be regulated by the Notch pathway (Kang et al., 2010). Delta-like 4 (Dll4)/Notch signaling has been also found to crosstalk with VEGF receptors (VEGFRs) and directly and indirectly regulate lymphangionegesis (Garcia & Kandel, 2012) (Figure. 9)
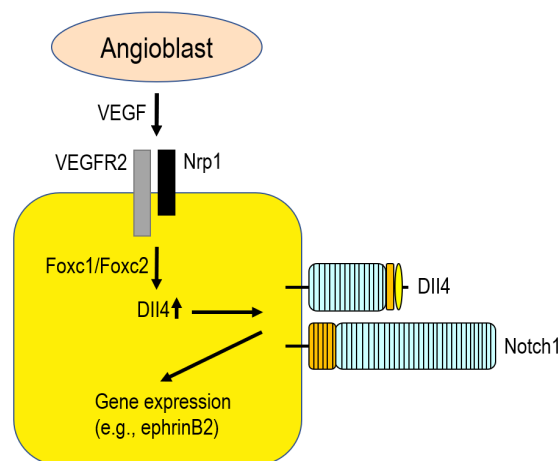
Figure 9. Cell specification mediated by Dll4-Notch signalling. During early development, VEGF (in concert with Foxc1/c2 transcription factors) induces Dll4 expression in endothelial cells, and Dll4-Notch signalling promotes other gene expression (Adapted from (Kume, 2009)).

Loss of the Notch gene or reduction in Notch signalling has been shown to result in enlarged dysmorphic embryonic dermal lymphatic vessels as a result of significant increases in LEC proliferation and sprouting from JLS (Fatima et al., 2014; Murtomaki et al., 2014). Downregulation of DLL4 or inhibition of Notch signalling in zebrafish also leads to impaired lymphatic development, emphasizing the importance of the Notch signalling

pathway (Geudens et al., 2010). Furthermore, it has been shown that the downregulation of ephrinB2 results in the inhibition of DLL4/Notch signalling, which subsequently decreases postnatal lymphangiogenesis (Niessen et al., 2011).

Biomechanical signalling is another critical element in lymphatic vasculature development. Intrinsic and extrinsic mechanical forces applied to lymphatic vessels contribute to both the lymphangiogenic response and lymphatic vascular maturation during development. The origin of these forces is the uptake and propulsion of lymphatic fluids (Hargens & Zweifach, 1977; Olszewski & Engeset, 1980; Weid & Zawieja, 2004).

During the studies where the contribution of Neuropilin2 and Ccbe1 (collagen and calcium-binding EGF domain 1) in lymphatic vasculature development was investigated in deficient mice, the importance of mechanical stimuli including tissue fluid pressure in the regulation of VEGFC/VEGFR3 signalling and its contribution to growth and maturation of lymphatic vasculature during early development was also highlighted (Planas-Paz et al., 2012; Planas-Paz & Lammert, 2013; Mecker et al., 2011; BOs et al., 2011).

Tissue stiffness is a mechanical force which regulates the nuclear localisation of GATA2 and expression of VEGFR3, important for LEC proliferation and migration (Frye et al., 2018). Moreover, the regulation of GATA2 by oscillatory shear stress (OSS) was examined by Kazenwadel et al. In this study, an elevated level of GATA2 in developing valves was shown in the presence of OSS (Kazenwadel et al., 2015). Earlier it was also shown that GATA2 lies upstream of *Prox1* and *Foxc2* transcription factors, both highly essential for valve development. It was reported that a reduction in Gata2 levels significantly diminished levels of *Prox1* and *Foxc2* (Kazenwadel et al., 2012). Previously, the importance of mechanotransduction and FOXC2 in lymphatic valve development was also shown by Sabine and Petrova (Sabine & Petrova, 2014). Together, these data suggested elevated levels of FOXC2 in response to OSS are also dependent on GATA2.

Moreover, it was also reported that PIEZO1 is required for lymphatic valve formation (Nonomura et al., 2018) and studies of patients with lymphatic dysfunction showed that mechanically activated ion channel PIEZO1 is essential in the lymphatic system (Lukacs et al., 2015; Datkhaeva et al., 2018). A study of a mouse line lacking PIEZO1 in endothelial cells (*Tie2Cre*) showed PIEZO1 knockout mice exhibit pleural effusion and

breathing difficulties and PIEZO1 was shown to be one of the mechanosensors essential in lymphatic and venous valve formation (Nonomura et al., 2018). However, previous findings showed that knockout of *PIEZO1* does not affect transcriptional up-regulation of *GATA2* induced by oscillatory shear stress (Lukacs et al., 2015), suggesting there is more than one mechanotransduction pathway involved in lymphatic vessel valve formation.

1.3.5 Molecular markers important in lymphatic vessels and their role in lymphatic vascular development and function

1.3.5.1 Prospero-Related Homeobox Domain (Prox1)

Prospero-related homeobox domain 1 (*Prox1*), known as the master regulator and gold standard LEC marker was originally isolated due to its high homology to the *Drosophila melanogaster* homeobox gene, *prospero* (Oliver et al., 1993). Regulation of Prox1 is essential during the development of various organ systems. In mammalians, Prox1 facilitates the differentiation of many cell types in tissues such as the lens, retina, heart, pancreas and liver (Jeffery et al., 2000; Oliver et al., 1993; Tomarev et al.,1996). The Lymphatic vasculature begins to form when *Prox1* expression initiates in a subset of venous EC on the dorso-lateral side of the anterior cardinal veins at E9.5. These cells ultimately bud off and migrate to form a primary lymphatic plexus and eventually form lymph sacs to start the lymphatic network. Prox1 has also been shown to be crucial for LEC fate specification (Lavado et al., 2010; Wigle & Oliver, 1999). The essential role of *Prox1* in lymphatic vascular development was demonstrated through a mouse study, where it was shown that homozygous *Prox1* mutant embryos (*Prox1$^{-/-}$*) were lacking lymphatic vessels and died at E14.5. *Prox1*-deficient EC started to bud and sprout in these embryos, but they could not acquire markers essential for cell identity in LECs and their migration was arrested around E11.5-E12.0. However, the blood vasculature was completely unaffected in *Prox1*-null mice (Harvey et al., 2005; Wigle & Oliver, 1999). Moreover, *Prox1* expression levels have been shown to be critical for postnatal survival. A substantial proportion of *Prox1* heterozygous pups present with evidence of lymphatic dysfunction. These pups develop chylous ascites and extravasation of milky chyle from the mesenteric lymphatic vessels into the peritoneal or thoracic cavities and subsequently

die soon after birth. However, one genetic background was identified by Wigle et al where several heterozygous mice survived until adulthood. However, these mice developed adult-onset obesity, which suggested a potential link between lymphatic vascular dysfunction and adipogenesis (Harvey et al., 2005; Wigle & Oliver, 1999).

In the research conducted by Oliver and his team, the necessity of Prox1 in different aspects of developmental and postnatal lymphangiogenesis was investigated where Prox1 activity was removed conditionally in a time-specific manner. This study confirmed that Prox1 is constantly required to maintain lymphatic endothelial cell identity (Johnson et al., 2008). Furthermore, it was illustrated that the differentiated LEC phenotype is a plastic, reversible state (Johnson et al., 2008). Although the importance of *Prox1* is very well known, the mechanism by which *Prox1* expression is controlled in EC is not fully understood yet. Studies suggest that the transcription factor SOX18 has a direct influence on the expression of *Prox1* by binding to its proximal promoter. François et al. demonstrated that lack of *Sox18* expression leads to the complete arrest of embryonic lymphatic vascular development, which subsequently results in embryonic lethality and oedema (François et al., 2008).

It was also shown that chicken ovalbumin upstream promoter-transcription factor 2 (Coup-TFII) which is a regulator of venous identity is essential for the induction of *Prox1* expression in lymphatic endothelial progenitor cells within the embryonic venous endothelium. Up until E13.5, binding of COUP-TFII to PROX1 is essential for the maintenance of *Prox1* expression. After E13.5, the expression of *Prox1* becomes independent of this regulator (Srinivasan et al., 2010).

1.3.5.2   SRY-Related HMG-box 18 and SoxF Group Transcription Factors

SRY-related HMG-box 18 (SOX18) is part of a subfamily of transcription factors known as F-group, which also contains the closely related SOX7 and SOX17 family members. These transcription factors play critical roles during vascular development (Downes & Koopman, 2001).

As mentioned earlier, SOX18 initiates the expression of *Prox1* during LEC fate induction. (François et al., 2008). In contrast to PROX1, lymphatic endothelial cells do not express

SOX18 during later stages of lymphangiogenesis, suggesting that Sox18 may not be further involved in the expansion and maturation of the lymphatic plexus (~E14.5) or the maintenance of LEC identity.

1.3.5.3 Forkhead Box Protein c2 (FOXC2)

Foxc2 is a forkhead transcription factor known for its essential role in lymphatic valve development. Initially, Foxc2 plays a critical role in regulating arterio-venous differentiation in cooperation with Foxc1 (Dagenais et al., 2004). High expression of Foxc2 is observed in lymphatic vessels up until E14.5 where it starts to downregulate as LECs mature into a collecting lymphatic phenotype, except in lymphatic valves. Foxc2 expression remains high. Mouse studies demonstrated severe morphological defects in lymphatic vessel development especially in valve formation in *Foxc2* mutant mice (Petrova et al., 2004). Interestingly, in humans, Foxc2 was found to be associated with the rise of lymphoedema distichiasis (inherited primary lymphoedema), whereby individuals display lymphatic vascular morphogenesis defects including aberrant pericyte recruitment and absence of valve formation (Irrthum et al., 2003).

Recent data also suggested the close function of Foxc2 with another transcription factor Nuclear Factor of Activated T Cells 1 (Nfatc1). Nfatc1 also controls cardiac valve formation, suggesting that different endothelial valvular morphogenesis programs may be controlled by the common transcriptional regulators (Norrmén et al., 2009).

1.3.5.4 Nuclear Factor of Activated T-Cells, Cytoplasmic 1

Nfatc1 is a calcium-sensitive transcription found to be highly expressed by PROX1-positive LEC precursors in cardinal veins and LECs in developing lymph sacs (Schulz & Yutzey, 2004). By interacting directly with several developmental transcription factors, Nfatc1 was identified to play an essential role in normal lymphatic vascular patterning and cardiac valve morphogenesis (Sater et al., 2012; Olson, 2006). Reduction of Nfatc1 was also shown to be associated with poorly organised jugular lymph sacs (Kulkarni et al., 2009).

Activation and nuclear localisation of Nfatc1 are directed by the Calcineurin pathway via dephosphorylation of NfatC1. In a study undertaken by Rishikesh and colleagues, inhibition of Calcineurin phosphatase was demonstrated to result in disorganised development of lymph sacs. Assessing the level of Prox1 and Vegfr3 when levels of NfatC1 were reduced, indicated that the expression of Prox1 and Vegfr3 were unaltered. This result suggested that the role of NfatC1 is independent of Prox1 (Kulkarni et al., 2009).

In a different study using a genome-wide chromatin immunoprecipitation (ChIP) analysis, a large set of Foxc2 binding sites were identified and mapped; data showed consistent enrichment of Nfat binding sites co-located with Foxc2 binding sites. These data, together with characterisation of the Nfatc1 and Foxc2 phenotypes, illustrate cooperation between Foxc2 and Nfatc1 signalling in the transcriptional control of lymphatic vessel differentiation and maturation (Norrmén et al., 2009).

1.3.5.5 LYVE1

LYVE-1 (Lymphatic Vessel Endothelial Receptor 1) is a transmembrane receptor found on lymphatic endothelial cells. Expression of LYVE1 has been also reported on hepatic sinusoids, macrophages, Kupffer cells, cortical neurons, renal epithelium and the islets of Langerhans (Banerji et al., 1999; Prevo et al., 2001). The function of LYVE1 has been defined to be similar to CD44, which is important for the transportation and turnover of hyaluronan (HA), as well as HA localisation to the surface of lymphatic endothelium (Banerji et al., 1999). HA is a component in skin and connective tissues which is recognized for its roles in cell migration, inflammation, tissue morphogenesis and tumour metastasis. As mentioned earlier LYVE1 is expressed widely in intra-embryonic blood vessels prior to the induction of *Prox1* in the cardinal veins (Harvey et al., 2005). Levels of LYVE1 are high in Prox1-positive LEC progenitors in embryonic stages and remain high postnatally on EC of lymphatic capillaries, but are downregulated in collecting lymphatic vessels (Gordon et al., 2008; Mäkinen et al., 2005). LYVE1 has also been demonstrated as the most common marker for secondary lymphoid tissues and is important in cornea and skin lymphangiogenesis and inflammatory conditions (Chauhan et al., 2014). The specificity of LYVE1 antibodies for lymphatics made it a great candidate

as a marker of lymphangiogenesis in cancer models even though the contribution of lymphangiogenesis in metastatic spread is still unclear. Using LYVE1 as a marker for tumour lymphangiogenesis has identified patients at high risk of nodal metastasis, relapse and poor prognosis.

1.3.5.6   Integrin Alpha-9

Integrin-alpha 9 (Itga-9) is part of a family of heterodimeric cell surface transmembrane glycoproteins important in cell-cell and cell-matrix interactions. Integrins have two subunits, α and β, which facilitate their role in extracellular matrix protein binding (Srichai & Zent, 2010). Cell anchorage to the extracellular matrix is predominantly mediated through integrin-based linkages, where they create strong connections between the intracellular and extracellular environments.

Studying the function of Itga-9 in corneal lymphatic valve formation, Altiok et al revealed an essential role of Itga-9 in lymphatic valve development, as well as its involvement in LEC processes such as migration, proliferation and adhesion (Altiok et al., 2015). Fibronectin has been reported as one of the main ligands for Itga-9. LEC adhesion to fibronectin was shown to be significantly inhibited upon the depletion of Itga-9. The role of Itga-9 in LEC migration was also shown through wound healing scratch assays where it was demonstrated that LECs lacking Itga-9 never fully migrated over the scratch wound in comparison to control LECs (Altiok et al., 2015).

1.4 Lymphatic Endothelial Cell (LEC) heterogeneity

As described earlier, LECs are specialized to play various vital roles in the body. Their function is not limited to the drainage of interstitial fluid but also includes the transportation of tissue-derived immune cells and antigens to lymph nodes to activate immune responses (Földi, 2003; Randolph et al., 2005). The lymphatic system also has a crucial role in the uptake of dietary fats and the clearance of cholesterol from peripheral tissues (Dixon, 2010). Any dysfunction in the lymphatic system can contribute to an array of pathogenic disorders (Alitalo, 2011). The most important fact to consider when studying

lymphatic anomalies is that lymphatic vessels show significant plasticity and heterogeneity within different organs and under different pathological and physiological processes, which reflect the tissue-specific nature of the lymphatic system (Ulvmar & Mäkinen, 2016). LECs of different vascular beds were compared recently in a study where Vegfc was deleted in postnatal mice. The study showed the failure of function in specialised lacteal lymphatic vessels within the intestinal villi, whereas dermal lymphatic vessels showed no changes in function or integrity (Nurmi et al., 2015). In a different study, the lymphatic vascular of different tissues was analysed where Vegfc was overexpressed (Yao et al., 2014). The result indicated lymphatic vessel growth in the respiratory tract was only observed during a critical period in perinatal development, however overexpression of vegfc in skin-activated lymphangiogenesis even in adult stages (Yao et al., 2014).

Still very little is known about the lymphatic patterning and maintenance or how LEC plasticity is controlled in different tissues. Only recently have researchers started to investigate more to understand the molecular difference, function, and cellular origin of LECs in different organs and biological contexts. The studies using single-cell transcriptomics of lymphatic endothelial cells (LECs) have shown that LECs consist of multiple cell subsets, which together will serve a different physiological and pathological function in each organ setting (Fujimoto et al., 2020; Sibler et al., 2021; Takeda et al., 2019). It has been identified that these LEC subsets have been defined based on their gene expression patterns and anatomical locations. Further investigation is required to fully understand their role, as well as their interactions with other cell types in lymphoid tissues, which subsequently will aid in a better understanding of lymphatic-associated diseases in various organs and in examining how diseases can affect these LEC heterogeneities in each tissue.

1.4.1 Dermal lymphatics

Understanding the lymphatic origin and molecular mechanisms involved in regulating lymphatic vessel formation in the skin is vital to unravel the context of pathological conditions arising as a result of lymphatic vasculature abnormalities in the dermal

lymphatics. Although the epidermis is avascular, the dermis is rich in both blood and lymphatic vessels. Lymphatic capillaries in the skin, like in other organs can dilate up to 10-50 times when there is an increase in interstitial pressure. This gives LVs in the skin the essential feature required to maintain the fluid balance in these tissue beds (Skobe & Detmar, 2000). LVs in the skin can also initiate immune responses by directing the migration of Langerhans cells to lymph nodes (Romani et al., 2012). Dermal lymphatics are the most well-studied lymphatic bed, however, information on their origin and molecular mechanisms regulating their formation in different regions of the skin is still lacking. Dermal LVs consist of two plexuses; a superficial one that extends to the dermal papillae and consists of thin vessels devoid of valves, and a deep lymphatic network that comprises larger collecting vessels and numerous valves (Sabin, 1904).

During embryonic development in mice, LVs start sprouting from the JLS and reach the cervical region by E12.5. Several dermal lymphatics then start emerging from the lateral side of the embryo between E12.5 and E13.5. These dermal lymphatics then continue extending both ventrally and dorsally to form a fine superficial lymphatic network, which is visible at E15.5 (Corral et al., 2015; Wigle & Oliver, 1999). Based on various studies, LECs in early LVs can originate from both venous and non-venous cells (Hen et al., 2015; Klotz et al., 2015a; Nicenboim et al., 2015; Ny et al., 2005; Okuda et al., 2012; Stanczuk et al., 2015; Wilting et al., 2006). It has been demonstrated that non-venous derived LEC progenitors are the sources of dorsal dermal lymphatic vessel formation in the lumbar and cervical regions of the skin (Corral et al., 2015). In addition, a contribution from PROX1-positive cells arising in the blood vascular capillaries contributes to dermal lymphatic development (Thievend et al., 2018).

Over the past few decades, several transcription factors and molecular players essential for dermal LV development were identified. *Prox1* and *Nr2f2* have been shown to be critical for the formation of dermal lymphatics in *vivo* (Lin et al., 2010; Srinivasan et al., 2014; Wigle & Oliver, 1999a). VEGFR3 signalling is also critical during LV formation. Disruption of VEGFR3 signalling results in drastic hypoplasia of the embryonic dermal lymphatic network due to defective LV sprouting (Dellinger et al., 2007; Haiko et al., 2008; L. Zhang et al., 2010). NRP2 is a transmembrane receptor in lymphatic endothelial cells and is essential for lymphatic capillary development in embryonic skin (Yuan et al., 2002). Studies have also shown that the reduction of fatty acid oxidation as a result of lymphatic-

specific loss of Carnitine Palmitoyltransferase 1A (Cpt1a), which is being controlled by PROX1 in differentiating LECs, results in several defects in the formation of dermal LVs and induces embryonic lymphoedema (Wong et al., 2018). Moreover, glycolysis was also demonstrated to be important for embryonic dermal lymphatic development. Loss of Hexokinase 2 (Hk2) which is a glycolytic enzyme, is associated with the reduced migration of dermal lymphatic capillaries and vessel branching (Yu & Li, 2016).

Normal lymphatic transport is essential for skin homeostasis. Lymphatic vessel abnormalities in the skin are implicated in conditions such as psoriasis and dermatitis. The density and function of dermal LVs were also found to be related to age-related skin disorders (Karaman et al., 2015). Impairment in dermal LV function can also lead to lymphoedema, hyperpigmentation, keratosis, and papillomatosis (Carlson, 2014).

1.4.2   Dural lymphatics

The meningeal lining in the brain consists of three layers: the pia mater, the avascular arachnoid matter and the vascularized dura mater. For decades the central nervous system (CNS) was considered to lack lymphatic vessels, which raised the question of how the brain drains waste material. With no clear evidence of the existence of an organized lymphatic network, the brain was considered immunoprivileged for years, though work done by anatomists centuries ago had described lymphatic vessels in the meninges (Mesquita et al., 2018).

Upon the discovery of specific lymphatic EC markers such as PROX1, CCL21, PECAM1, LYVE1, VEGFR3 and PDPN, the visualisation of lymphatic vessels was facilitated in the CNS. The findings demonstrated the existence of lymphatic vessels in the brain meninges. Generally, it was found that lymphatic vessels are relatively scarce in the superior portions of the skull, whereas the base of the skull contains a more extensive lymphatic vessel network. No lymphatic vessels were identified in the brain parenchyma or pia mater, however, an extensive network of lymphatic vessels was observed in the meninges underlying the skull bones (Ahn et al., 2019; Aspelund et al., 2015; Louveau et al., 2015). Interestingly, a relatively small number of lymphatic valves were found in

the lymphatic vessels at the base of the skull. These valves appeared to be separated by long stretches of valveless vessel segments (Ahn et al., 2019).

Functional studies have since demonstrated the crucial role of the dural lymphatic network in the drainage and clearance of cerebrospinal fluid and macromolecules, as well as the transport of immune cells into the cervical lymph nodes (Aspelund et al., 2015; Louveau et al., 2015). The importance of dural LVs suggests their association with the accumulation of proteins or altered immunity contributing to various diseases, including Alzheimer's disease and Parkinson's disease (Louveau et al., 2016). These findings highlight the importance of more detailed analyses to uncover the function of dural LVs in CNS health and diseases.

1.4.3   Ocular lymphatics

Like other tissues and organs in the body, proper fluid haemostasis is crucial for the maintenance of ocular health. Ocular tissues are heterogeneous by nature, lymphatic vessels are not distributed equally throughout the eye. Some parts such as conjunctiva and eyelids are rich in lymphatics, while other parts like the retina, uveal tract and cornea are devoid of any lymphatic vasculature (Neto et al., 2015; Yücel et al., 2009). This heterogeneity in ocular tissue suggests fluid homeostasis in the eye is controlled by more than one drainage system.

A specialised fluid drainage system of the eye, Schlemm's canal, was recently demonstrated to share significant similarities with the lymphatic vasculature. Schlemm's canal originates from a subset of venous endothelial cells which upregulate Prox1 and undergo lymphatic differentiation by upregulating LEC and downregulating BEC-specific genes. In Schlemm's canal, a subset of limbal BECs starts to express Prox1 (which plays a vital role in canal development), which subsequently clusters to form the primitive tube structure in a manner similar to the development of lymph sacs (Ulvmar & Mäkinen, 2016). Schlemm's canal is lined by a single layer of endothelial cells featuring both BEC and LEC features. These special endothelial cells express several endothelial cell markers such as CD31, cadherin 5, VEGF receptor 2, ITGA9 and vWF (Aspelund et al., 2014). The mature Schlemm's canal stays connected with the blood vessels via collecting channels from where it drains the aqueous humour to the systemic circulation (Wu et al.,

2020). The very low or lack of LYVE1 and PDPN expression is what prevents Schlemm's canal from being considered a "true" lymphatic vessel.

Identification of a broad spectrum of ocular disorders associated with lymphatic dysfunction in the eye, such as inflammatory diseases, transplant rejection, tumour and cancer metastasis, venous lymphatic malformations, glaucoma, and ocular manifestations of numerous systemic diseases led to a more detailed study of the lymphatic beds in ocular tissue. Studies have shown that even though the cornea is avascular, lymphatic vessels can be induced in this region under pathological situations. Findings suggest that lymphatics can be in fact stimulated in the cornea after inflammatory, traumatic, infectious, or chemical and toxic insults independently of blood vessels. These induced lymphatic vessels are absolutely essential for the induction of corneal transplantation immunity (Zhong et al., 2009).

It has been demonstrated that lymphatics in the conjunctiva are important in providing immune effectors to the anterior eye compartment and metabolic homeostasis of this tissue. However, the lymphatics in the posterior eye segment are not yet understood. Understanding the role of lymphatics in this segment may reveal novel ways to manage macular oedema (Yang et al., 2019).

1.4.4   Cardiac lymphatics

The crucial role of cardiac lymphatic vessels in the normal functioning of the cardiovascular system and their association with various pathologies justifies the significant interest directed to understanding the biology and development of cardiac lymphatic vessels. The lymphatic networks in the heart generally run alongside the blood vessels and are vital for the maintenance of interstitial fluid pressure (draining extravasated interstitial fluid and preventing myocardial oedema) and modulation of immune responses (Ratajska et al., 2014). Malformation in cardiac lymphatic vessels can result in severe heart dysfunction with it being shown that a 3.5% increase in myocardial fluids as a result of dysfunction in lymphatic vasculature can lead to a 40% reduction in cardiac output (Dongaonkar et al., 2010).

Various studies have confirmed the lineage heterogeneity of the cardiac lymphatics during development and their crucial role in fibrotic repair after myocardial infarction (MI) in non-regenerative animal models, such as adult mice and regenerative models, such as zebrafish. These findings provide evidence that lymphatic vessels in the heart could be a potential therapeutic target in cardiovascular diseases, whereby promoting the growth and repair of new lymphatic vessels provides an opportunity to promote regeneration of the damaged myocardium, subsequently reducing myocardial oedema and modulating the immune response after MI (Klaourakis et al., 2021).

In-depth analyses of lymphatic development in the heart over recent years demonstrated that the localisation of lymphatic capillaries and routes of collecting vessels in the heart are diverse among different species. Understanding these differences in normal structure and development of lymphatic vessels across species is important for studying the evolutionary changes in animals. In species such as monkeys, rodents and birds the cardiac lymphatics begin to establish soon after the blood vasculature develops during embryogenesis. In contrast, the development of the cardiac lymphatics in fish starts in the juvenile-adult stages and sprouts towards the ventricle after coronary blood vessel formation (Gancz et al., 2020). In mice, the first cardiac lymphatic sprout appears at the anterior part of the heart between E12 and E14, after the formation of the first coronary vessels yet before the onset of coronary blood circulation. During cardiac development, lymphangiogenesis highly depends on the ingrowth of cardinal vein LEC precursors that first migrate onto the dorsal epicardial surface. Subsequently, these cells extend towards the apex of the heart, expand through the coronaries, and end up covering a large part of the heart surface by E14.5. These early cardiac PROX1$^+$ LECs then differentiate in situ, by expressing lymphatic markers, including LYVE1 and podoplanin, and organize into a net-like structure covering the atria and ventricles of the heart (Brakenhielm & Alitalo, 2019). Moreover, 20% of cardiac lymphatic vessels have been identified to be initiated from non-venous-derived LECs with unknown origin and are proposed to be involved in the process of lymphvasculogenesis, suggesting substantial heterogeneity of the lymphatics in the heart (Klotz et al., 2015; Lioux et al., 2020). In mice, cardiac lymphatic vessel maturation and remodelling continue postnatally until 2-3 weeks after birth where the key lymphangiogenic growth factors, VEGFC and VEGFD, play important roles in these processes.

Understanding the mechanisms of regulation and function of lymphatic vessels in the heart is important to obtain a better understanding of cardiovascular diseases associated with malfunction in this network, thereby offering new therapeutic approaches to promote cardiac repair (Henri et al., 2016; Klotz et al., 2015; Vuorio et al., 2017).

1.4.5 Pulmonary lymphatics

Lymphatic vessels in the lungs have critical roles in the maintenance of fluid homeostasis, immune system and gas exchange by draining fluid from tissues and returning it to the vascular circulatory system. All these vital functions make lymphatic circulation a vital component in health and lung diseases (Jakus et al., 2014).

Like lymphatics in other organs, the pulmonary lymphatic vasculature consists of thin-walled capillaries and larger vessels, which are lined by a layer of endothelial cells. The interstitial space and thin layer of epithelium in the lung are constantly exposed to great hydrodynamic, osmotic and hydrostatic forces. The existence of pulmonary lymphatics in the lung facilitates the adaptation to this constant shift of fluid, protein and cells.

Identification of specific lymphatic markers, such as Prox1 and Nrp2, receptors including LYVE1 and VEGFR3 involved in lymphatic development, as well as production of transgenic mice enabled a better understanding of pulmonary lymphatic development and the consequence of lymphatic dysfunction in a variety of lung diseases.

Various lung disorders associated with dysfunction in pulmonary lymphatics have been identified so far and much evidence from animal models supported the involvement of lymphatics in lung disease (Maltzman et al., 2015; Reed et al., 2019; Summers et al., 2022). While there is a clear role established for pulmonary lymphatic vessels in the severe lymphatic disease lymphangioleiomyomastosis (LAM), the involvement of lymphatic vessels in other lung pathologies remains to be fully established (McCarthy et al, 2021). Understanding the role of lymphatics in human is vital to identifying their specific contributions to the pathogenesis of lung disease and thereby the development of novel therapeutic approaches.

Studies have shown that lymphangiogenesis in the lung contributes to small-cell lung cancer (SCLC) and non-small-cell lung cancer (NSCLC) (Remark et al., 2015). Pre-existing peritumoral lymphatics undergo lymphangiogenesis in the presence of high levels of the growth factor VEGFC. Subsequently, metastases spread to the regional lymph nodes. Suppressing high expression of VEGFC by blocking VEGFR3 signalling has provided a new approach to control and prevent tumour growth and metastasis in animal studies, representing new opportunities for human cancer treatment. Although blockage of VEGFR3 has not provided long-term survival benefits for patients, efforts remain in progress to develop more efficacious agents (Persaud et al, 2004; Saif et al,2016). In contrast, impaired lymphangiogenesis has been shown to be involved in cases of chronic asthma. Asthma occurs when there is a chronic airflow obstruction and bronchial hyperreactivity. The pathogenesis of chronic airflow obstruction involves remodelling of the airway wall secondary to inflammatory cell infiltration, myocyte and myofibroblast hyperplasia, mucus metaplasia, subepithelial fibrosis and oedema formation. The lymphatic system in the lung has been identified to play an important role in attenuating airway wall remodelling in asthma. Studies have suggested that impaired lymphangiogenesis results in the accumulation of extravasated fluid which leads to bronchial lymphoedema and contributes to airway remodelling with persistent airflow obstruction in asthmatic lungs (Chemaly et al., 2008; Elias et al., 1999; Esther & Barker, 2004).

The role of lymphangiogenesis in human allograft rejection of organs, such as the kidney and heart, has also been documented. It is also believed that lymphangiogenesis in the lung is responsible for cases of obliterative bronchiolitis (OB) which eventually leads to failure in lung transplantation. However, there are no published reports on this hypothesis yet (Cui et al., 2015). Idiopathic pulmonary fibrosis (IPF) is another lung disorder, which is believed to be associated with angiogenic processes in lung tissues. In animal models, IPF occurs as a result of bleomycin use, as well as excess deposition of collagen IV and collagen I which are associated with lymphatic vascular development. Like OB there is no published evidence on this hypothesis.

Furthermore, pulmonary lymphangiectasia which is a rare respiratory disorder in newborns and infants resulting in death is associated with pulmonary lymphatics (Bellini et al., 2006). Primary pulmonary lymphangiectasia is suggested to be associated with congenital anomalies and secondary pulmonary lymphangiectasia is believed to be associated with both lymphatic and cardiovascular obstruction. Thoracic duct agenesis causing lymphatic obstruction, hypoplastic left heart syndrome, anomalous pulmonary venous return, pulmonary vein atresia, and congenital mitral stenosis are all associated with pulmonary lymphangiectasia (Esther & Barker, 2004).

Chylous pleural effusion is another lung disease with a clear connection to abnormalities in pulmonary lymphatic vascular function. Chylomicrons and very low-density lipoproteins produced by dietary fats (contained in chyle) are delivered to cisterna chyli and need to be returned to the vascular circulation. The thoracic duct, which is a major lymphatic vessel in the body plays a vital role in this transportation process. Entering and accumulation of chyle in the pleural space results in the formation of chylothorax. Chylothorax can occur for various reasons such as lymphoma, trauma/surgery, or as a consequence of other disorders like tuberculosis, sarcoidosis, or Kaposi's Sarcoma. Idiopathic chylothorax such as congenital chylothorax, however, is the most common cause of pleural effusion that occurs frequently in babies (Attar & Donn, 2017; Bellini, et al., 2006; Chemaly et al., 2008).

1.4.6   Intestinal lymphatics

The intestinal lymphatic vasculature is essential in absorbing nutrients and conducting immunosurveillance of intestinal microbiota. The intestine is one of the largest immunological organs in the body (Latmani & Petrova, 2017). The lymphatic vasculature also regulates the removal of cholesterol from peripheral tissues. Specialised lymphatic capillaries, known as lacteals, in the intestine are located solely in the intestinal villi and collect lymphatic vessels in the mesentery. Lacteals are covered by a highly organized cage-like structure of arterial and venous blood capillaries and a tree-like set of smooth muscle fibres, which are essential for the drainage of dietary lipids. Lacteal contraction regulated by the autonomic nervous system is also an important factor in the drainage of dietary lipids and other lipophilic molecules in this setting.

Lymphatic capillaries lack mural cells (SMCs and pericytes) but are connected to the extracellular matrix via anchoring filaments (Cifarelli & Eichmann, 2019). Intestinal capillary LECs express common markers such as PROX1, CCL21, LYVE1, NRP2 and the growth factor receptor VEGFR3 (Latmani & Petrova, 2017). Collecting vessels are equipped with smooth muscle cells, which provide intrinsic pumping activity required for drainage of the lipid-rich lymph through gut lymphatics and numerous intraluminal lymphatic valves which prevent lymph backflow. Collecting lymphatic vessels display continuous zipper-like junctions at the cell borders, which provides less permeability to prevent lymph leakage during transport from capillaries to lymph nodes. Lacteals display a mix of discontinuous and continuous junctions, the essential features for both sprouting and quiescent lymphatic capillaries (Cifarelli & Eichmann, 2019).

Lymphangiogenesis in the intestine is regulated by the interaction of extracellular matrix proteins in intestinal villi with LEC membrane proteins, specifically integrins (Integrin β1 was shown to be essential for LECs proliferative response to fluid accumulation and cell stretching, and integrin α9 was shown to be important in providing fibronectin matrix support to LECs during lymphatic valve morphogenesis). Tenascin C, periostin and Milk fat globule-EGF factor 8 protein are additional active-matrix components, which have been found to be important in tissue stretching, tissue remodelling and influencing intestinal lipid absorption respectively (Conway et al., 2014; Järvinen et al., 2000; Soltani et al., 2016).

Adult lacteals in the intestine go through continuous remodelling and regeneration, unlike other lymphatic beds that are more quiescent. Dysfunction in gut and mesenteric lymphatics can lead to impaired dietary lipid absorption. Genetic deletion of specific lymphatic markers such as Prox1, VEGFC and DLL4 (Notch ligand) are associated with defective lymphangiogenesis in intestinal lymphatics. Deletion of the *Dll4* gene in transgenic mice highlighted the vital role of this gene in LECs' survival and migration. Loss of DLL4 in lymphatics promoted the transition from mixed adherens junctions to mostly continuous junctions in lacteals, negatively affecting Chylomicrons uptake and transport (Latmani et al., 2015). In addition, CD36, which is a heavily glycosylated transmembrane protein, was identified recently as a facilitator in fatty acid transportation, intestinal lipid absorption and transportation into the lymph. A study of a mouse model revealed that endothelial CD36 plays an important role in vascular homeostasis.

Defective lymphatic vessels in the mesentery were also identified in mouse models lacking either *Nrp2* or *Ang2* genes (Gale et al., 2002; Yuan et al., 2002).

The association of gut lymphatics with cases of metabolic syndrome is not fully understood yet and investigation into understanding the molecular mechanisms involved in this process is insufficient. A better understanding of both metabolic and molecular pathways, as well as a detailed characterisation of intestinal LV maintenance and function is necessary in order to develop new therapies for the treatment of gut-related disorders like inflammatory disease, obesity development and colon cancers (Alexander et al., 2010; Latmani & Petrova, 2017).

1.4.7   Hepatic lymphatics

The liver is the largest and most important lymphatic fluid production organ in the body and the source of up to 50% of lymph entering the thoracic duct (Chung & Iwakiri, 2013; Tanaka & Iwakiri, 2016). The lymphatic system in the liver has a different structure compared to other tissues. The liver has sinusoids, which consist of one layer of liver sinusoidal cells (LSECs), which lack basement membranes. The high permeability of these LSECs is found to be the reason for the higher protein content of hepatic lymph (Courtice et al., 1962; Witte et al., 1969). Lymphatic fluids in the liver are composed of plasma membrane components, which filter through the junctions in LSECs into the space of Disse, then flow to the space of Mall and move through into the lymphatic capillaries (Ohtani & Ohtani, 2008). The movement of hepatic fluid is supported by collagen fibres and proteoglycan in sinusoids, which provides essential morphological support for fluid transportation. The backflow of lymph is prevented by the existence of lymphatic valves downstream of collecting vessels. The lymphatic fluid then drains into the lymphatic vessels surrounded by lymphatic muscle cells, which are required to pump the lymph from the liver to lymph nodes (LNs) and subsequently into the cisterna chyli (Barbier et al., 2012; Chakraborty et al., 2015; Harrell et al., 2008; Trutmann & Sasse, 1994; Zheng et al., 2014).

Like other organs, *Prox1* expression initiates the development of lymphatic vessels in the liver by differentiating LECs from the blood vasculature. However, Prox1 is also

expressed in the liver hepatocytes (Dudas et al., 2004; Wigle & Oliver, 1999). Various other molecules expressed by LECs are also expressed in other cells in the liver such as LYVE1 which is also expressed by macrophages and LSECs and VEGFR3, which is expressed by cholangiocytes and LSECs. Liver resident cells also express lymphatic markers such as CCL21, integrin α9 and Mitochondrial MYO2 receptor-related protein 1. The only lymphatic marker that can be used specifically to detect LVs in the human liver is found to be PDPN, which is still challenging to visualise in mouse liver. Therefore, distinguishing the lymphatic vasculature in the liver especially in mice has been difficult and requires a combination of lymphatic markers to confirm their identity (Finlon et al., 2019; Gaudio et al., 2006; Petrova et al., 2002).

Hepatic lymphangiogenesis has been identified to be connected to various pathogenic conditions like liver fibrosis/cirrhosis, post-transplantation complications, chronic hepatitis, non-alcoholic steatohepatitis (NASH), portal hypertension and malignant tumours. During inflammation, lymphangiogenesis occurs in response to VEGFC expression by infiltrating macrophages (Kataru et al., 2009). However, the precise production of VEGF-C as the main element in the VEGF-C/VEGFR3 signalling pathway required for regulating lymphangiogenesis is not yet clear in the liver setting (Secker & Harvey, 2015; Tanaka & Iwakiri, 2016). It has been reported that during various liver diseases, lymphatic vessel density increases which is correlated with increases in VEGFC/D in the liver. Other findings demonstrated that the frequency of lymphatics during disease increases whereas the permeability of lymphatics decreases which subsequently prevents the proper removal of cells and inflammatory mediators from this organ. Further investigation into understanding the development, structure and mechanisms involved in the hepatic lymphatic network are required to identify any clear linkage to liver-associated diseases.

1.4.8 Renal lymphatics

Renal lymphatics are vital in removing excess fluid, macromolecules and solutes from the renal interstitium and have a critical role in maintaining body fluid homeostasis. Kidneys are the central organs for filtering the entire blood volume >35 times a day, with the renal interstitium responsible for >99% of the filtrate in the body. Activation of the

immune system and inflammatory processes are also the other two important roles of the kidneys (Seeger et al., 2012; Lopez et al., 2015).

Similar to other organs, the identification of LEC-specific markers played a major role in providing insight into lymphatic vasculature development in the kidney. Blind-ended lymphatic capillaries originate in the cortex of the kidney and run near renal tubules, pass along the glomerulus and follow the renal arteries to form interlobular, arcuate and interlobar lymphatics. In the cortex, interlobular lymphatics do not have valves and lymph can exit the kidney freely through two different routes: either towards the hilum or capsular lymphatic plexus penetrating the capsule. Arcuate, interlobar and hilar lymphatics, however, contain smooth muscle for pumping the lymph and valves which aid in facilitating the unidirectional flow of lymph (Seeger et al., 2012). Renal interstitial fluid enters the lymphatics via inter-junctional gaps between LECs. This entry is aided by tethering filaments and a lack of basement membrane components. These endothelial cells are also highly endocytic which facilitates the transcellular uptake of fluid and macromolecules. Interstitial fluid and proteins can move freely into terminal lymphatics down hydrostatic and oncotic pressure gradients and exit through the venous or lymphatic systems. Lymphatics in the kidneys drain to local lymph nodes and connect eventually to the thoracic duct.

Lymphangiogenesis in the kidney occurs in response to inflammation. Induction of lymphangiogenesis enables the transportation of antigens and immune cells which initiates immune responses in the kidney. Lymphangiogenesis can also play a role in the removal of debris and noxious stimuli to promote the resolution of inflammation. Studies have shown that lymphangiogenesis may not always have a beneficial contribution during kidney injury. Lymphangiogenesis during acute injury results in the drainage of pro-fibrotic inflammatory cytokines and immune cells, which are produced in response to injuries thereby resulting in cases of kidney fibrosis. The chronicity of injury and inflammatory responses may influence the beneficial versus detrimental effects of lymphangiogenesis in kidney fibrosis. Therefore, care is required when approaching lymphangiogenesis processes as a therapeutic target in kidney diseases. Association of renal lymphatics with various diseases such as Polycystic kidney diseases, peritoneal ultrafiltration failure, renal interstitial oedema and transplant rejection has been

demonstrated (Dudas et al., 2004; Goodwin & Kaufman, 1956; Stolarczyk & Carone, 1975).

1.5 Lymphatic anomalies

As described earlier, the lymphatic system is a highly specialised multipurpose system, specialised in the recognition, integration, rescue and transport of pathogenic material and macromolecules. As such, lymphatic vessels actively contribute to pathological and physiological processes. Defects in the lymphatic vasculature have been associated with metabolic disorders, cardiovascular diseases, lymphoedema and potentially, many more anomalies that have not been characterised yet (Brouillard et al., 2014). In order to have a better understanding of developmental lymphatic vascular anomalies and to provide precise diagnosis and treatments, incorporating a clear and global clinical classification is essential. This classification has been largely based on clinical presentation so far, however, the identification of various causative genes through molecular diagnosis has provided another way of categorizing lymphatic disorders.

The most well-characterised lymphatic disorder is lymphoedema which is classified into primary (genetic) and secondary (acquired) lymphoedema. Lymphoedema occurs when there is an impaired lymphatic function caused by lymphatic obstruction, malformation, misconnection, dysplasia or absence of functional lymphatic valves resulting in the accumulation of fluid between cells and tissues and ultimately leading to gross anatomical swelling. The underlying cause of Primary lymphedema (PLE) can be a mutation of genes involved in lymphatic development processes. Many of these lymphedema-associated mutations that result in lymphatic dysplasia can also lead to chylous ascites, chyluria, chylothorax, compromised lung function and protein losing enteropathy. PLE is a rare type which can be congenital or happen later in life, but it can go undiagnosed for a long time as well (Connell et al., 2008).

The diagnosis for PLE includes the presentation of unilateral or bilateral swelling in different parts of the body, including limbs, hands, abdomen, neck, head and arms. In some cases where the lymphatic vasculature in different organs is affected at the same time, multiple PLE phenotypes are also possible such as lung effusions, chylous ascites, intestinal lymphangiectasis and embryonic oedemas. Recently, a non-invasive technique

of imaging lymphatics through non-contrast magnetic resonance lymphangiography has provided a better insight to use for the classification of lymphatic system abnormalities resulting in primary lymphoedema (Brouillard et al., 2021; Mazzei et al., 2017). Genetic testing, especially in familial cases through whole genome sequencing has also recently become a method employed to provide a better clinical diagnosis in syndromic PLEs. Many identified variants in genes such as FOXC2, GATA2, CCBE1 and ADAMTS3 that are associated with lymphedema are involved in VEGFC, its receptor VEGFR3 or their downstream signalling pathways. Milroy's disease, lymphedema-distichiasis syndrome, cardiovascular failure, chylous ascites and chylothorax syndrome are some of the known disorders caused by loss of function of important lymphatic genes such as Prox1, LYVE1, SOX18. (Choi et al., 2012). A comprehensive list of genes associated with lymphatic abnormalities is presented in Appendix, Table.1.

Secondary lymphedemas are the more common type and occur as a result of impaired lymphatic function due to infection, surgery, radiotherapy, or lymphatic filariasis. Secondary lymphedema is accountable for most cases of clinical lymphedema. In developed countries more than 20% of breast cancer patients who had surgical operations present with upper extremity lymphedema (Cormier et al., 2010; Oremus et al., 2012).

cular Lymphatics Associated Anomalies
- Bilateral Subepicanthal folds
- Ectropion Uveae
- Ptosis
- Lymphedema-hypoparathyroidism
- Face edema
- Conjunctival edema
- Distichiasis
- Punched-out lesion
- Chorioretinopathy
- Hyperterlorism

Dural Lymphatics Associated Anomalies
- Lymphostatic Encephalopathy
- Microcephaly/Marcocephaly
- Intellectual disability
- Dysmorphism
- Stroke
- Parkinson disease (PD)
- Alzheimer
- Multiple Sclerosis (MS)
- Hydrocephalus

Cardiac Lymphatics Associated Anomalies
- Atherosclerosis
- Myocardial infraction
- Endocarditis
- Myocarditis
- Cyanosis
- Venous Valvular insufficiency
- Congenital heart disease
- Chylopericardium

Pulmonary Lymphatics Associated Anoma-lies
- Small cell lung cancer
- Non-small cell lung cancer
- Chronic asthma
- Myofibroblast hyperplasia
- Mucus metaplasia
- Subepithelial fibrosis
- Myocyte
- Obliterative bronchiolitis (OB)
- Idiopathic Pulmonary Fibrosis (IPF)
- Pulmonary lymphangiectasia
- Chylous pleural effusion
- Chylothorax
- Tuberculosis
- Kaposi's sarcoma
- Hydrops fetalis
- Respiratory failure
- Non-chylous effusion

Renal Lymphatics Associated Anomalies
- Polycystic kidney disease (PKDs)
- Peritoneal ultrafiltration failure (UFF)
- Renal intestinal edema
- Hydronephrosis
- Diuresis
- Ureteric obstruction
- Hyperglycaemia
- Kidney fibrosis
- Hypertension
- Transplant rejection

Intestinal Lymphatics Associated Anomalies
- Obesity
- Intestinal lymphatic hypoplasia
- Primary intestinal lymphangiectasia (PIL)
- Intestinal lymphatic hypoplasia (ILH)
- Nonne-Milroy-Meige syndrome (NMD)
- Lymphedema distichiasis (LD)
- Hennekam's syndrome
- Asgenae's syndrome
- Noonan syndrome (NS)
- Yellow-Nail syndrome
- Crohn's disease (CD)
- Ulcerative colitis (UC)
- Mesenteric venous thrombosic (MUT)
- Inflammatory bowel disease
- Pancreatitis
- Whipple's disease (WD)
- Cirrhosis
- Chylous ascites
- Sjogren's disease (SD)
- GI cancer
- Malnutrition
- Protein-losing enteropathy

Hepatic Lymphatics Associated Anomalies
- Chronic hepatitis
- Non-alcoholic steatohepatitis (NASH)
- Portal hypertension
- Fibrosis/Cirhosis

Dermal Lymphatics Associated Anomalies
- Lymphadenitis papillomatosis
- Psoriasis
- Keratosis
- Lymphedema
- Dermatitis
- Hyperpigmentation
- Lymphangitis
- Café-au-lait lesion
- Hypertrichosis or Hypotrichosis
- Vascular lesions
- Webbed neck

Figure 10. Lymphatic associated diseases and their impact on different organs.

1.6 Project rationale

Very little is known about the genetic and developmental basis of hydrops fetalis. Many questions regarding the aetiology and pathogenesis of hydrops remain unanswered. A careful and systematic evaluation of infants and foetuses is required to broaden our understanding of the mechanisms that underlie NIHF. Eventually, knowledge about aetiology and pathogenesis will allow us to intervene in a more tailored and successful manner in order to obtain a better prognosis. To date, syndromes including Turner syndrome, Noonan's syndrome, Nonne-Milroy disease, Acrocephalopolydactylous dysplasia (also known as Elejalde syndrome), lymphoedema distichiasis syndrome and congenital myotonic dystrophy have been associated with NIHF. A number of monogenic mutations have been associated with NIHF in humans including *FOXC2, PTPN11, SOX18* and *ITGA9* (Sparks et al., 2019), all of which are important for lymphatic vascular development. Recently, through genetic screening, we have identified autosomal recessive mutations in a novel gene, *MDFIC*, underlying hydrops fetalis.

1.7 Hypothesis and aims of the project

1.7.1   Hypothesis:

We hypothesise that MDFIC is important for the normal development and function of the lymphatic vasculature during development and that mutations in MDFIC disrupt lymphatic vascular development and/or function. The goal of this study was to understand how MDFIC functions to control cardiovascular development and dissect the mechanisms by which mutations in *MDFIC* lead to foetal hydrops.

Characterisation of a *Mdfic* knockout mouse model and identification of MDFIC interacting proteins and downstream regulated genes will reveal the mechanism by which *MDFIC* variants contribute to NIHF and unveil possible avenues for treatment.

Understanding the mechanisms by which *MDFIC* gene variants cause NIHF will shed light on the aetiology of this disease. This work will contribute knowledge important to understanding the cellular and molecular mechanisms important for lymphatic vascular

development and improve our ability to provide new diagnostic and prognostic information to guide genetic testing for families who experience miscarriage and stillbirth. Ultimately, we aim to identify opportunities for the development of novel therapeutics for these devastating lymphatic vascular disorders.

1.7.2   Aims:

Aim 1: To investigate the nature of lymphatic vascular defects in a mouse model caused by *Mdfic* mutations.

Aim 2: To determine the molecular mechanisms by which MDFIC controls lymphatic vascular development by identifying and characterising the role of MDFIC a) interacting proteins and b) regulated genes.

Aim 3: To investigate whether RAS/MAPK pathway activity and function are impacted by *MDFIC* variants.

Chapter 2: Methods and Materials

2.1 Materials

2.1.1 DS-33 antibody generation

Monoclonal antibody specific to mouse MDFIC was generated at the Monash Antibody Technologies Facility (MATF, Monash University, Melbourne, Australia, https://www.monash.edu/researchinfrastructure/matf). Following immunisation of mice with a combination of peptide antigen (KNGGHTRMSNGNGIPC), immune adjuvant (Sigma-Aldrich, Cat. #S6322) and methylated CpG, hybridomas were generated and analysed for their ability to recognise mouse MDFIC in immunoblotting analyses.

2.1.2   All other materials used are listed in appendix (Supplementary Table.2).

2.2 Methods

2.2.1   Sequencing

DNA was isolated from whole blood. Family LE-452 (Adelaide family) was subjected to whole genome sequencing (WGS), performed at the Kinghorn Centre for Clinical Genomics Sequencing Laboratory (Sydney, NSW, Australia). DNA was prepared using Illumina HiSeq X reagents and libraries sequenced (150bp paired-end) on an Illumina HiSeq X Ten. The index cases of families LE-230, LE-410 and LE-590 were subjected to whole-exome sequencing (WES) at Macrogen, using SureSelect v7 as a capture kit and (150 bp paired-end protocol) on Illumina NovaSeq. Family G764 was subjected to Trio-based WES at the Genome Analysis Centre (GAC) of the Helmholtz Zentrum München (Germany). DNA was prepared using the SureSelect human all exon v6 capture kit and libraries were sequenced on an Illumina platform with mean coverages of 103x to 116x (100 bp paired-end protocol). (Byrne et al., 2022).

2.2.2 Mapping/annotation and variant filtering

An Adelaide in house pipeline based on Picard was used to process genome sequencing data. Sequencing reads were aligned to the Human Genome Build 37 (hg19) using BWA. SNVs and small insertions/ deletions (termed indels) were called using GATK HaplotypeCaller V.3.4. Default filters were applied to variant calls using the GATK Variant Quality Score Recalibration approach. Variants were filtered for rare (gnomAD and in-house frequencies 0.5 in Polyphen2 (hdiv or hvar)). Validation of the selected changes and cosegregation analyses were performed using Sanger sequencing, with primers designed in introns to amplify the exons containing the changes. All possible homozygous variants were analysed in depth for the consanguineous families (LE-230, LE-410 and LE-590). For family G764, BWA and SAMtools were used for sequence alignment (reference genome hg19) and variant calling, respectively. Variants were filtered for rare (gnomAD minor allele frequency <1%) missense, nonsense, frameshift, indel or consensus splice-site changes in homozygous or compound-heterozygous state in the index case. Candidate variants were confirmed by Sanger sequencing.

2.2.3 CHOP-1 sequencing, mapping and variant filtering methodology

CHOP-1 sequencing, mapping and variant filtering methodology Trio exome was performed by the Children's Hospital of Philadelphia Division of Genomic Diagnostics. Genomic DNA was extracted from peripheral blood or other patient tissues following standard DNA extraction protocols. After extraction of genomic DNA, targeted regions were captured with the Agilent SureSelect XT Clinical Research Exome V2 kit (per manufacturer's protocol) and sequenced on the Illumina NovaSeq 6000 platform with 100 bp paired end reads. Mapping and analysis were based on the human genome build UCSC hg19 reference sequence. Sequencing data was processed using an in-house custom-built bioinformatics pipeline. Coding exons and splice sites targeted with the exome kit were analysed and reported. The following variant types were detectable: single nucleotide variants, small deletions, and small insertions.

2.2.4   Animal Husbandry

Experiments using mice were approved by and conducted in accordance with guidelines of the University of Adelaide, South Australian (SA) Pathology/Central Adelaide Local Health Network (CALHN) Animal Ethics Committee, the University of South Australia Animal Ethics Committee and the Australian code for the care and use of animals for scientific purposes (AEC Project Approval 44/17). Adult female mice subjected to timed pregnancies were scored by the presence of vaginal plugs, with 9:00am on the day of plug detection designated as 0.5 days post coitum.

2.2.5   Generation of MDFIC M131fs* mice

Aiming to mimic the common genetic mutation in humans c.391dup; p.(Met131Asnfs*3), guides were designed to generate a frameshift variant around the nucleotide c.394A in mouse (NM_175088) using an online CRISPR tool (http://benchling.com). The gRNA sequence used was as follows: 5'-GTTTCTCAGAAGATGCACAG-3'. C57BL/6J embryos were injected cytoplasmically with CRISPR reagents at the SA Genome Editing (SAGE) facility (Adelaide, Australia), transferred into pseudo-pregnant recipients on the same day and allowed to develop to term. Founder pups were screened for indels by PCR amplification across the targeted region to generate a 374 bp wild type amplicon (forward 5'-GAACGTCTGCCTCAACTCCA-3', reverse 5'-TGGAGAAAGTTAAGTGGTGTTTTCT-3') and PCR products from indel-carrying founders were Sanger sequenced to identify specific mutations. Two founders with 2 bp and 8 bp deletions leading to frameshifts and premature stop codons, were selected and backcrossed to wild-type mice to segregate individual mutant alleles in F1 progeny. These lines were further backcrossed for at least three generations to eliminate potential off-target artefacts. For routine colony maintenance, CRISPR mutant mice were screened by PCR and confirmed by Sanger sequencing of PCR products.

2.2.6   Plasmids and mutagenesis

The open reading frame of mouse Mdfic was cloned into pBluescript SKII for RNA probe synthesis and into pCMV-Entry (Origene) for protein expression studies. Human MDFIC was purchased from Origene (Cat# SC313109). MDFIC mouse and human frameshift mutants were made using QuikChange II XL site directed mutagenesis kit (Agilent Cat# 200522). Mouse point mutant c.735T>G (equivalent to human c.732T>G) was generated by PCR and cloned into pCMV-Entry using forward primer 5'-GAGGCGATCGCCATGTCCTGCGCGGGTGAAGCC-3' and reverse primer 5'-GCGACGCGTTTATGAAGGCAAACAGATGCCACAGC-3'.

2.2.7   Genotyping

DNA was extracted from mouse tail biopsies collected by University of South Australia animal facility. To isolate DNA, samples were incubated with 2.5ul of proteinase K mixed with genotyping buffer (20mM Tris pH8.0, 5mM EDTA, 400mM NACL, 1%SDS, H_2O) at 55℃, 800rpm overnight. 100% ethanol was subsequently added to the mix and spun for 15 mins at 13000rpm. The collected pellet was then spun with 75% ethanol for 3 minutes and resuspended in TE buffer (2mM Tris pH8.0, 0.2mM EDTA, H_2O).

PCR was carried out using PROMEGA GoTaq green master mix with the following conditions: 95°C 3 mins (1 cycle); 95°C 15 s, 53°C 20s, 72°C 60 s (30 cycles), 72°C 60s (1 cycle). Primers used for the analysis were as follows:
Forward primer (Sigma): 5'-GAACGTCTGCCTCAACTCCA-3'
Reverse Primer (Sigma): 5'-TGGAGAAAGTTAAGTGGTGTTTTCT-3'
DNA was run on a 4% (w/v) agarose at 100 V alongside the 1 Kb+ DNA Ladder. Gels were post stained with ethidium bromide for 10 minutes and visualised under UV on the Syngene Bioimaging apparatus (In Vitro Technologies, Victoria, Australia) using the GeneSnap image acquisition software version 7.05.

2.2.8   RNA in situ hybridisation

RNA in situ hybridisation was performed using digoxigenin-labelled riboprobes against full length *Mdfic*. Probes were hybridized to 20μm sections of cryopreserved wild-type E16.5 and E18.5 embryos. Probe specificity was confirmed using a corresponding sense probe. Immunostaining for PROX1 was performed following in situ hybridisation. Whole embryo brightfield scans were captured using 3DHistech Panoramic 250 Flash II. PROX1 co-staining was acquired using a Carl Zeiss LSM 800 Axio Observer 7 confocal microscope with Airyscan, equipped with 405nm, 488nm, 561nm and 640nm lasers. Images were compiled using ZEN 2.5 (blue edition; Zeiss) and Adobe Photoshop CC (version 21.1.1) software. (Protocol adapted from (Betterman et al., 2020).

2.2.9   Immunohistochemical staining

For cryopreserved sections embryos were fixed in 4% paraformaldehyde (PFA) overnight at 4°C. After fixing, embryos were transferred to 1x PBS containing 30% (w/v) sucrose at 4°C with gentle agitation to equilibrate. Embryos were embedded in a cryomold in O.C.T and transferred to -70°C freezer overnight. Embryos were sectioned coronally at 10　m on a cryostat and transferred to the slides which were stored at -20°C fridge prior to staining. Slides were allowed to air dry for 5 minutes, placed in Coplin staining jar(s) filled with TBS-T for 15 minutes with gentle agitation to remove excess O.C.T Compound from surrounding of tissue sections. Sections on slides were blocked in a humidified chamber for 1 hour followed by incubation overnight with primary antibody diluted in phosphate-buffered saline (PBS)-0.3% Triton X100 (TX100) (v/v) containing 1% (w/v) bovine serum albumin (BSA) (blocking solution).

Tissues were washed with Tris-buffered saline with Tween® 20 Detergent (TBS-T), 3 times for 10 minutes with gentle agitation. Secondary antibody diluted in block was added to the tissues after wash and incubated for 2-3 hours at room temperature (RT) in humidified dark chamber to prevent photobleaching. Tissues were washed 3 times with TBS-T for 10 minutes followed by a last wash with water for 5 minutes. Slides with tissues on it were air dried for approximately 15 minutes in the dark and mounted with DAPI Fluoromount G™ mounting medium and were covered with glass coverslip.

2.2.10 Histopathology

Embryos were removed from a pregnant female at embryonic day 18 and washed in Phosphate-buffered saline (PBS). A small amount of Bouins solution was injected into the thorax and abdomen of embryos to assist fixation. Embryos were incubated in Bouins solution for 48 hours at RT. This was followed by extensive washing in 70% ethanol at RT. Embryos were then placed in 4% PFA in PBS and delivered to the Australian Phenomics Network for paraffin embedding, sectioning (5µm) and H&E staining.

2.2.11 Whole mount DAB immunohistochemistry

Thoracic cavities were fixed in 4% PFA overnight at 4°C, washed with PBS and bleached with 3% hydrogen peroxide at RT for 30 minutes. After several washes, samples were blocked with 0.5% BSA in PBS-T (PBS-0.1% TX-100) at RT with gentle agitation for two hours, followed by incubation with anti-LYVE1 antibody diluted in blocking solution overnight at 4°C. Samples were washed thoroughly with PBS-T and incubated overnight at 4°C with biotinylated secondary antibody diluted in blocking solution. Following extensive washing with PBS-T, samples were incubated overnight at 4 ℃ with ABC-Peroxidase complex (VECTASTAIN Elite, Vector Laboratories) and developed using ImmPACT™ DAB Substrate Kit (Vector Laboratories), according to the manufacturer's instructions. Staining was imaged using an Olympus dissecting microscope (SZX7) digital camera, with associated software. Image acquisition was performed at RT.

2.2.12 Quantitation of lymphatic vessel width and area

Lymphatic vessel width in the skin and diaphragm was analysed and quantified using high resolution confocal microscopy and Imagej. Skin from the cervical-thoracic region of E16.5 and E18.5 embryos was analysed, 4-5 images (1280µm x1280µm) per sample were used for quantitation, using a $4000µm^2$ grid. The mesenteric lymphatic vasculature was also quantified using the same method (Figure 11 and 12).

E16.5   E18.5
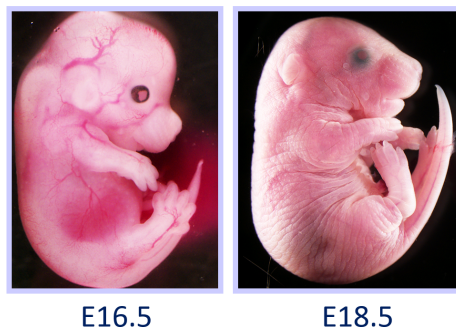
Figure 11. Mouse embryos at E16.5 and E18.5 used for lymphatic development analyses. Embryos at the embryonic stages of E16.5 and E18.5 were used to lymphatic vasculature analysis.

2.2.12.1 Dissection of Skin, diaphragm and mesentery

Mesentery   Diaphragm   Skin
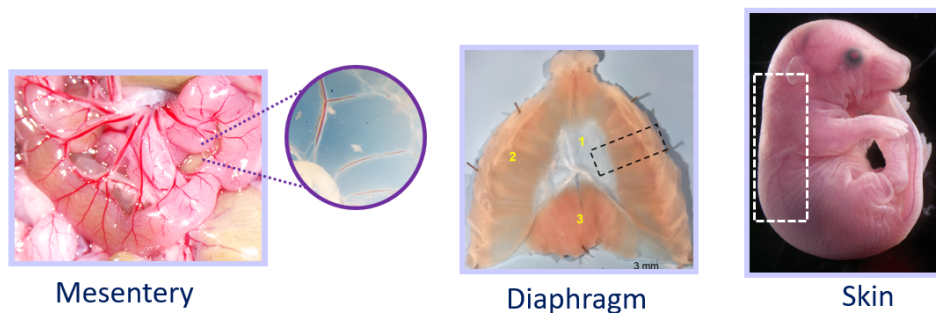
Figure 12. Tissues where lymphatic vessels were assessed in this study. Mesentery, diaphragm and skin of embryonic mice were dissected for lymphatic vessel analyses.

2.2.12.2 Wholemount staining of dissected tissues

For whole mount staining of skin and diaphragm from E16.5 and E18.5 wild-type and mutant embryos, tissues were dissected and fixed in 4% PFA overnight at 4°C. Mesenteries were dissected and pinned on 3% agarose then fixed in 4% PFA for 1 hour at RT. Subsequently samples were blocked in PBS- 0.3% TX100 containing 1% (w/v) bovine serum albumin (BSA) (PBS-0.3% TX100-1% BSA) overnight at 4°C with gentle agitation followed by incubation with primary antibody diluted in (PBS-0.3% TX100-1% BSA) block overnight at 4°C. After an extensive wash with PBS-0.3% TX100, tissues were incubated with Secondary antibody (Alexa Fluor® conjugated secondary

antibodies) diluted in (PBS-0.3% TX100-1% BSA) block overnight at 4°C with gentle agitation in the dark. After thorough washing with (PBS-0.3% TX100), samples were mounted and imaged using a Carl Zeiss LSM 800 Axio Observer 7 confocal microscope with Airyscan. Images were compiled using ZEN 2.5 (blue edition; Zeiss) and Adobe Photoshop CC (version 21.1.1) software. (Betterman and Harvey, 2018).

2.2.13 Blue dye injection for lymphatic transport analysis

To assess the integrity and function of lymphatic vessels in the thoracic cavity of postnatal mice, P10 WT and mutant mice were injected intraperitoneally with 50ul of 10 mg/ml Evans blue dye (Sigma-Aldrich). They were allowed to move freely in a warmed cage for 30 minutes before being humanely killed. Thoracic cavities were imaged using an Olympus DP20-5E digital camera (Olympus) attached to an Olympus SZX7 stereo microscope (Olympus) with images being processed using Adobe Photoshop CC (version 21.1.1) software.

2.2.14 HeLa cell transfection

HeLa cells were seeded on 8 well-ibidi plates at 2.5 x10^4 cells/well and cultured at 37 °C overnight. Cells were transfected using Lipofectamine 2000 (Thermo Fisher Scientific) according to the manufacturer's instructions. After 24 hours, cells were fixed for 10 minutes in 4% PFA, rinsed throughly with PBS and blocked with 0.5% BSA in PBS-T at RT for 30 minutes. Cells were incubated with anti-mouse MDFIC (DS33A-RC4) diluted in blocking solution for 2 hours, then washed with PBS-T and incubated with secondary antibody diluted in blocking solution for 2 hours. Cells were then extensively washed, mounted with DAPI and imaged using a Carl Zeiss LSM 800 Axio Observer 7 confocal microscope with Airyscan.

2.2.15   RNA isolation and analysis

Freshly dissected mouse tissues were snap frozen on dry ice and either processed immediately, or stored at -80°C. Tissue samples were homogenized using a rotor-stator and RNA extracted with TRIzol (Thermo Fisher Scientific), according to manufacturers recommendations.   Cultured cells were collected directly into TRIzol. cDNA was synthesized, including gDNA removal, using a QuantiTect Reverse Transcription Kit (Qiagen), quantitation performed using a QuantiTect SYBR Green PCR Kit (Qiagen) and analysed on a Qiagen Rotor-Gene Q. Data were normalised to the housekeeping gene Actb.

Endogenous levels of *MDFIC* mRNA were knocked down in cultured human lymphatic endothelial cells (hLECs) using Mission® esiRNA (endoribonuclease prepared small interfering RNA; Sigma Aldrich; MDFIC-human, Cat# EHU056121) and Lipofectamine 2000 (Thermo Fisher Scientific) following manufacturers recommendations.

2.2.16   Protein isolation

To assess endogenous MDFIC protein levels in primary human LECs and ectopically expressed MDFIC protein levels in HEK293 and HeLa cells, cells were directly harvested in ice-cold T-PER® Tissue Protein Extraction Reagent (Thermo Fisher Scientific), supplemented with Halt™ Protease and Phosphatase Inhibitor Cocktail (Thermo Fisher Scientific). After addition of 4x Laemmli sample buffer (277.8mM Tris pH 6.8, 355mM 2-mercaptoethanol, 44.4% (v/v) glycerol, 4.4% (w/v) SDS, Bromophenol blue) to give a final concentration of 1X, cell lysates were sonicated in a Diagenode Bioruptor® sonicator and heated at 98°C for 8 minutes. Following centrifugation at 12,000g for 1 minute at 20°C, protein lysates were stored at -80°C.

To determine the sub-cellular localisation of endogenous MDFIC in primary human LECs, cells were washed with PBS, trypsinised and pelleted by centrfugation at 200g for 5 min at 4°C. Cell pellets were resuspended in cell lysis buffer (10mM Tris-HCl pH 7.5, 10mM KCl, 0.1mM EDTA, 1mM Dithiothreitol, 0.5% IGEPAL® CA-630, Halt™ Protease and Phosphatase Inhibitor Cocktail (Thermo Fisher Scientific)) and allowed to swell on ice for 15 min with intermittent mixing. Samples were vortexed to disrupt cell membranes, then

centrifuged at 12,000g for 10 min at 4°C. The supernatant (cytoplasmic fraction) was stored on ice while pelleted nuclei were washed with cell lysis buffer, then pelleted at 12,000g for 5 min at 4°C. Washed nuclei were resuspended in lysis buffer, then both the resuspended nuclei and cytoplasmic fraction were processed as outlined above.

To investigate endogenous MDFIC protein levels in mouse tissues, dissected lung tissue was snap frozen on dry ice, then stored at -80°C. To prepare protein lysates, lung tissue was finely chopped, then transferred to a pre-cooled Dounce homogeniser containing ice-cold lysis buffer consisting of T-PER® Tissue Protein Extraction Reagent (Thermo Fisher Scientific) supplemented with Halt™ Protease and Phosphatase Inhibitor Cocktail (Thermo Fisher Scientific). Lysis buffer was used at 4µl/mg of tissue. Homogenisation of tissue was performed with 10 strokes of pestle 'A' followed by 15 strokes of pestle 'B'. Tissue lysates were processed as outlined above except that following centrifugation, the supernatant was removed and retained for analysis.

To assess ectopically expressed MDFIC protein secretion, HEK293 cells were exchanged into high-glucose DMEM supplemented with 5% serum prior to being transfected. On the day following transfection, conditioned media was collected and concentrated using a Pall Nanosep® Centrifugal Device with Omega™ Membrane 3K. With the exception of sonication, the concentrated conditioned media was processed as outlined above.

To investigate whether MDFIC protein levels are regulated by proteosomal/lysosomal degradation, HeLa cells were transfected with mouse MDFIC WT (NP_780297) in pCMV6-Entry (OriGene), or empty vector, using Lipofectamine® 2000 (Thermo Fisher Scientific), according to manufacturer's instructions. On the day following transfection, cells were treated with growth media supplemented with 20µM MG132 and 40µM Chloroquine for 3h, before being processed as outlined above.

To assess the stability of ectopically expressed MDFIC protein, HeLa cells were transfected with mouse MDFIC WT, MDFIC F245L or MDFIC M131fs* in pCMV6-Entry (OriGene), together with FLAG-tagged FOXC2 (NP_038547), FLAG-tagged NFATC1 (NP_001157581), FLAG-tagged PROX1 (NP_032963), GATA2 (NP_001342182), all in

pCMV6-Entry (OriGene), or empty vector, using Lipofectamine® 2000 (Thermo Fisher Scientific), according to manufacturer's instructions. On the day following transfection, cells were directly harvested in ice-cold T-PER® Tissue Protein Extraction Reagent (Thermo Fisher Scientific) supplemented with Halt™ Protease and Phosphatase Inhibitor Cocktail (Thermo Fisher Scientific) and processed as outlined above.

2.2.17 Immunoprecipitation

To analyse protein interactions by co-immunoprecipitation, HEK293 cells were co-transfected with mouse MDFIC WT, MDFIC F245L or MDFIC M131fs* in pCMV6-Entry (OriGene), together with FLAG-tagged FOXC2, FLAG-tagged NFATC1, FLAG-tagged PROX1 and GATA2, all in pCMV6-Entry (OriGene), or empty vector, using Lipofectamine® 2000 (Thermo Fisher Scientific) according to manufacturer's instructions. Co-transfected cells were scraped into ice-cold PBS and collected by centrifugation at 500g for 5 min at 4°C. Cell pellets were resuspended in lysis buffer (20mM Tris-HCl pH 7.5, 150mM NaCl, 1% IGEPAL® CA-630, Halt™ Protease and Phosphatase Inhibitor Cocktail (Thermo Fisher Scientific)), then sonicated in a Diagenode Bioruptor® sonicator. Cell debris was cleared by centrifugation at 12,000g for 15 min at 4°C and the resulting supernatant was incubated with primary antibody overnight at 4°C with mixing by inversion. To immunoprecipitate FLAG-tagged proteins, cell lysates were incubated with rabbit anti-DYKDDDDK Tag antibody (2368; Cell Signalling Technology) or normal rabbit IgG (2729; Cell Signalling Technology). To immunoprecipitate GATA2 protein, cell lysates were incubated with α-GATA2 antibody (NBP1-82581; Novus Biologicals) or normal rabbit IgG (2729; Cell Signalling Technology). Antibody-antigen complexes were precipitated by incubating with Dynabeads® Protein G (Life Technologies) for 1.5 h at 4°C with mixing by inversion. Immunoprecipitated complexes were washed with lysis buffer, resuspended in 2 x Laemmli sample buffer, and heated at 95°C for 7 min. Following centrifugation at 12,000g for 1 min at 20°C, supernatants were stored at -70°C.

2.2.18 Immunoblotting

Protein samples were resolved by SDS-PAGE (Bio-Rad Mini-PROTEAN® TGX Stain-Free™ 4-20% Precast Protein Gels), transferred to PVDF (PerkinElmer) and incubated with primary antibodies. Immunoblots were visualised using ECF reagent (GE Healthcare) or Immun-Star AP substrate (Biorad), on a Typhoon FLA 9000 (GE Healthcare) and quantified using ImageQuant TL 1D (version 8.1; GE Healthcare).

2.2.19 Protein structure prediction and alignment

The amino acid sequence of mouse MDFIC was analysed for a predicted transmembrane domain using TMpred , DAS Transmembrane Prediction server , OCTOPUS and Split 4.0 Membrane Protein Secondary Structure Prediction Server. Amino acid sequence alignments were performed using the T-COFFEE multiple sequence alignment server.

2.2.20 RNA Sequencing

2.2.20.1 Human lymphatic endothelial cell transfection

Three batches of human lymphatic endothelial cells (hLECs) from different donors (Lonza, Bioscience, USA) (Isolated from different donors; lot numbers 7F3304, 0000254463, 4F3029 and 4F3037) were plated and transfected with control or *MDFIC* esiRNA in 6cm petri dish, harvested with TrypLE™ Express Enzyme (Thermo Fisher Scientific) 48 h post transfection, spun down for 5 minutes, and resuspended in EGM-2MV.

2.2.20.2 Analysis of cell number and viability

Cell number and cell viability was routinely assessed during routine passaging using a haemocytometer. Cells were washed with 1X PBS, trypsinisied and 10µl of cell suspension was mixed with 10µl of 0.4% (w/v) Trypan Blue Solution (Sigma). Viable cells

within the haemocytometer grid were counted using an Olympus CX41 microscope (Olympus, Olympus Corporation, Tokyo, Japan).

Cell number was determined as the number of cells counted, divided by the number of squares that the cells were counted in. This was multiplied by the dilution factor of the Trypan Blue (2 in this experiment) and by 10^4 to express the cell number as cells per ml.

Cell number (cells/ml) = (number of cells counted/number of squares counted) x 2 x 10^4

2.2.20.3 RNA isolation

All ribonucleic acid (RNA) procedures were performed using ART® aerosol resistant filter tips (Molecular BioProducts, Inc., San Diego, CA). RNA extraction was performed using Direct-zol™ RNA MiniPrep kit according to the manufacturer's instructions for isolation of total RNA. To lyse the cells, 1ml of TRIzol® Reagent (Invitrogen, Carlsbad, CA) was added to each sample. Cells were homogenised using a 25G needle and syringe and incubated at RT for 5 minutes. Equal volumes of ethanol 1ml (95-100% v/v) was added to each lysate and mixed vigorously for 15 seconds. The mixed samples then transferred to Zymo-spin column in a collection tube provided by the kit and centrifuged at high speed for 30 seconds at 4ºC. Supernatant was removed following centrifugation. Next, for DNase treatment, 400µl of wash buffer was first added to the column followed by centrifugation at high speed for another 30 seconds at 4ºC. 5µl DNase to 75µl of DNA Digestion buffer was added to the column, mixed gently by inversion, and incubated for 15 minutes at RT. 400µl of RNA Prewash was added to the column, centrifuged at high speed for 1 minutes at 4ºC and supernatant was discarded. This step was performed twice. Following the wash step, 700µl of RNA wash buffer was added to the column and centrifuged for 1 minutes at high speed at 4ºC. After this step, the column was transferred to a new RNase free 1.5 ml tube. To elute the RNA, 50µl of DNase free water was added to the centre of the column, incubated for 1 minute, followed by centrifugation for 1 minute at 4ºC. Purity and concentration of extracted RNAs were determined and rest of collected RNA samples were stored at -80ºC.

2.2.20.4 Determination of RNA concentration

RNA concentrations were determined by NanoDrop™ 1000 spectrophotometer and version 3.7 software (NanoDrop Technologies, Inc., Wilmington, DE). RNA samples were diluted 1:1 with diethylpyrocarbonate (DEPC)-treated MQ-H2O and absorbance of the sample at 260nm was detected. The acceptable ratio of sample absorbance at 260/280nm of approximately 2.0 and a ratio of sample absorbance at 260/230nm of approximately 1.9-2.2 indicates high purity RNA and was assigned for this experiment.

2.2.20.5 First-strand cDNA synthesis

In order to investigate the messenger RNA (mRNA), isolated total RNA was reverse transcribed to form complementary deoxyribonucleic acid (cDNA) using SuperScript™ III First-Strand Synthesis SuperMix (Invitrogen), in a total reaction volume of 20µl. RNA (0.1-1µg) was combined with a mix of 2.5µM oligo(dT)20 and 50ng random hexamer primers and incubated in an Eppendorf Mastercycler (Eppendorf, Hamburg, Germany) at 65ºC for 5 minutes. Mixes were then immediately chilled on ice for at least 1 minute. This RNA-primer mixture was subsequently combined with First-Strand Reaction Mix and SuperScript™ III/RNaseOUT™ Enzyme Mix and incubated at 25ºC for 10 minutes, followed by 50 minutes at 50ºC. Reactions were terminated via a 5-minute incubation at 85ºC, followed by cooling to 4ºC. cDNA was diluted as necessary using DEPC treated MQ-H2O and stored at -20ºC.

2.2.20.6 Real-time RT-PCR

Real-time reverse transcription-polymerase chain reaction (RT-PCR) was performed in triplicate on each individual gene analysed using RT2 Real-Time™ SYBR Green/Rox Master Mix (SABiosciences, Frederick, MD). Real-time RT-PCRs were performed in 0.1ml polymerase chain reaction (PCR) tubes in a 15µl total reaction volume containing 2µl of cDNA (generated as per section 2.2.20.5), 7.5pmol of both forward and reverse primers and 1x RT2 Real-Time™ SYBR Green/Rox Master Mix. Amplification was

performed using a Corbett Research RotorGene™ 6000 real-time rotary analyser (QIAGEN, QIAGEN GmbH, Hilden, Germany) according to the following parameters: 95ºC for 15 minutes, followed by cycling at 95ºC for 15 seconds, 60ºC for 25 seconds and 72ºC for 10 seconds, for a maximum of 40 cycles, followed by a final extension at 72ºC for 3 minutes and melt from 72-99ºC. Data were collected and analysed using RotorGene™ 6000 Series Software version 1.7 (QIAGEN) and melt curves examined to validate the generation of single product amplicons following every real-time RT-PCR amplification run. Data were normalised to *Actb*.

2.2.21 RNA sequencing analysis

Sequencing was performed in ACRF cancer genomics facility. RNA was depleted of rRNA using RNAseH. RNA sequencing libraries were prepared using a stranded protocol, and with the addition of 18 nucleotide (nt) UMIs. Sequencing was performed on an Illumina Nextseq, producing 82 - 137 million 145 nt paired-end reads per sample. RNA sequencing analysis was performed by Nick Warnock (Australian Cancer Research Foundation (ACRF) Cancer Genomics Facility, Bioinformatics group) using Bioconductor package edgeR program.

2.2.22 Statistical analysis

Data are expressed as means ± SEM or SD, and statistical evaluation was performed using two-tailed Student's t test, two-way analysis of variance (ANOVA) with a Sidak multiple comparison test, or one-way ANOVA, using GraphPad Prism (version 8.2.1). P values less than 0.05 were considered statistically significant.

2.2.23 ERK signalling pathway analysis

hLECs were transfected with control or *MDFIC* esiRNA, harvested with TrypLE™ Express Enzyme (Thermo Fisher Scientific) 48 h post transfection, spun down and resuspended in EGM-2MV. Immediately after that, 5 x 10^4 cells in 500 l media per well

were added to 24 wells plate. Cells were allowed to sit for 5 hours, after which media was removed and cells were serum starved overnight (0.1% Foetal Bovine Serum (FBS) EBM). Cells were stimulated with full media (EGM-2MV) for 60 minutes, 30 minutes, and 15 minutes. Cells were immediately resuspended in 50µl of 2x Laemmli sample buffer (277.8mM Tris pH 6.8, 355mM 2-mercaptoethanol, 44.4% (v/v) glycerol, 4.4% (w/v) SDS, Bromophenol blue). Cell lysates were sonicated in a Diagenode Bioruptor® sonicator and heated at 98°C for 8 minutes. Following centrifugation at 12,000g for 1 minute at 20°C, protein lysates were stored at -80°C.

2.2.24 MEK inhibitor (Trametinib) treatment of hLECs

hLECs were transfected with control or MDFIC esiRNA, harvested with TrypLE™ Express Enzyme (Thermo Fisher Scientific) 48 h post transfection, spun down and resuspended in EGM-2MV. Immediately after that, 5×10^4 cells in 500 l media per well were added to 24 wells plate. Cells were allowed to sit for 5 hours, after which media was removed and cells were serum starved overnight (0.1%FBS EBM). Cells were treated with Trametinib (0.5nM-300nM) diluted in DMSO with full media (EGM-2MV) for 15 minutes. Cells were immediately resuspended in 50µl of 2x Laemmli sample buffer (277.8mM Tris pH 6.8, 355mM 2-mercaptoethanol, 44.4% (v/v) glycerol, 4.4% (w/v) SDS, Bromophenol blue). Cell lysates were sonicated in a Diagenode Bioruptor® sonicator and heated at 98°C for 8 minutes. Following centrifugation at 12,000g for 1 minute at 20°C, protein lysates were stored at -80°C.

Table 5. Commercial antibodies used in this study.

Immunostaining				
Antibody	Species	Supplier	Cat	Dilution
CD29 (Integrin β1 chain)	rat	BD Biosciences	553715	1:100
CD31	rat	BD Biosciences	550247	1:500
LYVE1	rabbit	AngioBio	11-034	1:1000
Laminin α5	goat	Ringelmann et al, 1999	-	1:1000
MDFIC (mouse)	mouse	This study	DS33A-RC4	1:500
NRP2	rabbit	Cell Signaling	3366	1:250
NRP2	Goat	R&D Systems	AF567	1:500
PROX1	goat	R&D Systems	AF2727	1:500
PROX1	rabbit	Abcam	ab101851	1:1000
ERK	rabbit	Cell Signalling	4370	1:1000

Immunoblotting				
Antibody	Species	Supplier	Cat	Dilution
β-actin	mouse	Sigma-Aldrich	A5441	1:5000
FLAG	rabbit	Cell Signalling Technology	2368	1:1000
GATA2	rabbit	Novus Biologicals	NBP1-82581	1:500
MDFIC (human)	rabbit	Oakley et al, 2017	-	1:1000
MDFIC (mouse)	mouse	This study	DS33A-RC4	1:1000
NFATC1	mouse	Santa Cruz Biotechnology	sc-7294	1:500
PROX1	goat	R&D Systems	AF2727	1:1000
α-tubulin	rabbit	Abcam	15246	1:1000
Immunoprecipitation				
Antibody	Species	Supplier	Cat	Dilution

FLAG	rabbit	Cell Signalling Technology	2368	1:100
GATA2	rabbit	Novus Biologicals	NBP1-82581	1:150
Normal Rabbit IgG	rabbit	Cell Signalling Technology	2729	1:250

Chapter 3: Defining a novel role for MDFIC in lymphatic vascular development through genetic and clinical presentation of patient cases

3.1 Genomic autopsy and clinical testing

Clinical autopsies started over a century ago on patients dying of natural causes, to advance the medical knowledge and understanding of human diseases. Autopsy results can provide information for quality control of the accuracy of diagnosis and effectiveness of treatments (Charlton, 1994). However, the high costs of performing autopsies on all patients, as well as improved methods of diagnosis such as imaging, blood-based testing and minimally invasive testing over the past few decades have led to better diagnosis of abnormalities during life which subsequently lessened the need for autopsies on all patients. Autopsies can still be highly valuable if performed properly on patients with diseases that have been missed or misdiagnosed.

The diminishing role of autopsies in discovery and education raised the question of what other approaches can be used to restore the status of autopsy in the modern clinical world. Sequence analysis of the patient's genome as a routine part of the clinical autopsy has been the best answer to this question. Next-generation sequencing technology introduced a way to analyse the nucleotide sequencing of many regions of DNA simultaneously (parallel sequencing). Advancements in bioinformatics methods also improved the quick sequencing of large regions of genomic DNA. Genomic DNA can be extracted from any tissue, including dead tissues, as it remains intact for a long period of time. Current efforts aim to obtain information from the DNA sequence of each patient in order to diagnose and identify the certain mutation associated with their disease and subsequently tailor a personalised targeted therapy for individual patients based on the pathogenic variants found in their DNA.

Analysis of inherited variants in patients has become an active area of clinical medical research over the past few decades, which is also highly valuable to identify the rare/unknown pathogenic variants associated with a wide range of diseases. The main advantages of genomic screening are as below:

1. Identify the true aetiology of a disease
2. Identifying the inherited mutation in deceased or alive patients to enable the prediction of future disease or prevent/control the arises of the same conditions in other relatives.

3. Helps to discover new genetic disorders.
4. Identify potential therapeutic approaches

A routine genomic autopsy has also raised various potential concerns, such as the cost of sequencing, data processing and genetic counselling services, confidentiality, the potential misuse of genetic information, as well as storage and ownership of information after death. Therefore, the appropriate set-up and highly skilled management are required to have a functional genomic autopsy program. It is also important to have proper thresholds set for reporting the sequence variants, based on various factors such as level of evidence for pathogenicity, physical injury, psychological stress, environmental factors and antigenic stimuli.

As mentioned earlier, a high percentage of stillbirths and prenatal deaths are unexplained or are associated with congenital abnormalities. A broader approach of genetic screening (whole exome/genome sequencing) provides an opportunity to identify the molecular origin of such congenital abnormalities and unexplained perinatal death (Goldenberg et al., 2009) An accurate identification of the cause of death can subsequently help in counselling families in understanding the reason for miscarriage or stillbirth and can provide the opportunity to monitor future pregnancies in order to optimise the chances of having a healthy child (Flenady et al., 2009).

In that regard, genomic autopsy study, a national research program in Adelaide, South Australia, has undertaken genomic research to address this matter and to understand the genomic contribution of perinatal death and stillbirth (Figure. 13). The aim of this study is to provide answers to families affected by these conditions and give them an accurate diagnosis of the cause of stillbirth and perinatal death to enable safe and viable future pregnancies.
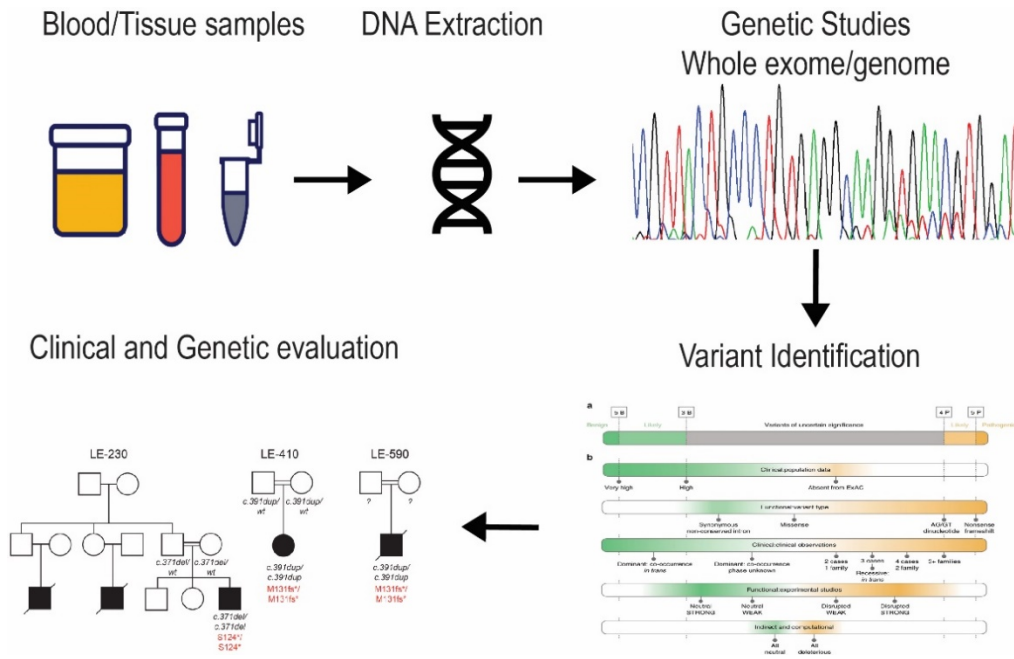
Figure 13. Genomic autopsy study framework adapted by national research program in Adelaide, South Australia. Genomic investigation of pregnancy loss and perinatal death begins with collecting samples from patients including parents and affected children. Following DNA extraction and whole genome or whole exome sequencing, the data will be analysed through variant calling where variant of interest is identified for further study and evaluation.

Genomic autopsy study in Adelaide currently focuses on families experiencing prenatal and perinatal death due to unexplained reasons or congenital abnormalities without genetic disorders identified through the standard of care testing.

Through genetic screening, novel homozygous and compound heterozygous, pathogenic variants in MDFIC in individuals with Central conducting lymphatic anomaly (CCLA) were identified (Figure.14). CCLA is a complex vascular condition, occurring when there is a dysfunction of major lymphatic vessels including the thoracic duct or cisterna chyli, leading to abnormal drainage, backflow and accumulation of lymphatic fluid. CCLA can manifest with overlapping clinical symptoms such as lymphoedema, chylous ascites, chylothorax, and pleural and pericardial effusions.
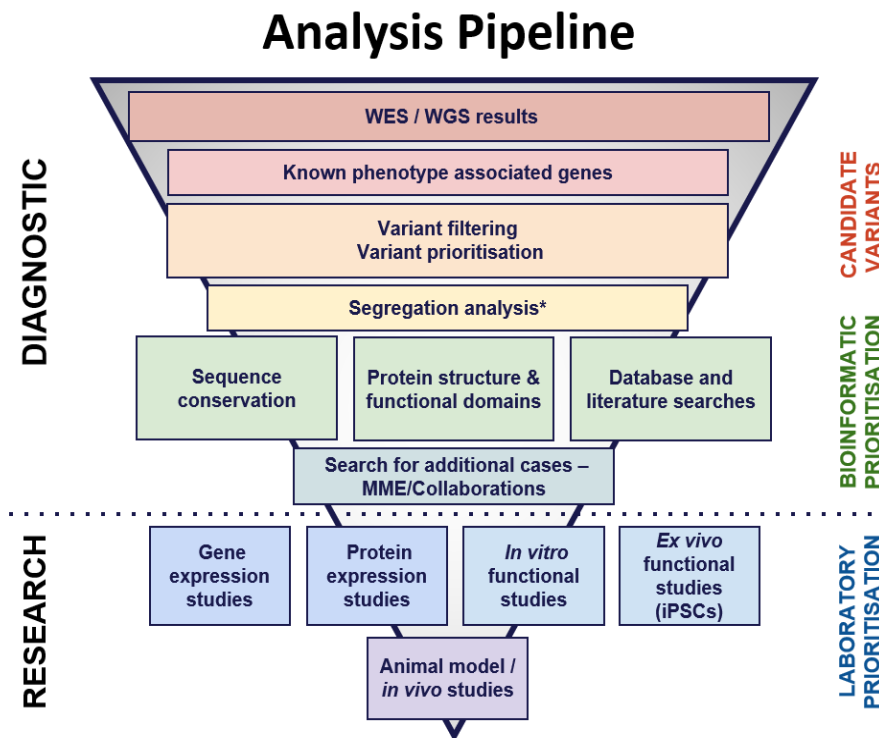
Analysis Pipeline

Figure 14. Analysis pipeline used by bioinformaticians to identify the pathogenic variants in patients exhibiting non-immune hydrops fetalis.

Compound heterozygous *MDFIC* variants were first discovered in a non-consanguineous family in Adelaide where two siblings exhibited severe hydrops fetalis. Our findings about this novel gene were shared with interstate and international collaborators. Through the exchange of information, we identified additional patients exhibiting similar phenotypes to the first proband in Adelaide including non-immune hydrops fetalis (NIHF) and stillbirth or NIHF followed by postnatal lymphoedema and recurrent pleural and pericardial effusions.

MDFIC encodes **M**yo**D** **f**amily **i**nhibitor domain-**c**ontaining protein, also known as HIC (Human I-mfs Domain containing protein) is a 246 amino acid protein about which little is known, but that has been documented to locate on chromosome 7 and regulates transcription factor activity (Figure. 15). MDFIC was discovered as a novel protein which binds Receptor Expressed in Lymphoid Tissues (RELT) family members. RELT is a

tumour necrosis factor receptor superfamily member (TNFRSF19L) that is expressed predominantly in the haematopoietic system (Cusick et al., 2020). The C-terminal region of MDFIC harbours a unique, cysteine-rich domain, demonstrated to mediate the interaction of MDFIC with transcription factors including the glucocorticoid receptor (GR), Heart- and neural crest derivatives-expressed protein 1 (HAND1) and TCF/LEF family members with key roles in the regulation of WNT signalling by targeting a group of basic helix-loop-helix (bHLH) proteins (Martindill et al., 2007; Oakley et al., 2017; Snider et al., 2001; Snider & Tapscott, 2005).

The exact process and mechanism in which MDFIC interacts with other transcription factors in this study or previous studies are not yet fully understood. What is known is in each case, the binding of MDFIC to transcriptional partners was demonstrated to tether transcription factors in the cytoplasm where MDFIC resides, thereby restricting their nuclear access and transcriptional activity.
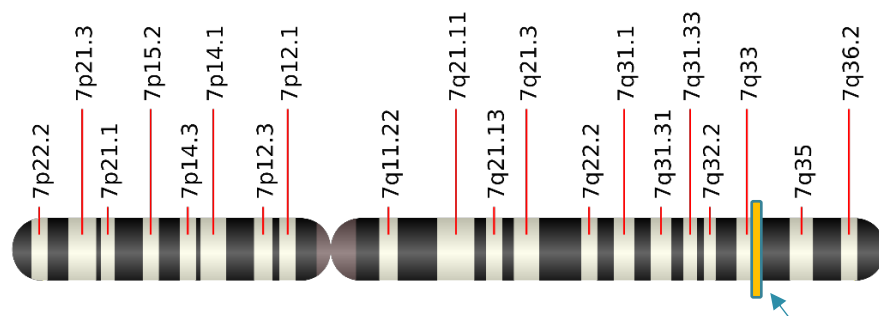
Figure 15. Location of MDFIC on chromosome 7. Location of HIC or MDFIC on chromosome 7 is highlighted in this picture.

To investigate the mechanisms by which *MDFIC* variants underlie hydrops fetalis and primary lymphoedema, we first investigated *Mdfic* expression and localisation throughout cardiovascular development in the mouse embryo. To study the role of the *Mdfic* gene, two mouse founders with a *Mdfic* frameshift variant p.(Met131Asnfs*3), found in five of seven participants in this study, were generated using CRISPR-Cas9 technology at the SA Genome Editing (SAGE) facility (Adelaide, Australia). Following the generation of the *Mdfic* mouse model, to investigate the consequences of truncation of either one or both copies of the *Mdfic* gene at embryonic stages in mice, timed matings were established between *Mdfic*$^{M131fs*/+}$ male and female mice. This resulted in a mixture of genotypes: *Mdfic*$^{+/+}$ (wild type), *Mdfic*$^{M131fs*/+}$ (heterozygous mutation) and *Mdfic*$^{M131fs*/}$

M131fs*(homozygous mutation). Postnatal mice were carefully monitored to assess the effect of *Mdfic* variants and lymphatic vessel growth, and maturation was subsequently investigated at a series of key embryonic and postnatal developmental stages, employing high-resolution immunostaining approaches.

3.2 Identification of *MDFIC* pathogenic variants in patients with foetal hydrops, postnatal lymphoedema, pleural and pericardial effusions.

Whole genome sequencing (WGS) or whole exome sequencing (WES) was performed on nineteen individuals including parents, affected children and unaffected children to investigate the genetics underlying stillbirth, NIHF and primary lymphoedema in both diagnostic and research settings.

3.2.1 Family LE452 (diagnosed and reported by Dr Eric Haan, Adelaide)

The proband was the first child of non-consanguineous Chinese parents (maternal age 33 years, paternal age 30 years). Hydrops fetalis was apparent on routine antenatal ultrasound screening at 19 weeks of gestation; the cause was not identified. He was delivered at 26 weeks of gestation by caesarean section because of deteriorating foetal dopplers. Birth weight was 1535 g (>97th percentile). He could not be resuscitated and died soon after birth. Autopsy documented severe hydrops fetalis with marked subcutaneous oedema, a pericardial effusion, bilateral pleural effusions, ascites, and severe pulmonary hypoplasia. Skeletal radiographs were normal, with femur length 47 mm (mean for 25 weeks of gestation). The placenta was markedly oedematous (406 g: 90th percentile for 26 weeks 280 g). The autopsy failed to find a cause for the hydrops.

Investigations, including studies for infection, maternal autoantibodies, inborn errors of metabolism, chromosome abnormalities, lysosomal storage disorders and mutations in the *VEGFR3* or *FOXC2* genes were all negative. The couple had two pregnancies subsequently: an early miscarriage and a blighted ovum.

First-trimester aneuploidy screening in the couple's fourth pregnancy demonstrated a trisomy 21 risk of 1:49 (nuchal translucency was 3.3 mm, a normal range for a foetus at 12 weeks is under 3.0mm). The normal risk of trisomy 21 for a woman at the age of 35 is

1:365. Amniocentesis at 16 weeks revealed a normal male karyotype (46, XY). Ultrasound scan at 16 weeks showed essentially normal foetal anatomy but the heart rate was consistently greater than 160 bpm. A further ultrasound scan at 18 weeks documented normal foetal heart rate and anatomy. However, ultrasound scans at 20 and 21 weeks showed bilateral pleural effusions (larger on the left with mediastinal shift to the right), abdominal ascites and subcutaneous oedema. A stent was inserted into the left chest at 23 weeks and the fluid obtained at the time was rich in lymphocytes (1.5×10^9 cells/L, lymphocytes 100%), consistent with a chylothorax. He was delivered at 38 weeks by emergency caesarean section after spontaneous labour. Apgar scores were 9 at 1 min and 9 at 5 min. Apgar score is the clinical indicator of a baby's condition right after birth, which is based on 5 characteristics pulse, reflex irritability, breathing, muscle tone and skin colour. Birth growth parameters were normal (weight 3,600 g, 75th percentile: length 49.7 cm, 50th percentile and head circumference 35.5 cm, 50-90th percentile). He required CPAP for a brief period. There were small chylothoraces at birth that resolved quickly, but no ascites or nuchal or subcutaneous oedema. He had undescended testes. Prolonged unconjugated neonatal jaundice was treated with phototherapy; no cause was identified.

At 5.5 months, growth and development were normal. He had a broad chest with pectus excavatum. Mild hepatomegaly, mild elevation of transaminases and mild lymphocytosis were attributed to intercurrent infection. *GATA2* gene sequencing was performed at 10 months of age and was normal. Bilateral orchidopexies were performed around 12 months of age.

At 4.5 years, growth (weight and height 75th percentile; head circumference 50th percentile) and development were normal. He had significant pectus excavatum with flattening of the lower part of the left hemithorax. Age-appropriate assessment of lung function and echocardiogram were normal. The couple had a fifth pregnancy; the pregnancy was normal, with no evidence of hydrops fetalis, and resulted in the birth of a healthy boy.

Genetic screening performed on family LE452, filtering for rare, protein-altering variants revealed compound heterozygous variants in *MDFIC* in both affected children; a paternally inherited Chr7(hg19):g.114619728C>CA; NM_001166345.1:c.391dup;

NP_001159817.1: p.(Met131Asnfs*3) and a maternally inherited g.114655980 T>G; c.732T>G; p.(Phe244Leu) (Figure. 16). The frameshift variant p.Met131Asnfs*3 led to a premature termination codon and is reported in gnomAD (v2.1) 50 times in heterozygosity (popmax allele frequency 0.026%) with no homozygous occurrences . Similarly, the p.(Phe244Leu) missense variant has only been observed in gnomAD in heterozygosity (25 times, popmax allele frequency 0.13%). This variant is also predicted to be deleterious by *in silico* prediction tools including CADD (24.9), Polyphen2 (Probably Damaging), SIFT (Damaging), and altogether by 8 out of 11 prediction tools in Varsome.

Figure 16. Pedigree of children diagnosed in Family LE452 with hydrops fetalis, pleural or pericardial effusions and lymphoedema. Pathogenic variants in the *MDFIC* gene sequence are indicated in black type and corresponding MDFIC protein changes in red. Affected individuals are shown in black. Sequencing method is designated (E, exome; G, genome). Second affected child was treated with shunt therapy in utero and showed normal growth and development following treatment.

Upon discovery of mutations in the *MDFIC* gene, information was exchanged with collaborators and four additional consanguineous and non-consanguineous families were identified displaying similar phenotypes consistent with CCLA and carrying homozygous truncating variants in *MDFIC* in their probands. Probands in Families LE410, LE590 and CHOP1 were homozygous for the p.Met131Asnfs*3 variant identified in Family LE452.

3.2.2   Family LE410 (reported by Dr Ariana Kariminejad, Iran 2000)

The proband in this family was the first child of distantly related apparently healthy Iranian parents. Pregnancy was uneventful. Delivery was by caesarean section at 9 months because of breech position. Birth weight, length and head circumference were 3600 g, 50 cm and 35 cm, respectively. She was hospitalised from birth in the Neonatal intensive care unit for 20 days because of meconium aspiration and respiratory problems. She had lymphoedema of both legs below the knees and oedema around the eyes from birth. Renal functional tests performed at that time were normal. She started wearing compression stockings at the age of three years with moderate control. She had a history of pleural effusions at 3 years and 5 years of age, managed by drainage and antibiotic treatment. Spiral thorax CT (axial without contrast) showed large left-sided pleural effusion and bilateral pleural thickening with compressive collapse of the left lower lobe. Peribronchiolar and parenchymal consolidation were noted in the rest of the left lung field and to a lesser degree in the right parahilar region. A colour Doppler of the pelvis and abdomen was performed at the age of 4 years showing normal venous flow of mesenteric veins and no gross lymphangiectasia in the small bowel walls. The aorta, mesenteric and renal branches, aorto-iliac bifurcations and aorto-iliac axis were all within normal limits. CT scan of the abdomen with oral and IV-contrast were normal with no fluid in the peritoneal cavity or enlarged lymph nodes. Liver, spleen, biliary tract, pancreas, diaphragmatic crura, adrenal glands, abdominal aorta and inferior vena cava were unremarkable. She had a fluid collection at the right knee at five years of age and was hospitalised with antibiotic treatment. At 6 years of age, she had bilateral lymphoedema below the ankles, which was painful when running or standing for prolonged periods. She

also had papillomatosis on her toes with hyperpigmentation on the dorsum of the feet and ankle area.

At 13 years of age, the patient had an injection of stem cells which was taken from bone marrow into the legs on the route of the lymphatic veins, without any significant change in lymphoedema.

Re-examination at the age of 20 years showed her weight and height were 80 kg and 168 cm, respectively. She has bilateral lymphoedema below the knees, papillomatosis on the toes, hyperkeratosis of the toes, and hyperpigmentation on the dorsum of the feet and ankle area. Periorbital oedema was not evident, but the patient claims that it is seen in the mornings. Echocardiography performed at 20 years of age showed mild mitral valve prolapse. A 24-hour holter electrocardiogram monitoring, which records the heart rate and rhythm for 24 hours showed 44 episodes of tachycardia (very fast heart rate over 100 beats a minute). The normal range of heart rate for an individual at a similar age is 60-100 heartbeats per minute. Otherwise, it was normal. Chest X-ray was unremarkable. Genetic analysis of this family revealed the parents of Family LE410 were heterozygous for p.Met131Asnfs*3 (Figure. 17).

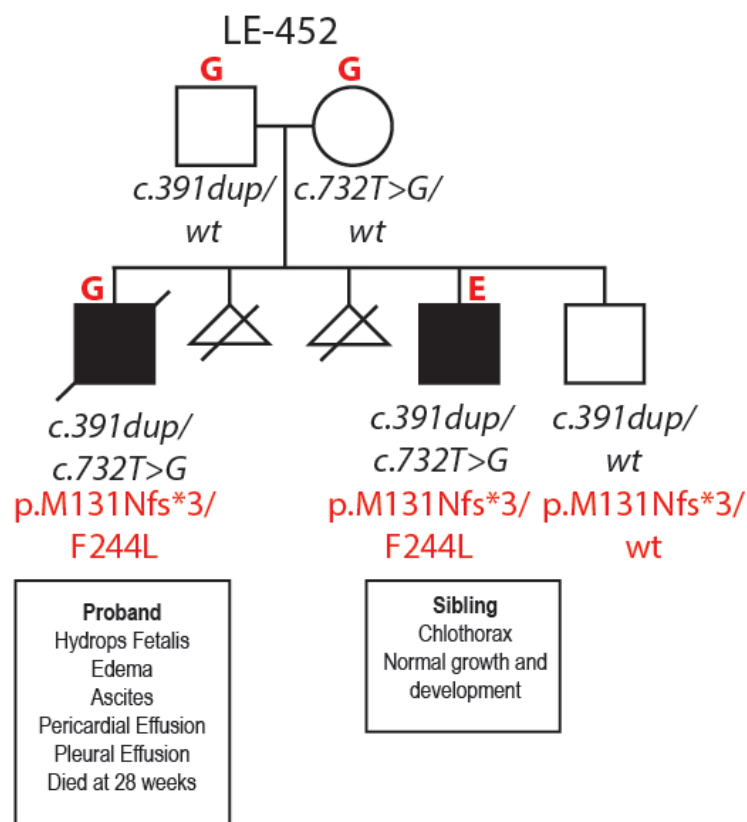**Figure 17. Pedigree of children diagnosed in Family LE410 with hydrops fetalis, pleural or pericardial effusions and lymphoedema.** Pathogenic variants in the *MDFIC* gene sequence are indicated in black type and corresponding MDFIC protein changes in red. Affected individuals are shown in black. Sequencing method is designated (E, exome; G, genome). Lymphoedema and papillomatosis in the proband are shown in the inset.

3.2.3 Family LE590 (reported by Dr Nicole Revencu and Dr Laurence Boon, Belgium 2009)

The proband in this family was a boy who died at the age 7 years. He was the first child of consanguineous parents. Hydrops fetalis with subcutaneous oedema and bilateral pleural effusion was diagnosed by ultrasound scan at 22 weeks of gestation. The analysis of the pleural liquid revealed a chylothorax (87% lymphocytes). Polyhydramnios was observed at 31 weeks of gestation. Infections, maternal antibodies and inborn errors of metabolism were all excluded. The standard karyotyping performed on the amniotic fluid was unaffected. The diagnosis of NIHF was considered (Figure. 18). He was delivered at 35 weeks and 3 days, with a weight of 3,180 kg (90th C) length of 49 cm (80th C), and occipital frontal circumference of 35 cm (97th C). APGAR score was 5/6/6. There are 0-2 points for each characteristic, with a total score of 1–10. At birth, he presented generalised subcutaneous oedema, bilateral important pleural effusion and moderate ascites. He needed respiratory support for ~2 months: high-frequency oscillatory ventilation for 7 days, conventional mechanical ventilation for 30 days and Continuous Positive Airway Pressure (CPAP) for another 30 days. Thoracic drains were placed for 11 days. Subsequently, he had several episodes of important pleural effusions, requiring drainage. He was hospitalised in a neonatal unit during the first 10 months of life.

Lymphoscintigraphy was compatible with the absence of the thoracic duct and possibly of all the truncal lymphatic system. The thorax was narrow and short, with thin ribs. Cardiac ultrasound was normal, apart from patent foramen ovale. He was put on furosemide for 2 months and developed nephrocalcinosis, possibly secondary to furosemide. Furosemide was stopped and the child was put on hydrochlorothiazide/triamterene. Spironolactone was added at the age of 10 months. At home, he needed oxygen therapy during the night (0.5L/min). The evolution was marked by the persistence of important bilateral inferior leg lymphoedema, which caused decreased mobility, recurrent pleural effusion, pericardial effusion with no haemodynamic consequences, and bilateral hydrocele.

His development was delayed especially the language. He could say some words only, at the age of 6 years. Comprehension was better than expression. He was able to walk

at 2 years. At the age of 1 year, he was operated on for a bilateral inguinal hernia. At the age of 20 months, he had cardiac and respiratory arrest during a physiotherapy session. He needed a brief cardio-respiratory resuscitation. He had recurrent unexplained fever episodes, which lasted 1 or 2 days. He also had frequent upper and lower tract infections. His growth was characterised by a height at -2.2 SD, weight at 0 SD and occipital frontal circumference at 0 SD.

Management included respiratory, motor and lymph drainage physiotherapy and speech therapy. The genetic investigation performed postnatally showed several homozygous regions larger than 10Mb on molecular karyotyping in relation to the parental consanguinity and normal *FLT4* and *FOXC2* sequencing. He died at the age of 7 years from multiorgan failure due to septic shock from *Streptococcus pyogenes* infection.
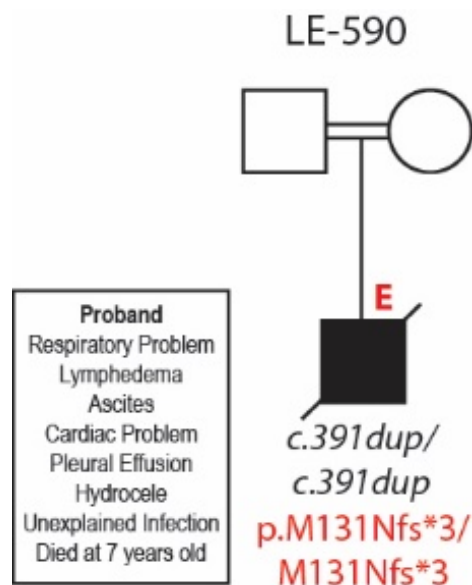
Figure 18. Pedigree of children diagnosed in Family LE590 with hydrops fetalis, pleural or pericardial effusions and lymphoedema. Pathogenic variants in the *MDFIC* gene sequence are indicated in black type and corresponding MDFIC protein changes in red. Affected individuals are shown in black. Sequencing method is designated (E, exome; G, genome).

3.2.4   Family LE230 (reported by Dr Denise Adams, USA 2009)

The proband in this family was a 12-month-old boy born in 2009, with a history of hydrops at birth, generalised lymphoedema and bilateral chylous effusions. His parents are first cousins of Arabic origin. There is a family history of two infants with the same illness, both of whom died of sepsis at 9 and 10 months. His generalised lymphoedema resolved and

bilateral effusions stabilised. He also had ptosis and hydrocele. In Family LE230, the proband was homozygous for a *MDFIC* p.Ser124* variant (Chr7(GRCh37): g.114619728TC>T; NM_001166345.1: c.371del), which results in a premature termination codon and is absent from gnomAD. Both parents were heterozygous for the variant (Figure. 19).
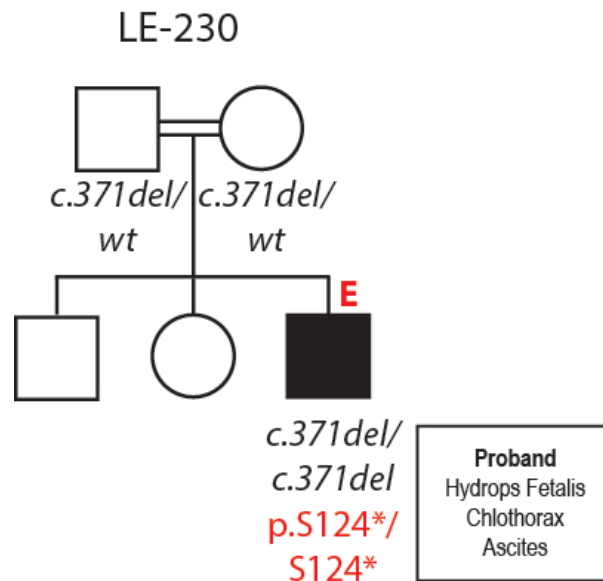
Figure 19. Pedigree of children diagnosed in Family LE230 family with hydrops fetalis, pleural or pericardial effusions and lymphoedema. Pathogenic variants in the *MDFIC* gene sequence are indicated in black type and corresponding MDFIC protein changes in red. Affected individuals are shown in black. Sequencing method is designated (E, exome; G, genome).

3.2.5 Family G764 (reported by Dr Matthias Rath, Dr G Christoph Korenke and Dr Ute Felbor, Germany)

The 11-year-old female proband was the first child of third- to fourth-degree consanguineous Kurdish parents. Bilateral pleural effusions were identified at 35 weeks gestation, requiring bilateral thoracocentesis after birth; pleural fluid analysis verified a chylothorax. The patient was discharged from hospital at the age of five weeks. At follow-up, she had recurrent asymptomatic uni- and bilateral pleural effusions, oedema of the eyelids, lymphoedema of the lower extremities and minimal ascites on sonography. There were no signs of autoimmune disease. In this family, the proband was homozygous for a

MDFIC p.Gly63* variant (Chr7(GRCh37):g.114582422G>T; NM_001166345.1:c187G>T), for which both parents were heterozygous. This variant results in a premature termination codon and is absent from gnomAD (Figure. 20).
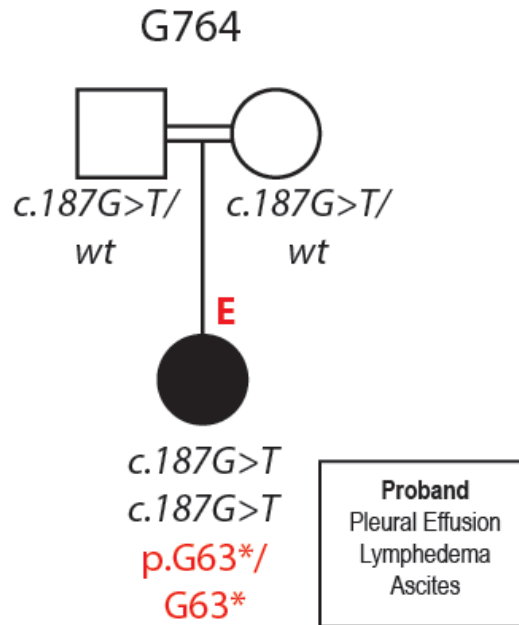
Figure 20. Pedigree of children diagnosed in Family G764 with hydrops fetalis, pleural or pericardial effusions and lymphoedema. Pathogenic variants in the *MDFIC* gene sequence are indicated in black type and corresponding MDFIC protein changes in red. Affected individuals are shown in black. Sequencing method is designated (E, exome, G, genome).

3.2.6 Family CHOP1 (reported by Dr Sarah Sheppard, USA)

A couple of European ancestry had a stillborn child due to NIHF at 23 weeks gestation in their first pregnancy. NIHF was identified in the proband on a 20-week anatomy scan. After birth, bilateral thoracentesis was performed confirming chylothorax. Magnetic resonance lymphangiography showed retrograde perfusion along the lower left intercostal distribution and extensive dermal backflow with bilateral groin node injection. Follow-up at 4 months of age showed lymphoedema of the bilateral lower extremities and bilateral hydroceles (Figure. 21).
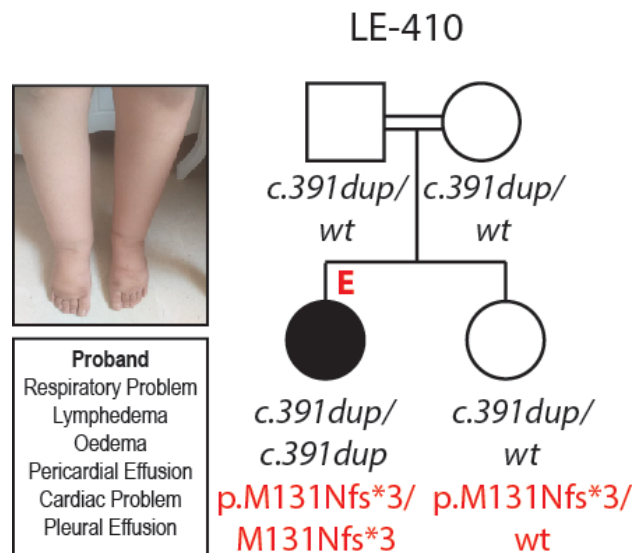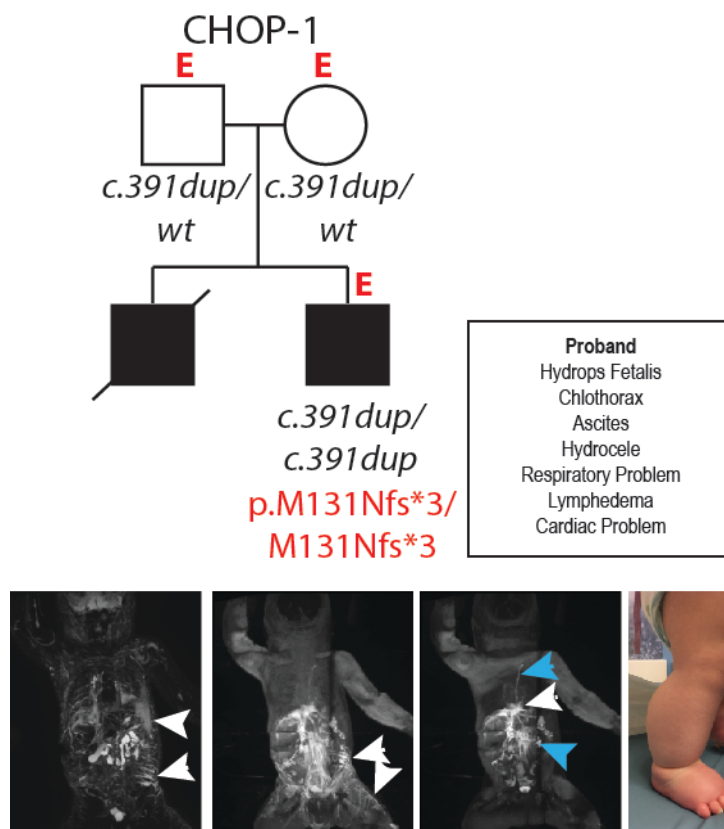
Figure 21. Pedigree of children diagnosed in Family CHOP1 with hydrops fetalis, pleural or pericardial effusions and lymphoedema. Pathogenic variants in the *MDFIC* gene sequence are indicated in black type and corresponding MDFIC protein changes in red. Affected individuals are shown in black. Sequencing method is designated (E, exome; G, genome). Pleural effusions (white arrowhead), large cutaneous lymphatic channels (white arrows), retrograde mesenteric lymphatic flow (blue arrowhead), dilated thoracic duct (blue arrow) and perfusion of the capsular lymphatics (dashed white arrow) visualised using T2 MRI, IN-DCMRL and IH-DCMRL, together with lymphoedema in the proband of CHOP1.

3.3 Mdfic is prominently expressed in cardiac and lymphatic valves.

To investigate the mechanisms by which *MDFIC* pathogenic variants underlie hydrops fetalis and primary lymphoedema, we first investigated *Mdfic* expression and localisation throughout cardiovascular development in the mouse embryo. RNA *in situ* hybridisation analyses performed in the mouse embryo at E16.5 and E18.5 revealed robust expression of *Mdfic* in the developing lung, kidney and salivary glands. In the cardiovascular system, *Mdfic* was detected in lymphatic valves and cardiac valves. These data were confirmed by immunostaining; MDFIC protein was prominent in lymphatic and cardiac valves and

appeared to be located both in the cytoplasm and in association with the extracellular matrix of cells within these regions (Figure. 22). (Experiments performed by Jan Kazenwadel and Gen Secker) (Byrne et al., 2022).
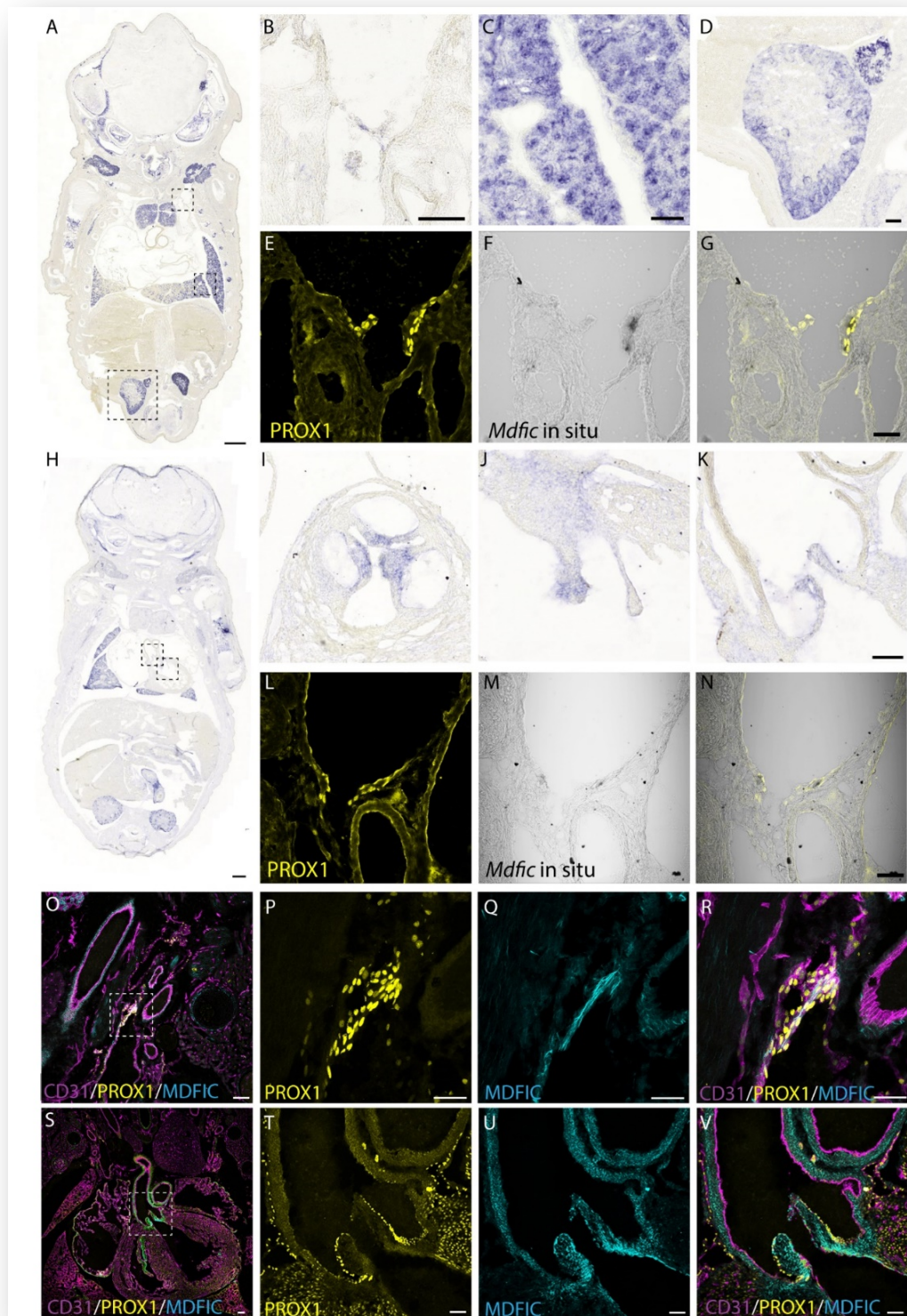
Figure 22. Mdfic is prominently expressed in cardiac and lymphatic valves. RNA in situ hybridisation on coronal E16.5 (A-G) and E18.5 (H-N) sections demonstrates Mdfic expression in lymphatic valves (B, F, G), lung (C), kidney (D) and cardiac valves (I, J, K). The identity of lymphatic valves in which Mdfic

expression was detected (F, G, M, N) was confirmed by immunostaining for PROX1 (E, G, L, N). Immunofluorescent staining of E17.5 sections (O-V) with antibodies to PROX1 (P, T), MDFIC (Q, U) and CD31 (R, V) reveals co-localisation of MDFIC with PROX1 positive lymphatic (O-R) and cardiac (S-V) valves. Scale bars, 500 μm (A, H), 200 μm (S), 100 μm (B-D, I-K, O, T, U, V), 50 μm (E-G, L-N, P, Q, R). Experiments performed by Jan Kazenwadel and Gen Secker (Byrne et al., 2022).

3.4 $Mdfic^{M131fs*/M131fs*}$ mice exhibit profound lymphatic vascular defects and perinatal lethality.

To investigate the consequences of *Mdfic* variants on cardiovascular development, CRISPR-Cas9 genome editing using a guide RNA targeting the region between c.379G and c.396C was used to generate a mouse model mimicking the most frequent human *MDFIC* truncating variants found in five of the seven patients (c.391dup/p.Met131Asnfs*3). Two founder mice were born harbouring small deletions in this region, one of two base pairs and one of eight base pairs. Each of these variants resulted in a frameshift and premature stop codon, predicted to generate proteins 142 and 140 amino acids in length, respectively. For simplicity, these lines are referred to as $Mdfic^{M131fs*}$. Mice in each line were back-crossed to wild-type mice for at least three generations to minimise potential off-target genome editing events, and heterozygous $Mdfic^{M131fs*/+}$ mice were then crossed together to generate homozygotes. One hundred percent of homozygous $Mdfic^{M131fs*/M131fs*}$ mice exhibited perinatal lethality, with the majority dying within 30 days of birth. Careful postnatal monitoring of mice revealed that, although otherwise indistinguishable from wild-type littermates initially, immediately before death, homozygous mutant mice appeared less active, were hunched, and exhibited laboured breathing. The development of symptoms was rapid and resulted in the demise of affected mice within hours of onset. Post-mortem analysis of $Mdfic^{M131fs*/M131fs*}$ mice revealed chylothorax, the filling of the thoracic cavity with chylous fluid (Figure. 23 A and B). Analysis of the lymphatic vasculature within the thoracic wall and diaphragm with chylothorax revealed dysmorphic, distended lymphatic vessels, together with elevated numbers of LYVE1-positive macrophages (Figure 24, D and H), phenotypes not observed in wild-type littermates (Figure. 24, C and G). Evans blue dye injection to the peritoneal cavity of $Mdfic^{M131fs*/M131fs*}$ mice revealed notable retrograde flow from the thoracic duct to the intercostal lymphatics, a phenotype reminiscent of that

observed in patients with CCLA (Figure 24, E and F). Investigation of the lymphatic vasculature in the mesentery of $Mdfic^{M131fs*/M131fs*}$ mice with chylothorax revealed no apparent leakage or breach in vessel integrity, although lymphatic vessel valves were clearly defective, appearing arrested at an early stage of development (Figure 24, I and J).
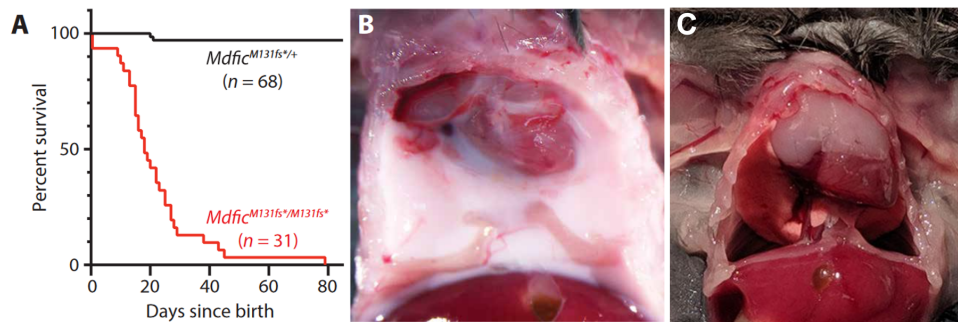
Figure 23. $Mdfic^{M131fs*/M131fs*}$ mice exhibit perinatal lethality. (A) Kaplan-Meier survival curve for mice with homozygous (red) and heterozygous (black) $Mdfic$ truncating mutations. n = 68 $Mdfic^{M131fs*/+}$ mice, n = 31 $Mdfic^{M131fs*/M131fs*}$ mice. (B) Post-mortem photograph of chylothorax in $Mdfic^{M131fs*/M131fs*}$ mice exhibiting laboured breathing. (C) Post-mortem photograph of chylothorax in Wild-type mice.

| | Mdfic$^{+/+}$ | Mdfic$^{M131fs*/M131fs*}$ |
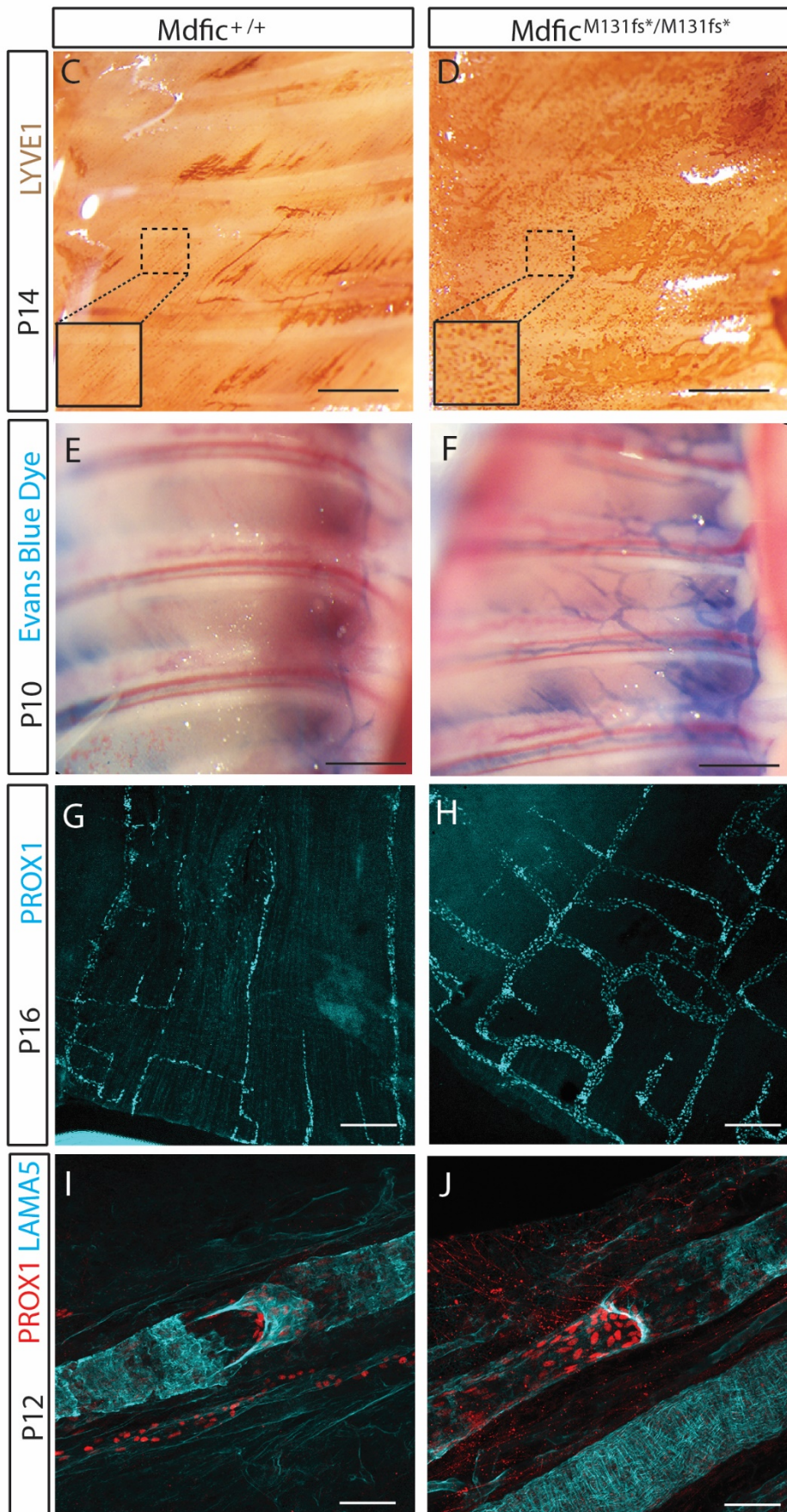
Figure 24. *Mdfic^M131fs*/M131fs** **mice exhibit profound lymphatic vascular defects.** (C and D) Whole-mount DAB staining of thoracic wall with an antibody to LYVE1 in *Mdfic^M131fs*/M131fs** mice (D) compared with WT littermates (C). Insets represent higher magnification images of the regions depicted in dashed boxes. (E and F) Evans blue dye injection to the peritoneal cavity of P10 pups to analyse retrograde flow of dye from the thoracic duct to the intercostal lymphatics in *Mdfic^M131fs*/M131fs** mice (F) and WT littermates (E). (G and H) Immunofluorescence immunostaining of diaphragm with an antibody to PROX1 in *Mdfic^M131fs*/M131fs** mice (H) compared with WT counterparts (G). (I and J) Whole-mount immunostaining of mesenteric lymphatic vessels focussing on lymphatic valves with antibodies to PROX1 (red) and laminin α5 (LAMA5, cyan) in *Mdfic^M131fs*/M131fs** mice (J) compared with WT littermates (I). Scale bars, 1 mm (C to F), 200 m (G and H), and 50 m (I and J).

We next investigated the lymphatic vascular phenotype of postnatal *Mdfic^M131fs*/M131fs** mice not exhibiting discernibly laboured breathing. In this case, chylothorax was not observed, though the lymphatic vessels in the thoracic wall were clearly enlarged and dysmorphic compared to littermate controls (Figure. 25).
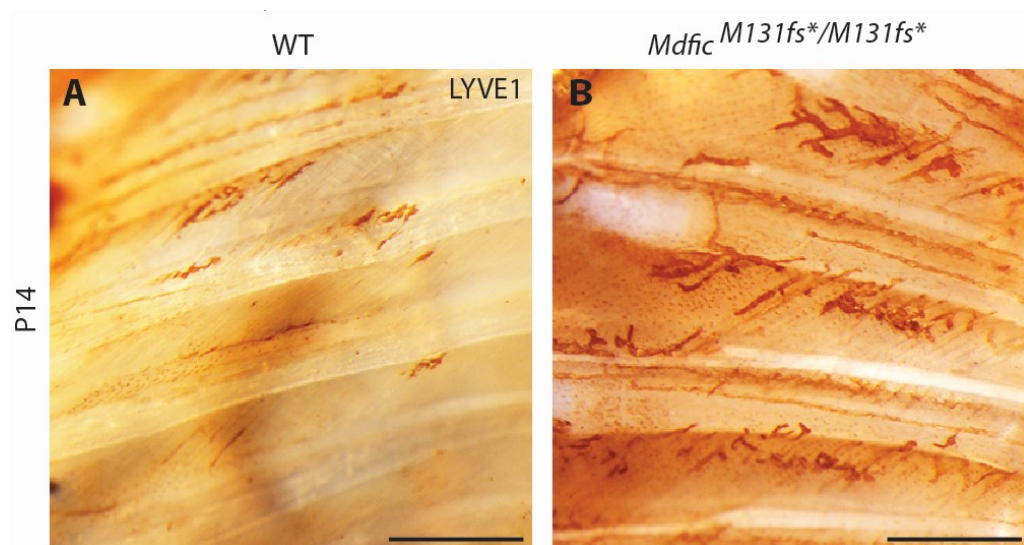
Figure 25. *Mdfic^M131fs*/M131fs** **mice exhibit lymphatic vascular defects in the absence of discernibly laboured breathing.** (A and B) Wholemount immunostaining of thoracic walls isolated from P14 wild-type (A) and *Mdfic^M131fs*/M131fs** (B) mice revealed distended, mis patterned lymphatic vessels in *Mdfic^M131fs*/M131fs** mice, even prior to exhibiting the phenotype of laboured breathing. N=3 Scale bars, 1mm (A, B).

3.5 *Mdfic*^{*M131fs*/M131fs**} mice exhibit mild subcutaneous oedema in skin

To investigate the possible consequences of *Mdfic* variants on the morphology of tissues in *Mdfic*^{*M131fs*/M131fs*} mice, we sent E18.5 embryos to the Australian Phenomics Network (University of Melbourne) for histopathology analysis. Tissue histology was examined in wild-type, *Mdfic*^{*M131fs*/+*} and *Mdfic*^{*M131fs*/M131fs*} mice. The microscopic examination of tissues showed mild subcutaneous oedema in the skin of both heterozygous and homozygous mice. Mild separation of muscle fibres was also observed in homozygous and heterozygous mice. No obvious difference was observed in heart tissues between different genotypes (N=3 embryonic mice per genotype were used for histopathology analysis) (Figure. 26).
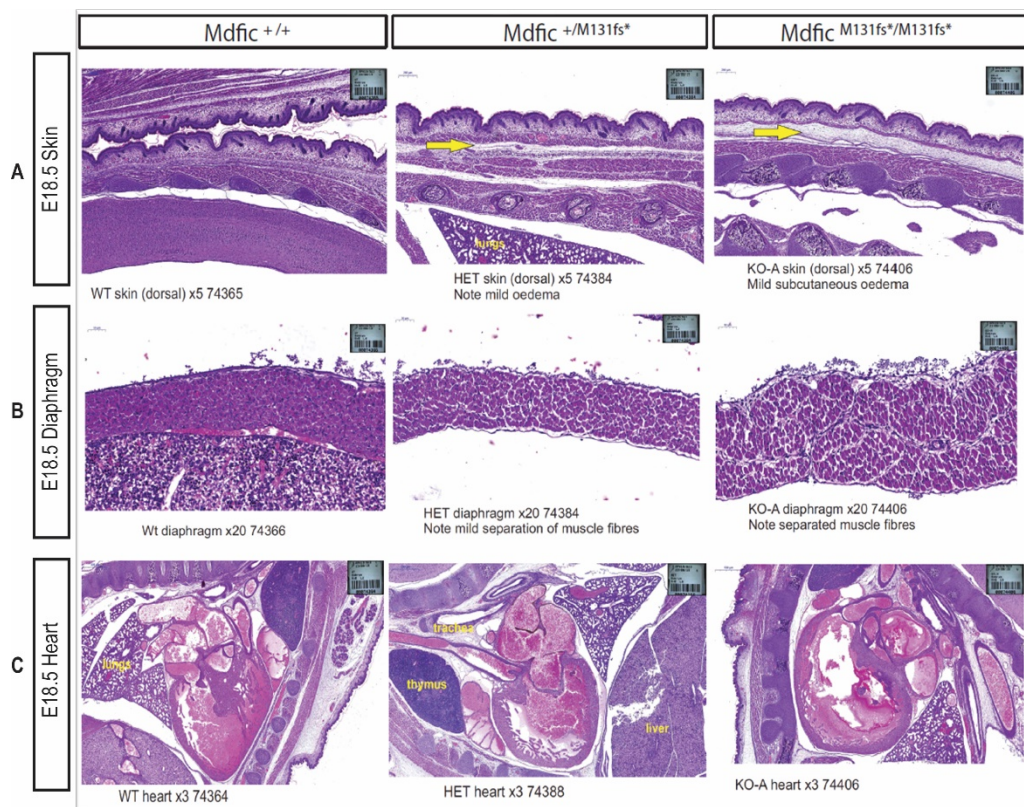
Figure 26. Morphological analysis of skin, diaphragm, and heart in *Mdfic*^{*M131fs*/M131fs**} mice. (A) Mild oedema was seen in skin of heterozygous and homozygous E18.5 mice (yellow arrows). (B) Mild separation of muscle fibres was observed in homozygous and heterozygous mice but not littermate controls. (C) No difference was observed in heart morphology.

The presence of mild oedema in mutant mice was subsequently confirmed through immunostaining of cryosections. Mutant embryos and their wild-type counterparts at E18.5 were collected, frozen, and sectioned sagittally. Analysis of lymphatic vascular patterning in the skin of mutant mice showed dilation and distension of lymphatic vessels. (Figure. 27).
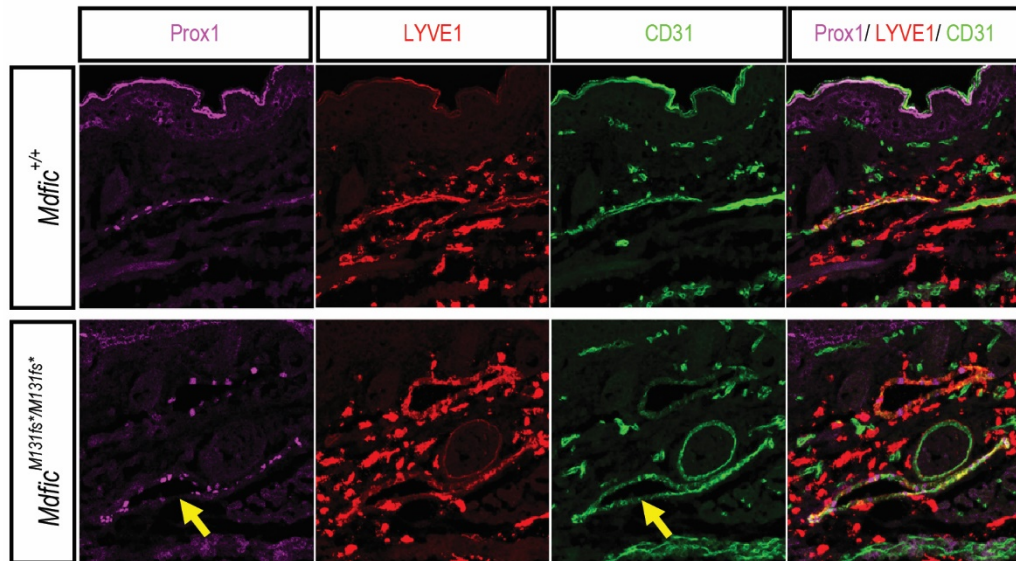
Figure 27. Morphological analysis of skin in *Mdfic*M131fs*/M131fs* mice through immunostaining using blood and lymphatic specific markers. Cryosections stained with lymphatic (PROX1 and LYVE1) and blood (CD31) markers. Yellow arrows point to the dilation of lymphatic vessels demonstrating the presence of oedema in skin of *Mdfic*M131fs*/M131fs* mice (N=3 mice per genotype).

3.6 Lymphatic vascular defects in the skin, diaphragm, and mesentery of E18.5 $Mdfic^{M131fs*/M131fs*}$ mice.

To investigate the nature and onset of lymphatic vessel defects in $Mdfic^{M131fs*/M131fs*}$ mice, lymphatic vessel structure and patterning during embryonic development were investigated. Analysis of lymphatic vascular patterning in the skin, diaphragm, and mesentery of E18.5 embryos revealed that the lymphatic vasculature of $Mdfic^{M131fs*/M131fs*}$ mice was wider in calibre and greater in surface area than the vessels of wild-type counterparts in all tissues analysed (Figure. 28, A to I). In addition, valve development was abnormal in $Mdfic^{M131fs*/M131fs*}$ mice at E18.5; significantly fewer valves were present in the mesenteric collecting lymphatic vessels of $Mdfic^{M131fs*/M131fs*}$ embryos compared with their wild-type counterparts (Figure. 28, H to J). In addition, the valves that had formed were less mature than those observed in wild-type littermates, evidenced by both the apparent arrest of valve development at the ring-like stage and by lower quantities of laminin $\alpha5$ deposition in valve territories compared with wild-type counterparts (Figure. 28, K to P). Coupled with the restricted expression of $Mdfic$ in valve endothelial cells, these data suggest that the primary cause of the lymphatic vascular phenotype in $Mdfic^{M131fs*/M131fs*}$ embryos is defective valve development.
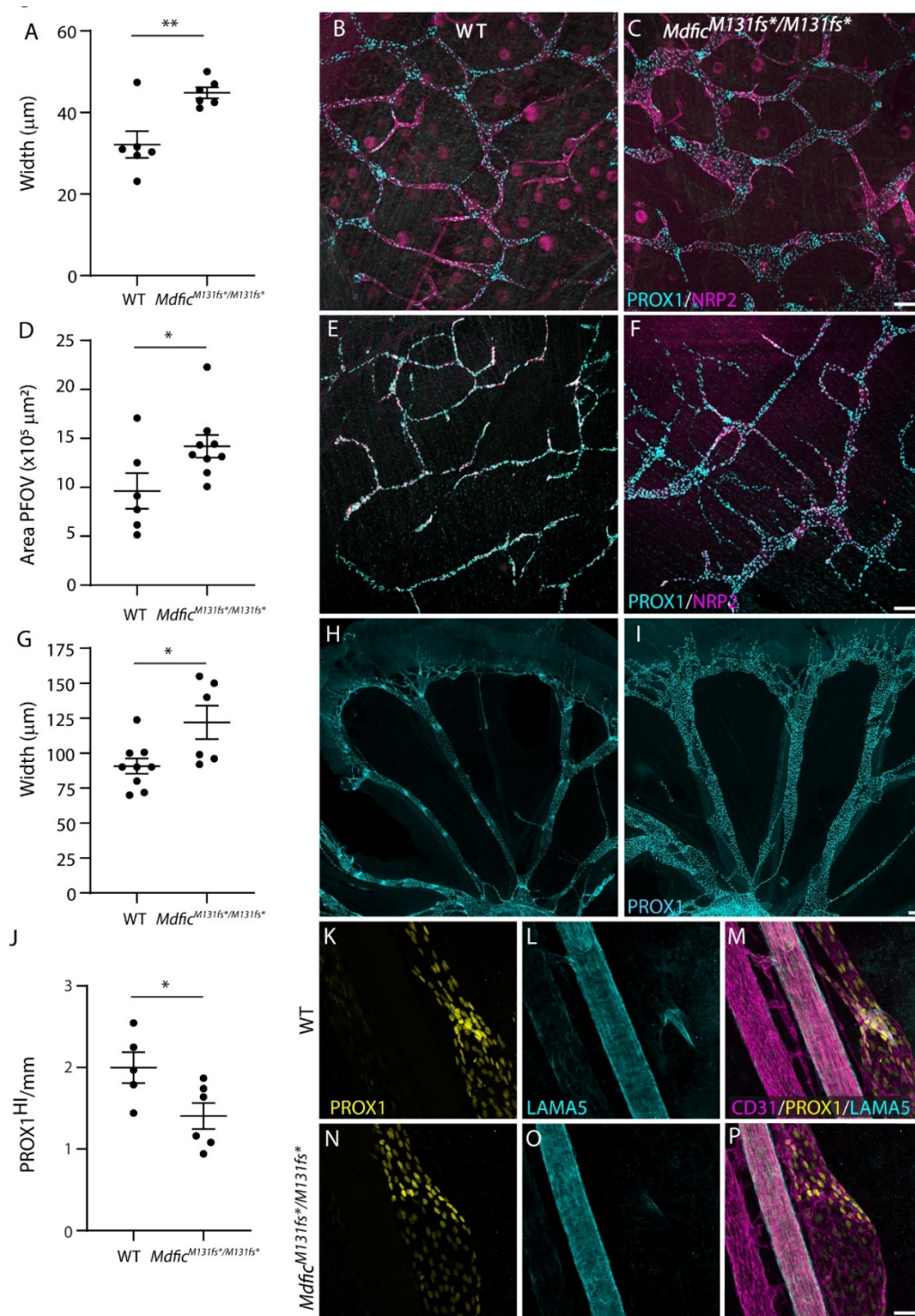
Figure 28. E18.5 Mdfic^M131fs*/M131fs* embryos exhibit distended lymphatic vessels and defective lymphatic vessel valve development. Analysis of lymphatic vessel calibre in E18.5 dermis (A-C), diaphragm (D-F) and mesentery (G-I) by wholemount immunostaining with lymphatic markers PROX1 (cyan) and NRP2 (magenta), demonstrates an increase in vessel width (A, G) and area (D) in Mdfic ^M131fs*/M131fs* embryos (C, F, I) compared to wild type littermates (B, E, H). Quantification of PROX1high valve territories in mesenteric collecting vessels (J) shows fewer valves in Mdfic^M131fs*/M131fs*

embryos (I) compared to wild-type littermates (H). Wholemount immunostaining of mesenteric collecting vessels (K-P) with PROX1 (yellow), laminin α5 (cyan) and CD31 (magenta) demonstrates immature valves in Mdfic$^{M131fs*/M131fs*}$ embryos (N-P) compared to wild-type littermates (K-M). Scale bars, 100μm (B, C, E, F, H, I), 40μm (K-M, N-P). Error bars represent SEM, *p<0.05, **p<0.01. Dots represent the number of embryos used per experiment. Analysis was done with the help of Genevieve Secker (Byrne et al., 2022).

3.7 No obvious defect was identified in heart valves of E16.5 Mdfic$^{M131fs*/M131fs*}$ mice

Due to the severe lymphatic dysfunction that was observed in the thoracic cavity of Mdfic$^{M131fs*/M131fs*}$ mice, further investigation was performed to study the potential heart defects due to the MDFIC variant. Micro-CT scanning was performed on the heart's tissues isolated from the Wild-type and homozygous Mdfic$^{M131fs*/M131fs*}$ embryos at E16.6 and cardiac and lymphatic valves were examined (n=3). Examination of cardiac valves showed no obvious defects in the mutant mice. Heart sizes appeared to be normal and valves such as tricuspid pulmonary valves, tricuspid aortic valves, both left and right atria, ventricular atrial septum and coronary arteries were present and intact (Figure. 29).
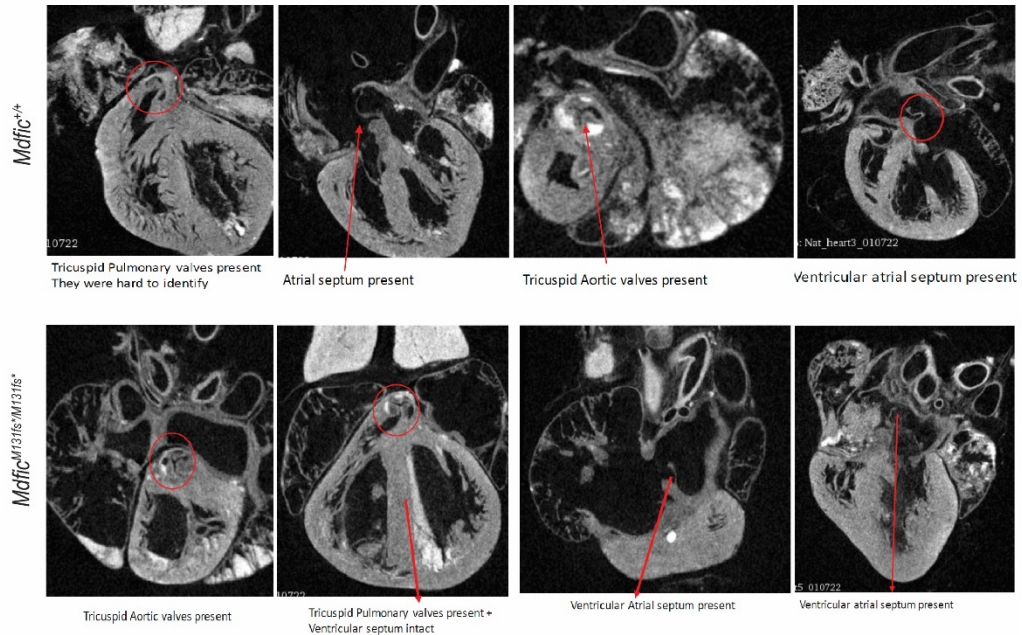
Figure 29. Micro-CT scanning of the isolated heart from embryos at E16.5 for cardiac valves examination. Analysis of the micro-CT scanning images from the hearts dissected from embryonic mice (E16.5) showed major cardiac valves including Tricuspid aortic valves, Tricuspid pulmonary valves, and

Ventricular atrial septum were present and intact in both wild-type and homozygous *Mdfic*[M131fs*/M131fs*] embryos (N=3 per genotype).

3.8 Discussion

Central collecting lymphatic anomaly (CCLA) is a devastating disorder characterised by abnormalities in the development and function of major, truncal lymphatic vessels, which is presented in seven affected individuals from six independent families in our study. The proband and affected brother from the non-consanguineous parents in Adelaide were diagnosed with foetal hydrops very early at 26 and 20 weeks of gestation, respectively. Both affected individuals inherited the exact same variants in *MDFIC* from their parents (p. (Met131Asnfs*3)/ c.732T>G; p. (Phe244Leu)). However, the severity of NIHF was different in these two babies. Given the high-risk pregnancies in this family, more frequent monitoring of the pregnancy helped with earlier diagnosis of hydrops in the second foetus, which subsequently facilitated the chance of performing shunt therapy that rescued the foetus. Furthermore, various severities of the disease caused by *MDFIC* mutation were also observed in the additional families that were presented in this study, all of which had the early onset of CCLA at early stages of development but progressed differently growing up. The neonate from family LE452 died at 28 weeks, whereas the proband from LE590 died at the age of 7 and the proband from family G764 and LE410 are still alive at the age of 11 and 20 years, respectively. Given that proband from LE590 and LE410 have a matched genotype and similar medical conditions it is interesting that one died, and one survives until today. It is interesting that p.Met131Asnfs*3 is observed in multiple probands and the exact mutation appears independently in different families with different ethnicities. It is evident that this is a mutation hotspot as it is found either in homozygosity or compound heterozygosity with another allele i.

Given that this frameshift variant was the most common and pathogenic mutation in this study, we generated a novel mouse model of CCLA in which homozygous truncating frameshift variants found in human *MDFIC* were recapitulated. Through studying this mouse model, a crucial role for MDFIC in the development of lymphatic vessel valves was revealed. Structural abnormalities in the lymphatic vasculature of homozygous mutant mice were observed concurrently with the onset of lymphatic vessel valve development during embryogenesis, and they progressively worsened over time, resulting in the lethality of mice due to chylothorax within the first 30 days of life. *Mdfic*[M131fs*/M131fs*] mice generated in this study exhibited the exact phenotype that was observed in humans. Breathing difficulties, increased heartbeat, and lack of movements were the major

phenotypes that these mutant mice showed abruptly. The severity of the phenotype has led mutant mice to be humanely euthanised. Autopsies performed on mutant mice revealed the underlying reason for breathing difficulties have been the accumulation of Chylous ascites in the thoracic cavity of these mice which was similar to the phenotype detected in our probands, confirming that the $Mdfic^{M131fs*/M131fs*}$ mice were a great model to study the function of *MDFIC*. Other than the accumulated lymphatic fluid in the thoracic cavity no other defect was observed during the autopsy examination. Lymphatic vessels in other tissues such mesenteric, heart and skin were intact, no obvious leakage was observed and so signs of blood in the lymphatic vessels were noted.

Our data reveal that biallelic *MDFIC* pathogenic variants are causative of CCLA, define a novel role for MDFIC in lymphatic vascular development, and identify a new gene important for the development and function of lymphatic vessel valves. It is intriguing that despite the presence of valves in collecting lymphatic vessels of all tissues analysed to date, the phenotypes of lymphatic vessel distension and, ultimately, dysfunction are predominant in the thoracic region of $Mdfic^{M131fs*/M131fs*}$ mice. All patients in our study exhibited pleural and pericardial effusions, which, in many cases, were recurrent. Chylothorax and pleural and pericardial effusions occur as a direct and severe consequence of thoracic duct dysfunction, resulting in retrograde flow of lymph into the pulmonary, cardiac, and intercostal lymphatics and fluid accumulation in the pleural/pericardial/thoracic spaces. This profound effect on the thoracic lymphatic beds may manifest as a result of the thoracic duct carrying the greatest lymph load in the body, thereby being the point at which lymphatic dysfunction reaches a critical threshold. In addition, the high degree of mechanical stress that the vessels of the thoracic region are subjected to during breathing, arterial pulsation, and heartbeat may result in these lymphatics being more susceptible to structural or functional impacts. Nonetheless, given that central and peripheral lymphatic symptoms are observed in patients with CCLA with *MDFIC* variants and that abnormalities in valve development are observed in the collecting lymphatics of all tissue beds analysed in embryonic and postnatal $Mdfic^{M131fs*/M131fs*}$ mice, it is likely that lymphatic vascular defects caused by *MDFIC* pathogenic variants are prominent in all tissues.

Micro-CT scanning, which was conducted to examine the severity of lymphatic dysfunction in the thoracic cavity of $Mdfic^{M131fs*/M131fs*}$ mice showed no obvious cardiac valve defects in mutant mice. However further analysis would be interesting to perform to record the electrodiagrams (ECGs) from these homozygous $Mdfic^{M131fs*/M131fs*}$ mice and their wild-type littermates and analyse the signals to assess animal health and cardiac diseases.

EC Genie™ is a great rapid non-invasive ECG system, which allows the detection of cardiac electrical activity from conscious animals including newborns. EC Genie™ captures the electrical signals at 2kHz and provides optimal fidelity in mapping the rapid ECG interval durations in mice. This instrument is safe and provides an ideal platform to detect the ECG signals through the paws, which is perfect for our mouse model.

This work and further investigation to analyse the additional impact of the *MDFIC* variant and understanding the mechanisms of MDFIC in development has immediate implications for improving the genetic diagnosis of patients affected by CCLA, sheds new light on the developmental aetiology of CCLA, and ultimately will inform the development of novel therapeutics to combat this disease.

Chapter 4: Investigating the molecular mechanisms by which MDFIC controls lymphatic vascular development.

4.1 Introduction

In this chapter, methods are taken to answer a big question of what MDFIC protein does in the body and how it affects lymphatic developmental processes in patients exhibiting central conducting lymphatic anomaly (CCLA). As mentioned earlier, CCLA is a disorder where the development and function of large, truncal-collecting lymphatic vessels are affected. It is a severe lymphatic malformation for which few effective treatments are available.

MDFIC encodes the MyoD family inhibitor domain-containing protein. This 246 amino acid protein has been documented to regulate the activity of transcription factors including the glucocorticoid receptor (GR), HAND1, and T cell factor/lymphoid enhancer factor (TCF/LEF) family members (Martindill et al., 2007; Oakley et al., 2017; Snider et al., 2001; Snider & Tapscott, 2005). The C-terminal region of MDFIC harbours a domain extremely rich in cysteine residues, reported to mediate protein-protein interactions between MDFIC and other transcription factors. In this manner, it is proposed that MDFIC tethers transcription factors in the cytoplasm where MDFIC predominantly resides, thereby restricting their nuclear access and transcriptional activity. To date, the roles of MDFIC remain enigmatic, and MDFIC has not been implicated in cardiovascular development.

An important aspect of lymphatic vessel maturation is the development of lymphatic vessel valves, which act to ensure that lymph is returned efficiently in a unidirectional manner to the bloodstream (Bazigou and Makinen, 2013). Valve development is dependent on key transcription factors including FOXC2 and GATA2, the abundance of which is elevated in valve-forming territories in response to flow-initiated signals (Kazenwadel et al., 2015; Norrmén et al., 2009; Petrova et al., 2004; Sabine et al., 2012).

Studies have shown that the failure of lymphatic vessel valves to form or function in mice deficient in expression of genes such as *Foxc2* and *Gata2*, or harbouring a pathogenic variant in *Kras*, can result in lymphatic phenotypes including oedema, chylous ascites, and chylothorax (Sepehr et al., 2021; Petrova et al., 2004). Patients with primary lymphoedema syndromes or lymphatic malformations caused by pathogenic variants in *FOXC2*, *GATA2* or *KRAS* also exhibit lymphatic vessel valve defects and, in some cases,

venous valve defects. This highlights the impact of valve defects on lymphatic function in human lymphatic disease (Hägerling, 2020; Sepehr et al., 2021; Lyons et al., 2017).

In Chapter 3, the crucial role of MDFIC in the development of lymphatic vessel valves was highlighted. A study of a mouse model revealed that pathogenic truncating *Mdfic* variants cause structural abnormalities in the lymphatic vasculature, specifically in the development of valves, which subsequently causes lethality in mice due to chylothorax. This impact of *Mdfic* mutation on lymphatic valve development suggests the existence of a potential direct/indirect interaction of MDFIC with transcription regulators crucial in lymphatic vessel valve development such as GATA2, PROX1, NFATC1 and FOXC2.

In this chapter, further analysis has been carried out to 1) Investigate the localisation and protein structure of MDFIC 2) investigate potential protein-protein interactions of MDFIC with transcriptional regulators important in valve development and 3)RNA sequencing as a ubiquitous tool in molecular biology was also performed on human lymphatic endothelial cells (LECs) treated with control and *Mdfic* esiRNA to provide more comprehensive information on the biological and cellular participation of MDFIC protein in the cells and investigate the consequences of removing *MDFIC* on gene expression in LECs.

Furthermore, we also took experimental approaches to characterise the mechanism by which MDFIC controls the activity of RAS/MAPK signalling. Signalling pathways play a critical role in translating extracellular signals originating from the environment into specific responses that regulate intracellular gene expression and cellular responses. The process of signal transduction is initiated by the binding of ligands such as hormones, growth factors, interleukins and neurotransmitters to membrane-bound receptors, subsequently triggering a cascade of intracellular signalling activities through phosphorylation of multiple kinases that control how transcription factors regulate downstream gene expression.

Activation of different signalling pathways within and between cells can regulate physiological and cellular responses such as metabolism, proliferation, differentiation, tissue repair, communication and death (Lefloch et al., 2009; Molina & Adjei, 2006). Disruption of these signalling communication chains can lead to the dysregulation of biological processes which can result in developmental disorders and cancers (Sever &

Brugge, 2015). Therefore, it is important to understand the critical pathways affected by disease processes to design rational treatment strategies.

The ERK/MAPK pathway (Figure 49) is one of the most important signalling networks in cells. Signal transduction through the ERK/MAPK pathway begins with the activation of Raf protein kinases by GTP-bound Ras. Ras is a group of proteins upstream of the Raf-MEK-ERK pathway, which plays a role as an on-and-off switch for signal transduction (Wennerberg et al., 2005). Ras can be activated by various stimulating factors such as epidermal growth factor (EGF), tumour necrosis factor, activators of protein kinase C (PKC) and Src family members. Activation of Raf results in phosphorylation of MEK, which leads to phosphorylation of ERK (MAPK), which in turn phosphorylates and regulates the activity of downstream targets, including other kinases and various transcriptional regulators (Peti & Page, 2013; Pimienta & Pascual, 2007; Vandamme et al., 2014; Zhang et al., 2004) (Figure. 30).
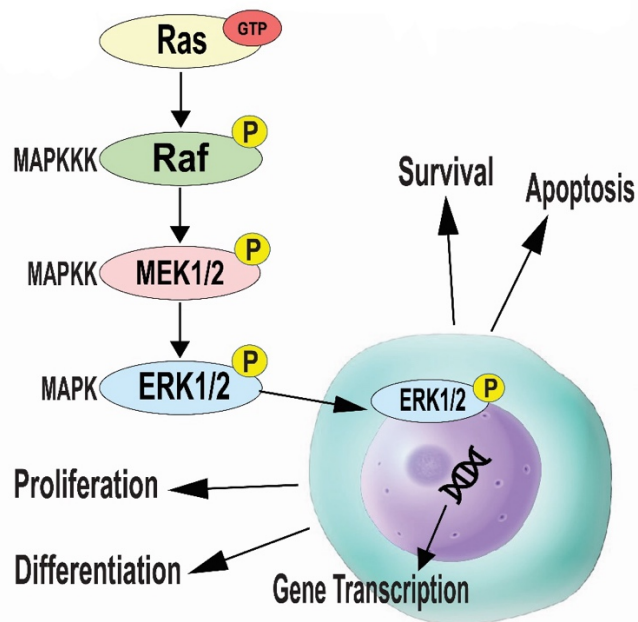
Figure 30. Simplified regulation of ERK/MAPK signalling pathway. Activation of Ras initiates the cascade of phosphorylation in Raf/MEK/ERK protein kinases leading to transmission of extracellular signals to the nucleus, thereby regulating transcription of downstream gene targets.

This pathway is also reported to be important for regulating SOX18 and PROX1 expression in LECs, thereby promoting lymphangiogenesis and lymphatic remodelling (Deng et al,2013). Mutations in genes encoding components of this signalling pathway can result in gain or loss of function in the Ras/Raf signalling cascade, dysregulating the ERK pathway and subsequently resulting in lymphatic abnormalities (Bui & Hong, 2020; Coso et al., 2014; Muraca & King, 2014).

Recent studies have revealed that the ERK signalling pathway is dysregulated in lymphatic anomalies and that targeting this pathway is a promising therapeutic option for the treatment of these disorders. In instances in which lymphatic defects were determined to arise from increased activity of this pathway, small molecule inhibitors such as Trametinib, Binimetinib and Dabrafenib were found to be effective therapies (Bui & Hong, 2020; Li et al., 2019; Song et al., 2022; Su et al., 2012). The similarities between the lymphatic phenotypes reported in CCLA due to pathogenic *MDFIC* variants and those described in patients with lymphatic anomalies due to pathogenic variants in components of the RAS/MAPK pathway raise the possibility that MDFIC might also influence RAS/MAPK signalling in lymphatic endothelial cells.

Thereby in this chapter, we also investigated whether RAS/MAPK pathway activity in the lymphatic vasculature is regulated by *MDFIC* deficiency. Linking MDFIC function to RAS/MAPK signalling pathways has the potential to facilitate the implementation of clinically approved modulators for patient treatment, as has been recently described for CCLA ((Li et al., 2019).

4.2 The MDFIC Met131Asnfs*3 variant results in protein truncation

The most C-terminal truncating variant identified in our patient cohort (p.M131Nfs*3) results in a stop codon 95 nucleotides before the last exon/intron junction (Figure. 31, A and B), suggesting that all truncating variants may be susceptible to nonsense-mediated decay (Supek et al., 2021).
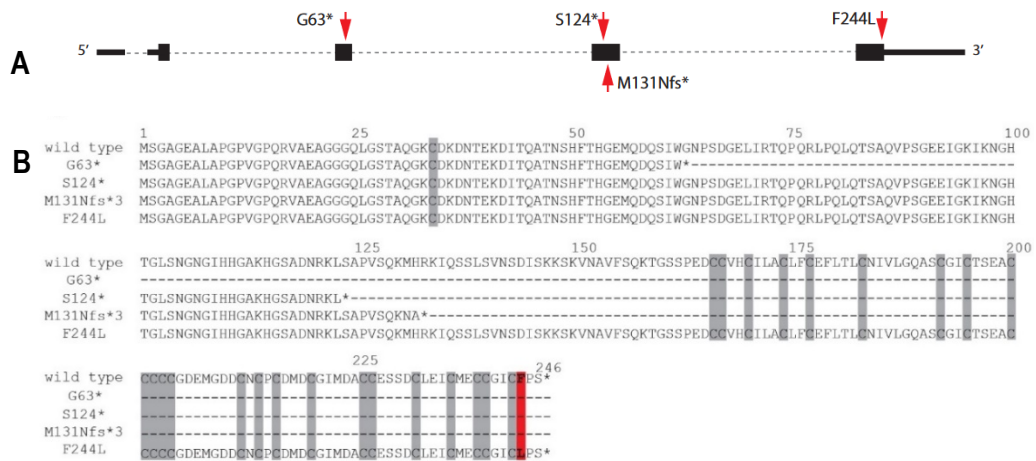
Figure 31. Schematic depicting exon/intron structure of *MDFIC* transcript. (A) Exons are shown as black boxes, and patient variants are shown with red arrows. (B) Human *MDFIC* sequence alignment comparing wild type and mutant proteins found in patients. Cysteine residues are highlighted in grey and the F244L amino acid substitution, in red.

To ascertain whether this was the case, RNA sequencing data from patients with compound heterozygous c.391dup/c.732T>G (p.M131Nfs*3/p.F244L) variants were interrogated. Both variant transcripts were present at an equivalent quantity, suggesting that the c.391dup variant predicted to give rise to a truncated protein was not subject to nonsense-mediated decay. Moreover, quantification of *MDFIC* transcripts in fibroblasts revealed comparable amounts of transcripts from both *MDFIC* variant alleles in fibroblasts from the proband of LE452 to those found in healthy controls (Byrne et al., 2022).

Analysis of *Mdfic* transcripts in the kidneys of *Mdfic*$^{M131fs*/M131fs*}$ mice harbouring either the 2 or 8 base pair deletion also revealed that expression of the M131fs* transcript was comparable to wild-type *Mdfic* mRNA in control littermates, providing further evidence that mRNA encoding the patient c.391dup variant is unlikely to be degraded (Figure. 32) (Byrne et al., 2022).
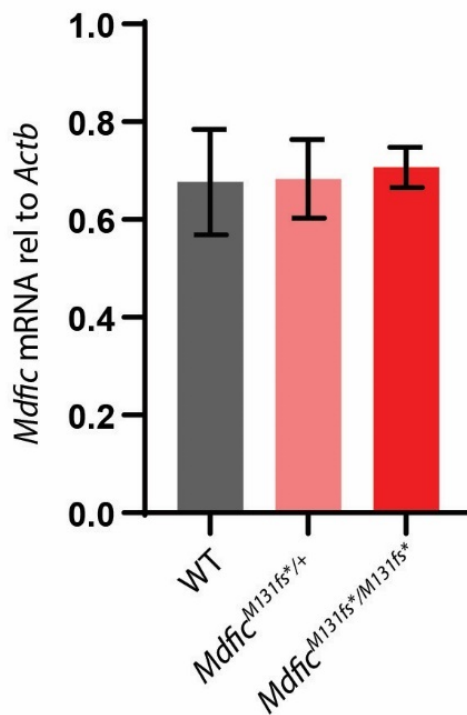
Figure 32. Expression level of *Mdfic M131fs** transcript is comparable to wild-type *Mdfic* mRNA. Analysis of RNA isolated from kidneys of *Mdfic*$^{M131fs*/M131fs*}$, *Mdfic*$^{M131fs*/+}$ and *Mdfic*$^{+/+}$ littermates demonstrates that mutant *Mdfic* transcript levels are comparable (Analysis was performed by Jan Kazenwadel).

4.3 MDFIC protein localisation and function

As mentioned earlier, MDFIC has previously been reported to tether transcription factors in the cytoplasm, thereby restricting their nuclear access and transcriptional activity. To investigate whether MDFIC is equipped with such characteristic domains essential for binding to other transcriptional regulators, the sequence of MDFIC protein was subjected to analysis using several prediction programs such as TMpred, DAS Transmembrane Prediction server , OCTOPUS and Split 4.0 Membrane Protein Secondary Structure Prediction Server. Amino acid sequence alignments were performed using the T-COFFEE multiple sequence alignment server. This analysis revealed a predicted transmembrane domain adjacent to the cysteine-rich C-terminal domain, suggesting that MDFIC might reside in membranes. In addition, the cysteine-rich region was found to be highly homologous to the somatomedin B (SMB) domain of vitronectin, which is known

to be responsible for binding integrins, plasminogen activator inhibitor (PAI1) and the receptor for urokinase plasminogen activator (uPAR), to control cell adhesion and migration (Figure. 33). These analyses suggest that MDFIC p.Met131Asnfs*3 potentially impacts the binding capacity of the C-terminal SMB domain, thereby affecting the function of MDFIC in the human body. MDFIC p.Met131Asnfs*3 variant is likely to act as a loss-of-function pathogenic variant and result in MDFIC losing the capacity to bind to other transcriptional regulators. Moreover, MDFIC localisation within the cell was also investigated to assess whether *MDFIC* pathogenic variants found in patients affect subcellular MDFIC localisation. Our findings revealed that both the F244L missense variant and wild-type MDFIC were present on the cell surface and could be secreted out of the cell, whereas the frameshift MDFIC variant was not detectable at the cell surface and lost its ability to be secreted (Byrne et al., 2022).
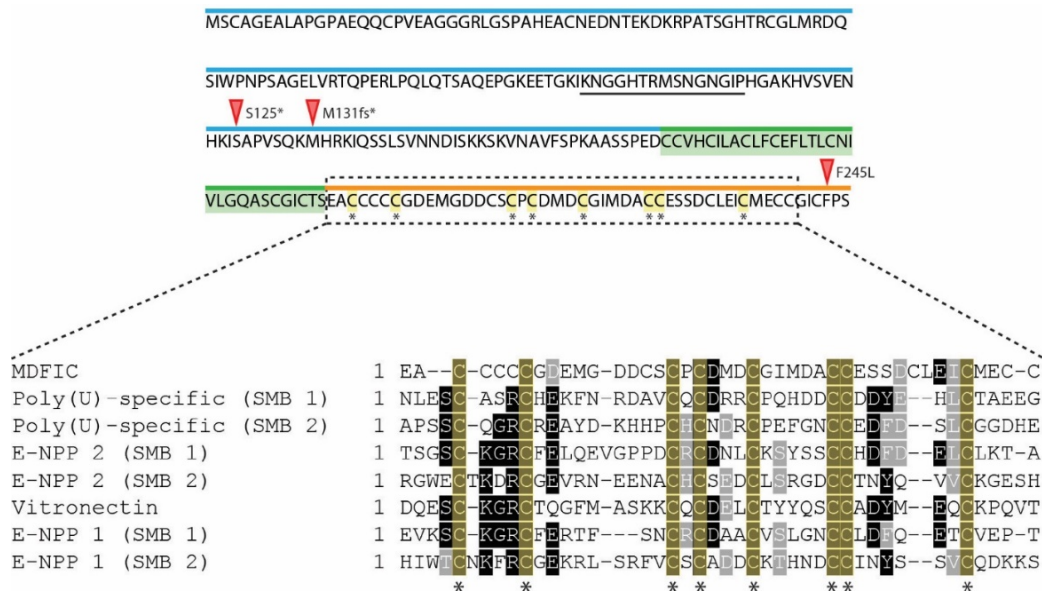
Figure 33. MDFIC protein contains predicted transmembrane and somatomedin B domains. The extracellular domain of mouse MDFIC protein (highlighted in blue) contains the epitope for the mouse monoclonal antibody developed in this study (underlined amino acids). Position of the M131fs*, S125* and F245L variants are shown with red arrowheads. The predicted transmembrane domain is highlighted in green and the intracellular domain, containing a predicted somatomedin B (SMB) domain, is highlighted in orange. Amino acid sequence alignment revealed that the putative MDFIC SMB domain contains a pattern of highly conserved cysteine residues (highlighted in yellow and with asterisks) that are characteristic of SMB protein domains. Protein names and UniProt database accession numbers: MDFIC, Q8BX65; Poly(U) - specific endoribonuclease, Q3V188; Ectonucleotide pyrophosphatase/phosphodiesterase family member 2, Q9R1E6; Vitronectin, P29788; Ectonucleotide pyrophosphatase/phosphodiesterase family member 1, P06802 (Analysis was performed by Drew Sutton).

4.4 MDFIC stability is regulated by FOXC2, GATA2 and NFATC1.

To explore the possibility that, as previously reported (Sklan et al., 2009). full-length MDFIC protein is post-translationally regulated and subject to rapid proteasomal degradation, constructs encoding full length and M131fs* MDFIC were ectopically expressed in HeLa cells and cells were treated with the proteasomal and lysosomal inhibitors MG132 and chloroquine. HeLa cells were used due to rapid growth, transfection efficiency and easy accessibility. In contrast to untreated cells, more full-length protein was consistently detected in cells treated with these inhibitors. In contrast, no striking differences in the levels of M131fs* were observed in cells treated with MG132 and chloroquine and higher levels of truncated protein were consistently observed (Figure. 34).
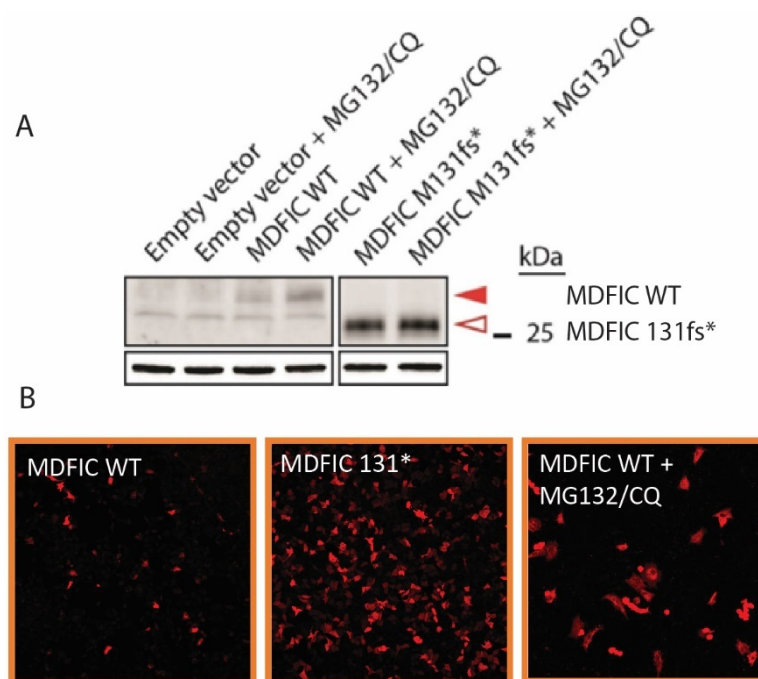
Figure 34. Inhibition of the proteasome and lysosome leads to increased levels of MDFIC protein in HeLa cells. (A) Treatment of HeLa cells ectopically expressing wild-type (WT) MDFIC protein along with a proteasomal inhibitor (MG132) and lysosomal inhibitor chloroquine (CQ) results in increased levels of detectable MDFIC protein compared to untreated cells. No striking differences in the levels of the M131fs* variant was observed following treatment with MG132 and CQ. Red arrowhead indicates full length MDFIC protein, open red arrowhead indicates truncated MDFIC M131fs* protein (N=3) (B) The number of MDFIC

positive cells was significantly increased when MDFIC was pro proteasomal inhibitor MG132 and lysosomal inhibitor chloroquine (CQ).

Given that we observed high MDFIC levels in valves and that MDFIC is reported to interact with several transcription factors, we investigated whether FOXC2, PROX1, GATA2 and NFATC1, all of which are elevated in valves and important for valve development, might also influence MDFIC stability and localisation. Expression levels of full-length MDFIC and MDFIC Phe245Leu appeared to be equal, while MDFIC M131fs* level was higher (Figure. 35 A to C). Co-expression of FOXC2 or GATA2 with MDFIC in HeLa cells resulted in increased levels of MDFIC, while co-expression with PROX1 or NFATC1 had no impact on MDFIC levels (Figure. 35 D to H). This data suggests that the stability of the truncated MDFIC M131fs* protein is increased upon removal of the cysteine-rich C-terminus, or/and that more protein is retained within the cell, particularly in valve endothelial cells where FOXC2 and GATA2 levels are elevated.
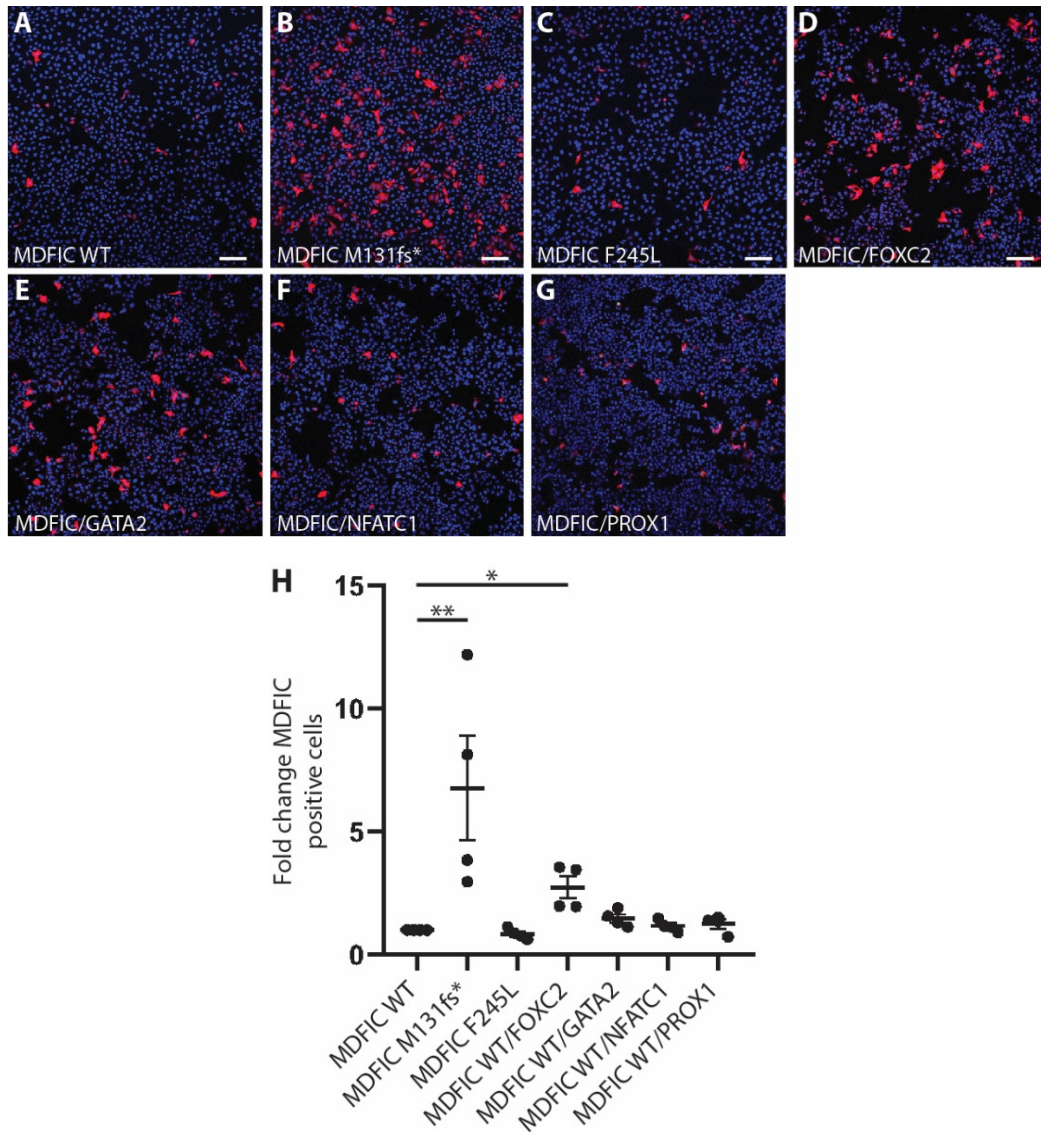
Figure 35. MDFIC protein levels are regulated by FOXC2 and GATA2. Ectopic expression of wild-type (WT) MDFIC, MDFIC M131fs* and MDFIC F245L proteins alone and co-expression of wild-type MDFIC together with PROX1, FOXC2, GATA2 or NFATC1 protein in HeLa cells was performed. Number of cells positive for MDFIC were assessed by immunostaining (A-G). MDFIC levels were increased when MDFIC was co-expressed with FOXC2 or GATA2 (D-E). The number of MDFIC positive cells was significantly increased when MDFIC was co-expressed with FOXC2 and trended towards an increase when MDFIC was co-expressed with GATA2 (H). Consistently increased numbers of cells positive for MDFIC M131fs* (B) were observed compared to WT MDFIC (A), suggesting that MDFIC M131fs* is more stable than wild-type MDFIC, or that it is retained intracellularly. Scale bars (A-G), 100 µm. (N=4) Error bars represent SEM, *p<0.05, **p<0.01. Successful transfection was confirmed by negative control cells transfected with control esiRNA and immune-stained with MDFIC Ab.

To investigate whether FOXC2, GATA2, PROX1 and NFATC1 influence MDFIC stability by binding in a complex with MDFIC, MDFIC was ectopically expressed in HEK293 cells together with GATA2 or FLAG-tagged FOXC2, PROX1 or NFATC1 and transcription factors were immunoprecipitated using antibodies to GATA2 or FLAG, respectively. HEK293 cells were used due to the high efficiency of transfection and high reproducibility. Strikingly, MDFIC co-immunoprecipitated selectively with GATA2 (Figure. 36). The impact of MDFIC M131fs* and Phe245Leu mutants on the interaction with GATA2 was also investigated. While Phe245Leu retained the ability to interact with GATA2, no interaction was detected between the M131fs* and GATA2, suggesting that the cysteine-rich C-terminus of MDFIC is required to mediate the interaction with GATA2. These data suggest that a physical interaction between MDFIC and GATA2 might contribute to the selective localisation of MDFIC in lymphatic vessels and cardiac valves where GATA2 levels are typically high.
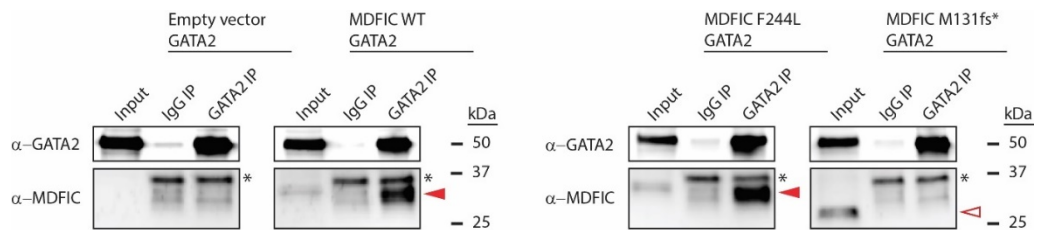
Figure 36. Interaction between MDFIC and GATA2 proteins is interrupted by the MDFIC M131fs* mutation. Wild-type (WT) MDFIC, M131fs* or F245L were ectopically co-expressed with GATA2 in HEK293 cells and immunoprecipitation was performed using an anti-GATA2 antibody. Immunoblotting of GATA2 immunoprecipitate revealed co-precipitation of WT and F245L MDFIC proteins with GATA2 (red arrowheads). In contrast, M131fs* did not co-precipitate with GATA2 (open red arrowhead denotes the expected size of M131fs*), suggesting that the C-terminus of MDFIC is essential for this interaction. (N=3) (experiment performed by Drew Sutton).

4.5 Changes to GATA2 localisation in MDFIC deficient LECs.

Our observation that MDFIC interacts with GATA2, prompted us to assess whether the localisation and transcriptional activity of GATA2 might be altered in MDFIC-deficient cells. Therefore, primary human lymphatic endothelial cells (hLECs) were treated with control and *MDFIC* endoribonuclease prepared siRNAs (esiRNA), which is a mixture of different siRNAs that target the same mRNA sequence to better silence the target gene. LEC lysates were then fractionated into nuclear and cytoplasmic compartments. MDFIC was predominantly localised to the cytoplasmic/membrane fraction of hLECs (Figure. 37 A). In *MDFIC* deficient hLECs, GATA2 levels marginally increased in the nucleus and decreased in the cytoplasm (Figure. 37 B) which is consistent with a role for MDFIC in sequestering transcription factors such as GATA2 in the cytoplasm. This experiment was performed three times. Even though we showed a consistent increase in the level of GATA2 in the nucleus of *MDFIC* deficient hLECs, the P-value is not significant. While this is an interesting observation it will require further experimental validation and quantification.
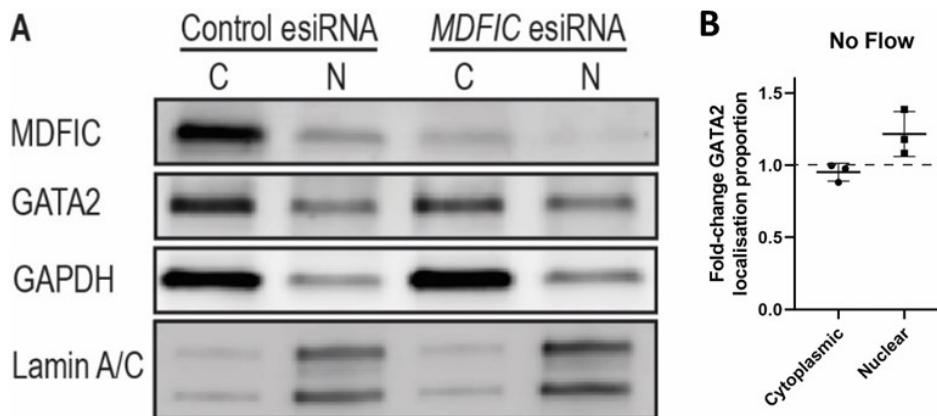
Figure 37 *MDFIC* deficiency results in slightly altered nuclear and cytoplasmic GATA2 levels. MDFIC and GATA2 are found largely in the cytoplasmic/membrane fraction of control esiRNA treated hLECs. In *MDFIC* deficient cells, levels of cytoplasmic GATA2 are decreased, whilst nuclear GATA2 is increased marginally. While GAPDH exists in both fractions, Lamin A/C is considered predominantly nuclear. Cytoplasmic fraction, C; nuclear fraction, N) (N=3). (Experiments performed by Drew Sutton).

4.6 Changes to GATA2 transcriptional activity in *MDFIC* deficient LECs.

To investigate the impact of reduced *MDFIC* levels on gene expression, control esiRNA and *MDFIC* esiRNA treated hLECs were investigated using RNA-sequencing (RNA-seq). The experimental workflow for this investigation is depicted in Figure 38.
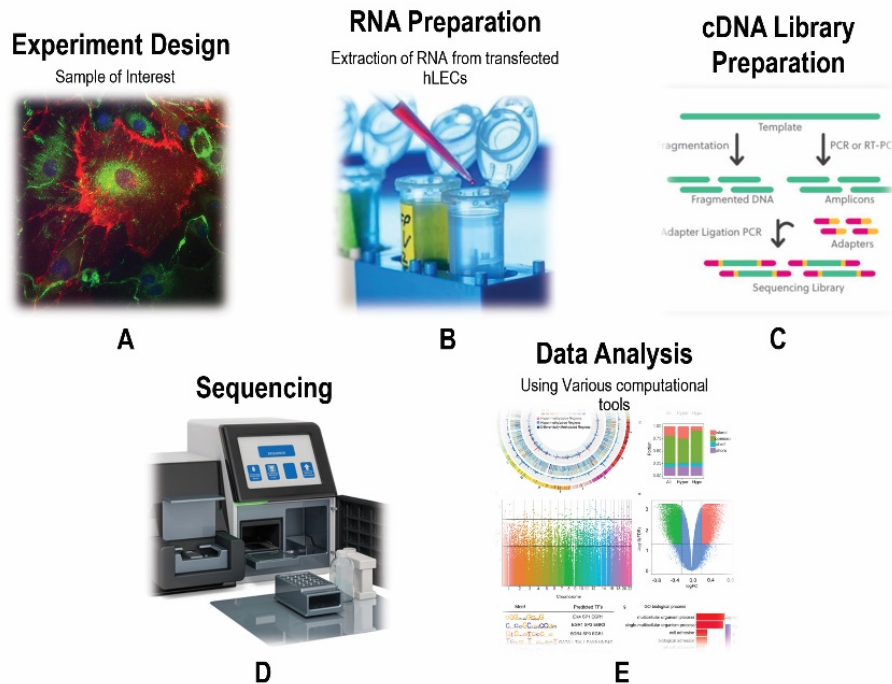
Figure 38 Experimental workflow for total RNA-seq analysis on control esiRNA and *Mdfic* esiRNA treated hLECs.

For analysing differential gene expression (DGE) in *MDFIC* esiRNA treated hLECs compared to control, three biological replicates were used to perform RNA-seq (hLECs batch 2, batch 4 and batch 5). (Isolated from different donors; lot numbers 7F3304, 0000254463, 4F3029 and 4F3037).

MDFIC gene knockdown via esiRNA was validated through both RT-qPCR by quantifying knockdown of mRNA (Figure. 39 A) and by Western blotting to investigate MDFIC protein levels (Figure.39 B). In both cases, reduced levels of MDFIC mRNA and protein were observed.
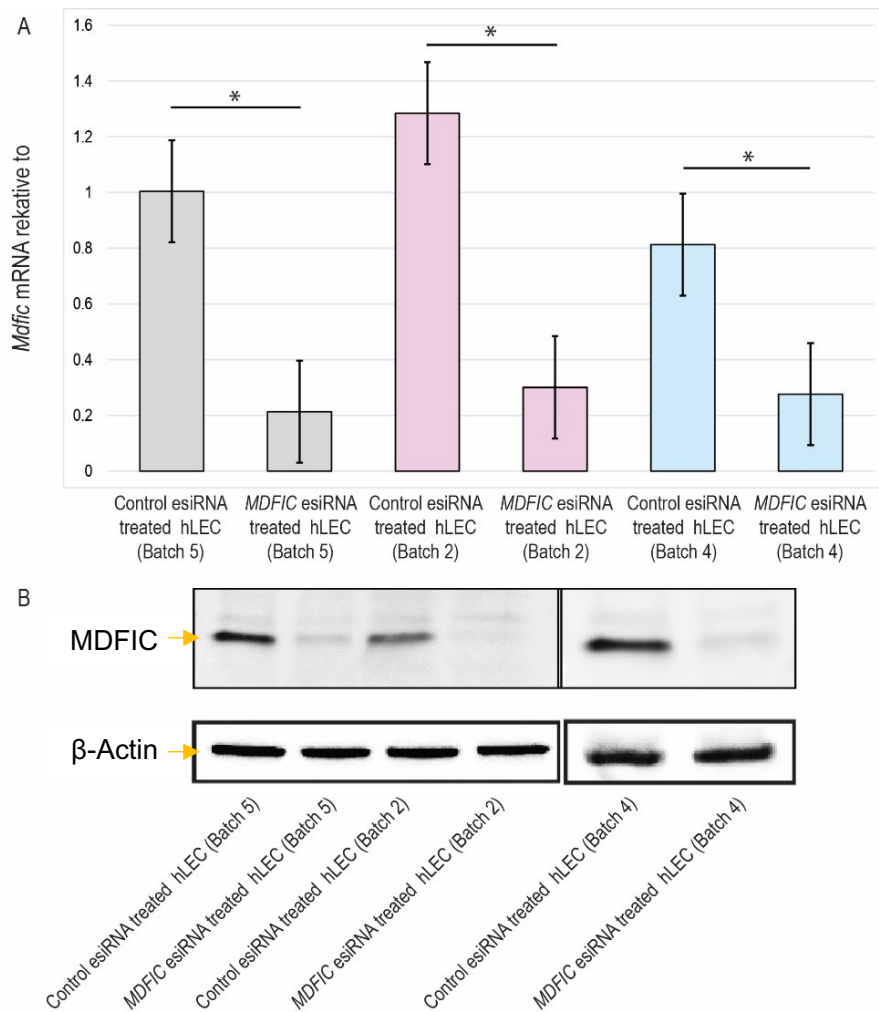
Figure 39. Relative knockdown of *MDFIC* gene expression levels in 3 independent batches of human lymphatic endothelial cells (hLECs). (A) Analysis of RNA isolated from control and *MDFIC* esiRNA treated hLECs (batch 5, 2, and 4). (B) MDFIC protein levels in control and *MDFIC* esiRNA treated hLECs. Decreased amounts of *MDFIC* mRNA and corresponding protein levels were detected in MDFIC knockdown hLECs compared to control cells. Error bars represent SEM (*p<0.05).

Levels of *GATA2* and *PROX1* mRNA were quantified and normalised to beta-actin mRNA, for both control and *MDFIC* esiRNA-treated hLECs in each batch. Elevated levels of *GATA2* mRNA were detected in batch 2 and 5, whilst decreased levels of GATA2 mRNA was seen in batch 4 in *MDFIC* esiRNA-treated hLECs compared to control cells. Varied levels of PROX1 mRNA were also shown across the different batches of hLECs. This data shows the variation among different samples and confirms the necessity of

using multiple biological samples/independent batches of cell lines in gene expression profiling studies (Figure. 40).
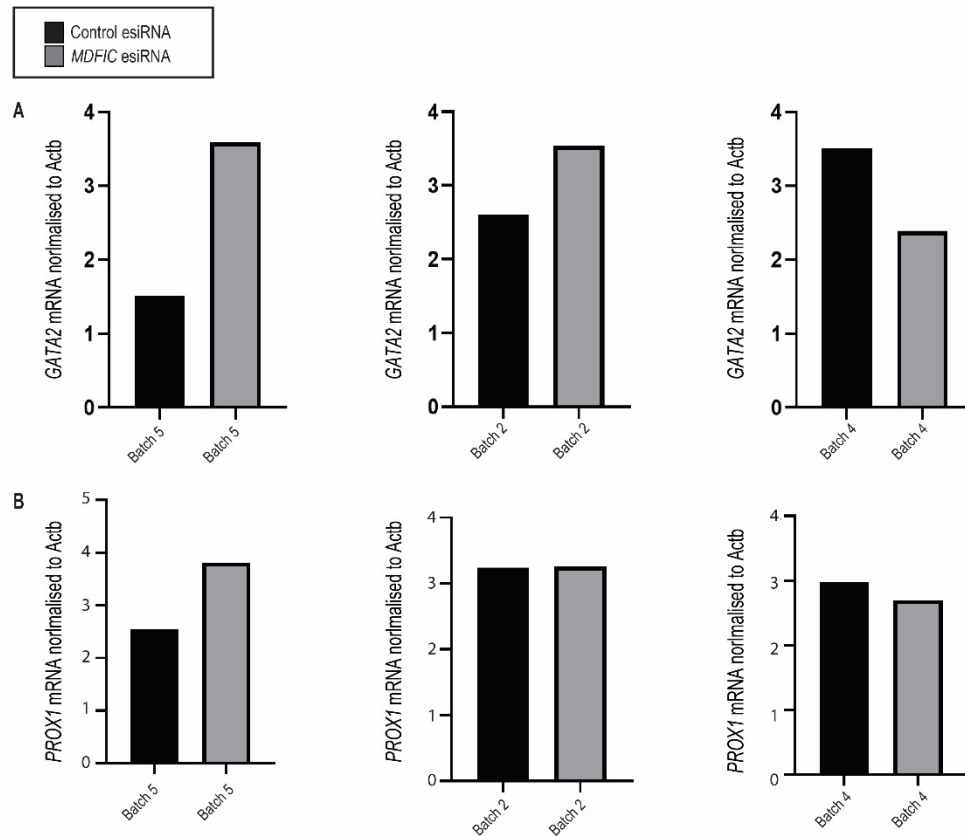
Figure 40. Expression levels of *GATA2* and *PROX1* vary among different biological replicates. Variation in *GATA2* and *PROX1* mRNA expression among different biological replicates is highlighted in this graph. (A) *MDFIC* deficient cells of batch 5 and 2 show elevated levels of GATA2, whereas decreased levels of GATA2 are observed in batch 4. (B) *PROX1* levels in *MDFIC* deficient hLECs are increased in batch 5, whilst no change was observed in either batch 2 and 4. Measurements of expression were normalised against the expression of the *ACTB* gene in the same sample.

4.6.1 Analysis of RNA-seq data

Sequencing reads were analysed using FastQC to assess quality and adapter contamination. Adapters were trimmed using cutadapt (Martin, 2011), then reads aligned to the hg19 reference genome using STAR (Dobin et al., 2013) PCR duplicates were removed using UMI-tools (Smith et al., 2017), Deduplicated reads were remapped using

STAR, and differential gene expression analysis performed on read counts produced by STAR using Bioconductor package edgeR. edgeR is an effective tool for differential expression analysis of RNA-seq expression profiles with biological replicates (Robinson et al., 2009). Lowly expressed genes were first filtered by requiring greater than 5 counts per million in at least three libraries. Normalisation factors were calculated using the calcNormFactors function of edgeR to enable accurate comparisons of gene expression between samples. Data were explored using multidimensional scaling (MDS) plots generated using the plotMDS function of edgeR, allowing assessment of replicate sample clustering and treatment effects (Figure. 41).

A linear model was fit to count data for each gene. A factor representing replicate was included in the model to account for differences between replicates. For genes to be called differentially expressed, a false discovery rate of (FDR<0.05) and fold change of (FC > 1.25 (log2FC 0.3)) was assigned. 319 differentially expressed genes (65 downregulated and 254 upregulated) were identified in MDFIC deficient cells compared to control treated hLECs (Figure. 42, Appendix table.8 and 9).
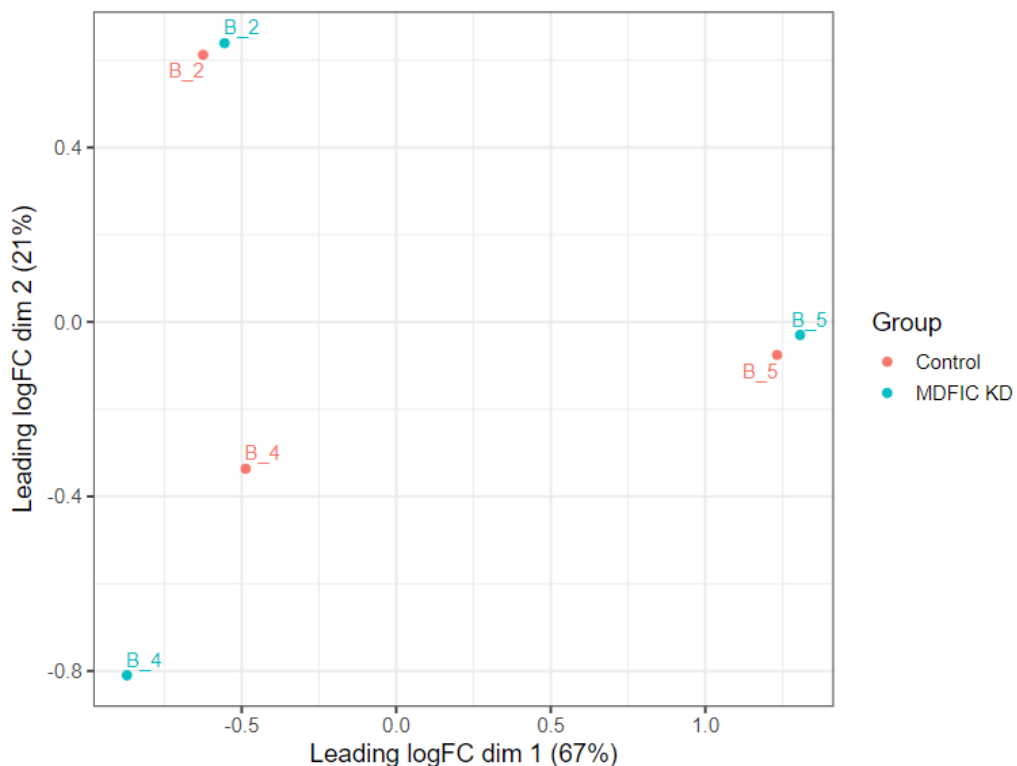
Figure 41. Multi-dimensional scaling (MDS) plot displaying overall variability in replicates. MDS plot visualises the difference between the expression profiles of Control and *MDFIC* esiRNA treated hLECs

(batch 5, 2 and 4). Replicate samples of the same batch cluster together, while samples from different batches form separate clusters, which indicates the differences between the three batches of hLECs are larger than those within batches (i.e. same batch of hLECs with different esiRNA treatments).
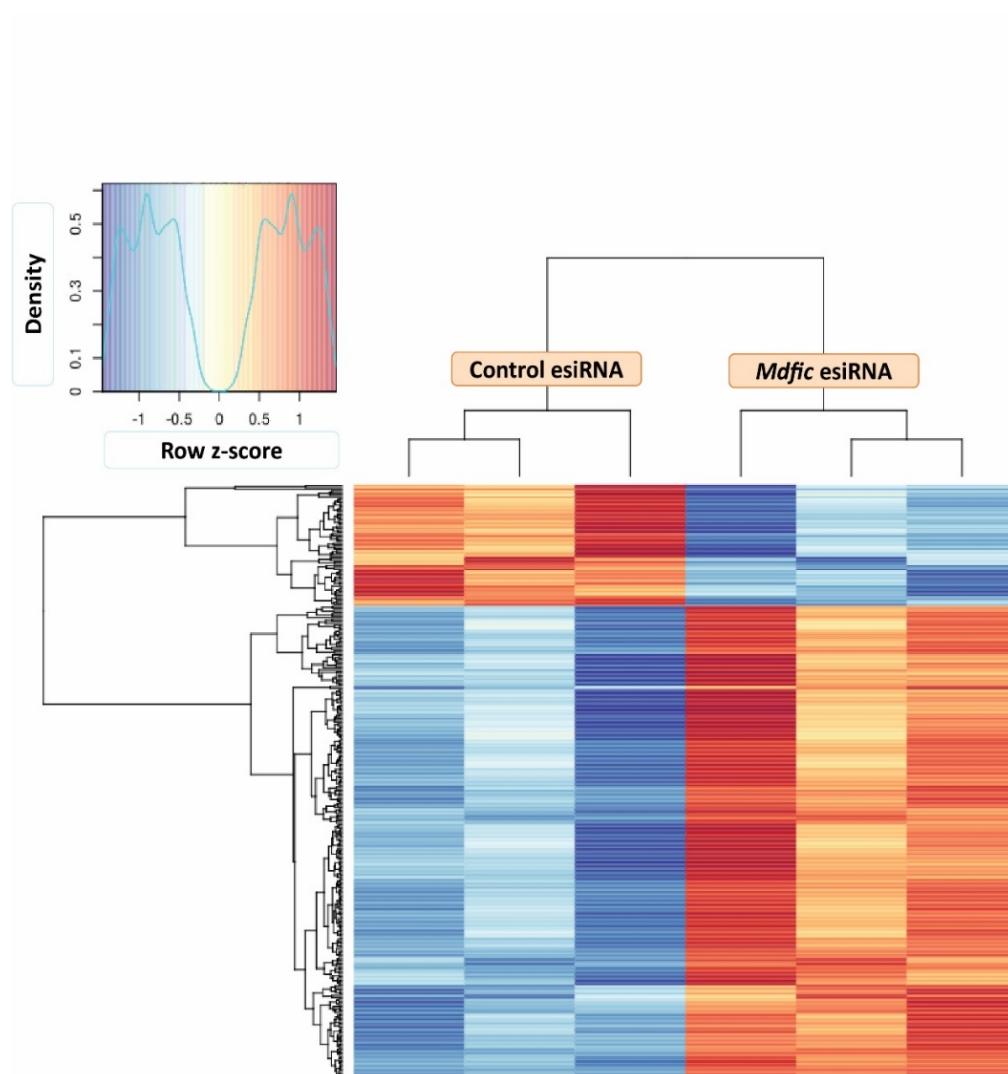
Figure 42. Heat map graph illustrating differentially expressed genes in MDFIC deficient cells compared to control treated hLECs. Heatmap comparing genes elevated (red) and decreased (blue) in expression in *MDFIC* esiRNA compared to control treated hLECs.

4.6.2 Validating the accuracy of RNA seq analysis

RNA-seq analysis data was confirmed for several important lymphatic genes using qRT-PCR by measuring the mRNA expression levels of *CDH5*, *VEGFC* and *ESAM* in hLECs treated with control and *MDFIC* esiRNA. In RNA-seq data showed that *CDH5* (1.4-fold) and *ESAM* (1.3-fold) were upregulated in *MDFIC* deficient hLECs, whilst *VEGFC* (1.3-fold) was downregulated (Appendix table 8 and 9, respectively). Similar levels of regulation were seen with qRT-PCR and Western blot (Figure. 43).

Upregulated genes in *MDFIC* deficient cells in compared to control treated hLECs

Gene	logFC	logCPM	LR	PValue	FDR
ESAM	0.389024	6.898431	17.9883	2.22E-05	0.002614
CDH5	0.535307	9.662647	14.42345	0.000146	0.010169

Downregulated gene in *MDFIC* deficient cells in compared to control treated hLECs

Gene	logFC	logCPM	LR	PValue	FDR
VEGFC	-0.34798	4.241051	10.87357	0.000975	0.035727

Figure 43. Validation of differentially expressed genes between control and *MDFIC* deficient hLECs. Increasing in level of ESAM and VECAD and decrease level of VEGFC in *MDFIC* deficient cells is consistent with differentially expressed gene analysis data.

4.6.3 Analysis of topmost differentially expressed genes upregulated in *MDFIC* esiRNA treated hLECs.

The volcano plot (Figure. 44) illustrates the topmost differentially expressed genes between control and *MDFIC* esiRNA-treated hLECs, whilst a more in-depth description of the top 9 upregulated genes (red) in *MDFIC* cells can be found in Table 6.
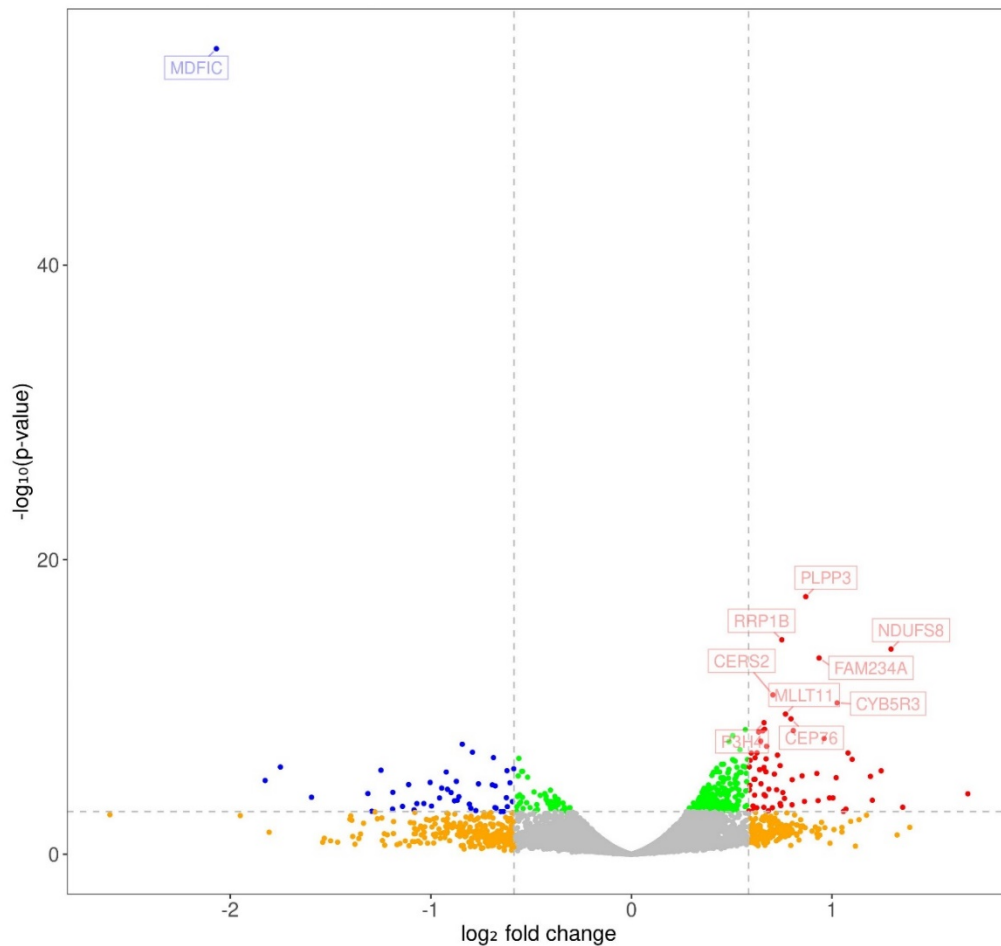
Figure 44. Volcano plot illustrating the *MDFIC* gene knockdown and topmost genes upregulated in MDFIC deficient human dermal lymphatic endothelial cells. *MDFIC* (blue, top left of graph) is the most differentially downregulated gene, illustrating efficient knockdown of *MDFIC*.

Table 6. Description of topmost differentially expressed genes upregulated in *MDFIC* esiRNA treated hLECs.

Gene Name		References
PLPP3 (Phospholipid Phosphatase 3)	PLPP3 is responsible for encoding lipid phosphate phosphatase (LPP3), which is an integral membrane enzyme. A heritable single nucleotide polymorphism (SNPs) in the PLPP3 gene has been identified to be associated with cases of coronary artery disease (CAD). CAD is a complex cardiovascular disease and leading cause of death worldwide.	Busnelli et al., 2018; Schunkert et al., 2011)
RRP1B (Ribosomal RNR processing 1B)	RRP1B is a novel candidate metastasis modifier. ECM gene expression was found to be consistently associated with Rrp1b expression. Expression of Rrp1b significantly alters ECM gene expression and tumour growth. RRP1B may also be a novel susceptibility gene for breast cancer progression and metastasis.	(Crawford et al., 2007; Lee et al., 2014)
CERS2 (Ceramide synthase 2)	CERS2 influences albuminuria. Fittingly SNP in *CERS2* has been associated with an increased rate of albuminuria and cardiovascular disease among patients with diabetes.	(Imgrund et al., 2009; Shiffman et al., 2014)
NDUFS2 (NADH: Ubiquinone Oxidoreductase Core Subunit S8)	*NDUFS2* mutations are associated with Mitochondrial Complex I Deficiency, which is an autosomal recessive disorder which has been found to cause a wide range of clinical symptoms, ranging from lethal neonatal disease to adult-onset neurodegenerative disorders including myopathy, liver disease, Leigh syndrome and cardiomyopathy.	(Loeffen et al., 2001; Ngu et al., 2012; marin et al., 2013)
P3H4 (Prolyl 3-Hydroxylase Family Member 4)	P3H4 is vital for cross-linking of collagen fibrils in regulating bone density and maintaining skin stability. Collagen fibrils are a major mechanical component in the extracellular matrix.	(Heard et al., 2016; Onursal., 2021)
CEP76 (Centrosomal Protein 76)	CEP76 is important in the cell cycle and localises to centrosomes and is expressed in a cell cycle-dependent manner. CEP76 is a centrosome-intrinsic factor that limits the reproduction of centrioles to once per cell cycle.	(Barbelanne et al., 2016; Hassan et al., 2008; Spektor 2007)

CYB5R3 (Cytochrome B5 Reductase 3)	CYB5R3 is located on the chromosome 22 and encodes a 34.2 kDa protein. Mutations in the gene can cause methemoglobinaemia types I and II, which are rare autosomal recessive diseases due to a deficiency in the isoform of NADH-cytochrome b5 reductase. *CYB5R3* deficiency was also found to be associated with neurological disorders. Loss of CYB5R3 in smooth muscle cells also showed to have an effect on the development of vascular and organ pathology including cardiopulmonary system in sickle cell disease.	(Percy and Lappin 2008; Wood et al., 2019)
FAM234A (Family with sequence similarity 234 Member A)	FAM234A is a protein encoded by the ITFG3 gene. Little is known about the function of this gene. An a^0-thalassaemia deletion has been found within the second intervening sequence of the FAM234A gene which is associated with multiple red blood cell phenotypes in African Americans.	(Ravenhill et al., 2019)
MLLT11 (Myeloid/Lymphoid or Mixed-Lineage Leukemia; Translocated To, 11)	MLLT1 was first identified in leukaemia cells as a fusion partner for mixed lineage leukaemia (MLL) protein. MLLT11 is a 90 amino acid protein with highly conserved residues, containing a MLLT11 motif and a nuclear export signal. MLLT11 is an oncogenic protein, although its function in haematopoietic malignancies is not well understood. MLLT11 also plays a role in cell fate specification. Recent findings demonstrate that MLLT11 is a marker for post-mitotic neurons and suggests a role in neuronal differentiation or maintenance during development.	(Parcelier et al., 2011; Yamada et al., 2014).

4.6.4   Biological process analysis

An enrichment analysis web tool (WebGestalt (WEB-based Gene SeT AnaLysis Toolkit) was used for the assessment of gene pathways and biological processes most highly affected by *MDFIC* knockdown. This revealed a significant enrichment of genes involved in biological processes associated with vascular development (Figure. 45), including some with established roles in lymphatic vessel valve development, for which MDFIC is crucial (Table 7 and Appendix table.10). Over-Representation Analysis (ORA) method was employed, and biological process analysis was performed via the gene ontology (GO) database (http://www.webgestalt.org/).
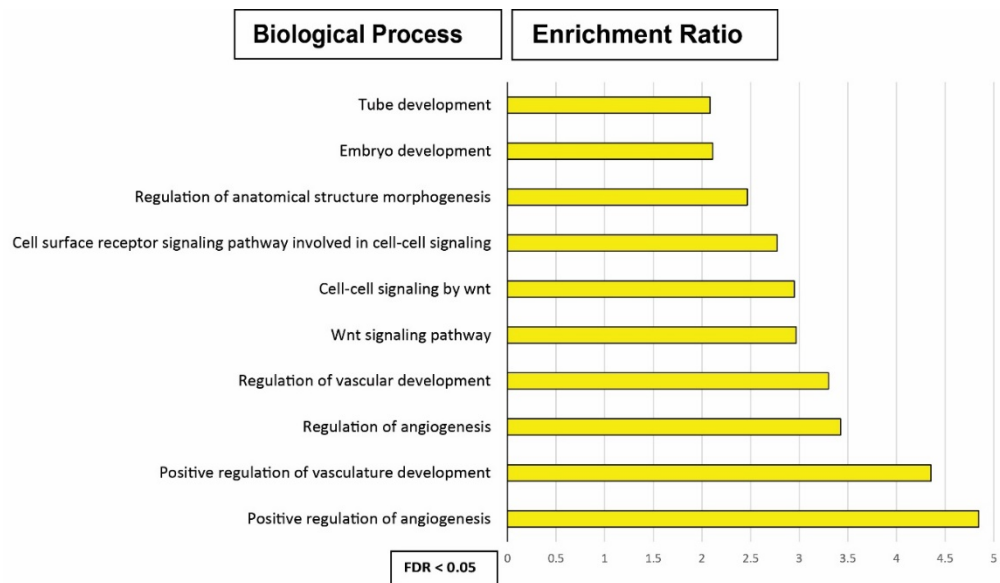
Figure 45. Biological process analysis on differentially expressed genes in *MDFIC* deficient hLECs. Biological processes associated with differentially regulated genes in *MDFIC* deficient hLECs.

Table 7. Differentially regulated genes with established roles in lymphatic vessel valve development in *MDFIC* deficient hLECs.

Differentially expressed genes with established roles in lymphatic vessel valve development		Fold change
VEGFC	VEGFC signalling is crucial for sprouting and migration of PROX-1 positive LECs from the veins to form the initial lymphatic plexus, lymph sacs and valve development (Karkkainen et al., 2004).	1.27
ITGA9	ITGA9 is an essential regulator of the morphogenetic processes controlling the formation of lymphatic valve leaflets (Alitalo et al., 2005).	1.89
CDH5	VE-cadherin (encoded by *CDH5*) regulates vascular mechanotransduction (Dejana & Vestweber, 2013). Well-established regulator of endothelial permeability (Giannotta et al., 2013). Differential expression in the lymphatic vasculature helps establish discontinuous "button" junctions in the lymphatic capillaries and continuous "zipper" junctions in the larger lymphatic collecting vessels (Baluk et al., 2007). VE-cadherin is particularly required for the valve maturation step.	1.44
PIEZO1	Mechanosensitive ion channel PIEZO1 was shown to regulate the condensation and elongation steps of valve formation (Fotiou et al., 2015b; Nonomura et al., 2018). Piezo1 activation induces cytoskeletal remdoeling and changes in cell-cell adhesion (Bon et al., 2019).	1.42
SOX18	Sox18 initiates the transactivation of *Prox1* promoter during LEC fate induction (Francois et al., 2011).	1.38
FLI1	FLI1 regulates haematopoietic cell differentiation and haemorrhage crucial for endothelial development (Hart et al, 2000; Spyropoulos et al., 2000).	1.35
NFATC1	NFATc1 controls the morphogenesis of cardiac valves and is expressed in the developing lymphatic vasculature and intraluminal valves (Johnson et al., 2003; Wu et al., 2011).	1.27

4.6.5   Gene set enrichment analysis

Direct interaction of MDFIC with GATA2 was shown earlier. In order to investigate the possible impact of MDFIC on the transcriptional activity of GATA2, gene set enrichment analysis was performed comparing gene expression changes in *MDFIC* deficient hLECs with genes either up-or down-regulated in GATA2 ChIP-seq data (*i.e.,* GATA2 target genes) in response to siRNA treatment. A significant overlap was revealed in genes established to be transcriptional targets of GATA2 (Figure. 46). Genes downregulated in response to siRNA treatment in the GATA2 experiment were significantly enriched in the MDFIC knockdown experiment (FDR < 0.05). The leading edge of this analysis consisted of 175 genes 40 of which were significantly upregulated in *MDFIC*-deficient cells. These included *ITGA9, ESAM, FLI1* and *SOX18* which are important in lymphatic vessel development (Appendix Table.11) (Figure. 47). These data provide compelling evidence in support of the hypothesis that pathogenic *MDFIC* variants impact lymphatic vessel valve development by interfering with the localisation and transcriptional activity of GATA2.
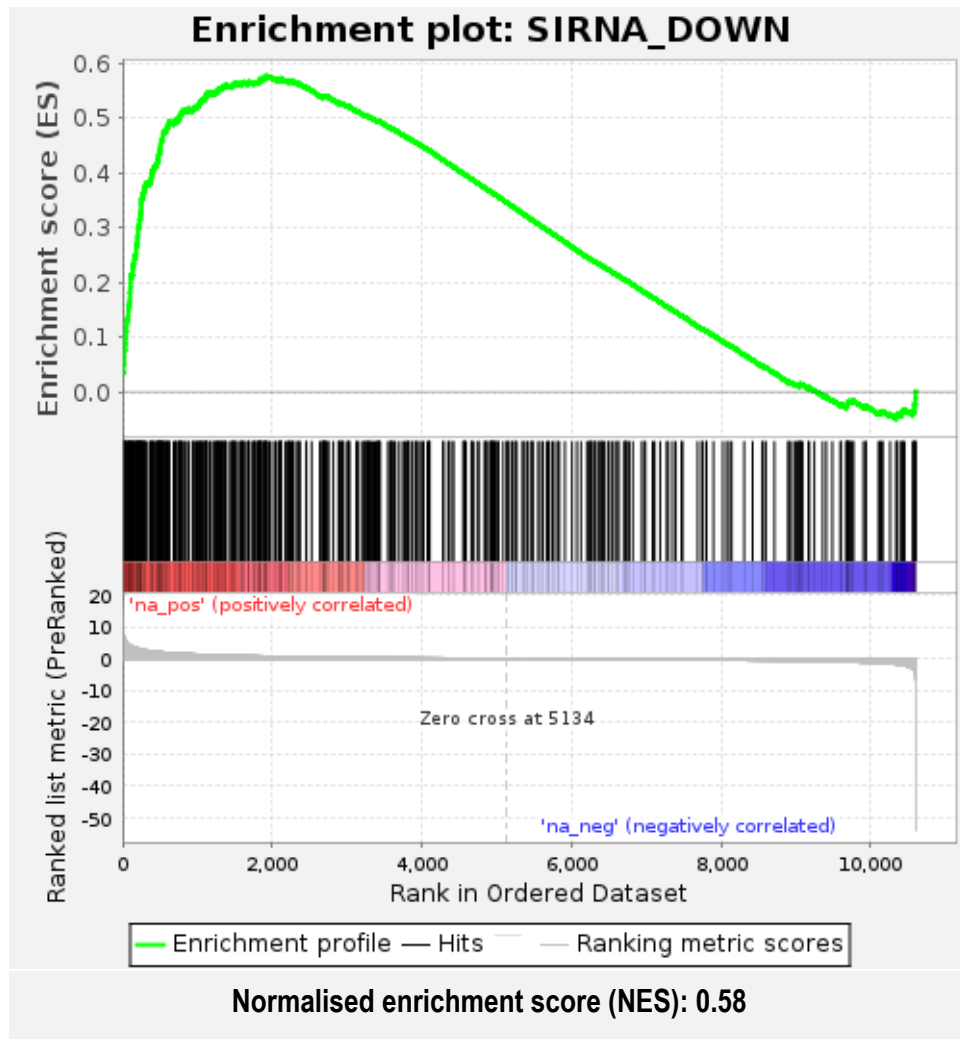
Figure 46. Gene expression analysis reveal enrichment of GATA2 target genes in *MDFIC* deficient hLECs. Gene set enrichment analysis (GSEA) comparing genes increased in expression in *MDFIC* deficient hLECs with GATA2 target genes reveals significant overlap.
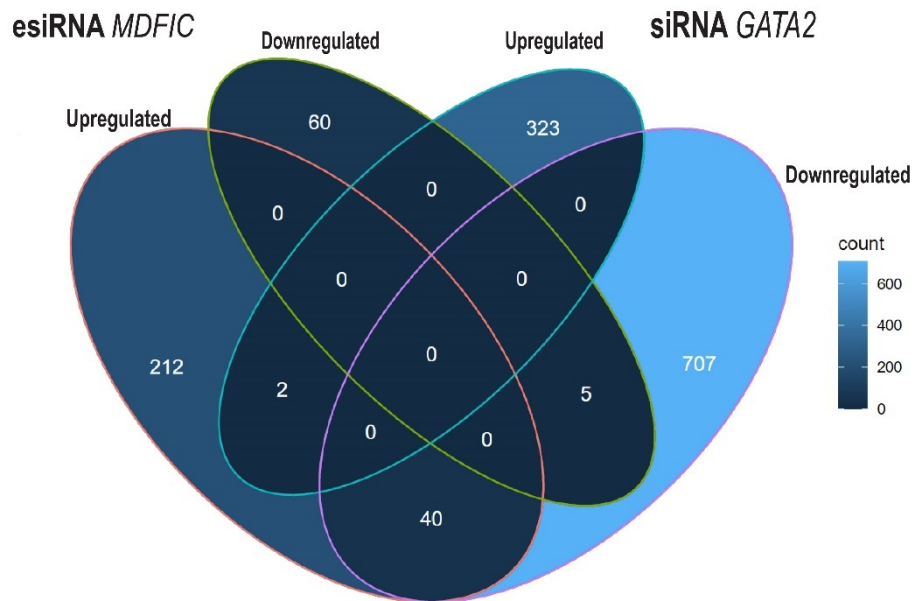
Figure 47. Venn diagram illustrating 40 mutual genes in differentially upregulated genes in *MDFIC* deficient cells and genes downregulated in *GATA2* deficient cells. Comparing genes most differentially upregulated in expression in *MDFIC* deficient cells with a GATA2 target genes database revealed 40 mutual genes including genes important in lymphatic vessel development.

4.7 Alteration in GATA2 localisation in the lymphatic vasculature of *Mdfic^M131*/M131*^* mutant mice

To assess whether the localisation and transcriptional activity of GATA2 is also altered *in vivo*, mesenteries dissected from wild-type and mutant *Mdfic^M131fs*/M131fs*^* embryos at E18.5 were stained with GATA2 and VE-Cadherin (a marker of lymphatic vessel valve maturation and LEC junctional marker, respectively) and mounted with DAPI to determine where nuclei are. Localisation of GATA2 was quantified in lymphatic vascular valves using high-resolution confocal microscopy and ImageJ was utilised to quantify the ratio of nuclear to cytoplasmic GATA2 based on the measure of area GATA was stained. A substantial level of GATA2 was observed in both the nucleus and cytoplasm of lymphatic endothelial cells in the mesenteric lymphatic vessels of both wild-type and mutant mice. However, decreased levels of GATA2 were observed in the nucleus of lymphatic endothelial cells in *Mdfic^M131fs*/M131fs*^* mesenteries compared to control littermates, whilst no significant change in the level of cytoplasmic GATA2 was observed (Figure. 48 A and

B). These subcellular localisation data are consistent with an interaction of MDFIC with GATA2, and suggest that the effect on GATA2 function might be different for a complete loss of full-length MDFIC (*e.g.* hLECs treated with esiRNA) compared to a truncated protein such as M131fs* (loss of cysteine-rich C-terminal domain). These findings add to our previous findings that the interaction of GATA2 and MDFIC depends on the cysteine-rich C-terminal domain in the MDFIC, but also suggests the potential existence of a third factor/element that interacts with both MDFIC and GATA2. The interaction of MDFIC with a third factor is likely not dependent on the cysteine-rich C-terminal domain in MDFIC sequence.

These data reveal that loss of full-length MDFIC *in vitro* might not be equivalent to the impact of truncated MDFIC[M131*] variant *in vivo*, with respect to GATA2 localisation and activity.
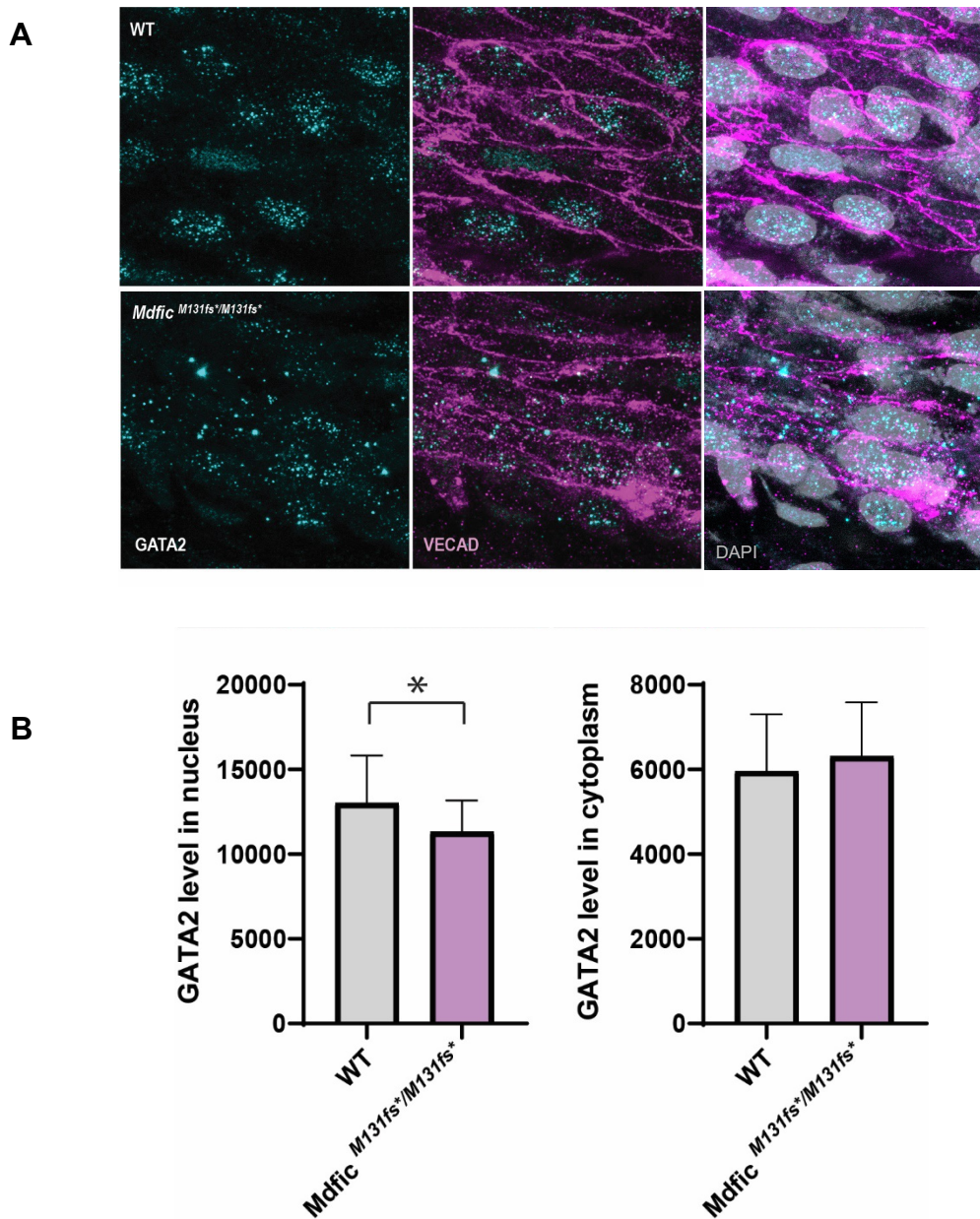
Figure 48. GATA2 levels in mesenteric lymphatic vessel valve cells. (A) Immunostaining using VE-cadherin (purple) to demarcate the cell border revealed GATA2 (cyan) is found in both the cytoplasm and nucleus of both wild-type (WT) and $Mdfic^{M131fs*/M131fs*}$ mesenteric lymphatic vessel valve cells. (B) Quantification of immunostaining indicated that in $Mdfic^{M131fs*/M131fs*}$ valve cells levels of nuclear GATA2 decreased significantly, whilst cytoplasmic GATA2 was only slightly increased. Error bars represent SEM, *$p<0.05$. 3 WT and 3 $Mdfic^{M131fs*/M131fs*}$ from 3 different litters were used for this analysis.

4.8 *MDFIC* deficient hLECs exhibit elevated ERK activity

To investigate whether the activity of ERK/MAPK is affected by *MDFIC* deficiency in hLECs, control and *MDFIC* esiRNA-treated hLECs were serum starved and then stimulated with full media or the potent lymphangiogenic growth factor VEGFC. In both cases, phosphorylation of ERK was rapidly promoted. In the case of *MDFIC* deficient cells treated with full media or VEGFC (Figure. 49, A and B), levels of phosphorylated ERK were significantly increased compared to control cells 15 minutes following stimulation These data suggest that activity of the RAS/MAPK pathway is increased in the setting of MDFIC deficiency, which could be proposed to be the scenario in the case of biallelic truncating *MDFIC* variants in patients, raising the question as to whether dampening activity of this pathway might provide a therapeutic opportunity for the treatment of CCLA caused by MDFIC variants.
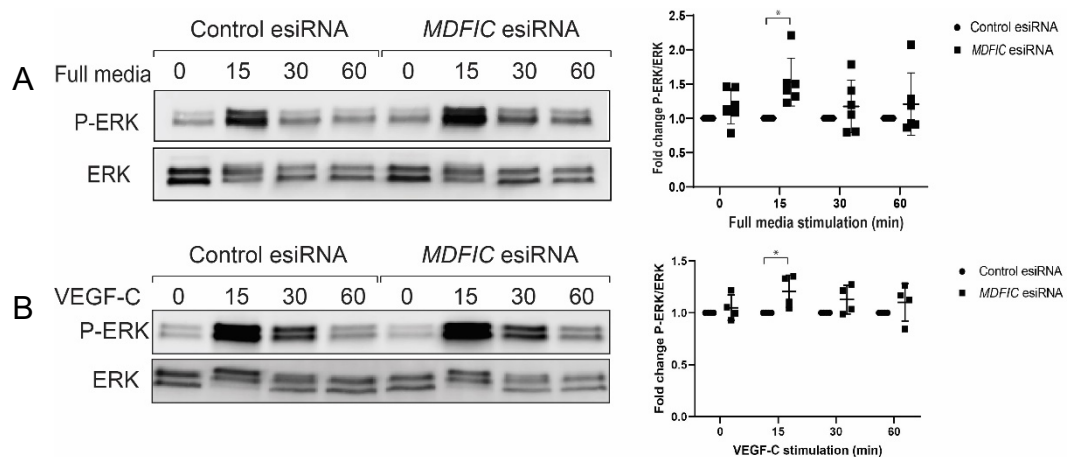
Figure 49. Elevated ERK activity in MDFIC deficient hLECs. Stimulation of serum starved, control and *MDFIC* esiRNA treated hLECs with full media (A) and VEGFC (B) initiates robust ERK phosphorylation, which is increased in MDFIC deficient cells. Quantification of ERK phosphorylation in 6 independent experiments is represented as fold change in P-ERK/ERK in MDFIC deficient, compared to control hLECs. Error bars represent SD, N=6, *$p<0.05$, calculated using Kruskal-Wallis test. Measurements of expression were normalised against the expression of the *ACTB* gene in the same sample. (VEGFC western blot was performed by Drew Sutton).

4.9 Investigation of small molecule inhibitors for correction of RAS/MAPK signalling in *MDFIC* esiRNA treated hLECs

To determine whether small molecule inhibitors of the RAS/MAPK signalling pathway might prove to be effective in correcting the level of ERK1/2 activity in *MDFIC* esiRNA treated hLECs, we assessed whether Trametinib was effective in reducing ERK phosphorylation back to levels observed in control esiRNA-treated hLECs. Trametinib is a small molecule inhibitor of MEK1/2 that prevents Raf dependent MEK phosphorylation and activation, which subsequently reduces the ERK activity. We hypothesised that Trametinib might potentially rescue the lymphatic phenotypes that result from *MDFIC* variants in patients and mice. Trametinib was used effectively by Li and colleagues in a study where a gain-of-function (GOF) *ARAF* mutation was found to underlie CCLA. In their study, they successfully rescued the elevated activity of *ARAF* in primary hLECs *in vitro*, in a zebrafish model *in vivo,* and ultimately, in patients with ARAF gain-of-function mutations (Li et al., 2019) . In this study, a high dosage of Trametinib was used since ERK activity was tremendously elevated due to the gain-of-function *ARAF* mutation. In *MDFIC*-deficient hLECs, elevated levels of phospho-ERK were detected when compared to control esiRNA-treated cells, though levels of active ERK due to *MDFIC* mutation were much lower than those observed as a result of the *ARAF* GOF mutation. To identify the appropriate dosage of trametinib to reduce ERK phosphorylation back to baseline in *MDFIC* deficient cells, a dose response assay was undertaken.

Control and *MDFIC* esiRNA treated hLECs were serum starved and then stimulated with full media, together with a range of concentrations of Trametinib diluted in dimethyl sulfoxide (DMSO) (300nM, 100nM, and 30nM) for 15 min. No P-ERK signalling was detected in either control or *MDFIC* deficient hLECs treated with trametinib, indicating complete inhibition of a signal in the pathway at these concentrations (Figure. 50). Moreover, a surprisingly slight decrease in levels of P-ERK/ERK in *MDFIC* deficient cells compared to control cells was observed. We hypothesise that DMSO had a negative effect on hLECs, more so on *MDFIC* deficient than control hLECs.
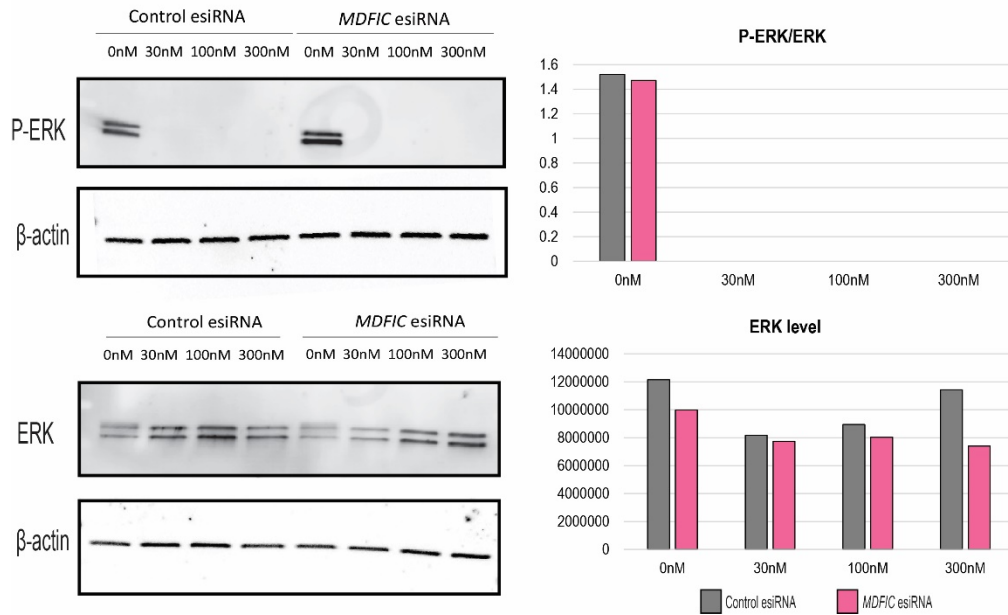
Figure 50. **Complete inhibition of ERK phosphorylation in control and *MDFIC* esiRNA treated hLECs treated with 300nM, 100nM and 30nM trametinib.** Stimulation of serum starved, control and *MDFIC* esiRNA treated hLECs with trametinib and full media completely inhibited the phosphorylation of ERK.

This experiment was repeated with lower dosages of trametinib. Control and *MDFIC* esiRNA-treated hLECs were serum starved and then stimulated with full media and trametinib diluted in DMSO (10nM, 2nM, and 0.5nM) for 15 min. To investigate whether DMSO has toxic effects on hLECs in this experiment, one additional control was added where hLECs had no treatment at all. For these lower dosages of trametinib, partial inhibition of ERK phosphorylation was achieved even down to 0.5 nM (Figure. 51). This finding confirmed suitable concentrations of trametinib to be used for future experiments (10nM, 2nM, and 0.5nM).
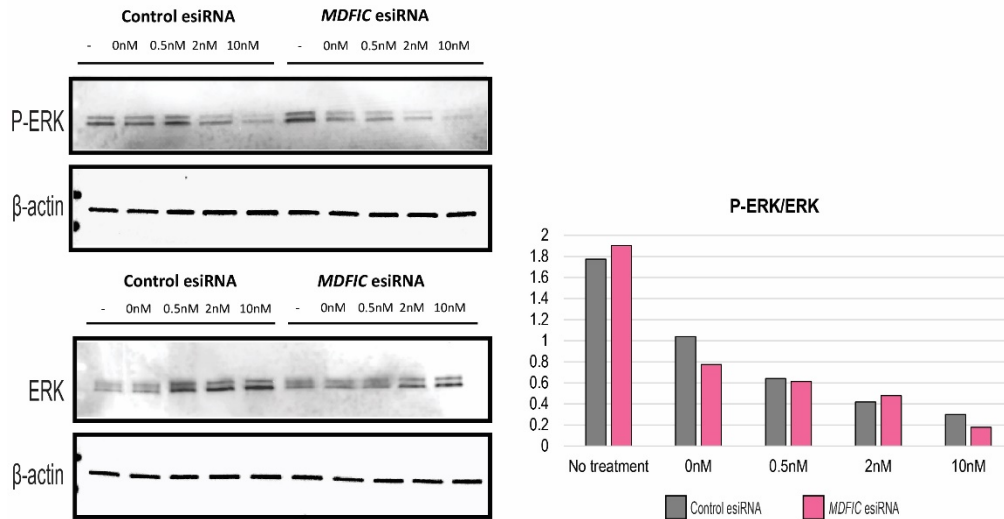
Figure 51. Levels of ERK phosphorylation decrease when treated with 0.5nM, 2nM and 10nM trametinib. Stimulation of serum starved, control and *MDFIC* esiRNA treated hLECs with trametinib showed decrease in levels of phosphorylation of ERK.

Interestingly, the elevated level of phosphorylated ERK was observed once again in *MDFIC* deficient hLECs, confirming our finding earlier that the RAS/MAPK pathway is increased in the setting of *MDFIC* deficiency. However, decreased P-ERK/ERK in *MDFIC* deficient cells compared to control cells was again seen with 0.4% DMSO alone (0nM in Figure 51), suggesting that DMSO generally inhibited ERK phosphorylation due to possible toxic effects on human dermal endothelial cells. This possibility was further investigated, and it was found that recently the off-target effect of DMSO was demonstrated in functional signalling networks and their downstream substrates. A study by Baldelli and colleagues revealed that even an ultra-low DMSO concentration (e.g. 0.002% and 0.004% *v/v*) has broad and heterogeneous effects on signalling proteins (Baldelli et al., 2021).

Therefore, in addition to trametinib dosage optimisation, careful optimisation of DMSO concentrations used in experiments is essential to be addressed in future work.

4.10 Discussion

In previous chapters, we identified novel pathogenic *MDFIC* variants underlying the severe complex lymphatic vascular anomaly CCLA and demonstrated a crucial role of MDFIC in lymphatic vessel valve development. Here we investigated the cellular and biological mechanisms by which *MDFIC* variants interrupt normal MDFIC function. Phenotypic analysis of a *Mdfic* mouse model in addition to protein work demonstrated that *Mdfic* mRNA and protein are most highly expressed in valves in the lymphatic valve vasculature.

Through protein analysis, we found that a C-terminal truncating variant (p.M131Nfs*3) in MDFIC is not susceptible to nonsense mediated decay and gives rise to a truncated protein. This results in loss of MDFIC function with respect to appropriate subcellular localisation and interaction with other transcriptional regulators possibly via deletion of the SMB domain region. Our findings on the stability of MDFIC however revealed C-terminal truncating variant (p.M131Nfs*3) in MDFIC resulting in truncated protein can lead to possible gain of function with respect to protein stability. Our data suggests that full-length MDFIC protein is post-translationally regulated and subject to rapid proteasomal degradation, however, the stability of the truncated MDFIC M131fs* protein is increased upon removal of the cysteine-rich C-terminus, or as mentioned earlier more protein is retained within the cell, particularly in valve endothelial cells. Given that MDFIC is known for tethering with other transcription factor, elevated levels of MDFIC protein in the lymphatic valve where FOXC2 and GATA2 are elevated suggest that this truncated protein can result in a negative gain of function which subsequently disrupts lymphatic valve development. The mechanisms via which *Mdfic* mRNA is selectively transcribed or the protein selectively stabilised in valve territories remain to be established.

Further analysis revealed that MDFIC protein co-precipitates with GATA2 and is stabilised when ectopically expressed with GATA2, FOXC2, and NFATC1. This data confirms that MDFIC is stabilised in valve-forming territories. We further studied the localisation of GATA2 *in vitro* using primary hLECs treated with control and *MDFIC* esiRNA and *in vivo* by staining the mesenteric tissues dissected from wild-type and *Mdfic*^{M131fs*/M131fs*} embryonic mice. Preliminary *In vitro* findings indicated increased levels

of GATA2 in the nucleus of *MDFIC* deficient hLECs. However, quantification of the level of GATA2 in lymphatic endothelial cells *in-vivo* showed a decreased trend in the levels of GATA2 in the nucleus of these cells. These findings together confirm our prediction that MDFIC interacts with GATA2 and alters its subcellular localisation but also suggest that loss of full-length MDFIC *in vitro* is possibly not equivalent to the impact of truncated *Mdfic*[M131fs*] *in vivo*, with respect to GATA2 localisation and activity. The existence of other factors/elements directly interacting with both GATA2 and MDFIC is also a possibility and cannot be ruled out. The presence of a trio interaction might control the nuclear localisation of GATA2 in cells. There is also a possibility that GATA2 and MDFIC are part of a larger complex that facilitates this protein-protein interaction. While full-length MDFIC has the capacity to interact with both GATA2 and possibly unknown factors (Figure. 52A), *MDFIC* esiRNA-treated cells lose that ability, resulting in the release of tethered GATA2, which subsequently moves into the nucleus (Figure. 52B). However, truncated *Mdfic*[M131fs*] is hypothesised to lose interaction with GATA2 due to deletion of the cysteine-rich C-terminus including the SMB domain, and remains connected to an unknown factor, which possibly has a different binding site in MDFIC. Subsequently, the interaction of an unknown factor with GATA2 also remains intact and inhibits GATA2 translocation in the cells, thereby disrupting lymphatic valve development (Figure. 52, C).
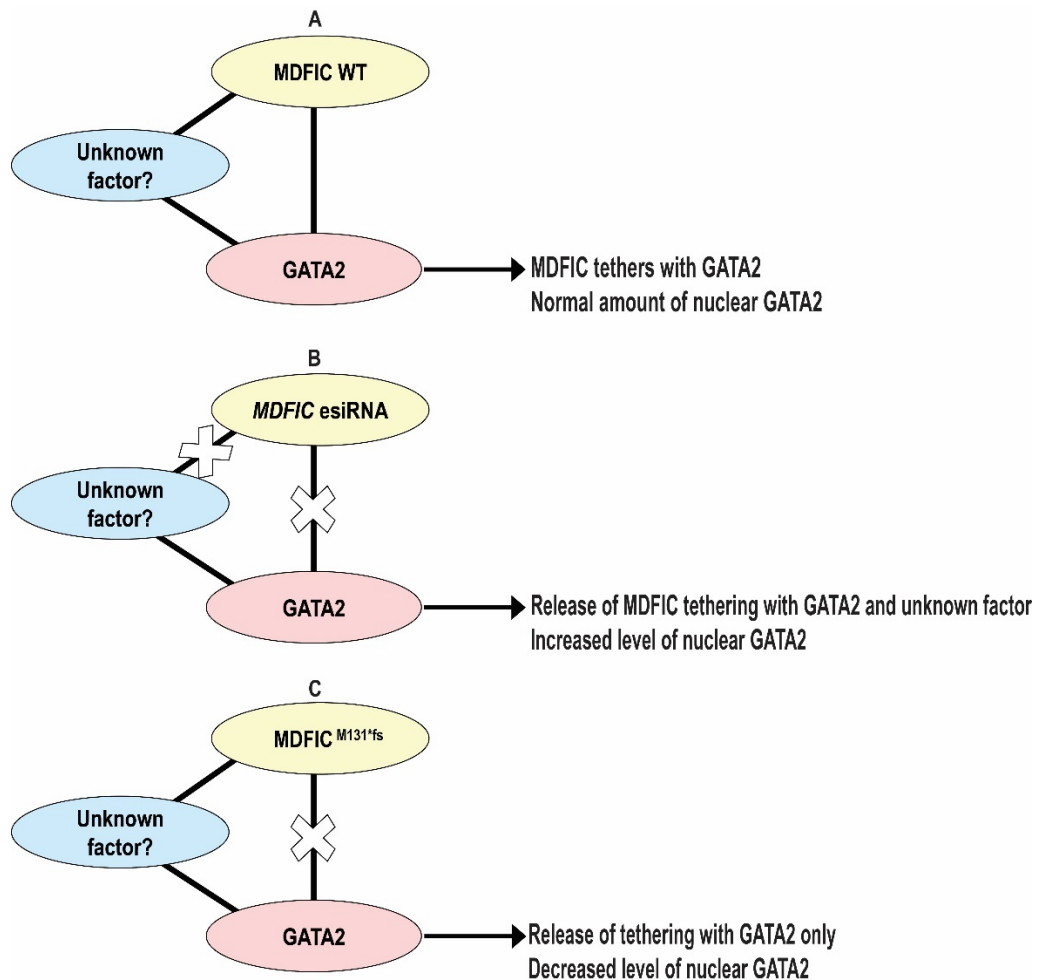
Figure 52. Proposed model of a trio interaction of MDFIC, GATA2 with and an unknown factor. (A) Depicts full-length MDFIC interacts with both GATA2 and an unknown factor and leads to normal GATA2 expression levels in the nucleus. (B) Illustrates that *MDFIC* esiRNA results in total loss of MDFIC function, thereby disrupting interaction of MDFIC with GATA2 and the unknown factor, leading to translocation of excess amounts of GATA2 to the nucleus and subsequently increased levels of GATA2 in the nucleus. (C) Shows truncated MDFIC M131fs* remains connected to an unknown factor, whilst losing direct interaction with GATA2. Here GATA2 and the unknown factor remain intact, keeping GATA2 in the cytoplasm and leading to decreased expression of GATA2 in the nucleus.

It is important to consider that the LECs chosen for *in vivo* analysis were only from the valve region territory, which is not properly formed in our mutant animal model. Therefore, there is a possibility that the level of GATA2 in lymphatic vessels of mutant tissues was generally lower in cells because lymphatic valve development was arrested in these regions. Future work will address these possibilities and the proposed trio model.

To confirm whether MDFIC has an impact on the transcriptional activity of GATA2, gene expression profiles of control esiRNA and *MDFIC* esiRNA-treated hLECs were investigated using RNA sequencing. For this purpose, lymphatic endothelial cell lines from 3 different donors were used. The primary analysis showed significant biological variation in these cell lines which was further confirmed in the MDS plot displaying significant differences in expression profiles of control and *MDFIC* esiRNA treated hLECs. This finding highlighted the importance of using biological replicates in gene expression profiling studies. Assessment of the most differentially regulated genes revealed enrichment of genes involved in biological processes associated with vascular development including some with established roles in lymphatic vessel valve development. Comparison of genes increased in MDFIC-deficient hLECs, also showed significant overlap in genes established to be transcriptional targets of GATA2. Together, these data provide preliminary evidence that pathogenic *MDFIC* variants impact lymphatic vessel valve development by interfering with the localisation and transcriptional activity of GATA2. Further investigation is required to confirm this hypothesis.

Furthermore, in this study, we took experimental approaches to characterise the mechanism by which MDFIC controls signalling pathways in the cells. Recent work by Li and colleagues identifying a gain-of-function *ARAF* mutation in a CCLA patient whose symptoms were greatly improved following treatment with the MEK inhibitor trametinib, provided an outstanding example of the power of identifying the genetic and molecular basis of this human disease (Li et al., 2019). This study also brought up the possibility that MDFIC might influence the activity of RAS/MAPK signalling. This question was raised due to similarities in lymphatic phenotypes reported in our MDFIC patients and those with lymphatic anomalies due to mutations in components of the RAS/MAPK signalling pathway. *In vitro* analyses showed a significant increase in the level of phosphorylated ERK in *MDFIC* deficient hLECs treated with either full media or VEGFC, suggesting that biallelic truncating *MDFIC* variants in patients might also result in increased MAPK/ERK signalling activity. Future work will address whether the dampening activity of this pathway might provide a therapeutic opportunity for the treatment of CCLA caused by MDFIC variants and will assess the level of RAS/MAPK pathway activity *in vivo*. Additional investigation is required to identify which components of the RAS/MAPK pathway leading to ERK phosphorylation are most impacted by loss of MDFIC. Once the

association of *MDFIC* variants in dysregulation of the RAS/MAPK signalling pathway is confirmed, it should be assessed whether small molecule inhibitors of RAS/MAPK signalling pathway, such as trametinib, selumetinib, dabrafenib or other FDA-approved MEK inhibitors that are active in clinical development might prove to be effective in rescuing or halting the phenotypes that result from *MDFIC* variants in patients and mice.

Chapter 5: Final discussion and future direction

5.1 Discussion

The latest report published by the Australian government on prenatal, stillbirth and neonatal death indicates that every day in Australia, 6 babies are stillborn, and 2 babies die within 28 days of birth (neonatal death). Unfortunately, even with modern advances in medical and healthcare practices, the proportion of deaths due to these conditions has not changed over the past two decades (Figure.2).

The majority of stillbirth cases occur between 20-22 weeks followed by 23-36 weeks of gestation. Various underlying causes leading to stillbirth have been identified. However, based on the latest records in Australia (2018), congenital abnormalities and unexplained causes were the main reasons for stillbirth before and after 28 weeks of gestation, respectively; congenital abnormality (31.3%) <28 weeks of gestation, unexplained causes (39.9%) >28 weeks of gestation).

Genetic screening (whole exome/genome sequencing) provides an opportunity for the detection of the molecular origin of congenital abnormalities and these unexplained perinatal deaths. Genetic studies are a powerful tool to provide answers to families affected by these distressing conditions and a valuable approach to provide them with an accurate diagnosis of the cause of stillbirth and perinatal death to enable safe and viable future pregnancies.

In that regard, the Genomic Autopsy Study research program was initiated in Adelaide by Hamish Scott and Chris Barnett to address the genetic contribution of perinatal death and stillbirth. The aim of the program has been to privide better diagnosis, prevention, and treatment to reduce the occurrence of these devastating conditions in Australia.

In 2016, through genomic autopsy of an affected non-consanguineous family in Adelaide, South Australia, with two diagnosed foetuses with hydrops fetalis exhibiting lymphoedema, pleural and pericardial effusions, two unknown pathogenic variants of *MDFIC* were identified. Through the exchange of information with national and international collaborators to identify similar cases around the world, five more families were found carrying *MDFIC* variants and patients displaying similar phenotypes, which have been diagnosed as central conducting lymphatic anomaly (CCLA). CCLA is a severe congenital lymphatic malformation characterised by dysfunctional central

collecting lymphatic vessels including the thoracic duct. The failure of lymphatics to return lymph to the bloodstream in this disorder results in lymph reflux into tributary vessels resulting in pleural, pericardial effusion, peritoneal effusion and lymphoedema. Effusions in the pleural and pericardial spaces are particularly damaging, as they impact heart and lung function.

When this study started, very little information was published on MDFIC. MDFIC was identified as a 246 amino acid protein which was documented to regulate the activity of other transcription factors by tethering them in the cytoplasm and preventing their access to the nucleus. The C-terminal region of MDFIC harbours a unique, cysteine-rich domain, demonstrated to mediate interactions of MDFIC with transcription factors including the glucocorticoid receptor (GR), HAND1 and TCF/LEF family members with key roles in the regulation of WNT signalling. No association or possible role of MDFIC with cardiovascular development had been reported before this study.

Upon confirming the high expression of MDFIC and its localisation in cardiovascular tissues in the mouse embryo, we generated a mouse model mimicking the *MDFIC* homozygous truncating variants identified in humans using CRISPR-Cas9 technology at the SA Genome Editing (SAGE) facility (Adelaide, Australia). A crucial role of MDFIC in the development of lymphatic vessel valves was revealed by analysis of lymphatic vascular development in homozygous mutant mice compared to their wild-type counterparts. Phenotypic analysis of mutant mice in this study showed structural abnormalities in the lymphatic vasculature, particularly in lymphatic vessel valves, initiating at early stages of embryogenesis. Abnormalities in the lymphatic vasculature were shown to progressively worsen over time and lead to lethality in homozygous mutant mice. Our data indicated that 100% of mutant mice died of chylothorax and breathing difficulties, with the majority showing phenotypes within 10-20 days of birth. Development of the lymphatic vasculature was analysed in various tissues such as skin, mesentery, thoracic cavity, and diaphragm. It is interesting that even though malformations in lymphatic vessels were observed in all tissues, the phenotypes of lymphatic vessel distension and, ultimately, dysfunction were predominant in the thoracic region of $Mdfic^{M131fs*/M131fs*}$ mice. Chylothorax, pleural and pericardial effusions are phenotypes exhibited by all patients in this study. These phenotypes are a result of direct and severe consequences of thoracic duct dysfunction, leading to retrograde flow of lymph into the

pulmonary, cardiac, and intercostal lymphatics and fluid accumulation in the pleural/pericardial/thoracic spaces. This profound effect on the thoracic lymphatic beds might be explained by the fact that the thoracic duct carries the greatest lymph load in the body and tolerates a high degree of mechanical stress during breathing, arterial pulsation, and heartbeat. Therefore, lymphatic vessels of the thoracic region are more susceptible to structural or functional impacts and as a result, are the first lymphatic beds in which lymphatic dysfunction reaches a critical threshold for disease manifestation.

The development of lymphatic vessel valves is one of the crucial aspects of lymphatic vessel maturation, which depends on various key transcription factors such as GATA2, FOXC2, NFATC1 and PROX1. Therefore, after the essential role of MDFIC in the development of lymphatic vessel valves was highlighted, we first investigated the structure, localisation and stability of MDFIC protein and its variants (MDFIC p.Met131fs* and Phe245Leu) *in vivo* and *in vitro*. Next, the interaction of MDFIC with transcription factors important for lymphatic valve development was investigated.

Given that most C-terminal truncating variant identified in our patient cohort (p.M131Nfs*3) results in a stop codon 95 nucleotides before the last exon/ intron junction, it was hypothesised that all truncating variants may be susceptible to mRNA nonsense-mediated decay. Quantification of *MDFIC* transcripts revealed comparable amounts of both *MDFIC* variant alleles in fibroblasts from the proband of LE452 to those found in healthy controls. In addition, *Mdfic* transcripts in the kidney of our mutant mouse model revealed that the expression of the M131fs* transcript was comparable to wild-type *Mdfic* mRNA in control littermates. This suggested that the c.391dup; p.M131Nfs*3 variant gives rise to a truncated protein that is not subjected to nonsense-mediated decay.

The structure of full-length MDFIC as well as p.M131Nfs*3 and p.Phe245Leu variants were then investigated using several prediction programs. We identified a transmembrane domain adjacent to the cysteine-rich C-terminal domain of MDFIC, suggesting that MDFIC might reside in membranes. Moreover, the cysteine-rich region was found to be highly homologous to the somatomedin B (SMB) domain of vitronectin, which is known to be responsible for binding integrins, plasminogen activator inhibitor 1 (PAI1) and the receptor for urokinase plasminogen activator (uPAR) to control cell adhesion and migration. p.M131Nfs*3 results in the deletion of the cysteine-rich C-

terminal domain and SMB domain preventing interaction of MDFIC with other transcriptional regulators. The C-terminal domain of MDFIC in p.Phe245Leu however remains intact. The impact on MDFIC function as a result of p.Phe245Leu has not yet been identified.

It was also previously reported that full-length MDFIC protein is post-translationally regulated and subjected to rapid proteasomal degradation. We investigated this possibility and confirmed that full-length MDFIC is indeed susceptible to rapid degradation, while M131fs* MDFIC appeared to be more stable. Given the high level of MDFIC in valves and the possible interaction of MDFIC with a number of transcription factors, we investigated whether FOXC2, PROX1, GATA2 and NFATC1, all of which are elevated in valves and important for valve development, might also influence MDFIC stability and localisation. Our data reveal that MDFIC protein directly interacts with GATA2 and is stabilised when ectopically expressed with GATA2 and FOXC2. This provides insight into the mechanisms by which MDFIC protein is detected selectively in lymphatic and cardiac valves, where these transcription factors are prominent.

The interaction of GATA2 and MDFIC was further investigated to provide a deeper insight into the regulatory mechanisms of MDFIC. Our findings revealed that MDFIC interacts directly with GATA2 and that p.M131fs* MDFIC loses capacity to interact with GATA2. We studied the localisation of GATA2 *in vitro* using primary human LECs treated with control and *MDFIC* esiRNA. Our findings indicated increased levels of GATA2 in the nucleus of *MDFIC* deficient hLECs, with reduced cytoplasmic GATA2 levels. To assess whether the subcellular localisation of GATA2 was also altered *in vivo*, we used mesenteric tissues dissected from wild-type and *Mdfic*^M131fs*/M131fs* embryonic mice. Quantification of the level of GATA2 in lymphatic vascular cells revealed a significant decrease in levels of GATA2 in the nucleus of lymphatic endothelial cells within the mesenteric lymphatic vessels of *Mdfic*^M131fs*/M131fs* mice compared to littermate controls and slightly increased levels of GATA2 in the cytoplasm. These findings are consistent with our prediction that MDFIC interacts with GATA2 and alters its localisation, but also suggest that loss of full-length MDFIC *in vitro* might not be equivalent to the impact of a truncated *Mdfic*^M131fs* variant *in vivo*, with respect to GATA2 localisation and activity. The identified differences in nuclear localisation of GATA2 in *MDFIC* deficient hLECs and lymphatic vascular cells in mouse tissue need further investigation. There is a possibility

that nuclear GATA2 levels were lower in lymphatic endothelial cells in mesenteric tissue due to lack of valve development and absence/reduction in the levels of other transcriptional regulators essential for valve formation. Another possibility discussed in this study is the existence of another factor/element directly interacting with both GATA and MDFIC, proposed to control the nuclear localisation of GATA2. Future investigation is required to assess the above-mentioned possibilities.

To confirm if MDFIC has an impact on the transcriptional activity of GATA2, gene expression profiles of control and *MDFIC* esiRNA-treated hLECs were investigated using RNA-seq. Assessment of the genes most changed in expression revealed a significant enrichment of genes involved in biological processes associated with vascular development, including some with established roles in lymphatic vessel valve development, for which MDFIC is crucial. Comparison of genes increased in *MDFIC* deficient hLECs, harbouring higher levels of nuclear GATA2, also showed significant overlap in genes established to be transcriptional targets of GATA2. Together, these data provide compelling evidence in support of the hypothesis that pathogenic *MDFIC* variants impact lymphatic vessel valve development by interfering with the localisation and transcriptional activity of GATA2. However, further investigation is required to fully understand the mechanisms by which MDFIC interacts with GATA2 and subsequently changes its transcriptional activity.

This study also examined the possibility that MDFIC might influence the activity of RAS/MAPK signalling. This question was raised because of the similarities we observed in lymphatic phenotypes reported in our MDFIC patients and those with lymphatic anomalies due to mutations in components of the RAS/MAPK signalling pathway. We examined the levels of phosphorylated ERK in control and *MDFIC* esiRNA-treated hLECs and found a significant increase in the level of phosphorylated ERK in *MDFIC* deficient hLECs compared to controls. These data suggest that like mutations in RAS pathway genes found in CCLA, the activity of MAPK/ERK is elevated in the setting of *MDFIC* deficiency. This finding suggests that biallelic truncating *MDFIC* variants in patients increases MAPK/ERK signalling activity, raising the question as to whether the dampening activity of this pathway might provide a therapeutic opportunity for the treatment of CCLA caused by *MDFIC* variants. Answering this question requires further investigation to characterise the mechanism by which MDFIC controls the activity of

RAS/MAPK signalling and to examine the efficacy of an inhibitor of RAS/MAPK signalling in rescuing the symptoms and lethality of CCLA in our novel genetic mouse model of this disease.

5.2 Future direction

Future work will provide information regarding the mechanisms in which MDFIC interacts with GATA2, influences its localisation, and subsequently changes GATA2 transcriptional activity. Characterising the mechanism by which MDFIC controls the activity of RAS/MAPK signalling in the lymphatic vasculature will be also critical. We will determine whether correcting the level of GATA2 or utilising small molecule inhibitors of RAS/MAPK signalling would be effective in rescuing the phenotypes and lethality of CCLA in our novel mouse model of disease to provide the foundation upon which effective treatments for CCLA patients could be realised.

We hypothesise that targeting GATA2 activity or RAS/MAPK signalling will provide novel therapeutic approaches to treat CCLA.

Specific aims for future studies:

1. To understand the mechanisms by which MDFIC controls GATA2 localisation, transcriptional activity and expression levels *in vivo* and *in vitro*.
2. To investigate whether correcting the levels of GATA2 will rescue CCLA in $Mdfic^{M131fs*/M131fs*}$ mice.
3. To investigate whether RAS/MAPK pathway activity is elevated *in vivo*, and subsequently to understand which components of the RAS/MAPK signalling pathway are being targeted by *MDFIC* variants and how these mutations impact that function.
4. To investigate whether small molecule inhibitors of RAS/MAPK signalling such as Trametinib, can rescue CCLA in our $Mdfic^{M131fs*/M131fs*}$ mouse model.

While this study provided evidence to validate the interaction of MDFIC with GATA2, the underlying mechanism is not understood yet. The first step to dissect the mechanism by which MDFIC controls GATA2 localisation and transcriptional activity is addressing the differences in impact of loss of full-length MDFIC *in vitro* and truncated $MDFIC^{M131*}$ variant *in vivo*. To this end, an *in vivo* experiment could be designed to isolate the lymphatic

endothelial cells from $Mdfic^{M131fs*/M131fs*}$ mice and their wild-type littermates at E18.5, fractioning the LECs lysate into nuclear and cytoplasmic compartments and measuring the level of GATA2 via immunoblotting. This experiment can provide a better result in regard to comparing GATA2 localisation *in vivo* and *in vitro*. Further, gene expression profiling of mouse lymphatic endothelial cells in wild-type and $Mdfic^{M131*/M131*}$ mutant mice can be investigated through RNA-seq. Together, the findings of these analyses are likely to provide valuable information to complement our preliminary data in addressing the mechanism involved in the interaction of GATA2 with MDFIC and to identify whether there is any other gene that would play a part in this process. Once we establish the underlying mechanism, further experiments can be designed to target GATA2 for rescuing the phenotype in our $Mdfic^{M131*/M131*}$ mouse model. Depending on the future findings, correction of GATA2 levels can be performed using small molecule inhibitors of GATA2, such as dilazep, or using a GATA2 mouse line to influence the level of GATA2 dosage genetically and rescue the phenotypes associated with CCLA in $Mdfic^{M131*/M131*}$ mice.

Our preliminary data also suggest that RAS/MAPK signalling pathway activity, culminating in ERK phosphorylation, is elevated in *MDFIC* deficient hLECs. We also identified the optimal concentration of small molecule inhibitors (trametinib) that can be used to rescue the phenotype in *MDFIC* deficient hLECs. Future studies will need to first demonstrate whether RAS/MAPK pathway activity is also elevated *in vivo* and to identify whether increased ERK activity is present throughout the lymphatic vasculature or is constrained to lymphatic vessel valves. To that end, immunostaining of the lymphatic vasculature will be performed in tissues and sections of $Mdfic^{M131fs*/M131fs*}$ mice at different embryonic stages (E14.5, E16.5 and E18.5) using a phosphorylated ERK antibody along with lymphatic and junctional markers (PROX1 and VE-Cadherin).

To investigate which components of the RAS/MAPK pathway leading to ERK phosphorylation are most impacted by loss of MDFIC, pathway activity will be investigated *in vitro* using ERK Signalling Phospho Antibody Arrays (Full Moon Biosystems). Data from this experiment will reveal specific components of the pathway upstream of ERK activation that are affected as a result of reduced MDFIC levels, elucidating the point at which MDFIC connects to RAS/MAPK signalling. Identification of these components has the potential to reveal more specific opportunities for therapeutically targeting this pathway for the treatment of CCLA.

Once the association of *MDFIC* variants in the dysregulation of RAS/MAPK signalling pathway is established, we can assess whether small molecule inhibitors of RAS/MAPK signalling pathway might prove to be effective in rescuing the phenotypes that result from *MDFIC* variants in patients and mice. This experiment needs to be performed *in vitro* first. Control and *MDFIC* esiRNA-treated hLECs will be serum-starved overnight and then treated with full media and optimal concentrations of trametinib identified in his study (10nM, 2nM and 0.5nM) for 15 min. Cells will be collected and the level of phosphorylated ERK will be assessed through western blot. After the optimal concentration of trametinib that could rescue the phenotype is identified, an experiment *in vivo* can be initiated, where trametinib will be administered intra-peritoneally to pregnant females at an embryonic stage prior to initiation of lymphatic vessel valve development. Lymphatic vascular patterning and lymphatic vessel valve development will then be investigated by immunostaining and confocal microscopy.

Once the impact of these small molecules on embryonic lymphatic vascular development and valve development has been established, we will investigate whether trametinib can rescue lymphatic vessel valve defects and prevent the onset of chylothorax in postnatal mice. The ability of small molecule inhibitors to rescue phenotypes associated with CCLA, including death due to chylothorax, should be obvious after 21 days (the majority of *Mdfic*$^{M131fs*/M131fs*}$ pups die within 20 days of birth). Should survival be promoted, further studies will investigate the requirement for ongoing therapy.

5.3 Conclusion

In this study, the role of novel pathogenic *MDFIC* variants in cases of severe complex lymphatic vascular anomaly CCLA was established. A crucial role of MDFIC in lymphatic vessel valve development was demonstrated and the interaction of MDFIC with GATA2, a key transcriptional regulator in lymphatic valve development was identified. We found that the MAPK/ERK pathway is elevated in the setting of *MDFIC* deficiency. Dysregulation of RAS/MAPK signalling is associated with CCLA. Future work will provide information regarding the mechanisms by which MDFIC interacts with GATA2 and subsequently changes its transcriptional activity as well as characterising the mechanism by which MDFIC controls the activity of RAS/MAPK signalling in the lymphatic vasculature to provide new diagnostic and prognostic information for families who experience CCLA.

Appendix

Supplementary table.1: list of genes associated with lymphatic anomalies, their clinical feature, and therapies currently available.

Causative gene	Associated disorder	Clinical feature	Drug/Therapy	Reference
PIK3CA	Cystic hygroma (Macrocystic LM) Capillary and cavernous lymphangioma, simple lymphangioma (Microcystic LM) Lymphangiomatosis, diffuse LM (GLA)	Single lesion of variable size consisting of multiple large fluid-filled cysts, commonly in the neck area Small fluid-filled cysts and locally diffuse infiltrative lesions Diffuse and multicentric proliferative lesions with multiple organ involvement	mTOR Inhibitor rapamycin (Sirolimus)/ p110a inhibitor Alpelisib (BYL719)	(Blesinger et al., 2018)
NRAS	Lymphangiomatosis (KLA)			(Liu et al., 2021)
CBL	Lymphangiomatosis (KLA)	A subtype of GLA, foci of spindle shaped LECs, thrombocytopenia		(Bülow et al., 2015)
KRAS	Vanishing bone disease (GSD)	Lymphatic vessel growth in any bone, leading to progressive bone destruction and resorption		(Mooij et al., 2011)
ARAF	Lymphangiectasia, channel type LA (CCLA)	Dilation of large lymphatic vessels	MEK inhibitor Trametinib	(Li et al., 2019)
EPHB4	Lymphangiectasia, channel type LA (CCLA) Generalised lymphatic dysplasia (GLD)	Dilation of large lymphatic vessels Abnormal lymphovenous and lymphatic valve development Subcutaneous oedema		(Almedina et al., 2021)
SHOC2	Noonan like syndrome with loose angen hair	Mitral valve anomaly		(Croonen et al., 2013; Lee & Yoo, 2019)
CBL	Casitas B-cell lymphoma syndrome	Pleural effusion Chylothorax Hydrops		(Mardy et al., 2019)

Gene	Syndrome	Phenotype	Drug	Reference
HRAS	Costelo syndrome	Hydrops Foetal atrial tachycardia/arrhythmia		(Croonen et al., 2013; Lin et al., 2002, 2009)
MAP2K2	Cardiofaciocutaneous syndrome			(Gos et al., 2018)
PTPN11	Noonan syndrome	Distended jugular lymphatic sacs (JLS) Cystic hygroma Hydrops fetalis Pleural effusion, Polyhydramnios CHD and renal abnormalities		(Croonen et al., 2013)
SOS1	Noonan syndrome	Distended jugular lymphatic sacs (JLS) Cystic hygroma Hydrops fetalis Pleural effusion, Polyhydramnios CHD and renal abnormalities		(Croonen et al., 2013)
RAF1	Noonan syndrome	Distended jugular lymphatic sacs (JLS) Cystic hygroma Hydrops fetalis Pleural effusion, Polyhydramnios CHD and renal abnormalities		(Croonen et al., 2013)
RIT1	Noonan syndrome	Distended jugular lymphatic sacs (JLS) Cystic hygroma Hydrops fetalis Pleural effusion, Polyhydramnios CHD and renal abnormalities		(Croonen et al., 2013)
FLT4 (VEGFR3)	Hereditary lymphoedema type 1A (153100)		VGX-300/OPT-302, IMC-3C5	(Sagie et al., 2003; Schneider et al., 2022)
KDR (VEGFR2)		Capillary infantile haemangioma	Axitinib, Tivozanib, Cediranib	(Simons et al., 2016)
TIE1	n.d.	Defective valve development Increased recruitment of SMCs (embryonic)		(Eklund et al., 2017)

Gene	Disease	Phenotype	Drugs	Reference
		Impaired valve maintenance in ear pre-collectors, reduced valve number (postnatal)	154	
TEK (TIE2)	Dominantly inherited venous malformations Primary congenital glaucoma-3E			(Eklund et al., 2017)
NRP1		Defective valve formation		(Guo & Vander Kooi, 2015)
NRP2		Defective valve formation		(Guo & Vander Kooi, 2015)
LYVE1				(Jackson et al., 2001)
PDPN		Dysregulation of epithelial-mesenchymal transition (EMT) Abnormal valve development	Lymphactin,VGX-100	(Astarita et al., 2012; Ugorski et al., 2016)
VEGFC	Hereditary lymphoedema type 1D			(Rauniyar et al., 2018)
VEGFD				(Stacker & Achen, 2018)
ANGPT2	Hydrops fetalis		Nesvacumab,MEDI3617,Vanucizumab,RG7716	(Eklund et al., 2017; Leppänen et al., 2020)
ADAMTS3	Hennekam lymphangiectasia-lymphoedema syndrome	Abnormal lymphangiogenesis		(Janssen et al., 2016)
CCBE1	Hennekam lymphangectasia-lymphoedema syndrome 1	Oedema Lack of lymphatic vessels		(Vaahtomeri et al., 2017) (Bos et al., 2011)
SOX18	Hypotrichosis-lymphoedema-telangiectasia syndrome (HLTS, 607823) Hypotrichosis lymphoedema-telangiectasia- renal defect syndrome (HLTRS)			(Francois et al., 2011; Irrthum et al., 2003)

Gene	Human disease	Mouse phenotype		Reference
NR2F2 (COUP-TFI)	Congenital heart defects multiple types, 4 (CHTD4)			(Francois et al., 2011)
PROX1				(Francois et al., 2011)
FOXC2	Lymphoedema-distichiasis syndrome			(Francois et al., 2011; Gulati et al., 2018)
GATA2	Primary lymphoedema (Emberger syndrome)	Reduced initiation of valve development Dilated collecting vessels (embryonic) Valve regression Dilated collecting vessels (postnatal)		(Ostergaard et al., 2011)
Foxc1	Axenfeld-Rieger syndrome	Reduced number of valves (embryonic)		(Tümer & Bach-Holm, 2009)
Foxc2	Lymphoedema-distichiasis syndrome	Valve agenesis, failure to form collecting vessels (embryonic) Valve regression, loss of collecting LV integrity Chylothorax, chylous ascites (postnatal)		(Mansour et al., 2019)
Hdac3	n.d.	Arrested valve development		(Gu et al., 2019)
Ppp3ir1 (Cnb1)	n.d.	Failure of leaflet formation in embryos Valve regression (postnatal)		(Loyola & Petrova, 2021)
Celsr1	Primary lymphoedema*	Arrested valve development Defective cell re-orientation for leaflet formation (postnatal) Normal valve maintenance		(Garay et al., 2016)
Dchs1	Mitral valves prolapse-2 (607829)	Arrested valve development		(Durst et al., 2015)
Fat4	Van Maldergem syndrome-1 (601390) Hennekam lymphangiectasia-lymphoedema	Defective cell re-orientation for leaflet formation Reduced number of valves (embryonic)		(Alders et al., 2014; Rakhmanov et al., 2018)

Gene	Human disease (OMIM)	Mouse phenotype		Reference
	syndrome-2 (616006*)		156	
Vangl2	n.d.	Arrested valve development Defective cell re-orientation for leaflet formation (embryonic)		(Wang et al., 2016)
Emilin1	n.d.	Ring-like valves (embryonic)		(Vittet, 2014)
FnEIIIa	n.d.	Ring-like valves (embryonic and postnatal)		(Pujol et al., 2017)
Itga9	Congenital chylothorax*	Ring-like valves (embryonic and postnatal), chylothorax		(Yang et al., 2012)
Svep1	n.d.	Agenesis of lymphatic valves Defective LV remodelling (embryonic)		(Loyola & Petrova, 2021)
Pecam1	n.d.	Arrested valve development Failure of leaflet formation Defective LV remodelling (embryonic)		(Wang et al., 2016)
Cdh5	n.d.	Normal valve initiation Defective leaflet formation (embryonic) Reduced number of valves Ring-like valves Chylous ascites (postnatal) Atrophy of mesenteric but not dermal valves (adult)		(Hägerling et al., 2018; Yang et al., 2019)
Ctnnb1	n.d.	Agenesis of valves (embryonic)		(Geng et al., 2016)
Bmp9	Hereditary haemorrhagic telangiectasia type 5 (615506)	Arrested valve development failure of leaflet formation (embryonic and postnatal)		(Levet et al., 2013)
Angpt2	Primary lymphoedema*	Impaired maturation of collecting vessels Agenesis of lymphatic valves		(Dellinger et al., 2008; Leppänen et al., 2020)

		Disruption of "zipper"-like junctions in collecting vessels (embryonic) No effect on valve maintenance		157
Notch1	Aortic valve disease-1 (109730), Adams-Oliver syndrome-5 (616028)	Arrested valve development Failure of valve cell clustering and polarisation (embryonic)		(Murtomaki et al., 2014)
Efnb2	Lymphatic malformation-7 (617300*),	Agenesis of lymphatic valve		(Katsuta et al., 2013)
Ephb4	Capillary malformation-arteriovenous malformation-2 (618196)	Dilated collecting vessels Loss of valves Disruption of collecting LEC cell-cell junctions (juvenile and adult mice)	Defective valve development in embryos and in neonates is rescued by an agonistic α-EphB4 antibody	(Frye et al., 2020; Almedina et al., 2016)
Sdc4	n.d.	Arrested valve development Failure of leaflet formation Defective LV remodelling (embryonic) Aggravated defects of LV remodelling Excessive SMC coverage (embryonic)		(Wang et al., 2016)
Gja4		Normal valve initiation, but defective formation of ring-like regions (embryonic) Almost complete absence of valves (adult)		(Kanady et al., 2011; Sabine et al., 2012)
Gja1	Oculodentodigital dysplasia (164200)	Reduced number of valves (embryonic) Reduced number of valves, short valve leaflets, chylothorax (postnatal and adult)		(Kanady et al., 2011; Munger et al., 2017)
Piezo1	Lymphatic malformation-6 (generalised lymphatic dysplasia, 616843*) Dehydrated hereditary stomatocytosis (194380*)	Reduced number of valves (postnatal) Regression of valves (adult)		(Fotiou et al., 2015)

Sema3a	n.d.	Abnormal SMC Coating of valve regions Reduced valve leaflet length		(Bouvrée et al., 2012)
Clec2	n.d.	Reduced valve initiation and valve number Increased SMC coverage		(Bertozzi et al., 2010)
Akt1	n.d.	Lack of valves in hypoplastic pre-collectors of adult ears		(Loyola & Petrova, 2020)
Pik3r1	SHORT syndrome, (269880) Immunodeficiency-36 (616005)	Lack of mesenteric valves in newborns		(Deau et al., 2014; Dyment et al., 2013)
Rasa1	Capillary malformation-arteriovenous malformation-1 (608354	Normal valve initiation followed by apoptosis of valve cells (embryonic) Valve leaflet atrophy Impaired valve function chylothorax (adult)		(Revencu et al., 2020)
Cdk5	n.d.	Arrested valve development Reduced number of lymphatic valves (embryonic)		(Liebl et al., 2015; Sharma & Sicinski, 2020)
Epsin 1 & 2	n.d.	Ring-like valves in neonates, rescued by small molecule inhibitor of Vegfr3		(Sabine et al., 2016)
Cdc42	n.d.	Agenesis of lymphatic valve		(Francine, 2016)
Rasip1	n.d.	Arrested collecting vessel maturation (embryonic)		(Xiaolei Liu et al., 2018)
ApoE	Alzheimer's disease-2 (104310)	Decreased number of valves, decreased SMC coverage (adult)		(Majesky, 2016)
Mir126	n.d.	Absent lymphatic valves (embryonic)		(Kontarakis et al., 2018)
JAG1	Lymphatic Dysplasia			(Li et al., 2021)
NFATC1	Not formally linked to lymphatic disease, this gene has been found to be dysregulated in Down syndrome. This altered activity of NFATC1 may contribute to the			(Yang & Oliver, 2014)

	aetiology of lymphatic hypoplasia during childhood in Down syndrome patients, but further study is required.		159	

Supplementary table.2: List of materials used in this study.

Materials and Manufacturers	
1 Kb+ DNA Ladder	NEB, MA, USA
2-mercaptoethanol	Sigma-Aldrich Pty Ltd, NSW, Australia
ABC-Peroxidase complex	VECTASTAIN Elite, Vector Laboratories, USA
Agarose	Promega, USA
ART® aerosol resistant filter tips	Molecular BioProducts, Inc., San Diego, CA
Big Dye terminator cycle reagent	Thermo Fisher Scientific, USA
Bromophenol blue	Sigma-Aldrich Pty Ltd, NSW, Australia
BSA	Sigma-Aldrich Pty Ltd, NSW, Australia
Cold T-PER® Tissue Protein Extraction Reagent	Thermo Fisher Scientific, USA
DAPI	ProSciTech, Australia
Dithiothreitol	Bi-Rad, USA
DMEM	Lonza, Bioscience, USA
DMSO	Sigma-Aldrich Pty Ltd, NSW, Australia
Dynabeads® Protein G	Life Technologies, Australia
EBM	Lonza, Bioscience
ECF reagent	GE Healthcare
ECM	Bio-strategy Pty limited Australia
EDTA	Sigma-Aldrich Pty Ltd, NSW, Australia
Ethanol	Sigma-Aldrich Pty Ltd, NSW, Australia
Evans blue dye	Sigma-Aldrich Pty Ltd, NSW, Australia
FBS	Lonza, Bioscience
FCS	Sigma-Aldrich Pty Ltd, NSW, Australia

Glycerol	QIAGEN, Victoria, Australia
GoTaq Green PCR master mix	PROMEGA, USA
Halt™ Protease	Thermo Fisher Scientific, USA
Halt™ Protease and Phosphatase Inhibitor Cocktail	Thermo Fisher Scientific, USA
HCL	Sigma-Aldrich Pty Ltd, NSW, Australia
Heparin	Sigma-Aldrich, USA
IGEPAL® CA-630	IGEPAL® CA-630
ImmPACT™ DAB Substrate Kit	Vector Laboratories, USA
Immun-Star AP substrate	Bi-Rad, USA
KCL	Sigma-Aldrich Pty Ltd, NSW, Australia
Lipofectamine 2000	Thermo Fisher Scientific, USA
$MgCl_2$	Roche, NSW, Australia
Mission® esiRNA	Sigma Aldrich Pty Ltd, NSW, Australia
NaCl	Sigma-Aldrich Pty Ltd, NSW, Australia
Nuclease-free glycogen	Roche, Roche Diagnostics GmbH, Mannheim, Germany
PBS	Sigma-Aldrich Pty Ltd, NSW, Australia
pCMV6-Entry	OriGene
PFA	QIAGEN, Victoria, Australia
PVDF	PerkinElmer, USA
Qiagen, Germany	Qiagen, Germany
QuantiTect SYBR Green PCR Kit	Qiagen, Germany
QuikChange II XL site directed mutagenesis kit	Agilent, USA
Real-Time™ SYBR Green/Rox Master Mix	SABiosciences, Frederick, MD
RNAase Extraction Kit	Invitrogen, Carlsbad, CA
RNaseOUT™ Enzyme Mix	Thermo Fisher Scientific, USA
RT2 Real-Time™ SYBR Green/Rox Master Mix	SABiosciences, Frederick, MD
SDS	Sigma-Aldrich Pty Ltd, NSW,

SuperScript™ III First-Strand Synthesis SuperMix	Invitrogen, Carlsbad, CA
Taq DNA polymerase	Roche, NSW, Australia
T-PER® Tissue Protein Extraction Reagent	Thermo Fisher Scientific, USA
Tris	AMRESCO, Ohio, USA
Triton X-100	Sigma-Aldrich, USA
TRIzol® Reagent	Invitrogen, Carlsbad, CA
Trypan Blue Solution	Sigma-Aldrich Pty Ltd, NSW, Australia
TrypLE™ Express Enzyme	Thermo Fisher Scientific, USA
Trypsan Blue	Invitrogen, CA, USA
Tween20	Sigma-Aldrich, USA

Supplementary table. 3: Analysis of lymphatic vessel calibre in E18.5 dermis

Vessel calibre width (µm)	
WT	**Mdfic$^{M131fs*/M131fs*}$**
30.34693	50.02568
47.39554	46.99006
30.95424	41.0718
23.11634	45.50785
29.48224	42.93828
31.5895	42.47347

Supplementary table.4: Analysis of lymphatic vessel calibre in E18.5 diaphragm

Area PFOV (µm2)	
WT	**Mdfic$^{M131fs*/M131fs*}$**
614824.8	1007173
912270.033	1333127.405
1707809.16	1440940.217
1251418.38	1431499.71
772388.056	1576577.661
513700.024	2227534.005
	1313351.814
	1290267.307
	1149261.084

Supplementary table.5: Analysis of lymphatic vessel calibre in E18.5 mesentery

Vessel calibre width (µm)	
WT	**Mdfic$^{M131fs*/M131fs*}$**
71.7692308	99.20833
103.129032	96.95
100.586207	92.47059
123.8	108.913
90.3939394	155.3043
84.55	147.5333
90	143.5789
104.689655	
69.3333333	
94.8695652	

Supplementary table.6: Quantification of PROX1 high cells within mesenteric collecting vessel valve territories

PROX1HI/mm	
WT	**Mdfic$^{M131fs*/M131fs*}$**
2.2478878	1.7410897
2.5456088	0.940938
1.9689346	1.86957
1.441052	1.639551
1.7881979	1.1604294
	1.0802318

Supplementary table.7: Fold-change in the number of HeLa cells ectopically expressing MDFIC, MDFIC M131fs* and MDFIC F245L proteins alone and together with PROX1, FOXC2, GATA2 or NFATC1 compared to MDFIC alone

MDFIC	MDFIC M131fs*	MDFIC F245L	MDFIC + FOXC2	MDFIC + GATA2	MDFIC + NFATC1	MDFIC + PROX1
1	12.19589	1.131840532	3.5580556	1.9078709	1.48086114	1.524709
1	8.133729	0.879606	3.45764059	1.57196937	1.17190938	0.729752
1	2.9694227	0.61632364	1.97653777	1.12916467	0.90698365	1.35251
1	3.84722	0.778679	1.952036951	1.299950926	1.134956982	1.3979

Supplementary table.8: Differentially expressed downregulated gene in *MDFIC* deficient cells in compared to control treated hLECs.

Gene	log₂FC	logCPM	FC	LR	PValue	FDR
MDFIC	**-2.06958**	**4.391272**	**4.1**	**242.9781**	**8.82E-55**	**9.40E-51**
TLR2	-1.39956	4.447079	2.6	9.90153	0.001651	0.049914
SMOC1	-1.08407	2.824439	2.1	11.0485	0.000888	0.033907
THG1L	-0.7928	2.700275	1.7	29.10922	6.84E-08	3.57E-05
THBD	-0.76285	5.696905	1.7	18.30526	1.88E-05	0.00236
SMIM14	-0.70082	6.523764	1.6	10.15501	0.001439	0.045218
RNU5B-1	-0.69382	4.623948	1.6	17.98014	2.23E-05	0.002614
HMGA2	-0.68812	5.369057	1.6	25.97415	3.46E-07	0.000118
RNU5E-1	-0.67931	5.799281	1.6	18.03772	2.17E-05	0.002614
GREM1	-0.65356	3.725284	1.5	10.12991	0.001459	0.045596
RNU5A-1	-0.62064	4.819426	1.5	21.66356	3.25E-06	0.000568
UBD	-0.61877	3.348736	1.5	11.56997	0.00067	0.027905
APOBEC3B	-0.60568	3.218985	1.5	18.76314	1.48E-05	0.001947
MSR1	-0.58709	2.821104	1.5	24.31873	8.16E-07	0.000223
HELB	-0.5717	3.040971	1.4	11.6303	0.000649	0.027319
ICAM1	-0.56842	6.253283	1.4	14.40858	0.000147	0.010183
LAPTM4A	-0.56486	7.730873	1.4	20.24969	6.80E-06	0.001006
TMEM64	-0.56155	4.060502	1.4	26.79767	2.26E-07	9.26E-05
RNU11	-0.5577	3.012289	1.4	15.66428	7.56E-05	0.006297
ABLIM2	-0.54963	4.284629	1.4	9.889094	0.001663	0.049916
AOX1	-0.54807	3.801017	1.4	22.96664	1.65E-06	0.000359
UCP2	-0.54324	4.356713	1.4	22.84281	1.76E-06	0.000367
SDC4	-0.54021	6.217524	1.4	11.06231	0.000881	0.033776
HLA-H	-0.51792	4.453959	1.4	20.84754	4.97E-06	0.000758
AXL	-0.50582	7.377038	1.4	11.27774	0.000784	0.031079
ARMCX1	-0.48572	6.035262	1.4	15.66283	7.57E-05	0.006297
TMEM60	-0.47946	4.246592	1.3	10.35547	0.001291	0.041693
CPNE7	-0.47245	3.755641	1.3	12.50167	0.000407	0.020767
TTC39B	-0.46886	4.488636	1.3	10.6833	0.001081	0.038031
C12orf75	-0.45485	3.825735	1.3	15.55909	8.00E-05	0.006457
MND1	-0.43883	2.171296	1.3	10.02746	0.001542	0.047369

TFRC	-0.43206	6.315075	1.3	15.28705	9.23E-05	0.007237
ABI3BP	-0.4262	8.20101	1.3	14.67948	0.000127	0.009239
GNG2	-0.42519	3.758724	1.3	14.32422	0.000154	0.010463
IMPAD1	-0.41936	6.940715	1.3	13.41062	0.00025	0.015066
C1RL-AS1	-0.41693	2.758481	1.3	10.09193	0.001489	0.046409
SCAMP1	-0.41597	6.135587	1.3	12.35269	0.00044	0.021333
UHMK1	-0.40574	7.899616	1.3	11.76099	0.000605	0.025959
M6PR	-0.40412	6.697215	1.3	17.2557	3.27E-05	0.003448
TNRC6A	-0.40386	7.396206	1.3	13.19821	0.00028	0.015939
PRNP	-0.40279	7.570853	1.3	10.88493	0.00097	0.035727
POMK	-0.40181	3.750898	1.3	13.78582	0.000205	0.012845
ASNS	-0.38475	3.306613	1.3	11.49756	0.000697	0.028677
RASD1	-0.38456	4.464036	1.3	11.47107	0.000707	0.028866
MZT1	-0.38203	4.59838	1.3	12.16662	0.000487	0.022545
C6orf120	-0.38201	5.568458	1.3	16.03562	6.22E-05	0.005615
LARP4	-0.38179	7.686871	1.3	10.04019	0.001532	0.04731
MTHFD2	-0.38097	5.813023	1.3	11.24596	0.000798	0.031383
NUF2	-0.38075	4.228956	1.3	10.6169	0.001121	0.038903
TIPIN	-0.38028	3.484105	1.3	12.24757	0.000466	0.022166
HDAC9	-0.37923	6.557175	1.3	13.21536	0.000278	0.015939
CCNA2	-0.37834	6.020391	1.2	14.01114	0.000182	0.011739
LSM6	-0.3779	3.968214	1.2	12.47469	0.000413	0.020767
MAP2	-0.37669	8.46908	1.2	10.43509	0.001236	0.040767
NDC80	-0.36613	5.218501	1.2	12.39408	0.000431	0.021252
SNX27	-0.3661	6.119133	1.2	13.16159	0.000286	0.015939
GFPT1	-0.36552	7.036003	1.2	14.55315	0.000136	0.009747
GADD45A	-0.36531	5.437613	1.2	13.93729	0.000189	0.012063
NBPF10	-0.34864	3.539148	1.2	10.40419	0.001257	0.041105
VEGFC	-0.34798	4.241051	1.2	10.87357	0.000975	0.035727
BBIP1	-0.34442	4.211529	1.2	11.14026	0.000845	0.032859
SCARNA9	-0.34134	4.687949	1.2	13.15816	0.000286	0.015939
BUB1	-0.33815	6.00351	1.2	10.54409	0.001166	0.03969
GTF2E1	-0.33495	4.89296	1.2	11.43504	0.000721	0.029207
NFKB2	-0.32397	4.875214	1.2	10.29672	0.001333	0.042653

Supplementary table.9: Differentially expressed upregulated gene in *MDFIC* deficient cells in compared to control treated hLECs.

Gene	Log₂FC	FC	logCPM	LR	PValue	FDR
NDUFS8	1.294183	2.4	4.531199	58.48223	2.05E-14	5.47E-11
CPNE5	1.100262	2.1	3.017429	25.60375	4.19E-07	0.000131
FAM78A	1.07951	2.1	2.460944	29.05773	7.03E-08	3.57E-05
CYB5R3	1.025084	2.0	7.944295	41.54977	1.15E-10	1.75E-07
FAM124B	0.960576	1.9	4.258737	31.46987	2.03E-08	1.27E-05
FAM234A	0.935383	1.9	5.27797	56.34458	6.08E-14	1.30E-10
ITGA9	0.924372	1.8	4.686814	21.35953	3.81E-06	0.000644
PLPP3	0.868841	1.8	4.89942	75.21696	4.22E-18	2.25E-14
HOXD1	0.850737	1.8	3.39122	20.44593	6.13E-06	0.000921
PLA2G15	0.801158	1.7	4.351185	19.70561	9.03E-06	0.001284
CELSR1	0.800513	1.7	4.602641	12.32467	0.000447	0.021461
CEP76	0.795208	1.7	3.163089	39.21736	3.79E-10	5.05E-07
MLLT11	0.768653	1.7	4.721549	38.11407	6.67E-10	7.90E-07
MALL	0.762576	1.6	3.597437	14.0777	0.000175	0.01154
TSPAN18	0.754508	1.6	7.310922	15.65114	7.62E-05	0.006297
RRP1B	0.74946	1.6	5.797048	65.77464	5.06E-16	1.80E-12
CYYR1	0.744579	1.6	4.086544	11.93882	0.00055	0.024313
ANKRD55	0.741473	1.6	3.932636	12.53713	0.000399	0.020686
ADA	0.741126	1.6	3.16264	23.7922	1.07E-06	0.000266
NPR1	0.727461	1.6	4.808672	25.98659	3.44E-07	0.000118
SOX4	0.723536	1.6	6.570422	16.5535	4.73E-05	0.004577
SLC22A23	0.712784	1.6	6.554831	21.09918	4.36E-06	0.00071
CERS2	0.704993	1.6	6.658715	46.35317	9.87E-12	1.75E-08
DMTN	0.685071	1.6	4.956348	16.4408	5.02E-05	0.004734
CABLES2	0.682506	1.6	2.780945	10.59538	0.001134	0.03913
RHOB	0.673409	1.5	8.384768	28.84082	7.86E-08	3.64E-05

EVA1A	0.670311	1.5	3.519883	22.13546	2.54E-06	0.000492
PCBD1	0.667539	1.5	4.64133	14.52904	0.000138	0.009761
EPN1	0.663251	1.5	5.873018	34.99226	3.31E-09	2.52E-06
HID1	0.66094	1.5	5.676934	15.34649	8.95E-05	0.007065
P3H4	0.660679	1.5	4.53006	37.89847	7.45E-10	7.94E-07
NRG3	0.660512	1.5	2.90488	24.40751	7.80E-07	0.000219
GDPD5	0.660352	1.5	4.125009	22.67673	1.92E-06	0.000385
TLE2	0.659776	1.5	2.525594	12.08633	0.000508	0.023036
SPNS2	0.65462	1.5	6.15333	33.58293	6.83E-09	4.55E-06
NRARP	0.645614	1.5	4.684992	17.80592	2.45E-05	0.002774
KLHDC3	0.644184	1.5	5.051763	30.66704	3.06E-08	1.81E-05
PLOD1	0.638658	1.5	7.631038	21.88995	2.89E-06	0.000531
KIAA1161	0.633929	1.5	3.641859	36.04703	1.93E-09	1.87E-06
RAB11FIP1	0.625626	1.5	5.276404	27.83527	1.32E-07	5.87E-05
C1QTNF6	0.616275	1.5	4.586109	26.20289	3.07E-07	0.000113
RUNX1T1	0.616184	1.5	4.883518	18.99928	1.31E-05	0.001764
SMPDL3A	0.613025	1.5	2.118965	16.87895	3.98E-05	0.004083
CNPY4	0.610414	1.5	3.54371	19.93569	8.01E-06	0.001154
PIK3R2	0.596952	1.5	3.764165	28.86454	7.76E-08	3.64E-05
MMP15	0.591528	1.5	4.261741	26.2963	2.93E-07	0.000111
EID2	0.590605	1.5	3.173694	18.11755	2.08E-05	0.002544
KCTD12	0.587933	1.5	10.02568	15.6352	7.68E-05	0.006297
LRRC8B	0.587462	1.5	4.0576	23.69113	1.13E-06	0.000274
SCN3B	0.585248	1.5	4.108629	10.46184	0.001219	0.040767
LINC00704	0.578433	1.4	4.538906	25.92863	3.54E-07	0.000118
LOC728715	0.576804	1.4	2.397475	13.1584	0.000286	0.015939
PTGFRN	0.574432	1.4	6.954385	18.79164	1.46E-05	0.001942
TNFAIP1	0.572485	1.4	7.003326	21.52861	3.49E-06	0.000599
MEX3D	0.569963	1.4	4.459405	16.17939	5.76E-05	0.005249
SCAMP5	0.568177	1.4	2.705318	10.15068	0.001442	0.045218
TNFRSF11A	0.56798	1.4	4.967678	35.03329	3.24E-09	2.52E-06
H3F3A	0.567197	1.4	6.072647	23.08262	1.55E-06	0.000345

KATNB1	0.556833	1.4	3.505283	24.77983	6.43E-07	0.00019
SEMA6C	0.551266	1.4	3.376976	15.04077	0.000105	0.00801
FZD1	0.546249	1.4	3.236303	22.88905	1.72E-06	0.000366
CDKN1A	0.540875	1.4	7.06451	29.78629	4.82E-08	2.71E-05
SLC40A1	0.539424	1.4	5.548058	22.75959	1.84E-06	0.000376
H3F3AP4	0.535987	1.4	4.555341	16.30967	5.38E-05	0.004942
CDH5	0.535307	1.4	9.662647	14.42345	0.000146	0.010169
CXorf36	0.535157	1.4	7.249296	13.15255	0.000287	0.015939
PROB1	0.530404	1.4	2.579823	14.43831	0.000145	0.010155
JAG2	0.530082	1.4	5.54039	12.25973	0.000463	0.022121
GNPDA1	0.528062	1.4	5.384667	18.57149	1.64E-05	0.002101
NDUFS7	0.525498	1.4	3.833118	21.83491	2.97E-06	0.000537
FURIN	0.525454	1.4	6.719182	23.93451	9.97E-07	0.000257
HOMER3	0.524835	1.4	4.552378	12.10795	0.000502	0.023036
ZHX2	0.524429	1.4	3.333637	10.74233	0.001047	0.037325
KDM6B	0.521936	1.4	3.578387	21.93854	2.82E-06	0.000526
ALDH2	0.52001	1.4	4.996973	16.77922	4.20E-05	0.004262
C17orf58	0.519301	1.4	3.153889	21.21782	4.10E-06	0.000683
BLCAP	0.517095	1.4	6.135503	25.16396	5.27E-07	0.00016
PIEZO1	0.515718	1.4	8.19161	18.20636	1.98E-05	0.002456
HN1L	0.515705	1.4	6.369131	19.45607	1.03E-05	0.001444
C14orf1	0.509616	1.4	5.365	26.62106	2.48E-07	9.77E-05
MYO5C	0.505704	1.4	5.208126	11.0072	0.000908	0.034424
ITGB4	0.504865	1.4	5.330318	35.62232	2.40E-09	2.13E-06
TUBB2A	0.504404	1.4	4.343536	27.69773	1.42E-07	6.05E-05
FILIP1	0.504219	1.4	4.072284	10.44172	0.001232	0.040767
CAPZB	0.500728	1.4	7.665719	16.58604	4.65E-05	0.004577
TSPAN7	0.499575	1.4	3.832259	12.06669	0.000513	0.023181
NACC2	0.493389	1.4	4.198538	10.9823	0.00092	0.034529
PTPN21	0.490989	1.4	4.750923	17.84752	2.39E-05	0.002773
APLN	0.486655	1.4	8.378917	15.82088	6.96E-05	0.006083
TRPV4	0.486337	1.4	2.49836	14.06196	0.000177	0.011566
RAB12	0.486293	1.4	5.75571	33.73059	6.33E-09	4.50E-06
CABLES1	0.485854	1.4	5.689799	23.9039	1.01E-06	0.000257

RNPEPL1	0.485103	1.3	5.125421	11.32029	0.000767	0.030603
DUSP7	0.484233	1.3	4.486299	20.84928	4.97E-06	0.000758
FAM89B	0.483869	1.3	3.485816	11.26109	0.000791	0.031243
NOS3	0.481918	1.3	5.49741	23.10703	1.53E-06	0.000345
PLXNA4	0.481613	1.3	4.58232	15.06619	0.000104	0.007976
TMC7	0.481024	1.3	4.238904	15.38205	8.78E-05	0.006985
DOT1L	0.480393	1.3	4.97735	21.70711	3.18E-06	0.000564
CCM2L	0.479301	1.3	3.797864	10.58519	0.00114	0.03913
DTX4	0.478861	1.3	3.515348	16.45765	4.97E-05	0.004734
BTBD9	0.478691	1.3	4.234346	16.72229	4.33E-05	0.004351
SERINC2	0.476748	1.3	4.79299	13.10467	0.000295	0.016266
RNASE1	0.475871	1.3	4.528726	14.03647	0.000179	0.011652
ACER2	0.47446	1.3	3.422243	15.64711	7.63E-05	0.006297
MGP	0.472816	1.3	6.436629	12.90676	0.000327	0.017363
BCAT2	0.472156	1.3	3.845903	10.62222	0.001117	0.038903
MAF	0.470582	1.3	5.646011	11.55262	0.000677	0.028057
SPPL2B	0.469559	1.3	3.681947	16.66566	4.46E-05	0.004441
CSF2RB	0.469519	1.3	2.702139	13.04459	0.000304	0.01671
ISOC2	0.468438	1.3	4.096156	16.5397	4.76E-05	0.004577
CNTNAP3	0.466846	1.3	4.28598	12.53158	0.0004	0.020686
SOX18	0.465322	1.3	5.453131	12.33193	0.000445	0.021461
TMEM35B	0.465101	1.3	3.859415	20.84572	4.98E-06	0.000758
GRAMD4	0.465021	1.3	3.809104	17.65752	2.64E-05	0.002936
NYNRIN	0.46459	1.3	5.10577	15.13687	1.00E-04	0.007779
TFPI2	0.464058	1.3	8.699766	15.82484	6.95E-05	0.006083
SEMA4C	0.462434	1.3	3.395904	12.37239	0.000436	0.021333
TBC1D13	0.461799	1.3	5.029418	20.01109	7.70E-06	0.001124
MARCKSL1	0.459981	1.3	6.240812	10.36982	0.001281	0.041622
GYS1	0.458711	1.3	4.966249	24.63645	6.92E-07	0.000199
GSPT1	0.457041	1.3	7.317922	19.39688	1.06E-05	0.00147
BCR	0.456845	1.3	6.924907	21.05539	4.46E-06	0.00071
CEP68	0.455193	1.3	5.421331	13.18973	0.000281	0.015939
CD151	0.455041	1.3	7.252829	13.18544	0.000282	0.015939
MLXIP	0.451578	1.3	6.783369	15.75727	7.20E-05	0.00624

PARVB	0.451518	1.3	5.778669	17.81488	2.43E-05	0.002774
FAM171A1	0.450305	1.3	6.418194	10.9781	0.000922	0.034529
C2CD2	0.449155	1.3	5.271471	25.7167	3.95E-07	0.000128
UBTD1	0.448924	1.3	3.946416	11.62817	0.00065	0.027319
RHOJ	0.447035	1.3	7.653014	12.52394	0.000402	0.020686
SMPD1	0.445267	1.3	5.80109	21.05861	4.45E-06	0.00071
LINC01013	0.444379	1.3	4.199011	15.98551	6.38E-05	0.005696
LZTS3	0.440334	1.3	3.223245	12.09921	0.000504	0.023036
ANKRD52	0.439693	1.3	6.759924	23.46113	1.27E-06	0.0003
UAP1L1	0.434418	1.3	5.294085	12.48631	0.00041	0.020767
CARM1	0.434078	1.3	5.78538	19.12249	1.23E-05	0.001675
FLI1	0.433905	1.3	8.138948	16.32356	5.34E-05	0.004942
PGM5	0.432914	1.3	3.912201	16.53856	4.77E-05	0.004577
POU6F1	0.429969	1.3	3.181231	12.57475	0.000391	0.020427
KSR2	0.429252	1.3	4.583047	13.41578	0.00025	0.015066
DYRK1B	0.428389	1.3	3.644416	10.84557	0.00099	0.036023
GPRC5A	0.427035	1.3	3.452867	10.37882	0.001275	0.041546
SLC16A5	0.42653	1.3	2.715138	9.965759	0.001595	0.048843
TOMM20	0.425427	1.3	6.8378	17.29373	3.20E-05	0.003413
ELAC2	0.424833	1.3	5.978091	24.01679	9.55E-07	0.000254
PLXNB3	0.424779	1.3	4.149224	14.1132	0.000172	0.011466
SHROOM1	0.424671	1.3	2.524882	10.03509	0.001536	0.04731
CCNJ	0.423936	1.3	5.021224	22.43945	2.17E-06	0.000428
TTYH3	0.422586	1.3	7.705978	10.61776	0.00112	0.038903
ALPK3	0.420725	1.3	6.826634	13.35726	0.000257	0.015242
CNTNAP3B	0.419882	1.3	5.502016	12.92898	0.000324	0.017363
PM20D2	0.419827	1.3	3.360039	11.57252	0.000669	0.027905
FAM213A	0.417157	1.3	7.57623	10.25755	0.001361	0.043051
ZNF219	0.416543	1.3	3.1111	10.43081	0.001239	0.040767
TRIM8	0.416437	1.3	6.870257	15.66069	7.58E-05	0.006297
CCDC85B	0.415817	1.3	4.608994	14.98207	0.000109	0.008204
PERP	0.415586	1.3	5.791262	14.143	0.000169	0.011357
NDRG4	0.414545	1.3	6.142248	17.42695	2.99E-05	0.003247
RASSF4	0.414099	1.3	3.069769	12.62548	0.000381	0.019978

CTHRC1	0.413715	1.3	4.454276	11.3043	0.000773	0.030752
BCL7B	0.413554	1.3	4.832695	14.78563	0.00012	0.008853
GLRB	0.411843	1.3	3.040162	10.1642	0.001432	0.045153
MOB3A	0.410967	1.3	5.732588	14.96393	0.00011	0.008225
ENG	0.410945	1.3	9.703638	12.23054	0.00047	0.022171
WIPI2	0.410105	1.3	5.767749	13.88064	0.000195	0.012285
COMMD2	0.40857	1.3	5.245181	23.42789	1.30E-06	0.0003
SH3GL1	0.402252	1.3	6.777586	13.3811	0.000254	0.015219
TMCO1	0.401334	1.3	5.95328	22.01418	2.71E-06	0.000515
ZNF366	0.40117	1.3	4.200462	16.38159	5.18E-05	0.004842
TMED7	0.400915	1.3	6.631478	15.66254	7.57E-05	0.006297
MAPK3	0.399614	1.3	6.434204	12.90642	0.000327	0.017363
HECTD3	0.398898	1.3	5.918316	17.68138	2.61E-05	0.00293
NARF	0.395431	1.3	5.025587	10.36281	0.001286	0.041654
PIM3	0.393587	1.3	6.221267	13.74678	0.000209	0.012962
NAPRT	0.393096	1.3	3.309079	11.624	0.000651	0.027319
BMP2	0.39157	1.3	4.762564	10.06038	0.001515	0.046936
RIN3	0.391463	1.3	3.973828	14.71179	0.000125	0.009144
HMOX2	0.391273	1.3	5.762862	15.44407	8.50E-05	0.00681
PAK4	0.389919	1.3	4.458221	13.88738	0.000194	0.012285
ARVCF	0.389665	1.3	4.315369	11.4886	0.0007	0.028705
IGSF3	0.389537	1.3	3.532532	10.72975	0.001054	0.03733
ESAM	0.389024	1.3	6.898431	17.9883	2.22E-05	0.002614
SLC29A1	0.388801	1.3	6.081409	12.47207	0.000413	0.020767
RPN1	0.388473	1.3	8.073034	13.18326	0.000282	0.015939
TMCC3	0.388354	1.3	4.229403	12.4135	0.000426	0.02113
HSPB8	0.386313	1.3	4.1687	14.32116	0.000154	0.010463
CARD10	0.386034	1.3	4.930829	13.47263	0.000242	0.014827
NPAS2	0.38459	1.3	4.36451	12.42625	0.000423	0.021084
COPS6	0.384143	1.3	6.139483	18.4579	1.74E-05	0.002204
MEIS2	0.383591	1.3	3.665319	12.21248	0.000475	0.022191
MOV10L1	0.383357	1.3	5.027304	17.07108	3.60E-05	0.003726
ABCG1	0.381159	1.3	6.330515	10.68308	0.001081	0.038031
ZNF768	0.378732	1.3	3.942274	11.99613	0.000533	0.023774

Gene						
STRN4	0.378314	1.3	5.926707	18.01224	2.19E-05	0.002614
SLC27A3	0.377426	1.2	4.644445	11.11965	0.000854	0.033105
STARD8	0.376627	1.2	5.492034	17.56845	2.77E-05	0.003045
SLC45A3	0.376255	1.2	3.148069	10.47063	0.001213	0.040767
TGFBRAP1	0.376037	1.2	6.404305	13.46178	0.000243	0.014828
TRIM47	0.375949	1.2	5.035632	14.91355	0.000113	0.008389
TMEM8A	0.375307	1.2	5.560397	14.09925	0.000173	0.01148
PLEKHG5	0.37453	1.2	4.742747	11.98122	0.000537	0.023865
SLC16A13	0.372769	1.2	3.49663	10.7717	0.001031	0.036861
NLRX1	0.372213	1.2	3.816746	12.22175	0.000472	0.022178
HYAL1	0.372113	1.2	4.030947	11.65749	0.000639	0.027152
UNC13D	0.371461	1.2	4.107519	12.08944	0.000507	0.023036
PIP5K1C	0.370282	1.2	7.036449	13.60125	0.000226	0.013925
PKD1L1	0.370036	1.2	2.957409	10.30074	0.00133	0.042653
RAMP2	0.369937	1.2	5.323112	11.91948	0.000556	0.024364
TBC1D12	0.369536	1.2	4.275135	12.05406	0.000517	0.023241
FERMT2	0.368526	1.2	6.692585	13.76559	0.000207	0.012908
GON7	0.367929	1.2	2.916033	9.908866	0.001645	0.049914
ST6GAL1	0.367398	1.2	5.977303	10.90754	0.000958	0.035443
WFS1	0.366177	1.2	6.460174	15.97645	6.41E-05	0.005696
VOPP1	0.364207	1.2	6.07277	12.44017	0.00042	0.021026
PREP	0.362457	1.2	5.30574	18.60158	1.61E-05	0.002094
INPP5K	0.359648	1.2	4.554602	11.90912	0.000559	0.0244
SDHAF2	0.359554	1.2	4.770579	14.52524	0.000138	0.009761
GAS2L1	0.358562	1.2	3.984426	10.80959	0.00101	0.036349
NDEL1	0.358418	1.2	5.98854	17.3129	3.17E-05	0.003413
FAM43A	0.357909	1.2	7.647211	10.51415	0.001185	0.04021
MLLT1	0.355429	1.2	6.269268	14.78566	0.00012	0.008853
PLOD3	0.355093	1.2	6.534226	14.56344	0.000136	0.009747
MARCH2	0.351907	1.2	4.530563	10.44076	0.001233	0.040767
PEG10	0.351805	1.2	5.575276	12.35746	0.000439	0.021333
BTG2	0.351509	1.2	5.32268	17.22836	3.31E-05	0.003463
INTS1	0.349839	1.2	6.266828	13.34501	0.000259	0.015258
DNAJB4	0.34962	1.2	8.030773	10.32046	0.001316	0.042363

CEP170B	0.347519	1.2	4.864271	12.99446	0.000312	0.017075
PXDC1	0.346268	1.2	6.215601	10.961	0.00093	0.034676
MFNG	0.346063	1.2	6.00857	11.66603	0.000637	0.027136
NFATC1	0.344957	1.2	4.940054	11.8978	0.000562	0.024448
MAML1	0.343396	1.2	5.833238	15.06227	0.000104	0.007976
FAM234B	0.342342	1.2	4.484701	11.75603	0.000606	0.025959
MAN1B1	0.34018	1.2	5.767579	15.59061	7.86E-05	0.006398
AGAP3	0.33928	1.2	5.234718	13.27947	0.000268	0.015713
DENND6A	0.338386	1.2	5.049921	11.16025	0.000836	0.032636
ST3GAL2	0.337359	1.2	5.491194	13.24939	0.000273	0.01588
KDELC1	0.337301	1.2	4.437332	13.36416	0.000256	0.015242
KLHL3	0.336724	1.2	4.993047	14.39252	0.000148	0.010204
ZNF746	0.335973	1.2	4.358875	12.23619	0.000469	0.022171
NHSL2	0.334991	1.2	5.762945	11.522	0.000688	0.028412
SHARPIN	0.334941	1.2	4.214703	12.92386	0.000324	0.017363
TLE1	0.333204	1.2	6.005548	13.98669	0.000184	0.011821
ZBED4	0.332746	1.2	5.202053	12.97928	0.000315	0.017127
PPP2R1B	0.332716	1.2	6.468165	10.65978	0.001095	0.038386
PIAS4	0.332139	1.2	4.62576	10.84612	0.00099	0.036023
ABHD17A	0.331862	1.2	4.843737	12.02607	0.000525	0.023493
CDC34	0.330142	1.2	4.80392	9.89437	0.001658	0.049914
PLD3	0.329925	1.2	6.384585	11.09848	0.000864	0.033364
FAM84B	0.328012	1.2	4.037821	10.29021	0.001337	0.042676
SYNGR2	0.3263	1.2	5.460391	12.92047	0.000325	0.017363
SLC2A12	0.325529	1.2	7.263762	10.87359	0.000975	0.035727
ARHGEF3	0.323401	1.2	5.215862	11.85334	0.000576	0.024836

Supplementary table.10: "GATA2 siRNA down" genes enriched in the genes upregulated in MDFIC deficient LECs compared to control. 175 genes from the "GATA2 siRNA down" are present with statistical significance of FDR which is <0.05.

	SYMBOL	TITLE	RANK IN GENE LIST	RANK METRIC SCORE	RUNNING ES	CORE ENRICHMENT	
1	PLPP3	phospholipid phosphatase 3 [Source:HGNC Symbol;Acc:HGNC:9229]	0	17.375	0.0354	Yes
2	SPNS2	sphingolipid transporter 2 [Source:HGNC Symbol;Acc:HGNC:26992]	14	8.166	0.0508	Yes

3	MMP15	matrix metallopeptidase 15 [Source:HGNC Symbol;Acc:HGNC:7161]	24	6.533	0.0632	Yes
4	NPR1	natriuretic peptide receptor 1 [Source:HGNC Symbol;Acc:HGNC:7943]	26	6.464	0.0763	Yes
5	CABLES1	Cdk5 and Abl enzyme substrate 1 [Source:HGNC Symbol;Acc:HGNC:25097]	36	5.995	0.0876	Yes
6	NOS3	nitric oxide synthase 3 [Source:HGNC Symbol;Acc:HGNC:7876]	41	5.815	0.099	Yes
7	SLC40A1	solute carrier family 40 member 1 [Source:HGNC Symbol;Acc:HGNC:10909]	44	5.736	0.1105	Yes
8	ITGA9	integrin subunit alpha 9 [Source:HGNC Symbol;Acc:HGNC:6145]	54	5.419	0.1207	Yes
9	SLC22A23	solute carrier family 22 member 23 [Source:HGNC Symbol;Acc:HGNC:21106]	56	5.36	0.1315	Yes
10	ESAM	endothelial cell adhesion molecule [Source:HGNC Symbol;Acc:HGNC:17474]	76	4.653	0.1391	Yes
11	NRARP	NOTCH regulated ankyrin repeat protein [Source:HGNC Symbol;Acc:HGNC:33843]	79	4.612	0.1483	Yes
12	STARD8	StAR related lipid transfer domain containing 8 [Source:HGNC Symbol;Acc:HGNC:19161]	82	4.557	0.1574	Yes
13	PGM5	phosphoglucomutase 5 [Source:HGNC Symbol;Acc:HGNC:8908]	95	4.322	0.165	Yes
14	ZNF366	zinc finger protein 366 [Source:HGNC Symbol;Acc:HGNC:18316]	98	4.286	0.1736	Yes
15	FLI1	"Fli-1 proto-oncogene, ETS transcription factor [Source:HGNC Symbol;Acc:HGNC:3749]"	99	4.272	0.1823	Yes
16	APLN	apelin [Source:HGNC Symbol;Acc:HGNC:16665]	105	4.157	0.1902	Yes
17	TSPAN18	tetraspanin 18 [Source:HGNC Symbol;Acc:HGNC:20660]	109	4.118	0.1983	Yes
18	ACER2	alkaline ceramidase 2 [Source:HGNC Symbol;Acc:HGNC:23675]	110	4.117	0.2067	Yes
19	PLXNA4	plexin A4 [Source:HGNC Symbol;Acc:HGNC:9102]	117	3.984	0.2143	Yes
20	MALL	"mal, T cell differentiation protein like [Source:HGNC Symbol;Acc:HGNC:6818]"	137	3.756	0.22	Yes
21	TRPV4	transient receptor potential cation channel subfamily V member 4 [Source:HGNC Symbol;Acc:HGNC:18083]	138	3.752	0.2277	Yes
22	CARD10	caspase recruitment domain family member 10 [Source:HGNC Symbol;Acc:HGNC:16422]	146	3.616	0.2344	Yes
23	CEP68	centrosomal protein 68 [Source:HGNC Symbol;Acc:HGNC:29076]	155	3.551	0.2408	Yes
24	CSF2RB	colony stimulating factor 2 receptor subunit beta [Source:HGNC Symbol;Acc:HGNC:2436]	160	3.517	0.2476	Yes
25	NPAS2	neuronal PAS domain protein 2 [Source:HGNC Symbol;Acc:HGNC:7895]	178	3.373	0.2528	Yes
26	SOX18	SRY-box transcription factor 18 [Source:HGNC Symbol;Acc:HGNC:11194]	183	3.351	0.2592	Yes
27	CELSR1	cadherin EGF LAG seven-pass G-type receptor 1 [Source:HGNC Symbol;Acc:HGNC:1850]	184	3.35	0.266	Yes
28	TSPAN7	tetraspanin 7 [Source:HGNC Symbol;Acc:HGNC:11854]	195	3.29	0.2718	Yes
29	CYYR1	cysteine and tyrosine rich 1 [Source:HGNC Symbol;Acc:HGNC:16274]	200	3.26	0.278	Yes
30	RAMP2	receptor activity modifying protein 2 [Source:HGNC Symbol;Acc:HGNC:9844]	202	3.255	0.2845	Yes
31	MFNG	MFNG O-fucosylpeptide 3-beta-N-acetylglucosaminyltransferase [Source:HGNC Symbol;Acc:HGNC:7038]	207	3.196	0.2907	Yes
32	HYAL1	hyaluronidase 1 [Source:HGNC Symbol;Acc:HGNC:5320]	208	3.194	0.2972	Yes
33	ADCY4	adenylate cyclase 4 [Source:HGNC Symbol;Acc:HGNC:235]	215	3.147	0.303	Yes

34	FAM171A1	family with sequence similarity 171 member A1 [Source:HGNC Symbol;Acc:HGNC:23522]	227	3.035	0.3081	Yes
35	ST6GAL1	"ST6 beta-galactoside alpha-2,6-sialyltransferase 1 [Source:HGNC Symbol;Acc:HGNC:10860]"	229	3.019	0.3141	Yes
36	ABCG1	ATP binding cassette subfamily G member 1 [Source:HGNC Symbol;Acc:HGNC:73]	238	2.966	0.3194	Yes
37	TTYH3	tweety family member 3 [Source:HGNC Symbol;Acc:HGNC:22222]	241	2.951	0.3252	Yes
38	FAM43A	family with sequence similarity 43 member A [Source:HGNC Symbol;Acc:HGNC:26888]	246	2.926	0.3308	Yes
39	SCN3B	sodium voltage-gated channel beta subunit 3 [Source:HGNC Symbol;Acc:HGNC:20665]	248	2.914	0.3366	Yes
40	GALNT18	polypeptide N-acetylgalactosaminyltransferase 18 [Source:HGNC Symbol;Acc:HGNC:30488]	249	2.913	0.3426	Yes
41	FILIP1	filamin A interacting protein 1 [Source:HGNC Symbol;Acc:HGNC:21015]	251	2.909	0.3484	Yes
42	MARCKSL1	MARCKS like 1 [Source:HGNC Symbol;Acc:HGNC:7142]	256	2.892	0.3539	Yes
43	SEMA6B	semaphorin 6B [Source:HGNC Symbol;Acc:HGNC:10739]	274	2.773	0.3579	Yes
44	CD276	CD276 molecule [Source:HGNC Symbol;Acc:HGNC:19137]	276	2.77	0.3634	Yes
45	MERTK	"MER proto-oncogene, tyrosine kinase [Source:HGNC Symbol;Acc:HGNC:7027]"	289	2.716	0.3678	Yes
46	CD200	CD200 molecule [Source:HGNC Symbol;Acc:HGNC:7203]	297	2.68	0.3725	Yes
47	C1orf115	chromosome 1 open reading frame 115 [Source:HGNC Symbol;Acc:HGNC:25873]	305	2.656	0.3773	Yes
48	EPAS1	endothelial PAS domain protein 1 [Source:HGNC Symbol;Acc:HGNC:3374]	317	2.593	0.3815	Yes
49	SEMA6A	semaphorin 6A [Source:HGNC Symbol;Acc:HGNC:10738]	360	2.444	0.3823	Yes
50	TANC2	"tetratricopeptide repeat, ankyrin repeat and coiled-coil containing 2 [Source:HGNC Symbol;Acc:HGNC:30212]"	379	2.393	0.3854	Yes
51	CDC42EP5	CDC42 effector protein 5 [Source:HGNC Symbol;Acc:HGNC:17408]	381	2.386	0.3902	Yes
52	RNF144B	ring finger protein 144B [Source:HGNC Symbol;Acc:HGNC:21578]	388	2.35	0.3944	Yes
53	PRAG1	"PEAK1 related, kinase-activating pseudokinase 1 [Source:HGNC Symbol;Acc:HGNC:25438]"	392	2.33	0.3988	Yes
54	MMRN2	multimerin 2 [Source:HGNC Symbol;Acc:HGNC:19888]	394	2.322	0.4035	Yes
55	TSPAN15	tetraspanin 15 [Source:HGNC Symbol;Acc:HGNC:23298]	410	2.273	0.4066	Yes
56	ABI3	ABI family member 3 [Source:HGNC Symbol;Acc:HGNC:29859]	420	2.232	0.4103	Yes
57	DLL4	delta like canonical Notch ligand 4 [Source:HGNC Symbol;Acc:HGNC:2910]	439	2.185	0.413	Yes
58	FRY	FRY microtubule binding protein [Source:HGNC Symbol;Acc:HGNC:20367]	456	2.141	0.4158	Yes
59	MYO7A	myosin VIIA [Source:HGNC Symbol;Acc:HGNC:7606]	464	2.119	0.4194	Yes
60	RASSF2	Ras association domain family member 2 [Source:HGNC Symbol;Acc:HGNC:9883]	473	2.094	0.4229	Yes
61	ACE	angiotensin I converting enzyme [Source:HGNC Symbol;Acc:HGNC:2707]	479	2.08	0.4266	Yes
62	ST6GALNAC3	"ST6 N-acetylgalactosaminide alpha-2,6-sialyltransferase 3 [Source:HGNC Symbol;Acc:HGNC:19343]"	483	2.061	0.4305	Yes
63	PLXND1	plexin D1 [Source:HGNC Symbol;Acc:HGNC:9107]	487	2.053	0.4344	Yes
64	CGNL1	cingulin like 1 [Source:HGNC Symbol;Acc:HGNC:25931]	496	2.04	0.4378	Yes

65	PLEKHG1	pleckstrin homology and RhoGEF domain containing G1 [Source:HGNC Symbol;Acc:HGNC:20884]	498	2.039	0.4418	Yes
66	DCHS1	dachsous cadherin-related 1 [Source:HGNC Symbol;Acc:HGNC:13681]	509	2.013	0.445	Yes
67	APOLD1	apolipoprotein L domain containing 1 [Source:HGNC Symbol;Acc:HGNC:25268]	510	2.012	0.4491	Yes
68	EGFL7	EGF like domain multiple 7 [Source:HGNC Symbol;Acc:HGNC:20594]	513	2.004	0.4529	Yes
69	ZDHHC7	zinc finger DHHC-type palmitoyltransferase 7 [Source:HGNC Symbol;Acc:HGNC:18459]	517	1.995	0.4567	Yes
70	ICAM2	intercellular adhesion molecule 2 [Source:HGNC Symbol;Acc:HGNC:5345]	520	1.989	0.4606	Yes
71	TSPAN13	tetraspanin 13 [Source:HGNC Symbol;Acc:HGNC:21643]	538	1.958	0.4629	Yes
72	KANK3	KN motif and ankyrin repeat domains 3 [Source:HGNC Symbol;Acc:HGNC:24796]	540	1.957	0.4668	Yes
73	VWF	von Willebrand factor [Source:HGNC Symbol;Acc:HGNC:12726]	541	1.957	0.4708	Yes
74	PRICKLE1	prickle planar cell polarity protein 1 [Source:HGNC Symbol;Acc:HGNC:17019]	545	1.941	0.4744	Yes
75	ZNF423	zinc finger protein 423 [Source:HGNC Symbol;Acc:HGNC:16762]	571	1.897	0.4758	Yes
76	FAM189A2	family with sequence similarity 189 member A2 [Source:HGNC Symbol;Acc:HGNC:24820]	584	1.872	0.4785	Yes
77	PREX2	"phosphatidylinositol-3,4,5-trisphosphate dependent Rac exchange factor 2 [Source:HGNC Symbol;Acc:HGNC:22950]"	590	1.855	0.4817	Yes
78	SEMA3G	semaphorin 3G [Source:HGNC Symbol;Acc:HGNC:30400]	605	1.827	0.4841	Yes
79	PPP1R13B	protein phosphatase 1 regulatory subunit 13B [Source:HGNC Symbol;Acc:HGNC:14950]	611	1.82	0.4873	Yes
80	RASIP1	Ras interacting protein 1 [Source:HGNC Symbol;Acc:HGNC:24716]	618	1.803	0.4904	Yes
81	MAMLD1	mastermind like domain containing 1 [Source:HGNC Symbol;Acc:HGNC:2568]	625	1.79	0.4935	Yes
82	LMCD1	LIM and cysteine rich domains 1 [Source:HGNC Symbol;Acc:HGNC:6633]	683	1.693	0.4913	Yes
83	SH2D3C	SH2 domain containing 3C [Source:HGNC Symbol;Acc:HGNC:16884]	706	1.665	0.4925	Yes
84	ZCCHC24	zinc finger CCHC-type containing 24 [Source:HGNC Symbol;Acc:HGNC:26911]	707	1.663	0.4959	Yes
85	BCAM	basal cell adhesion molecule (Lutheran blood group) [Source:HGNC Symbol;Acc:HGNC:6722]	742	1.599	0.4958	Yes
86	FAM102A	family with sequence similarity 102 member A [Source:HGNC Symbol;Acc:HGNC:31419]	748	1.59	0.4986	Yes
87	SHROOM2	shroom family member 2 [Source:HGNC Symbol;Acc:HGNC:630]	764	1.557	0.5003	Yes
88	IL4R	interleukin 4 receptor [Source:HGNC Symbol;Acc:HGNC:6015]	765	1.556	0.5035	Yes
89	ABCG2	ATP binding cassette subfamily G member 2 (Junior blood group) [Source:HGNC Symbol;Acc:HGNC:74]	771	1.549	0.5061	Yes
90	EHD2	EH domain containing 2 [Source:HGNC Symbol;Acc:HGNC:3243]	790	1.524	0.5075	Yes
91	TP53I11	tumour protein p53 inducible protein 11 [Source:HGNC Symbol;Acc:HGNC:16842]	794	1.517	0.5102	Yes
92	MAML3	mastermind like transcriptional coactivator 3 [Source:HGNC Symbol;Acc:HGNC:16272]	798	1.514	0.513	Yes
93	ARRB1	arrestin beta 1 [Source:HGNC Symbol;Acc:HGNC:711]	828	1.481	0.5132	Yes
94	AFAP1L1	actin filament associated protein 1 like 1 [Source:HGNC Symbol;Acc:HGNC:26714]	845	1.462	0.5146	Yes
95	EML1	EMAP like 1 [Source:HGNC Symbol;Acc:HGNC:3330]	879	1.416	0.5143	Yes

175

96	CRTC3	CREB regulated transcription coactivator 3 [Source:HGNC Symbol;Acc:HGNC:26148]	882	1.414	0.5169	Yes
97	FZD4	frizzled class receptor 4 [Source:HGNC Symbol;Acc:HGNC:4042]	936	1.368	0.5145	Yes
98	RAPGEF4	Rap guanine nucleotide exchange factor 4 [Source:HGNC Symbol;Acc:HGNC:16626]	947	1.353	0.5163	Yes
99	ROBO4	roundabout guidance receptor 4 [Source:HGNC Symbol;Acc:HGNC:17985]	949	1.349	0.5189	Yes
100	DLL1	delta like canonical Notch ligand 1 [Source:HGNC Symbol;Acc:HGNC:2908]	971	1.327	0.5196	Yes
101	KLHL6	kelch like family member 6 [Source:HGNC Symbol;Acc:HGNC:18653]	990	1.306	0.5205	Yes
102	ITGA6	integrin subunit alpha 6 [Source:HGNC Symbol;Acc:HGNC:6142]	999	1.293	0.5223	Yes
103	NOD1	nucleotide binding oligomerisation domain containing 1 [Source:HGNC Symbol;Acc:HGNC:16390]	1023	1.267	0.5226	Yes
104	PCDH12	protocadherin 12 [Source:HGNC Symbol;Acc:HGNC:8657]	1024	1.267	0.5252	Yes
105	ESM1	endothelial cell specific molecule 1 [Source:HGNC Symbol;Acc:HGNC:3466]	1028	1.265	0.5275	Yes
106	STON2	stonin 2 [Source:HGNC Symbol;Acc:HGNC:30652]	1038	1.254	0.5292	Yes
107	SEMA3F	semaphorin 3F [Source:HGNC Symbol;Acc:HGNC:10728]	1055	1.235	0.5301	Yes
108	SHE	Src homology 2 domain containing E [Source:HGNC Symbol;Acc:HGNC:27004]	1057	1.234	0.5325	Yes
109	PPP1R16B	protein phosphatase 1 regulatory subunit 16B [Source:HGNC Symbol;Acc:HGNC:15850]	1073	1.214	0.5335	Yes
110	ICA1	islet cell autoantigen 1 [Source:HGNC Symbol;Acc:HGNC:5343]	1085	1.207	0.5349	Yes
111	RGS3	regulator of G protein signalling 3 [Source:HGNC Symbol;Acc:HGNC:9999]	1105	1.191	0.5355	Yes
112	UPP1	uridine phosphorylase 1 [Source:HGNC Symbol;Acc:HGNC:12576]	1113	1.186	0.5372	Yes
113	ABCA1	ATP binding cassette subfamily A member 1 [Source:HGNC Symbol;Acc:HGNC:29]	1117	1.183	0.5393	Yes
114	COLEC12	collectin subfamily member 12 [Source:HGNC Symbol;Acc:HGNC:16016]	1119	1.179	0.5416	Yes
115	PLCB4	phospholipase C beta 4 [Source:HGNC Symbol;Acc:HGNC:9059]	1123	1.177	0.5437	Yes
116	NOTCH1	notch receptor 1 [Source:HGNC Symbol;Acc:HGNC:7881]	1132	1.17	0.5453	Yes
117	MAP4K2	mitogen-activated protein kinase 2 [Source:HGNC Symbol;Acc:HGNC:6864]	1168	1.143	0.5442	Yes
118	GPRC5B	G protein-coupled receptor class C group 5 member B [Source:HGNC Symbol;Acc:HGNC:13308]	1176	1.134	0.5458	Yes
119	TCF7L1	transcription factor 7 like 1 [Source:HGNC Symbol;Acc:HGNC:11640]	1211	1.103	0.5447	Yes
120	CLEC14A	C-type lectin domain containing 14A [Source:HGNC Symbol;Acc:HGNC:19832]	1232	1.085	0.545	Yes
121	TNFAIP8L1	TNF alpha induced protein 8 like 1 [Source:HGNC Symbol;Acc:HGNC:28279]	1235	1.083	0.547	Yes
122	LDB2	LIM domain binding 2 [Source:HGNC Symbol;Acc:HGNC:6533]	1250	1.076	0.5478	Yes
123	DOCK8	dedicator of cytokinesis 8 [Source:HGNC Symbol;Acc:HGNC:19191]	1271	1.057	0.548	Yes
124	TSPAN9	tetraspanin 9 [Source:HGNC Symbol;Acc:HGNC:21640]	1276	1.055	0.5498	Yes
125	MAP2K6	mitogen-activated protein kinase kinase 6 [Source:HGNC Symbol;Acc:HGNC:6846]	1277	1.055	0.5519	Yes
126	BMX	BMX non-receptor tyrosine kinase [Source:HGNC Symbol;Acc:HGNC:1079]	1297	1.039	0.5522	Yes
127	KCNK6	potassium two pore domain channel subfamily K member 6 [Source:HGNC Symbol;Acc:HGNC:6281]	1306	1.033	0.5535	Yes
128	IGF1	insulin like growth factor 1 [Source:HGNC Symbol;Acc:HGNC:5464]	1324	1.019	0.5539	Yes

129	TPCN1	two pore segment channel 1 [Source:HGNC Symbol;Acc:HGNC:18182]	1335	1.014	0.555	Yes
130	C8orf58	chromosome 8 open reading frame 58 [Source:HGNC Symbol;Acc:HGNC:32233]	1340	1.013	0.5566	Yes
131	SORBS3	sorbin and SH3 domain containing 3 [Source:HGNC Symbol;Acc:HGNC:30907]	1359	1.003	0.5569	Yes
132	BMP2K	BMP2 inducible kinase [Source:HGNC Symbol;Acc:HGNC:18041]	1371	0.993	0.5578	Yes
133	HIPK1	homeodomain interacting protein kinase 1 [Source:HGNC Symbol;Acc:HGNC:19006]	1373	0.991	0.5598	Yes
134	CAV2	caveolin 2 [Source:HGNC Symbol;Acc:HGNC:1528]	1387	0.981	0.5605	Yes
135	PLA2G4A	phospholipase A2 group IVA [Source:HGNC Symbol;Acc:HGNC:9035]	1436	0.949	0.5577	Yes
136	PKIG	cAMP-dependent protein kinase inhibitor gamma [Source:HGNC Symbol;Acc:HGNC:9019]	1463	0.93	0.557	Yes
137	RFTN2	raftlin family member 2 [Source:HGNC Symbol;Acc:HGNC:26402]	1464	0.928	0.5589	Yes
138	MMRN1	multimerin 1 [Source:HGNC Symbol;Acc:HGNC:7178]	1479	0.918	0.5594	Yes
139	TM6SF1	transmembrane 6 superfamily member 1 [Source:HGNC Symbol;Acc:HGNC:11860]	1484	0.915	0.5609	Yes
140	SHANK3	SH3 and multiple ankyrin repeat domains 3 [Source:HGNC Symbol;Acc:HGNC:14294]	1491	0.912	0.5622	Yes
141	SMAGP	small cell adhesion glycoprotein [Source:HGNC Symbol;Acc:HGNC:26918]	1509	0.899	0.5623	Yes
142	EMILIN1	elastin microfibril interfacer 1 [Source:HGNC Symbol;Acc:HGNC:19880]	1518	0.894	0.5634	Yes
143	HMCN1	hemicentin 1 [Source:HGNC Symbol;Acc:HGNC:19194]	1548	0.877	0.5623	Yes
144	INKA1	inka box actin regulator 1 [Source:HGNC Symbol;Acc:HGNC:32480]	1584	0.852	0.5606	Yes
145	KIAA1217	KIAA1217 [Source:HGNC Symbol;Acc:HGNC:25428]	1586	0.85	0.5622	Yes
146	GSN	gelsolin [Source:HGNC Symbol;Acc:HGNC:4620]	1599	0.84	0.5628	Yes
147	NFIC	nuclear factor I C [Source:HGNC Symbol;Acc:HGNC:7786]	1605	0.837	0.564	Yes
148	SNCG	synuclein gamma [Source:HGNC Symbol;Acc:HGNC:11141]	1616	0.833	0.5647	Yes
149	ARHGEF15	Rho guanine nucleotide exchange factor 15 [Source:HGNC Symbol;Acc:HGNC:15590]	1627	0.827	0.5654	Yes
150	ADGRA2	adhesion G protein-coupled receptor A2 [Source:HGNC Symbol;Acc:HGNC:17849]	1674	0.806	0.5625	Yes
151	PRKAR2B	protein kinase cAMP-dependent type II regulatory subunit beta [Source:HGNC Symbol;Acc:HGNC:9392]	1675	0.806	0.5642	Yes
152	CLEC1A	C-type lectin domain family 1 member A [Source:HGNC Symbol;Acc:HGNC:24355]	1683	0.8	0.5651	Yes
153	VAV3	vav guanine nucleotide exchange factor 3 [Source:HGNC Symbol;Acc:HGNC:12659]	1694	0.797	0.5657	Yes
154	TIE1	tyrosine kinase with immunoglobulin like and EGF like domains 1 [Source:HGNC Symbol;Acc:HGNC:11809]	1731	0.78	0.5638	Yes
155	ATG4A	autophagy related 4A cysteine peptidase [Source:HGNC Symbol;Acc:HGNC:16489]	1755	0.77	0.5631	Yes
156	PIEZO2	piezo type mechanosensitive ion channel component 2 [Source:HGNC Symbol;Acc:HGNC:26270]	1761	0.767	0.5642	Yes
157	DEPP1	DEPP1 autophagy regulator [Source:HGNC Symbol;Acc:HGNC:23355]	1769	0.763	0.565	Yes
158	SLC9A3R2	SLC9A3 regulator 2 [Source:HGNC Symbol;Acc:HGNC:11076]	1797	0.748	0.5639	Yes
159	IGFBP4	insulin like growth factor binding protein 4 [Source:HGNC Symbol;Acc:HGNC:5473]	1806	0.743	0.5646	Yes
160	USHBP1	USH1 protein network component harmonin binding protein 1 [Source:HGNC Symbol;Acc:HGNC:24058]	1813	0.739	0.5655	Yes

161	LHFPL2	LHFPL tetraspan subfamily member 2 [Source:HGNC Symbol;Acc:HGNC:6588]	1825	0.733	0.566	Yes
162	HLX	H2.0 like homeobox [Source:HGNC Symbol;Acc:HGNC:4978]	1836	0.728	0.5665	Yes
163	SIGIRR	single Ig and TIR domain containing [Source:HGNC Symbol;Acc:HGNC:30575]	1838	0.727	0.5678	Yes
164	ATP2B4	ATPase plasma membrane Ca2+ transporting 4 [Source:HGNC Symbol;Acc:HGNC:817]	1840	0.725	0.5692	Yes
165	IGFBP3	insulin like growth factor binding protein 3 [Source:HGNC Symbol;Acc:HGNC:5472]	1841	0.725	0.5707	Yes
166	BMP4	bone morphogenetic protein 4 [Source:HGNC Symbol;Acc:HGNC:1071]	1845	0.722	0.5719	Yes
167	ITGB3	integrin subunit beta 3 [Source:HGNC Symbol;Acc:HGNC:6156]	1878	0.711	0.5702	Yes
168	STEAP1B	STEAP family member 1B [Source:HGNC Symbol;Acc:HGNC:41907]	1880	0.709	0.5715	Yes
169	PRICKLE2	prickle planar cell polarity protein 2 [Source:HGNC Symbol;Acc:HGNC:20340]	1881	0.709	0.573	Yes
170	CD34	CD34 molecule [Source:HGNC Symbol;Acc:HGNC:1662]	1904	0.699	0.5722	Yes
171	ST8SIA4	"ST8 alpha-N-acetyl-neuraminide alpha-2,8-sialyltransferase 4 [Source:HGNC Symbol;Acc:HGNC:10871]"	1914	0.696	0.5728	Yes
172	KLHL4	kelch like family member 4 [Source:HGNC Symbol;Acc:HGNC:6355]	1916	0.695	0.5741	Yes
173	KIAA1191	KIAA1191 [Source:HGNC Symbol;Acc:HGNC:29209]	1918	0.694	0.5754	Yes
174	AAK1	AP2 associated kinase 1 [Source:HGNC Symbol;Acc:HGNC:19679]	1924	0.691	0.5763	Yes

Supplementary table.11: Differentially expressed common genes between genes upregulated in *MDFIC* esiRNA treated hLECs and those downregulated in *GATA2* siRNA treated hLECs compared to control cells.

No.	Gene symbol and name	
1	PLPP3	phospholipid phosphatase 3 [Source:HGNC Symbol;Acc:HGNC:9229]
2	SPNS2	sphingolipid transporter 2 [Source:HGNC Symbol;Acc:HGNC:26992]
3	MMP15	matrix metallopeptidase 15 [Source:HGNC Symbol;Acc:HGNC:7161]
4	NPR1	natriuretic peptide receptor 1 [Source:HGNC Symbol;Acc:HGNC:7943]
5	CABLES1	Cdk5 and Abl enzyme substrate 1 [Source:HGNC Symbol;Acc:HGNC:25097]
6	NOS3	nitric oxide synthase 3 [Source:HGNC Symbol;Acc:HGNC:7876]
7	SLC40A1	solute carrier family 40 member 1 [Source:HGNC Symbol;Acc:HGNC:10909]
8	ITGA9	integrin subunit alpha 9 [Source:HGNC Symbol;Acc:HGNC:6145]
9	SLC22A23	solute carrier family 22 member 23 [Source:HGNC Symbol;Acc:HGNC:21106]
10	ESAM	endothelial cell adhesion molecule [Source:HGNC Symbol;Acc:HGNC:17474]
11	NRARP	NOTCH regulated ankyrin repeat protein [Source:HGNC Symbol;Acc:HGNC:33843]
12	STARD8	StAR related lipid transfer domain containing 8 [Source:HGNC Symbol;Acc:HGNC:19161]

13	PGM5	phosphoglucomutase 5 [Source:HGNC Symbol;Acc:HGNC:8908]
14	ZNF366	zinc finger protein 366 [Source:HGNC Symbol;Acc:HGNC:18316]
15	FLI1	Fli-1 proto-oncogene, ETS transcription factor [Source:HGNC Symbol;Acc:HGNC:3749]
16	APLN	apelin [Source:HGNC Symbol;Acc:HGNC:16665]
17	TSPAN18	tetraspanin 18 [Source:HGNC Symbol;Acc:HGNC:20660
18	ACER2	alkaline ceramidase 2 [Source:HGNC Symbol;Acc:HGNC:23675]
19	PLXNA4	plexin A4 [Source:HGNC Symbol;Acc:HGNC:9102]
20	MALL	mal, T cell differentiation protein like [Source:HGNC Symbol;Acc:HGNC:6818]
21	TRPV4	transient receptor potential cation channel subfamily V member 4 [Source:HGNC Symbol;Acc:HGNC:18083]
22	CARD10	caspase recruitment domain family member 10 [Source:HGNC Symbol;Acc:HGNC:16422]
23	CEP68	centrosomal protein 68 [Source:HGNC Symbol;Acc:HGNC:29076]
24	CSF2RB	colony stimulating factor 2 receptor subunit beta [Source:HGNC Symbol;Acc:HGNC:2436]
25	NPAS2	neuronal PAS domain protein 2 [Source:HGNC Symbol;Acc:HGNC:7895]
26	SOX18	SRY-box transcription factor 18 [Source:HGNC Symbol;Acc:HGNC:11194]
27	CELSR1	cadherin EGF LAG seven-pass G-type receptor 1 [Source:HGNC Symbol;Acc:HGNC:1850]
28	TSPAN7	tetraspanin 7 [Source:HGNC Symbol;Acc:HGNC:11854]
29	CYYR1	cysteine and tyrosine rich 1 [Source:HGNC Symbol;Acc:HGNC:16274]
30	RAMP2	receptor activity modifying protein 2 [Source:HGNC Symbol;Acc:HGNC:9844]
31	MFNG	MFNG O-fucosylpeptide 3-beta-N-acetylglucosaminyltransferase [Source:HGNC Symbol;Acc:HGNC:7038]
32	HYAL1	hyaluronidase 1 [Source:HGNC Symbol;Acc:HGNC:5320]
33	FAM171A1	family with sequence similarity 171 member A1 [Source:HGNC Symbol;Acc:HGNC:23522]
34	ST6GAL1	ST6 beta-galactoside alpha-2,6-sialyltransferase 1 [Source:HGNC Symbol;Acc:HGNC:10860]
35	ABCG1	tweety family member 3 [Source:HGNC Symbol;Acc:HGNC:22222]
36	TTYH3	tweety family member 3 [Source:HGNC Symbol;Acc:HGNC:22222]
37	FAM43A	family with sequence similarity 43 member A [Source:HGNC Symbol;Acc:HGNC:26888]
38	SCN3B	sodium voltage-gated channel beta subunit 3 [Source:HGNC Symbol;Acc:HGNC:20665]
39	FILIP1	filamin A interacting protein 1 [Source:HGNC Symbol;Acc:HGNC:21015]
40	MARCKSL1	MARCKS like 1 [Source:HGNC Symbol;Acc:HGNC:7142]

References

Abdul-Sater, Z., Yehya, A., Beresian, J., Salem, E., Kamar, A., Baydoun, S., ... & Nemer, G. (2012). Two heterozygous mutations in NFATC1 in a patient with Tricuspid Atresia. *PloS one*, *7*(11), e49532.

Adler, Y., Finkelstein, Y., Guindo, J., Rodriguez de la Serna, A., Shoenfeld, Y., Bayes-Genis, A., ... & Spodick, D. H. (1998). Colchicine treatment for recurrent pericarditis: a decade of experience. *Circulation*, *97*(21), 2183-2185.

Ahn, J. H., Cho, H., Kim, J. H., Kim, S. H., Ham, J. S., Park, I., ... & Koh, G. Y. (2019). Meningeal lymphatic vessels at the skull base drain cerebrospinal fluid. *Nature*, *572*(7767), 62-66.

Alby, C., Boutaud, L., Bonnière, M., Collardeau-Frachon, S., Guibaud, L., Lopez, E., ... & Attié-Bitach, T. (2018). In utero ultrasound diagnosis of corpus callosum agenesis leading to the identification of orofaciodigital type 1 syndrome in female fetuses. *Birth Defects Research*, *110*(4), 382-389.

Alders, M., Al-Gazali, L., Cordeiro, I., Dallapiccola, B., Garavelli, L., Tuysuz, B., ... & Hennekam, R. C. (2014). Hennekam syndrome can be caused by FAT4 mutations and be allelic to Van Maldergem syndrome. *Human genetics*, *133*, 1161-1167.

Alexander, J. S., Ganta, V. C., Jordan, P. A., & Witte, M. H. (2010). Gastrointestinal lymphatics in health and disease. *Pathophysiology*, *17*(4), 315-335.

Alitalo, K. (2011). The lymphatic vasculature in disease. *Nature medicine*, *17*(11), 1371-1380.

Alitalo, K., Tammela, T., & Petrova, T. V. (2005). Lymphangiogenesis in development and human disease. *Nature*, *438*(7070), 946-953.

Almomani, R., Verhagen, J. M., Herkert, J. C., Brosens, E., van Spaendonck-Zwarts, K. Y., Asimaki, A., ... & van de Laar, I. M. (2016). Biallelic truncating mutations in ALPK3 cause severe pediatric cardiomyopathy. *Journal of the American College of Cardiology*, *67*(5), 515-525.

Altiok, E., Ecoiffier, T., Sessa, R., Yuen, D., Grimaldo, S., Tran, C., ... & Chen, L. (2015). Integrin alpha-9 mediates lymphatic valve formation in corneal lymphangiogenesis. *Investigative Ophthalmology & Visual Science*, *56*(11), 6313-6319.

Amarillo, I. E., O'Connor, S., Lee, C. K., Willing, M., & Wambach, J. A. (2015). De novo 9q gain in an infant with tetralogy of Fallot with absent pulmonary valve: patient report and review of congenital heart disease in 9q duplication syndrome. *American Journal of Medical Genetics Part A*, *167*(12), 2966-2974.

Anuwutnavin, S., Wanitpongpan, P., Chungsomprasong, P., Soongswang, J., Srisantiroj, N., & Wataganara, T. (2013). Fetal long QT syndrome manifested as

atrioventricular block and ventricular tachycardia: a case report and a review of the literature. *Pediatric cardiology*, *34*, 1955-1962.

Aoki, Y., Niihori, T., Inoue, S. I., & Matsubara, Y. (2016). Recent advances in RASopathies. *Journal of human genetics*, *61*(1), 33-39.

Apkon, M. (1995, December). Pathophysiology of hydrops fetalis. In *Seminars in perinatology* (Vol. 19, No. 6, pp. 437-446). WB Saunders.

Aranguren, X. L., Beerens, M., Coppiello, G., Wiese, C., Vandersmissen, I., Lo Nigro, A., ... & Luttun, A. (2013). COUP-TFII orchestrates venous and lymphatic endothelial identity by homo-or hetero-dimerisation with PROX1. *Journal of cell science*, *126*(5), 1164-1175.

Arcasoy, M. O., & Gallagher, P. G. (1995, December). Hematologic disorders and nonimmune hydrops fetalis. In *Seminars in perinatology* (Vol. 19, No. 6, pp. 502-515). WB Saunders.

Aspelund, A., Antila, S., Proulx, S. T., Karlsen, T. V., Karaman, S., Detmar, M., ... & Alitalo, K. (2015). A dural lymphatic vascular system that drains brain interstitial fluid and macromolecules. *Journal of Experimental Medicine*, *212*(7), 991-999.

Aspelund, A., Tammela, T., Antila, S., Nurmi, H., Leppänen, V. M., Zarkada, G., ... & Alitalo, K. (2014). The Schlemm's canal is a VEGF-C/VEGFR-3–responsive lymphatic-like vessel. *The Journal of clinical investigation*, *124*(9), 3975-3986.

Astarita, J. L., Acton, S. E., & Turley, S. J. (2012). Podoplanin: emerging functions in development, the immune system, and cancer. *Frontiers in immunology*, *3*, 283.

Attar, M. A., & Donn, S. M. (2017, August). Congenital chylothorax. In *Seminars in Fetal and Neonatal Medicine* (Vol. 22, No. 4, pp. 234-239). WB Saunders.

Au, O. (2009). *Clinical Practice Guideline for Perinatal Mortality The Perinatal Society Of Australia And New Zealand Perinatal Mortality Group Second edition, Version 2.2.* http://www.psanzpnmsig.org.au

Aula, N., & Aula, P. (2006). Prenatal diagnosis of free sialic acid storage disorders (SASD). *Prenatal Diagnosis: Published in Affiliation With the International Society for Prenatal Diagnosis*, *26*(8), 655-658.

Baala, L., Romano, S., Khaddour, R., Saunier, S., Smith, U. M., Audollent, S., ... & Attié-Bitach, T. (2007). The Meckel-Gruber syndrome gene, MKS3, is mutated in Joubert syndrome. *The American Journal of Human Genetics*, *80*(1), 186-194.

Badiner, N., Taylor, S. P., Forlenza, K., Lachman, R. S., University of Washington Center for Mendelian Genomics, Bamshad, M., ... & Krakow, D. (2017). Mutations in DYNC2H1, the cytoplasmic dynein 2, heavy chain 1 motor protein gene, cause short-rib polydactyly type I, Saldino–Noonan type. *Clinical genetics*, *92*(2), 158-165.

Baldelli, E., Subramanian, M., Alsubaie, A. M., Oldaker, G., Emelianenko, M., El Gazzah, E., ... & Pierobon, M. (2021). Heterogeneous Off-Target Effects of Ultra-Low

Dose Dimethyl Sulfoxide (DMSO) on Targetable Signaling Events in Lung Cancer In Vitro Models. *International Journal of Molecular Sciences*, *22*(6), 2819.

Baluk, P., Fuxe, J., Hashizume, H., Romano, T., Lashnits, E., Butz, S., ... & McDonald, D. M. (2007). Functionally specialized junctions between endothelial cells of lymphatic vessels. *The Journal of experimental medicine*, *204*(10), 2349-2362.

Banait, N., Fenton, A., & Splitt, M. (2015). Cornelia de Lange syndrome due to mosaic NIPBL mutation: antenatal presentation with sacrococcygeal teratoma. *Case Reports*, *2015*, bcr2015211006.

Banerji, S., Ni, J., Wang, S. X., Clasper, S., Su, J., Tammi, R., ... & Jackson, D. G. (1999). LYVE-1, a new homologue of the CD44 glycoprotein, is a lymph-specific receptor for hyaluronan. *The Journal of cell biology*, *144*(4), 789-801.

Barbelanne, M., Chiu, A., Qian, J., & Tsang, W. Y. (2016). Opposing post-translational modifications regulate Cep76 function to suppress centriole amplification. *Oncogene*, *35*(41), 5377-5387.

Barbier, L., Tay, S. S., McGuffog, C., Triccas, J. A., McCaughan, G. W., Bowen, D. G., & Bertolino, P. (2012). Two lymph nodes draining the mouse liver are the preferential site of DC migration and T cell activation. *Journal of hepatology*, *57*(2), 352-358.

Basel-Vanagaite, L., Kornreich, L., Schiller, O., Yacobovich, J., & Merlob, P. (2008). Yunis–Varon syndrome: Further delineation of the phenotype. *American Journal of Medical Genetics Part A*, *146*(4), 532-537.

Bazigou, E., & Makinen, T. (2013). Flow control in our vessels: vascular valves make sure there is no way back. *Cellular and Molecular Life Sciences*, *70*, 1055-1066.

Beaujot, J., Joriot, S., Dieux, A., Vaast, P., Franquet-Ansart, H., Valat, A. S., ... & Devisme, L. (2013). Phenotypic variability of prenatally presenting Gaucher's disease. *Prenatal Diagnosis*, *33*(10), 1004-1006.

Bellini, C., & Hennekam, R. C. (2012). Non-immune hydrops fetalis: a short review of etiology and pathophysiology. *American journal of medical genetics Part A*, *158*(3), 597-605.

Bellini, C., Boccardo, F., Campisi, C., & Bonioli, E. (2006). Congenital pulmonary lymphangiectasia. *Orphanet journal of rare diseases*, *1*(1), 43.

Bellini, C., Hennekam, R. C., Boccardo, F., Campisi, C., Serra, G., & Bonioli, E. (2006). Nonimmune idiopathic hydrops fetalis and congenital lymphatic dysplasia. *American Journal of Medical Genetics Part A*, *140*(7), 678-684.

Bellini, C., Hennekam, R. C., Fulcheri, E., Rutigliani, M., Morcaldi, G., Boccardo, F., & Bonioli, E. (2009). Etiology of nonimmune hydrops fetalis: a systematic review. *American journal of medical genetics Part A*, *149*(5), 844-851.

Bernier-Latmani, J., & Petrova, T. V. (2017). Intestinal lymphatic vasculature: structure, mechanisms and functions. *Nature reviews Gastroenterology & hepatology*, *14*(9), 510-526.

Bernier-Latmani, J., Cisarovsky, C., Demir, C. S., Bruand, M., Jaquet, M., Davanture, S., ... & Petrova, T. V. (2015). DLL4 promotes continuous adult intestinal lacteal regeneration and dietary fat transport. *The Journal of clinical investigation*, *125*(12), 4572-4586.

Bernier-Latmani, J., Cisarovsky, C., Demir, C. S., Bruand, M., Jaquet, M., Davanture, S., ... & Petrova, T. V. (2015). DLL4 promotes continuous adult intestinal lacteal regeneration and dietary fat transport. *The Journal of clinical investigation*, *125*(12), 4572-4586.

Bertozzi, C. C., Schmaier, A. A., Mericko, P., Hess, P. R., Zou, Z., Chen, M., ... & Kahn, M. L. (2010). Platelets regulate lymphatic vascular development through CLEC-2–SLP-76 signaling. *Blood, The Journal of the American Society of Hematology*, *116*(4), 661-670.

Betterman, K. L., Sutton, D. L., Secker, G. A., Kazenwadel, J., Oszmiana, A., Lim, L., ... & Harvey, N. L. (2020). Atypical cadherin FAT4 orchestrates lymphatic endothelial cell polarity in response to flow. *The Journal of clinical investigation*, *130*(6), 3315-3328.

Blei, F., & Bittman, M. E. (2016). Congenital vascular anomalies: current perspectives on diagnosis, classification, and management. *Journal of vascular diagnostics and interventions*, *4*, 23.

Blesinger, H., Kaulfuß, S., Aung, T., Schwoch, S., Prantl, L., Rößler, J., ... & Becker, J. (2018). PIK3CA mutations are specifically localized to lymphatic endothelial cells of lymphatic malformations. *PLoS One*, *13*(7), e0200343.

Blitz, M. J., Rochelson, B., Sood, M., Bialer, M. G., & Vohra, N. (2018). Prenatal sonographic findings in a case of Wolman's disease. *Journal of Clinical Ultrasound*, *46*(1), 66-68.

Bos, F. L., Caunt, M., Peterson-Maduro, J., Planas-Paz, L., Kowalski, J., Karpanen, T., ... & Schulte-Merker, S. (2011). Brief UltraRapid Communication CCBE1 Is Essential for Mammalian Lymphatic Vascular.

Bouvrée, K., Brunet, I., Del Toro, R., Gordon, E., Prahst, C., Cristofaro, B., ... & Eichmann, A. (2012). Semaphorin3A, Neuropilin-1, and PlexinA1 are required for lymphatic valve formation. *Circulation research*, *111*(4), 437-445.

Bowe, E. T. (1970). Treatment and Prophylaxis of Rh Disease. *Gynecologic and Obstetric Investigation*, *1*(Suppl. 1), 13-25.

Brice, G., Child, A. H., Evans, A., Bell, R., Mansour, S., Burnand, K., ... & Mortimer, P. (2005). Milroy disease and the VEGFR-3 mutation phenotype. *Journal of medical genetics*, *42*(2), 98-102.

Bronsteen, R., Lee, W., Vettraino, I. M., Huang, R., & Comstock, C. H. (2004). Second-trimester sonography and trisomy 18. *Journal of ultrasound in medicine*, *23*(2), 233-240.

Brouillard, P., Boon, L., & Vikkula, M. (2014). Genetics of lymphatic anomalies. *The Journal of clinical investigation*, *124*(3), 898-904.

Bui, H. M., Enis, D., Robciuc, M. R., Nurmi, H. J., Cohen, J., Chen, M., ... & Kahn, M. L. (2016). Proteolytic activation defines distinct lymphangiogenic mechanisms for VEGFC and VEGFD. *The Journal of clinical investigation*, *126*(6), 2167-2180.

Bui, K., & Hong, Y. K. (2020). Ras pathways on Prox1 and lymphangiogenesis: insights for therapeutics. *Frontiers in Cardiovascular Medicine*, 7, 597374.

Bülow, L., Lissewski, C., Bressel, R., Rauch, A., Stark, Z., Zenker, M., & Bartsch, O. (2015). Hydrops, fetal pleural effusions and chylothorax in three patients with CBL mutations. *American Journal of Medical Genetics Part A*, *167*(2), 394-399.

Burden, C., Bradley, S., Storey, C., Ellis, A., Heazell, A. E., Downe, S., ... & Siassakos, D. (2016). From grief, guilt pain and stigma to hope and pride–a systematic review and meta-analysis of mixed-method research of the psychosocial impact of stillbirth. *BMC pregnancy and childbirth*, *16*(1), 1-12.

Busnelli, M., Manzini, S., Parolini, C., Escalante-Alcalde, D., & Chiesa, G. (2018). Lipid phosphate phosphatase 3 in vascular pathophysiology. *Atherosclerosis*, *271*, 156-165.

Byrne, A. B., Brouillard, P., Sutton, D. L., Kazenwadel, J., Montazaribarforoushi, S., Secker, G. A., ... & Harvey, N. L. (2022). Pathogenic variants in MDFIC cause recessive central conducting lymphatic anomaly with lymphedema. *Science translational medicine*, *14*(634), eabm4869.

Caciotti, A., Catarzi, S., Tonin, R., Lugli, L., Perez, C. R., Michelakakis, H., ... & Morrone, A. (2013). Galactosialidosis: review and analysis of CTSA gene mutations. *Orphanet journal of rare diseases*, *8*(1), 1-9.

Capobres, T., Sabharwal, G., & Griffith, B. (2016). A case of I-cell disease (mucolipidosis II) presenting with short femurs on prenatal ultrasound and profound diaphyseal cloaking. *BJR| case reports*, 20150420.

Cardwell, M. S. (1988). Successful treatment of hydrops fetalis caused by fetomaternal hemorrhage: a case report. *American journal of obstetrics and gynecology*, *158*(1), 131-132.

Carlson, J. A. (2014). Lymphedema and subclinical lymphostasis (microlymphedema) facilitate cutaneous infection, inflammatory dermatoses, and neoplasia: a locus minoris resistentiae. *Clinics in dermatology*, *32*(5), 599-615.

Chainarong, N., Muangpaisarn, W., & Suwanrath, C. (2021). Etiology and outcome of non-immune hydrops fetalis in relation to gestational age at diagnosis and intrauterine treatment. *Journal of Perinatology*, *41*(10), 2544-2548.

Chakraborty, S., Davis, M. J., & Muthuchamy, M. (2015, February). Emerging trends in the pathophysiology of lymphatic contractile function. In *Seminars in cell & developmental biology* (Vol. 38, pp. 55-66). Academic Press.

Charlton, R. (1994). Autopsy and medical education: a review. *Journal of the Royal Society of Medicine*, *87*(4), 232.

Chauhan, S. K., Dohlman, T. H., & Dana, R. (2014). Corneal lymphatics: role in ocular inflammation as inducer and responder of adaptive immunity. *Journal of clinical & cellular immunology*, *5*.

Chen, C. P. (2012). Prenatal diagnosis and genetic analysis of fetal akinesia deformation sequence and multiple pterygium syndrome associated with neuromuscular junction disorders: a review. *Taiwanese Journal of Obstetrics and Gynecology*, *51*(1), 12-17.

Chen, G., Wu, D. I., Guo, W., Cao, Y., Huang, D., Wang, H., ... & Ning, Q. (2020). Clinical and immunological features of severe and moderate coronavirus disease 2019. *The Journal of clinical investigation*, *130*(5), 2620-2629.

Cho, H. J., Shin, M. Y., Ahn, K. M., Lee, S. I., Kim, H. J., Ki, C. S., & Kim, J. W. (2006). X-linked Opitz G/BBB syndrome: identification of a novel mutation and prenatal diagnosis in a Korean family. *Journal of Korean Medical Science*, *21*(5), 790-793.

Choi, I., Lee, S., & Hong, Y. K. (2012). The new era of the lymphatic system: no longer secondary to the blood vascular system. *Cold Spring Harbor perspectives in medicine*, *2*(4).

Chui, D. H. (2005). Alpha-thalassaemia and population health in Southeast Asia. *Annals of human biology*, *32*(2), 123-130.

Chung, C., & Iwakiri, Y. (2013). The lymphatic vascular system in liver diseases: its role in ascites formation. *Clinical and molecular hepatology*, *19*(2), 99.

Cifarelli, V., & Eichmann, A. (2019). The intestinal lymphatic system: functions and metabolic implications. *Cellular and molecular gastroenterology and hepatology*, 7(3), 503-513.

Connell, F., Brice, G., & Mortimer, P. (2008). Phenotypic characterization of primary lymphedema. *Annals of the New York Academy of Sciences*, *1131*(1), 140-146.

Connell, F., Kalidas, K., Ostergaard, P., Brice, G., Homfray, T., Roberts, L., ... & Lymphoedema Consortium. (2010). Linkage and sequence analysis indicate that CCBE1 is mutated in recessively inherited generalised lymphatic dysplasia. *Human genetics*, *127*, 231-241.

Conway, S. J., Izuhara, K., Kudo, Y., Litvin, J., Markwald, R., Ouyang, G., ... & Kudo, A. (2014). The role of periostin in tissue remodeling across health and disease. *Cellular and Molecular Life Sciences*, *71*, 1279-1288.

Cormier, J. N., Askew, R. L., Mungovan, K. S., Xing, Y., Ross, M. I., & Armer, J. M. (2010). Lymphedema beyond breast cancer: A systematic review and meta-analysis of cancer-related secondary lymphedema. *Cancer*, *116*(22), 5138-5149.

Coso, S., Bovay, E., & Petrova, T. V. (2014). Pressing the right buttons: signaling in lymphangiogenesis. *Blood, The Journal of the American Society of Hematology*, *123*(17), 2614-2624.

Courtice, F. C., Woolley, G., & Garlick, D. G. (1962). The transference of macromolecules from plasma to lymph in the liver. *Australian Journal of Experimental Biology and Medical Science*, *40*(2), 111-120.

Crawford, N. P. S., Qian, X., Ziogas, A., Papageorge, A. G., Boersma, B. J., Walker, R. C., ... & Hunter, K. W. (2007). Rrp1b, a new candidate susceptibility gene for breast cancer progression and metastasis. *PLoS genetics*, *3*(11), e214.

Croonen, E. A., Nillesen, W., Schrander, C., Jongmans, M., Scheffer, H., Noordam, C., ... & Yntema, H. G. (2013). Noonan syndrome: comparing mutation-positive with mutation-negative dutch patients. *Molecular syndromology*, *4*(5), 227-234.

Cueni, L. N., & Detmar, M. (2008). The lymphatic system in health and disease. *Lymphatic research and biology*, *6*(3-4), 109-122.

Cui, Y. E., Liu, K., Monzon-Medina, M. E., Padera, R. F., Wang, H., George, G., ... & El-Chemaly, S. (2015). Therapeutic lymphangiogenesis ameliorates established acute lung allograft rejection. *The Journal of clinical investigation*, *125*(11), 4255-4268.

Cusick, J. K., Alhomsy, Y., Wong, S., Talbott, G., Uversky, V. N., Hart, C., ... & Shi, Y. (2020). RELT stains prominently in B-cell lymphomas and binds the hematopoietic transcription factor MDFIC. *Biochemistry and Biophysics Reports*, *24*, 100868.

Da Mesquita, S., Fu, Z., & Kipnis, J. (2018). The meningeal lymphatic system: a new player in neurophysiology. *Neuron*, *100*(2), 375-388.

Dagenais, S. L., Hartsough, R. L., Erickson, R. P., Witte, M. H., Butler, M. G., & Glover, T. W. (2004). Foxc2 is expressed in developing lymphatic vessels and other tissues associated with lymphedema–distichiasis syndrome. *Gene Expression Patterns*, *4*(6), 611-619.

Dagoneau, N., Goulet, M., Genevieve, D., Sznajer, Y., Martinovic, J., Smithson, S., ... & Cormier-Daire, V. (2009). DYNC2H1 mutations cause asphyxiating thoracic dystrophy and short rib-polydactyly syndrome, type III. *The American Journal of Human Genetics*, *84*(5), 706-711.

Dalal, A. B., & Phadke, S. R. (2006). Twin pregnancy with Roberts syndrome in one fetus and trisomy 18 in the other. *Journal of Clinical Ultrasound*, *34*(3), 146-149.

Dane, K. Y., Nembrini, C., Tomei, A. A., Eby, J. K., O'Neil, C. P., Velluto, D., ... & Hubbell, J. A. (2011). Nano-sized drug-loaded micelles deliver payload to lymph node immune cells and prolong allograft survival. *Journal of controlled release*, *156*(2), 154-160.

Datkhaeva, I., Arboleda, V. A., Senaratne, T. N., Nikpour, G., Meyerson, C., Geng, Y., ... & Janzen, C. (2018). Identification of novel PIEZO1 variants using prenatal exome sequencing and correlation to ultrasound and autopsy findings of recurrent hydrops fetalis. *American Journal of Medical Genetics Part A*, *176*(12), 2829-2834.

David, D. C., Hauptmann, S., Scherping, I., Schuessel, K., Keil, U., Rizzu, P., ... & Götz, J. (2005). Proteomic and functional analyses reveal a mitochondrial dysfunction in P301L tau transgenic mice. *Journal of Biological Chemistry*, *280*(25), 23802-23814.

De Bartolomeis, C., Collini, A., Rumberger, B., Barni, R., Ruggieri, G., Bernini, M., & Carmellini, M. (2008). Generalized lymphedema in a sirolimus-treated renal transplant patient. *Clinical transplantation*, *22*(2), 254-257.

De Lemos, J. A., McGuire, D. K., & Drazner, M. H. (2003). B-type natriuretic peptide in cardiovascular disease. *The Lancet*, *362*(9380), 316-322.

De Mooij, Y. M., van den Akker, N. M., Bekker, M. N., Bartelings, M. M., van Vugt, J. M., & Gittenberger-de Groot, A. C. (2011). Aberrant lymphatic development in euploid fetuses with increased nuchal translucency including Noonan syndrome. *Prenatal diagnosis*, *31*(2), 159-166.

De Titta, A., Ballester, M., Julier, Z., Nembrini, C., Jeanbart, L., Van Der Vlies, A. J., ... & Hubbell, J. A. (2013). Nanoparticle conjugation of CpG enhances adjuvancy for cellular immunity and memory recall at low dose. *Proceedings of the National Academy of Sciences*, *110*(49), 19902-19907.

Deau, M. C., Heurtier, L., Frange, P., Suarez, F., Bole-Feysot, C., Nitschke, P., ... & Kracker, S. (2014). A human immunodeficiency caused by mutations in the PIK3R1 gene. *The Journal of clinical investigation*, *124*(9), 3923-3928.

Degani, S. (2008). Fetal cerebrovascular circulation: a review of prenatal ultrasound assessment. *Gynecologic and obstetric investigation*, *66*(3), 184-196.

Dejana, E., & Vestweber, D. (2013). The role of VE-cadherin in vascular morphogenesis and permeability control. *Progress in molecular biology and translational science*, *116*, 119-144.

Dellinger, M. T., Hunter, R. J., Bernas, M. J., Witte, M. H., & Erickson, R. P. (2007). Chy-3 mice are Vegfc haploinsufficient and exhibit defective dermal superficial to deep lymphatic transition and dermal lymphatic hypoplasia. *Developmental Dynamics: An Official Publication of the American Association of Anatomists*, *236*(8), 2346-2355.

Dellinger, M., Hunter, R., Bernas, M., Gale, N., Yancopoulos, G., Erickson, R., & Witte, M. (2008). Defective remodeling and maturation of the lymphatic vasculature in Angiopoietin-2 deficient mice. *Developmental biology*, *319*(2), 309-320.

Dempsey, E., Homfray, T., Simpson, J. M., Jeffery, S., Mansour, S., & Ostergaard, P. (2020). Fetal hydrops–a review and a clinical approach to identifying the cause. *Expert Opinion on Orphan Drugs*, *8*(2-3), 51-66.

Den Hollander, N. S., Kleijer, W. J., Schoonderwaldt, E. M., Los, F. J., Wladimiroff, J. W., & Niermeijer, M. F. (2000). In-utero diagnosis of mucopolysaccharidosis type VII in a fetus with an enlarged nuchal translucency. *Ultrasound in Obstetrics and Gynecology: The Official Journal of the International Society of Ultrasound in Obstetrics and Gynecology*, *16*(1), 87-90.

Deng, Y., Atri, D., Eichmann, A., & Simons, M. (2013). Endothelial ERK signaling controls lymphatic fate specification. *The Journal of clinical investigation*, *123*(3), 1202-1215.

Dieterich, L. C., Klein, S., Mathelier, A., Sliwa-Primorac, A., Ma, Q., Hong, Y. K., ... & Detmar, M. (2015). DeepCAGE transcriptomics reveal an important role of the transcription factor MAFB in the lymphatic endothelium. *Cell reports*, *13*(7), 1493-1504.

Dixon, J. B. (2010). Mechanisms of chylomicron uptake into lacteals. *Annals of the New York Academy of Sciences*, *1207*, E52-E57.

Dobin, A., Davis, C. A., Schlesinger, F., Drenkow, J., Zaleski, C., Jha, S., ... & Gingeras, T. R. (2013). STAR: ultrafast universal RNA-seq aligner. *Bioinformatics*, *29*(1), 15-21.

Dongaonkar, R. M., Stewart, R. H., Geissler, H. J., & Laine, G. A. (2010). Myocardial microvascular permeability, interstitial oedema, and compromised cardiac function. *Cardiovascular research*, *87*(2), 331-339.

Doray, B., Girard-Lemaire, F., Gasser, B., Baldauf, J. J., De Geeter, B., Spizzo, M., ... & Flori, E. (2002). Pallister-Killian syndrome: difficulties of prenatal diagnosis. *Prenatal Diagnosis: Published in Affiliation With the International Society for Prenatal Diagnosis*, *22*(6), 470-477.

Downes, M., & Koopman, P. (2001). SOX18 and the transcriptional regulation of blood vessel development. *Trends in cardiovascular medicine*, *11*(8), 318-324.

Dudas, J., Papoutsi, M., Hecht, M., Elmaouhoub, A., Saile, B., Christ, B., ... & Wilting, J. (2004). The homeobox transcription factor Prox1 is highly conserved in embryonic hepatoblasts and in adult and transformed hepatocytes, but is absent from bile duct epithelium. *Anatomy and embryology*, *208*, 359-366.

Dunbar Iii, A. E., Moore, S. L., & Hinson, R. M. (2003). Fetal Diamond-Blackfan anemia associated with hydrops fetalis. *American journal of perinatology*, *20*(07), 391-394.

Dũng, V. C., Tomatsu, S., Montaño, A. M., Gottesman, G., Bober, M. B., Mackenzie, W., ... & Orii, T. (2013). Mucopolysaccharidosis IVA: correlation between genotype, phenotype and keratan sulfate levels. *Molecular genetics and metabolism*, *110*(1-2), 129-138.

Duong, T., Koltowska, K., Pichol-Thievend, C., Le Guen, L., Fontaine, F., Smith, K. A., ... & Francois, M. (2014). VEGFD regulates blood vascular development by modulating SOX18 activity. *Blood, The Journal of the American Society of Hematology*, *123*(7), 1102-1112.

Durst, R., Sauls, K., Peal, D. S., Devlaming, A., Toomer, K., Leyne, M., ... & Slaugenhaupt, S. A. (2015). Mutations in DCHS1 cause mitral valve prolapse. *Nature*, *525*(7567), 109-113.

Dursun, A., Gucer, S., Ebberink, M. S., Yigit, S., Wanders, R. J. A., & Waterham, H. R. (2009). Zellweger syndrome with unusual findings: non-immune hydrops fetalis, dermal erythropoiesis and hypoplastic toe nails. *Journal of Inherited Metabolic Disease: Official Journal of the Society for the Study of Inborn Errors of Metabolism*, *32*, 345-348.

Dyment, D. A., Smith, A. C., Alcantara, D., Schwartzentruber, J. A., Basel-Vanagaite, L., Curry, C. J., ... & Innes, A. M. (2013). Mutations in PIK3R1 cause SHORT syndrome. *The American Journal of Human Genetics*, *93*(1), 158-166.

Eklund, L., Kangas, J., & Saharinen, P. (2017). Angiopoietin–Tie signalling in the cardiovascular and lymphatic systems. *Clinical Science*, *131*(1), 87-103.

El Hokayem, J., Huber, C., Couvé, A., Aziza, J., Baujat, G., Bouvier, R., ... & Cormier-Daire, V. (2012). NEK1 and DYNC2H1 are both involved in short rib polydactyly Majewski type but not in Beemer Langer cases. *Journal of medical genetics*, *49*(4), 227-233.

El-Chemaly, S., Levine, S. J., & Moss, J. (2008). Lymphatics in lung disease. *Annals of the New York Academy of Sciences*, *1131*(1), 195-202.

Emrick, L. T., Murphy, L., Shamshirsaz, A. A., Ruano, R., Cassady, C. I., Liu, L., ... & Van den Veyver, I. B. (2014). Prenatal diagnosis of CLOVES syndrome confirmed by detection of a mosaic PIK3CA mutation in cultured amniocytes. *American Journal of Medical Genetics Part A*, *164*(10), 2633-2637.

Escobedo, N., & Oliver, G. (2016). Lymphangiogenesis: origin, specification, and cell fate determination. *Annual review of cell and developmental biology*, *32*, 677-691.

Esther Jr, C. R., & Barker, P. M. (2004). Pulmonary lymphangiectasia: diagnosis and clinical course. *Pediatric pulmonology*, *38*(4), 308-313.

Fang, J., Dagenais, S. L., Erickson, R. P., Arlt, M. F., Glynn, M. W., Gorski, J. L., ... & Glover, T. W. (2000). Mutations in FOXC2 (MFH-1), a forkhead family transcription factor, are responsible for the hereditary lymphedema-distichiasis syndrome. *The American Journal of Human Genetics*, *67*(6), 1382-1388.

Fatima, A., Culver, A., Culver, F., Liu, T., Dietz, W. H., Thomson, B. R., ... & Kume, T. (2014). Murine Notch1 is required for lymphatic vascular morphogenesis during development. *Developmental Dynamics*, *243*(7), 957-964.

Finlon, J. M., Burchill, M. A., & Tamburini, B. A. J. (2019). Digestion of the murine liver for a flow cytometric analysis of lymphatic endothelial cells. *JoVE (Journal of Visualized Experiments)*, (143), e58621.

Flenady, V., Frøen, J. F., Pinar, H., Torabi, R., Saastad, E., Guyon, G., ... & Gilshenan, K. (2009). An evaluation of classification systems for stillbirth. *BMC pregnancy and childbirth*, *9*, 1-13.

Földi, M., & Strossenreuther, R. (2005). *Foundations of manual lymph drainage.* Elsevier Health Sciences.

Fotiou, E., Martin-Almedina, S., Simpson, M. A., Lin, S., Gordon, K., Brice, G., ... & Ostergaard, P. (2019). Author Correction: Novel mutations in PIEZO1 cause an autosomal recessive generalized lymphatic dysplasia with non-immune hydrops fetalis. *Nature Communications*, *10*(1), 1951.

Francois, M., Caprini, A., Hosking, B., Orsenigo, F., Wilhelm, D., Browne, C., ... & Koopman, P. (2008). Sox18 induces development of the lymphatic vasculature in mice. *Nature*, *456*(7222), 643-647.

Francois, M., Harvey, N. L., & Hogan, B. M. (2011). The transcriptional control of lymphatic vascular development. *Physiology*, *26*(3), 146-155.

Freitas-Neto, C. A., Costa, R. A., Kombo, N., Freitas, T., Oréfice, J. L., Oréfice, F., & Foster, C. S. (2015). Subconjunctival indocyanine green identifies lymphatic vessels. *JAMA ophthalmology*, *133*(1), 102-104.

Fretts, R. C. (2005). Etiology and prevention of stillbirth. *American journal of obstetrics and gynecology*, *193*(6), 1923-1935.

Frøen, J. F., Cacciatore, J., McClure, E. M., Kuti, O., Jokhio, A. H., Islam, M., & Shiffman, J. (2011). Stillbirths: why they matter. *The Lancet*, *377*(9774), 1353-1366.

Frye, M., Stritt, S., Ortsäter, H., Hernandez Vasquez, M., Kaakinen, M., Vicente, A., ... & Mäkinen, T. (2020). EphrinB2-EphB4 signalling provides Rho-mediated homeostatic control of lymphatic endothelial cell junction integrity. *Elife*, *9*, e57732.

Frye, M., Taddei, A., Dierkes, C., Martinez-Corral, I., Fielden, M., Ortsäter, H., ... & Mäkinen, T. (2018). Matrix stiffness controls lymphatic vessel formation through regulation of a GATA2-dependent transcriptional program. *Nature communications*, *9*(1), 1-16.

Fujimoto, N., He, Y., D'Addio, M., Tacconi, C., Detmar, M., & Dieterich, L. C. (2020). Single-cell mapping reveals new markers and functions of lymphatic endothelial cells in lymph nodes. *PLoS biology*, *18*(4), e3000704.

Futerman, A. H., & Van Meer, G. (2004). The cell biology of lysosomal storage disorders. *Nature reviews Molecular cell biology*, *5*(7), 554-565.

Gale, N. W., Thurston, G., Hackett, S. F., Renard, R., Wang, Q., McClain, J., ... & Yancopoulos, G. D. (2002). Angiopoietin-2 is required for postnatal angiogenesis and

lymphatic patterning, and only the latter role is rescued by Angiopoietin-1. *Developmental cell*, *3*(3), 411-423.

Gancz, D., Perlmoter, G., & Yaniv, K. (2020). Formation and growth of cardiac lymphatics during embryonic development, heart regeneration, and disease. *Cold Spring Harbor perspectives in biology*, *12*(6), a037176.

Garcia, A., & Kandel, J. J. (2012). Notch: a key regulator of tumor angiogenesis and metastasis. *Histology and histopathology*, *27*(2), 151.

Gaucherand, P., Vavasseur-Monot, C., Ollagnon, E., Boisson, C., Labaune, J. M., Basset, T., & Yared, G. (2002). McKusik-Kaufman syndrome: prenatal diagnosis, genetics and follow up. *Prenatal Diagnosis: Published in Affiliation With the International Society for Prenatal Diagnosis*, *22*(11), 1048-1050.

Gaudio, E., Barbaro, B., Alvaro, D., Glaser, S., Francis, H., Ueno, Y., ... & Alpini, G. (2006). Vascular endothelial growth factor stimulates rat cholangiocyte proliferation via an autocrine mechanism. *Gastroenterology*, *130*(4), 1270-1282.

Gembruch, U., Hansmann, M., Redel, D. A., & Bald, R. (1988). Intrauterine therapy of fetal tachyarrhythmias: intraperitoneal administration of antiarrhythmic drugs to the fetus in fetal tachyarrhythmias with severe hydrops fetalis.

Geng, X., Cha, B., Mahamud, M. R., Lim, K. C., Silasi-Mansat, R., Uddin, M. K., ... & Srinivasan, R. S. (2016). Multiple mouse models of primary lymphedema exhibit distinct defects in lymphovenous valve development. *Developmental biology*, *409*(1), 218-233.

Geudens, I., Herpers, R., Hermans, K., Segura, I., Ruiz de Almodovar, C., Bussmann, J., ... & Dewerchin, M. (2010). Role of delta-like-4/Notch in the formation and wiring of the lymphatic network in zebrafish. *Arteriosclerosis, thrombosis, and vascular biology*, *30*(9), 1695-1702.

Ghalamkarpour, A., Morlot, S., Raas-Rothschild, A., Utkus, A., Mulliken, J. B., Boon, L. M., & Vikkula, M. (2006). Hereditary lymphedema type I associated with VEGFR3 mutation: the first de novo case and atypical presentations. *Clinical genetics*, *70*(4), 330-335.

Giannotta, M., Trani, M., & Dejana, E. (2013). VE-cadherin and endothelial adherens junctions: active guardians of vascular integrity. *Developmental cell*, *26*(5), 441-454.

Glass, H. C., & Rowitch, D. H. (2016). The role of the neurointensive care nursery for neonatal encephalopathy. *Clinics in perinatology*, *43*(3), 547-557.

Goldenberg, R. L., McClure, E. M., & Belizán, J. M. (2009). Commentary: reducing the world's stillbirths. *BMC Pregnancy and Childbirth*, *9*, 1-4.

Gonzalez-Garay, M. L., Aldrich, M. B., Rasmussen, J. C., Guilliod, R., Lapinski, P. E., King, P. D., & Sevick-Muraca, E. M. (2016). A novel mutation in CELSR1 is associated with hereditary lymphedema. *Vascular Cell*, *8*, 1-6.

González-Loyola, A., & Petrova, T. V. (2021). Development and aging of the lymphatic vascular system. *Advanced drug delivery reviews*, *169*, 63-78.

Goodwin, W. E., & Kaufman, J. J. (1956). Renal lymphatics, II: Preliminary experiments. *The Journal of Urology*, *76*(6), 702-707.

Gordon, E. J., Gale, N. W., & Harvey, N. L. (2008). Expression of the hyaluronan receptor LYVE-1 is not restricted to the lymphatic vasculature; LYVE-1 is also expressed on embryonic blood vessels. *Developmental dynamics: an official publication of the American Association of Anatomists*, *237*(7), 1901-1909.

Gordon, K., Spiden, S. L., Connell, F. C., Brice, G., Cottrell, S., Short, J., ... & Ostergaard, P. (2013). FLT 4/VEGFR 3 and M ilroy Disease: Novel Mutations, a Review of Published Variants and Database Update. *Human mutation*, *34*(1), 23-31.

Gos, M., Smigiel, R., Kaczan, T., Landowska, A., Abramowicz, A., Sasiadek, M., & Bal, J. (2018). MAP2K2 mutation as a cause of cardio-facio-cutaneous syndrome in an infant with a severe and fatal course of the disease. *American Journal of Medical Genetics Part A*, *176*(7), 1670-1674.

Gu, J., Lu, Y., Deng, M., Qiu, M., Tian, Y., Ji, Y., ... & Kong, X. (2019). Inhibition of acetylation of histones 3 and 4 attenuates aortic valve calcification. *Experimental & Molecular Medicine*, *51*(7), 1-14.

Gulati, N., Morris, R. K., Williams, D., & Kilby, M. D. (2018). Prenatal thoraco-amniotic chest drain insertion to manage a case of fetal hydrops secondary to FOXC2. *BMJ Case Reports*, *2018*.

Gunay-Aygun, M., Avner, E. D., Bacallao, R. L., Choyke, P. L., Flynn, J. T., Germino, G. G., ... & Gahl, W. A. (2006). Autosomal recessive polycystic kidney disease and congenital hepatic fibrosis: summary statement of a first National Institutes of Health/Office of Rare Diseases conference. *The Journal of pediatrics*, *149*(2), 159-164.

Guo, H. F., & Vander Kooi, C. W. (2015). Neuropilin functions as an essential cell surface receptor. *Journal of Biological Chemistry*, *290*(49), 29120-29126.

Gupta, A. K., Govindarajan, V., & Malhotra, A. (1999). Feedback-seeking behavior within multinational corporations. *Strategic management journal*, *20*(3), 205-222.

Gupta, P., Sharma, J. B., Sharma, R., Gadodia, A., Kumar, S., & Roy, K. K. (2011). Antenatal ultrasound and MRI findings of Pena–Shokeir syndrome. *Archives of gynecology and obstetrics*, *283*, 27-29.

Hägerling, R. (2020). Light sheet microscopy-based 3-dimensional histopathology of the lymphatic vasculature in Emberger syndrome. *Phlebologie*, *49*(04), 242-248.

Hägerling, R., Hoppe, E., Dierkes, C., Stehling, M., Makinen, T., Butz, S., ... & Kiefer, F. (2018). Distinct roles of VE-cadherin for development and maintenance of specific lymph vessel beds. *The EMBO journal*, *37*(22), e98271.

Hägerling, R., Pollmann, C., Andreas, M., Schmidt, C., Nurmi, H., Adams, R. H., ... & Kiefer, F. (2013). A novel multistep mechanism for initial lymphangiogenesis in mouse embryos based on ultramicroscopy. *The EMBO journal*, *32*(5), 629-644.

Haiko, P., Makinen, T., Keskitalo, S., Taipale, J., Karkkainen, M. J., Baldwin, M. E., ... & Alitalo, K. (2008). Deletion of vascular endothelial growth factor C (VEGF-C) and VEGF-D is not equivalent to VEGF receptor 3 deletion in mouse embryos. *Molecular and cellular biology*, *28*(15), 4843-4850.

Hargens, A. R., & Zweifach, B. W. (1977). Contractile stimuli in collecting lymph vessels. *American Journal of Physiology-Heart and Circulatory Physiology*, *233*(1), H57-H65.

Harrell, M. I., Iritani, B. M., & Ruddell, A. (2008). Lymph node mapping in the mouse. *Journal of immunological methods*, *332*(1-2), 170-174.

Hart, J., Hamersma, P. J., & Fortuin, J. M. H. (1991). Phase distribution during gas—liquid flow through horizontal dividing junctions. *Nuclear engineering and design*, *126*(3), 293-312.

Harvey, N. L., Srinivasan, R. S., Dillard, M. E., Johnson, N. C., Witte, M. H., Boyd, K., ... & Oliver, G. (2005). Lymphatic vascular defects promoted by Prox1 haploinsufficiency cause adult-onset obesity. *Nature genetics*, *37*(10), 1072-1081.

Hassan, M. J., Chishti, M. S., Jamal, S. M., Tariq, M., & Ahmad, W. (2008). A syndromic form of autosomal recessive congenital microcephaly (Jawad syndrome) maps to chromosome 18p11. 22–q11. 2. *Human genetics*, *123*, 77-82.

Hatzaki, A., Sifakis, S., Apostolopoulou, D., Bouzarelou, D., Konstantinidou, A., Kappou, D., ... & Velissariou, V. (2011). FGFR3 related skeletal dysplasias diagnosed prenatally by ultrasonography and molecular analysis: presentation of 17 cases. *American Journal of Medical Genetics part A*, *155*(10), 2426-2435.

Heard, M. E., Besio, R., Weis, M., Rai, J., Hudson, D. M., Dimori, M., ... & Morello, R. (2016). Sc65-null mice provide evidence for a novel endoplasmic reticulum complex regulating collagen lysyl hydroxylation. *PLoS genetics*, *12*(4), e1006002.

Heinrich, T., Nanda, I., Rehn, M., Zollner, U., Ernestus, K., Wirth, C., ... & Kunstmann, E. (2015). Co-Occurence of Reciprocal Translocation and COL2A1 Mutation in a Fetus with Severe Skeletal Dysplasia: Implications for Genetic Counseling. *Cytogenetic and genome research*, *145*(1), 25-28.

Hen, G., Nicenboim, J., Mayseless, O., Asaf, L., Shin, M., Busolin, G., ... & Yaniv, K. (2015). Venous-derived angioblasts generate organ-specific vessels during zebrafish embryonic development. *Development*, *142*(24), 4266-4278.

Henri, O., Pouehe, C., Houssari, M., Galas, L., Nicol, L., Edwards-Lévy, F., ... & Brakenhielm, E. (2016). Selective stimulation of cardiac lymphangiogenesis reduces myocardial edema and fibrosis leading to improved cardiac function following myocardial infarction. *Circulation*, *133*(15), 1484-1497.

Hillstrom, M. M., Brown, D. L., Wilkins-Haug, L., & Genest, D. R. (1995). Sonographic appearance of placental villous hydrops associated with Beckwith-Wiedemann syndrome. *Journal of ultrasound in medicine*, *14*(1), 61-64.

Hoeffler, C. D., Krenek, M. E., Brand, M. C., & Schierholz, E. (2016). Wolff–parkinson–white syndrome in a term infant presenting with cardiopulmonary arrest. *Advances in Neonatal Care*, *16*(1), 44-51.

Hogan, B. M., Bos, F. L., Bussmann, J., Witte, M., Chi, N. C., Duckers, H. J., & Schulte-Merker, S. (2009). Ccbe1 is required for embryonic lymphangiogenesis and venous sprouting. *Nature genetics*, *41*(4), 396-398.

Huntington, G. S. (1910). *The anatomy and development of the jugular lymph sacs in the domestic cat (Felis domestica).* Wistar Institute of Anatomy and Biology.

Imgrund, S., Hartmann, D., Farwanah, H., Eckhardt, M., Sandhoff, R., Degen, J., ... & Willecke, K. (2009). Adult ceramide synthase 2 (CERS2)-deficient mice exhibit myelin sheath defects, cerebellar degeneration, and hepatocarcinomas. *Journal of Biological Chemistry*, *284*(48), 33549-33560.

Irrthum, A., Devriendt, K., Chitayat, D., Matthijs, G., Glade, C., Steijlen, P. M., ... & Vikkula, M. (2003). Mutations in the transcription factor gene SOX18 underlie recessive and dominant forms of hypotrichosis-lymphedema-telangiectasia. *The American Journal of Human Genetics*, *72*(6), 1470-1478.

Jackson, D. G. prevo R, Clasper S, Banerji S (2001). LYVE-1, the lymphatic system and tumor lymphangiogenesis. *Trends Immunol*, *22*, 317-21.

Jafree, D. J., Moulding, D., Kolatsi-Joannou, M., Perretta Tejedor, N., Price, K. L., Milmoe, N. J., ... & Long, D. A. (2019). Spatiotemporal dynamics and heterogeneity of renal lymphatics in mammalian development and cystic kidney disease. *Elife*, *8*, e48183.

Jakus, Z., Gleghorn, J. P., Enis, D. R., Sen, A., Chia, S., Liu, X., ... & Kahn, M. L. (2014). Lymphatic function is required prenatally for lung inflation at birth. *Journal of Experimental Medicine*, *211*(5), 815-826.

Janssen, L., Dupont, L., Bekhouche, M., Noel, A., Leduc, C., Voz, M., ... & Colige, A. (2016). ADAMTS3 activity is mandatory for embryonic lymphangiogenesis and regulates placental angiogenesis. *Angiogenesis*, *19*, 53-65.

Järvinen, T. A. H., Kannus, P., Järvinen, T. L. N., Jozsa, L., Kalimo, H., & Järvinen, M. (2000). Tenascin-C in the pathobiology and healing process of musculoskeletal tissue injury. *Scandinavian Journal of Medicine & Science in Sports: Review Article*, *10*(6), 376-382.

Jeffery, W. R., Strickler, A. G., Guiney, S., Heyser, D. G., & Tomarev, S. I. (2000). Prox 1 in eye degeneration and sensory organ compensation during development and evolution of the cavefish Astyanax. *Development genes and evolution*, *210*, 223-230.

Jeltsch, K. M., Hu, D., Brenner, S., Zöller, J., Heinz, G. A., Nagel, D., ... & Heissmeyer, V. (2014). Cleavage of roquin and regnase-1 by the paracaspase MALT1 releases their cooperatively repressed targets to promote TH17 differentiation. *Nature immunology*, *15*(11), 1079-1089.

Jennings, E. R., Dibbern, H. H., Hodell, F. H., Monroe, C. H., Peckham, N. H., Sullivan, J. F., & Pollack, W. (1969). Prevention of Rh hemolytic disease of the newborn. *California Medicine*, *110*(2), 130.

Jewell, C. M., Bustamante López, S. C., & Irvine, D. J. (2011). In situ engineering of the lymph node microenvironment via intranodal injection of adjuvant-releasing polymer particles. *Proceedings of the National Academy of Sciences*, *108*(38), 15745-15750.

Jiang, X., Nicolls, M. R., Tian, W., & Rockson, S. G. (2018). **Lymphatic** dysfunction, leukotrienes, and lymphedema. *Annual review of physiology*, *80*, 49-70.

Johnson, N. C., Dillard, M. E., Baluk, P., McDonald, D. M., Harvey, N. L., Frase, S. L., & Oliver, G. (2008). Lymphatic endothelial cell identity is reversible and its maintenance requires Prox1 activity. *Genes & development*, *22*(23), 3282-3291.

Jones, G. E., & Mansour, S. (2017). An approach to familial lymphoedema. *Clinical Medicine*, *17*(6), 552.

Kadyrberdieva, F. Z., Shmakov, R. G., & Bokeria, E. L. (2019). Nonimmune hydrops fetalis: modern principles of diagnosis and treatment. *Obstetrics and gynecology*, (10), 28-35.

Kagan, M., Cohen, A. H., Matejas, V., Vlangos, C., & Zenker, M. (2008). A milder variant of Pierson syndrome. *Pediatric Nephrology*, *23*, 323-327.

Kaipainen, A., Korhonen, J., Mustonen, T., Van Hinsbergh, V. W., Fang, G. H., Dumont, D., ... & Alitalo, K. (1995). Expression of the fms-like tyrosine kinase 4 gene becomes restricted to lymphatic endothelium during development. *Proceedings of the National Academy of Sciences*, *92*(8), 3566-3570.

Kanady, J. D., Dellinger, M. T., Munger, S. J., Witte, M. H., & Simon, A. M. (2011). Connexin37 and Connexin43 deficiencies in mice disrupt lymphatic valve development and result in lymphatic disorders including lymphedema and chylothorax. *Developmental biology*, *354*(2), 253-266.

Karaman, S., Buschle, D., Luciani, P., Leroux, J. C., Detmar, M., & Proulx, S. T. (2015). Decline of lymphatic vessel density and function in murine skin during aging. *Angiogenesis*, *18*, 489-498.

Karkkainen, M. J., Haiko, P., Sainio, K., Partanen, J., Taipale, J., Petrova, T. V., ... & Alitalo, K. (2004). Vascular endothelial growth factor C is required for sprouting of the first lymphatic vessels from embryonic veins. *Nature immunology*, *5*(1), 74-80.

Kassab, K., Hariri, H., Gharibeh, L., Fahed, A. C., Zein, M., El-Rassy, I., ... & Nemer, G. (2016). GATA 5 mutation homozygosity linked to a double outlet right ventricle

phenotype in a Lebanese patient. *Molecular Genetics & Genomic Medicine*, *4*(2), 160-171.

Kataru, R. P., Jung, K., Jang, C., Yang, H., Schwendener, R. A., Baik, J. E., ... & Koh, G. Y. (2009). Critical role of CD11b+ macrophages and VEGF in inflammatory lymphangiogenesis, antigen clearance, and inflammation resolution. *Blood, The Journal of the American Society of Hematology*, *113*(22), 5650-5659.

Katsuta, H., Fukushima, Y., Maruyama, K., Hirashima, M., Nishida, K., Nishikawa, S. I., & Uemura, A. (2013). EphrinB2–EphB4 signals regulate formation and maintenance of Funnel-shaped valves in corneal lymphatic capillaries. *Investigative ophthalmology & visual science*, *54*(6), 4102-4108.

Kazenwadel, J., & Harvey, N. L. (2018). Lymphatic endothelial progenitor cells: origins and roles in lymphangiogenesis. *Current opinion in immunology*, *53*, 81-87.

Kazenwadel, J., Betterman, K. L., Chong, C. E., Stokes, P. H., Lee, Y. K., Secker, G. A., ... & Harvey, N. L. (2015). GATA2 is required for lymphatic vessel valve development and maintenance. *The Journal of clinical investigation*, *125*(8), 2979-2994.

Kazenwadel, J., Secker, G. A., Liu, Y. J., Rosenfeld, J. A., Wildin, R. S., Cuellar-Rodriguez, J., ... & Harvey, N. L. (2012). Loss-of-function germline GATA2 mutations in patients with MDS/AML or MonoMAC syndrome and primary lymphedema reveal a key role for GATA2 in the lymphatic vasculature. *Blood, The Journal of the American Society of Hematology*, *119*(5), 1283-1291.

Kerjaschki, D., Regele, H. M., Moosberger, I., Nagy-Bojarski, K., Watschinger, B., Soleiman, A., ... & Raab, I. (2004). Lymphatic neoangiogenesis in human kidney transplants is associated with immunologically active lymphocytic infiltrates. *Journal of the American Society of Nephrology*, *15*(3), 603-612.

Khan, A. A., Mudassir, J., Mohtar, N., & Darwis, Y. (2013). Advanced drug delivery to the lymphatic system: lipid-based nanoformulations. *International journal of nanomedicine*, 2733-2744.

Khazen, N. E., Faverly, D., Vamos, E., Van Regemorter, N., Flament-Durand, J., Carton, B., ... & Reynolds, J. F. (1986). Lethal osteopetrosis with multiple fractures in utero. *American journal of medical genetics*, *23*(3), 811-819.

Kim, M., Koh, Y. J., Kim, K. E., Koh, B. I., Nam, D. H., Alitalo, K., ... & Koh, G. Y. (2010). CXCR4 signaling regulates metastasis of chemoresistant melanoma cells by a lymphatic metastatic niche. *Cancer research*, *70*(24), 10411-10421.

Klaourakis, K., Vieira, J. M., & Riley, P. R. (2021). The evolving cardiac lymphatic vasculature in development, repair and regeneration. *Nature Reviews Cardiology*, *18*(5), 368-379.

Klotz, L., Norman, S., Vieira, J. M., Masters, M., Rohling, M., Dubé, K. N., ... & Riley, P. R. (2015). Cardiac lymphatics are heterogeneous in origin and respond to injury. *Nature*, *522*(7554), 62-67.

Koltowska, K., Lagendijk, A. K., Pichol-Thievend, C., Fischer, J. C., Francois, M., Ober, E. A., & Hogan, B. M. (2015). Vegfc regulates bipotential precursor division and Prox1 expression to promote lymphatic identity in zebrafish. *Cell reports*, *13*(9), 1828-1841.

Konstantinidou, A., Karadimas, C., Waterham, H. R., Superti-Furga, A., Kaminopetros, P., Grigoriadou, M., ... & Petersen, M. B. (2008). Pathologic, radiographic and molecular findings in three fetuses diagnosed with HEM/Greenberg skeletal dysplasia. *Prenatal Diagnosis: Published in Affiliation With the International Society for Prenatal Diagnosis*, *28*(4), 309-312.

Kontarakis, Z., Rossi, A., Ramas, S., Dellinger, M. T., & Stainier, D. Y. (2018). Mir-126 is a conserved modulator of lymphatic development. *Developmental biology*, *437*(2), 120-130.

Koronyo, Y., Biggs, D., Barron, E., Boyer, D. S., Pearlman, J. A., Au, W. J., ... & Koronyo-Hamaoui, M. (2017). Retinal amyloid pathology and proof-of-concept imaging trial in Alzheimer's disease. *JCI insight*, *2*(16).

Kranz, C., Basinger, A. A., Güçsavaş-Çalıkoğlu, M., Sun, L., Powell, C. M., Henderson, F. W., ... & Freeze, H. H. (2007). Expanding spectrum of congenital disorder of glycosylation Ig (CDG-Ig): sibs with a unique skeletal dysplasia, hypogammaglobulinemia, cardiomyopathy, genital malformations, and early lethality. *American Journal of Medical Genetics Part A*, *143*(12), 1371-1378.

Kulkarni, R. M., Greenberg, J. M., & Akeson, A. L. (2009). NFATc1 regulates lymphatic endothelial development. *Mechanisms of development*, *126*(5-6), 350-365.

Kume, T. (2009). Novel insights into the differential functions of Notch ligands in vascular formation. *Journal of angiogenesis research*, *1*, 1-9.

Kumru, P., Aka, N., Köse, G., Vural, Z. T., Peker, Ö., & Kayserili, H. (2005). Short rib polydactyly syndrome type 3 with absence of fibulae (Verma-Naumoff syndrome). *Fetal diagnosis and therapy*, *20*(5), 410-414.

Kunstfeld, R., Hirakawa, S., Hong, Y. K., Schacht, V., Lange-Asschenfeldt, B., Velasco, P., ... & Detmar, M. (2004). Induction of cutaneous delayed-type hypersensitivity reactions in VEGF-A transgenic mice results in chronic skin inflammation associated with persistent lymphatic hyperplasia. *Blood*, *104*(4), 1048-1057.

Kurjak, A., Azumendi, G., Andonotopo, W., & Salihagic-Kadic, A. (2007). Three-and four-dimensional ultrasonography for the structural and functional evaluation of the fetal face. *American journal of obstetrics and gynecology*, *196*(1), 16-28.

Lalanne, M., Paci, A., Andrieux, K., Dereuddre-Bosquet, N., Clayette, P., Deroussent, A., ... & Desmaële, D. (2007). Synthesis and biological evaluation of two glycerolipidic prodrugs of didanosine for direct lymphatic delivery against HIV. *Bioorganic & medicinal chemistry letters*, *17*(8), 2237-2240.

Lavado, A., Lagutin, O. V., Chow, L. M., Baker, S. J., & Oliver, G. (2010). Prox1 is required for granule cell maturation and intermediate progenitor maintenance during brain neurogenesis. *PLoS biology*, *8*(8), e1000460.

Le Guen, L., Karpanen, T., Schulte, D., Harris, N. C., Koltowska, K., Roukens, G., ... & Hogan, B. M. (2014). Ccbe1 regulates Vegfc-mediated induction of Vegfr3 signaling during embryonic lymphangiogenesis. *Development*, *141*(6), 1239-1249.

Lee, B. H., & Yoo, H. W. (2019). Noonan syndrome and RASopathies: Clinical features, diagnosis and management. *Journal of Genetic Medicine*, *16*(1), 1-9.

Lee, M., Dworkin, A. M., Lichtenberg, J., Patel, S. J., Trivedi, N. S., Gildea, D., ... & Crawford, N. P. (2014). Metastasis-associated protein ribosomal RNA processing 1 homolog B (RRP1B) modulates metastasis through regulation of histone methylation. *Molecular Cancer Research*, *12*(12), 1818-1828.

Lefloch, R., Pouysségur, J., & Lenormand, P. (2009). Total ERK1/2 activity regulates cell proliferation. *Cell cycle*, *8*(5), 705-711.

Leppänen, V. M., Brouillard, P., Korhonen, E. A., Sipilä, T., Jha, S. K., Revencu, N., ... & Alitalo, K. (2020). Characterization of ANGPT2 mutations associated with primary lymphedema. *Science translational medicine*, *12*(560), eaax8013.

Levet, S., Ciais, D., Merdzhanova, G., Mallet, C., Zimmers, T. A., Lee, S. J., ... & Vittet, D. (2013). Bone morphogenetic protein 9 (BMP9) controls lymphatic vessel maturation and valve formation. *Blood, The Journal of the American Society of Hematology*, *122*(4), 598-607.

Levick, J. R., & Michel, C. C. (2010). Microvascular fluid exchange and the revised Starling principle. *Cardiovascular research*, *87*(2), 198-210.

Lev-Sagie, A., Hamani, Y., Raas-Rothschild, A., Yagel, S., & Anteby, E. Y. (2003). Prenatal ultrasonographic diagnosis of atypical Nonne–Milroy lymphedema. *Ultrasound in Obstetrics and Gynecology: The Official Journal of the International Society of Ultrasound in Obstetrics and Gynecology*, *21*(1), 72-74.

Li, D., March, M. E., Gutierrez-Uzquiza, A., Kao, C., Seiler, C., Pinto, E., ... & Hakonarson, H. (2019). ARAF recurrent mutation causes central conducting lymphatic anomaly treatable with a MEK inhibitor. *Nature medicine*, *25*(7), 1116-1122.

Li, D., Sheppard, S. E., Peroutka, C., Barnes, C., Reid, J. R., Smith, C. L., ... & Hakonarson, H. (2021). Expanded phenotypic spectrum of JAG1-associated diseases: central conducting lymphatic anomaly with a pathogenic variant in JAG1. *Clinical genetics*, *99*(5), 742.

Li, S., Goins, B., Hrycushko, B. A., Phillips, W. T., & Bao, A. (2012). Feasibility of eradication of breast cancer cells remaining in postlumpectomy cavity and draining lymph nodes following intracavitary injection of radioactive immunoliposomes. *Molecular pharmaceutics*, *9*(9), 2513-2522.

Liebl, J., Zhang, S., Moser, M., Agalarov, Y., Demir, C. S., Hager, B., ... & Zahler, S. (2015). Cdk5 controls lymphatic vessel development and function by phosphorylation of Foxc2. *Nature communications*, *6*(1), 7274.

Lin, A. E., Grossfeld, P. D., Hamilton, R. M., Smoot, L., Gripp, K. W., Proud, V., ... & Nicholson, L. (2002). Further delineation of cardiac abnormalities in Costello syndrome. *American journal of medical genetics*, *111*(2), 115-129.

Lin, A. E., O'Brien, B., Demmer, L. A., Almeda, K. K., Blanco, C. L., Glasow, P. F., ... & Gripp, K. W. (2009). Prenatal features of Costello syndrome: ultrasonographic findings and atrial tachycardia. *Prenatal Diagnosis: Published in Affiliation With the International Society for Prenatal Diagnosis*, *29*(7), 682-690.

Lin, F. J., Chen, X., Qin, J., Hong, Y. K., Tsai, M. J., & Tsai, S. Y. (2010). Direct transcriptional regulation of neuropilin-2 by COUP-TFII modulates multiple steps in murine lymphatic vessel development. *The Journal of clinical investigation, 120*(5), 1694-1707.

Ling, R., Li, Y., Yao, Q., Chen, T., Zhu, D., Jun, Y., & Chen, J. (2005). Lymphatic chemotherapy induces apoptosis in lymph node metastases in a rabbit breast carcinoma model. *Journal of drug targeting*, *13*(2), 137-142.

Lioux, G., Liu, X., Temiño, S., Oxendine, M., Ayala, E., Ortega, S., ... & Torres, M. (2020). A second heart field-derived vasculogenic niche contributes to cardiac lymphatics. *Developmental cell*, *52*(3), 350-363.

Liu, X., Cheng, C., Chen, K., Wu, Y., & Wu, Z. (2021). Recent progress in lymphangioma. *Frontiers in Pediatrics*, *9*, 735832.

Liu, X., Gu, X., Ma, W., Oxendine, M., Gil, H. J., Davis, G. E., ... & Oliver, G. (2018). Rasip1 controls lymphatic vessel lumen maintenance by regulating endothelial cell junctions. *Development*, *145*(17), dev165092.

Loeffen, J., Elpeleg, O., Smeitink, J., Smeets, R., Stöckler-Ipsiroglu, S., Mandel, H., ... & Van Den Heuvel, L. (2001). Mutations in the complex I NDUFS2 gene of patients with cardiomyopathy and encephalomyopathy. *Annals of Neurology: Official Journal of the American Neurological Association and the Child Neurology Society*, *49*(2), 195-201.

Long, A., Sinkovskaya, E. S., Edmondson, A. C., Zackai, E., & Schrier Vergano, S. A. (2016). Kabuki syndrome as a cause of non-immune fetal hydrops/ascites. *American Journal of Medical Genetics Part A*, *170*(12), 3333-3337.

Louveau, A., Smirnov, I., Keyes, T. J., Eccles, J. D., Rouhani, S. J., Peske, J. D., ... & Kipnis, J. (2015). Structural and functional features of central nervous system lymphatic vessels. *Nature*, *523*(7560), 337-341.

Louveau, A., Smirnov, I., Keyes, T. J., Eccles, J. D., Rouhani, S. J., Peske, J. D., ... & Kipnis, J. (2016). Correction: Corrigendum: Structural and functional features of central nervous system lymphatic vessels. *Nature*, *533*(7602), 278-278.

Lui, K. O., Zangi, L., Silva, E. A., Bu, L., Sahara, M., Li, R. A., ... & Chien, K. R. (2013). Driving vascular endothelial cell fate of human multipotent Isl1+ heart progenitors with VEGF modified mRNA. *Cell research*, *23*(10), 1172-1186.

Lukacs, V., Mathur, J., Mao, R., Bayrak-Toydemir, P., Procter, M., Cahalan, S. M., ... & Krock, B. L. (2015). Impaired PIEZO1 function in patients with a novel autosomal recessive congenital lymphatic dysplasia. *Nature communications*, *6*(1), 8329.

Lyons, O., Saha, P., Seet, C., Kuchta, A., Arnold, A., Grover, S., ... & Smith, A. (2017). Human venous valve disease caused by mutations in FOXC2 and GJC2. *Journal of Experimental Medicine*, *214*(8), 2437-2452.

Machlitt, A., Tennstedt, C., Körner, H., Bommer, C., & Chaoui, R. (2002). Prenatal diagnosis of 22q11 microdeletion in an early second-trimester fetus with conotruncal anomaly presenting with increased nuchal translucency and bilateral intracardiac echogenic foci. *Ultrasound in Obstetrics and Gynecology: The Official Journal of the International Society of Ultrasound in Obstetrics and Gynecology*, *19*(5), 510-513.

Majesky, M. W. (2016). Vascular smooth muscle cells. *Arteriosclerosis, thrombosis, and vascular biology*, *36*(10), e82-e86.

Mäkinen, T., Adams, R. H., Bailey, J., Lu, Q., Ziemiecki, A., Alitalo, K., ... & Wilkinson, G. A. (2005). PDZ interaction site in ephrinB2 is required for the remodeling of lymphatic vasculature. *Genes & development*, *19*(3), 397-410.

Mäkinen, T., Norrmen, C., & Petrova, T. V. (2007). Molecular mechanisms of lymphatic vascular development. *Cellular and Molecular Life Sciences*, *64*, 1915-1929.

Mäkinen, T., Veikkola, T., Mustjoki, S., Karpanen, T., Catimel, B., Nice, E. C., ... & Alitalo, K. (2001). Isolated lymphatic endothelial cells transduce growth, survival and migratory signals via the VEGF-C/D receptor VEGFR-3. *The EMBO journal*, *20*(17), 4762-4773.

Makis, A., Georgiou, I., Traeger-Synodinos, J., Storino, M. R., Giuliano, M., Andolfo, I., ... & Grosso, M. (2021). A novel εγδβ-thalassemia deletion associated with severe anemia at birth and a β-thalassemia intermedia phenotype later in life in three generations of a Greek family. *Hemoglobin*, *45*(6), 351-354.

Maloy, K. J., Erdmann, I., Basch, V., Sierro, S., Kramps, T. A., Zinkernagel, R. M., ... & Kündig, T. M. (2001). Intralymphatic immunization enhances DNA vaccination. *Proceedings of the National Academy of Sciences*, *98*(6), 3299-3303.

Maltzman, J. S., Reed, H. O., & Kahn, M. L. (2015). HA-ving lymphatics improves lung transplantation. *The Journal of Clinical Investigation*, *125*(11), 3999-4001.

Mansour, S., Brice, G. W., Jeffery, S., & Mortimer, P. (2019). Lymphedema-distichiasis syndrome.

Mardy, A. H., Chetty, S. P., Norton, M. E., & Sparks, T. N. (2019). A system-based approach to the genetic etiologies of non-immune hydrops fetalis. *Prenatal diagnosis*, *39*(9), 732-750.

Marin, S. E., Mesterman, R., Robinson, B., Rodenburg, R. J., Smeitink, J., & Tarnopolsky, M. A. (2013). Leigh syndrome associated with mitochondrial complex I deficiency due to novel mutations In NDUFV1 and NDUFS2. *Gene*, *516*(1), 162-167.

Martin, M. (2011). Cutadapt removes adapter sequences from high-throughput sequencing reads. *EMBnet. journal*, *17*(1), 10-12.

Martin-Almedina, S., Martinez-Corral, I., Holdhus, R., Vicente, A., Fotiou, E., Lin, S., ... & Ostergaard, P. (2016). EPHB4 kinase–inactivating mutations cause autosomal dominant lymphatic-related hydrops fetalis. *The Journal of clinical investigation*, *126*(8), 3080-3088.

Martin-Almedina, S., Ogmen, K., Sackey, E., Grigoriadis, D., Karapouliou, C., Nadarajah, N., ... & Ostergaard, P. (2021). Janus-faced EPHB4-associated disorders: novel pathogenic variants and unreported intrafamilial overlapping phenotypes. *Genetics in Medicine*, *23*(7), 1315-1324.

Martindill, D. M., Risebro, C. A., Smart, N., Franco-Viseras, M. D. M., Rosario, C. O., Swallow, C. J., ... & Riley, P. R. (2007). Nucleolar release of Hand1 acts as a molecular switch to determine cell fate. *Nature cell biology*, *9*(10), 1131-1141.

Martinez-Corral, I., Ulvmar, M. H., Stanczuk, L., Tatin, F., Kizhatil, K., John, S. W., ... & Makinen, T. (2015). Nonvenous origin of dermal lymphatic vasculature. *Circulation research*, *116*(10), 1649-1654.

Massalska, D., Bijok, J., Ilnicka, A., Jakiel, G., & Roszkowski, T. (2017). Triploidy–variability of sonographic phenotypes. *Prenatal Diagnosis*, *37*(8), 774-780.

Mattos, E. P., Silva, A. A. D., Magalhães, J. A. A., Leite, J. C. L., Leistner-Segal, S., Gus-Kessler, R., ... & Sanseverino, M. T. V. (2015). Identification of a premature stop codon mutation in the PHGDH gene in severe Neu-Laxova syndrome—evidence for phenotypic variability. *American Journal of Medical Genetics Part A*, *167*(6), 1323-1329.

Mazzei, F. G., Gentili, F., Guerrini, S., Cioffi Squitieri, N., Guerrieri, D., Gennaro, P., ... & Mazzei, M. A. (2017). MR lymphangiography: a practical guide to perform it and a brief review of the literature from a technical point of view. *BioMed research international*, *2017*.

McCarthy, C., Gupta, N., Johnson, S. R., Jane, J. Y., & McCormack, F. X. (2021). Lymphangioleiomyomatosis: pathogenesis, clinical features, diagnosis, and management. *The Lancet Respiratory Medicine*, *9*(11), 1313-1327.

McClure, E. M., Saleem, S., Goudar, S. S., Tikmani, S. S., Dhaded, S. M., Hwang, K., ... & Goldenberg, R. (2022). The causes of stillbirths in south Asia: results from a prospective study in India and Pakistan (PURPOSe). *The Lancet Global Health*, *10*(7), e970-e977.

Meilhac, S. M., & Buckingham, M. E. (2018). The deployment of cell lineages that form the mammalian heart. *Nature Reviews Cardiology*, *15*(11), 705-724.

Melber, D. J., Andreasen, T. S., Mao, R., Tvrdik, T., Miller, C. E., Moore, T. R., ... & Lamale-Smith, L. M. (2018). Novel mutation in CCBE 1 as a cause of recurrent hydrops fetalis from Hennekam lymphangiectasia-lymphedema syndrome-1. *Clinical case reports*, *6*(12), 2358.

Meroni, G. (2018). X-linked opitz G/BBB syndrome.

Miller, M. A., & Zachary, J. F. (2017). Pathologic basis of veterinary disease. *Mechanisms and Morphology of Cellular Injury, Adaptation, and Death,*, 2-43.

Min, J. H., Lee, C. H., Ji, Y. W., Yeo, A., Noh, H., Song, I., ... & Lee, H. K. (2016). Activation of Dll4/notch signaling and hypoxia-inducible factor-1 alpha facilitates lymphangiogenesis in lacrimal glands in dry eye. *PloS one*, *11*(2), e0147846.

Mirzaa, G., Conway, R., Graham Jr, J. M., & Dobyns, W. B. (2013). PIK3CA-related segmental overgrowth.

Molina, J. R., & Adjei, A. A. (2006). The ras/raf/mapk pathway. *Journal of Thoracic Oncology*, *1*(1), 7-9.

Morris, C. A., Loker, J., Ensing, G., & Stock, A. D. (1993). Supravalvular aortic stenosis cosegregates with a familial 6; 7 translocation which disrupts the elastin gene. *American Journal of Medical Genetics*, *46*(6), 737-744.

Munger, S. J., Davis, M. J., & Simon, A. M. (2017). Defective lymphatic valve development and chylothorax in mice with a lymphatic-specific deletion of Connexin43. *Developmental biology*, *421*(2), 204-218.

Murtomaki, A., Uh, M. K., Kitajewski, C., Zhao, J., Nagasaki, T., Shawber, C. J., & Kitajewski, J. (2014). Notch signaling functions in lymphatic valve formation. *Development*, *141*(12), 2446-2451.

Nance, M. A., & Berry, S. A. (1992). Cockayne syndrome: review of 140 cases. *American journal of medical genetics*, *42*(1), 68-84.

Nanda, A., AL-ESSA, F. H., EL-SHAFEI, W. M., & Alsaleh, Q. A. (2010). Congenital yellow nail syndrome: a case report and its relationship to nonimmune fetal hydrops. *Pediatric dermatology*, *27*(5), 533-534.

Ngu, L. H., Nijtmans, L. G., Distelmaier, F., Venselaar, H., van Emst-de Vries, S. E., van den Brand, M. A., ... & Rodenburg, R. J. (2012). A catalytic defect in mitochondrial respiratory chain complex I due to a mutation in NDUFS2 in a patient with Leigh syndrome. *Biochimica et Biophysica Acta (BBA)-Molecular Basis of Disease*, *1822*(2), 168-175.

Nicenboim, J., Malkinson, G., Lupo, T., Asaf, L., Sela, Y., Mayseless, O., ... & Yaniv, K. (2015). Lymphatic vessels arise from specialized angioblasts within a venous niche. *Nature*, *522*(7554), 56-61.

Niessen, K., Zhang, G., Ridgway, J. B., Chen, H., Kolumam, G., Siebel, C. W., & Yan, M. (2011). The Notch1-Dll4 signaling pathway regulates mouse postnatal lymphatic development. *Blood, The Journal of the American Society of Hematology, 118*(7), 1989-1997.

Nikkels, P. G., Stigter, R. H., Knol, I. E., & van der Harten, H. J. (2001). Schneckenbecken dysplasia, radiology, and histology. *Pediatric Radiology, 31*, 27-30.

Nonomura, K., Lukacs, V., Sweet, D. T., Goddard, L. M., Kanie, A., Whitwam, T., ... & Patapoutian, A. (2018). Mechanically activated ion channel PIEZO1 is required for lymphatic valve formation. *Proceedings of the National Academy of Sciences, 115*(50), 12817-12822.

Norrmén, C., Ivanov, K. I., Cheng, J., Zangger, N., Delorenzi, M., Jaquet, M., ... & Petrova, T. V. (2009). FOXC2 controls formation and maturation of lymphatic collecting vessels through cooperation with NFATc1. *Journal of Cell Biology, 185*(3), 439-457.

Nurmi, H., Saharinen, P., Zarkada, G., Zheng, W., Robciuc, M. R., & Alitalo, K. (2015). VEGF-C is required for intestinal lymphatic vessel maintenance and lipid absorption. *EMBO molecular medicine, 7*(11), 1418-1425.

Ny, A., Koch, M., Schneider, M., Neven, E., Tong, R. T., Maity, S., ... & Carmeliet, P. (2005). A genetic Xenopus laevis tadpole model to study lymphangiogenesis. *Nature medicine, 11*(9), 998-1004.

Nyberg, R. H., Uotila, J., Kirkinen, P., & Rosendahl, H. (2005). Macrocephaly–cutis marmorata telangiectatica congenita syndrome—prenatal signs in ultrasonography. *Prenatal Diagnosis: Published in Affiliation With the International Society for Prenatal Diagnosis, 25*(2), 129-132.

Oakley, R. H., Busillo, J. M., & Cidlowski, J. A. (2017). Cross-talk between the glucocorticoid receptor and MyoD family inhibitor domain-containing protein provides a new mechanism for generating tissue-specific responses to glucocorticoids. *Journal of Biological Chemistry, 292*(14), 5825-5844.

Ohtani, O., & Ohtani, Y. (2008). Lymph circulation in the liver. *The Anatomical Record: Advances in Integrative Anatomy and Evolutionary Biology: Advances in Integrative Anatomy and Evolutionary Biology, 291*(6), 643-652.

Okuda, K. S., Astin, J. W., Misa, J. P., Flores, M. V., Crosier, K. E., & Crosier, P. S. (2012). lyve1 expression reveals novel lymphatic vessels and new mechanisms for lymphatic vessel development in zebrafish. *Development, 139*(13), 2381-2391.

Oliver, G. (2004). Lymphatic vasculature development. *Nature Reviews Immunology, 4*(1), 35-45.

Oliver, G., & Harvey, N. (2002). A stepwise model of the development of lymphatic vasculature. *Annals of the New York Academy of Sciences, 979*(1), 159-165.

Oliver, G., Sosa-Pineda, B., Geisendorf, S., Spana, E. P., Doe, C. Q., & Gruss, P. (1993). Prox 1, a prospero-related homeobox gene expressed during mouse development. *Mechanisms of development*, *44*(1), 3-16.

Olson, E. N. (2006). Gene regulatory networks in the evolution and development of the heart. *Science*, *313*(5795), 1922-1927.

Olszewski, W. L., & Engeset, A. R. N. F. I. N. N. (1980). Intrinsic contractility of prenodal lymph vessels and lymph flow in human leg. *American Journal of Physiology-Heart and Circulatory Physiology*, *239*(6), H775-H783.

Onursal, C., Dick, E., Angelidis, I., Schiller, H. B., & Staab-Weijnitz, C. A. (2021). Collagen biosynthesis, processing, and maturation in lung ageing. *Frontiers in Medicine*, *8*, 593874.

Oral, A., Caner, I., Yigiter, M., Kantarci, M., Olgun, H., Ceviz, N., & Salman, A. B. (2012). Clinical characteristics of neonates with VACTERL association. *Pediatrics International*, *54*(3), 361-364.

Oremus, M., Dayes, I., Walker, K., & Raina, P. (2012). Systematic review: conservative treatments for secondary lymphedema. *BMC cancer*, *12*(1), 1-15.

Ostergaard, P., Simpson, M. A., Connell, F. C., Steward, C. G., Brice, G., Woollard, W. J., ... & Mansour, S. (2011). Mutations in GATA2 cause primary lymphedema associated with a predisposition to acute myeloid leukemia (Emberger syndrome). *Nature genetics*, *43*(10), 929-931.

Overcash, R. T., Gibu, C. K., Jones, M. C., Ramos, G. A., & Andreasen, T. S. (2015). Maternal and fetal capillary malformation–arteriovenous malformation (CM–AVM) due to a novel RASA1 mutation presenting with prenatal non-immune hydrops fetalis. *American Journal of Medical Genetics Part A*, *167*(10), 2440-2443.

Pannier, E., Viot, G., Aubry, M. C., Grange, G., Tantau, J., Fallet-Bianco, C., ... & Cabrol, D. (2003). Congenital erythropoietic porphyria (Günther's disease): two cases with very early prenatal manifestation and cystic hygroma. *Prenatal diagnosis*, *23*(1), 25-30.

Papp, C., Beke, A., Mezei, G., Szigeti, Z., Bán, Z., & Papp, Z. (2006). Prenatal diagnosis of Turner syndrome: report on 69 cases. *Journal of Ultrasound in Medicine*, *25*(6), 711-717.

Parcelier, A., Maharzi, N., Delord, M., Robledo-Sarmiento, M., Nelson, E., Belakhdar-Mekid, H., ... & Canque, B. (2011). AF1q/MLLT11 regulates the emergence of human prothymocytes through cooperative interaction with the Notch signaling pathway. *Blood, The Journal of the American Society of Hematology*, *118*(7), 1784-1796.

Pascal, B., Witte, M. H., Erickson, R. P., Becker, C., Isabelle, Q., & Miikka, V. (2021). Primary lymphoedema (Primer). *Nature Reviews: Disease Primers*, 7(1).

Pasetti, M. F., Simon, J. K., Sztein, M. B., & Levine, M. M. (2011). Immunology of gut mucosal vaccines. *Immunological reviews*, *239*(1), 125-148.

Patel, M. S., Callahan, J. W., Zhang, S., Chan, A. K., Unger, S., Levin, A. V., ... & Chitayat, D. (1999). Early-infantile galactosialidosis: Prenatal presentation and postnatal follow-up. *American journal of medical genetics*, *85*(1), 38-47.

Peciuliene, S., Burnyte, B., Gudaitiene, R., Rusoniene, S., Drazdiene, N., Liubsys, A., & Utkus, A. (2016). Perinatal manifestation of mevalonate kinase deficiency and efficacy of anakinra. *Pediatric Rheumatology*, *14*, 1-4.

Percy, M. J., & Lappin, T. R. (2008). Recessive congenital methaemoglobinaemia: cytochrome b5 reductase deficiency. *British journal of haematology*, *141*(3), 298-308.

Persaud, K., Tille, J. C., Liu, M., Zhu, Z., Jimenez, X., Pereira, D. S., ... & Pytowski, B. (2004). Involvement of the VEGF receptor 3 in tubular morphogenesis demonstrated with a human anti-human VEGFR-3 monoclonal antibody that antagonizes receptor activation by VEGF-C. *Journal of Cell Science*, *117*(13), 2745-2756.

Peti, W., & Page, R. (2013). Molecular basis of MAP kinase regulation. *Protein science*, *22*(12), 1698-1710.

Petrova, T. V., Karpanen, T., Norrmén, C., Mellor, R., Tamakoshi, T., Finegold, D., ... & Alitalo, K. (2004). Defective valves and abnormal mural cell recruitment underlie lymphatic vascular failure in lymphedema distichiasis. *Nature medicine*, *10*(9), 974-981.

Petrova, T. V., Mäkinen, T., Mäkelä, T. P., Saarela, J., Virtanen, I., Ferrell, R. E., ... & Alitalo, K. (2002). Lymphatic endothelial reprogramming of vascular endothelial cells by the Prox-1 homeobox transcription factor. *The EMBO journal*, *21*(17), 4593-4599.

Petrova, T. V., Mäkinen, T., Mäkelä, T. P., Saarela, J., Virtanen, I., Ferrell, R. E., ... & Alitalo, K. (2002). Lymphatic endothelial reprogramming of vascular endothelial cells by the Prox-1 homeobox transcription factor. *The EMBO journal*, *21*(17), 4593-4599.

Petrovski, S., Aggarwal, V., Giordano, J. L., Stosic, M., Wou, K., Bier, L., ... & Wapner, R. J. (2019). Whole-exome sequencing in the evaluation of fetal structural anomalies: a prospective cohort study. *The Lancet*, *393*(10173), 758-767.

Pichol-Thievend, C., Betterman, K. L., Liu, X., Ma, W., Skoczylas, R., Lesieur, E., ... & Francois, M. (2018). A blood capillary plexus-derived population of progenitor cells contributes to genesis of the dermal lymphatic vasculature during embryonic development. *Development*, *145*(10), dev160184.

Pimienta, G., & Pascual, J. (2007). Canonical and alternative MAPK signaling. *Cell cycle*, *6*(21), 2628-2632.

Planas-Paz, L., & Lammert, E. (2013). Mechanical forces in lymphatic vascular development and disease. *Cellular and molecular life sciences*, *70*, 4341-4354.

Planas-Paz, L., Strilić, B., Goedecke, A., Breier, G., Fässler, R., & Lammert, E. (2012). Mechanoinduction of lymph vessel expansion. *The EMBO journal*, *31*(4), 788-804.

Ples, L., Sima, R. M., Nedelea, F., & Moga, M. (2018). First prenatal Diagnosis of a Niemann–pick Disease type C2 Revealed by a Cystic Hygroma: a Case Report and Review of the Literature. *Frontiers in Endocrinology*, *9*, 292.

Pretorius, D. H., Rumack, C. M., Manco-Johnson, M. L., Manchester, D., Meier, P., Bramble, J., & Clewell, W. (1986). Specific skeletal dysplasias in utero: sonographic diagnosis. *Radiology*, *159*(1), 237-242.

Prevo, R., Banerji, S., Ferguson, D. J., Clasper, S., & Jackson, D. G. (2001). Mouse LYVE-1 is an endocytic receptor for hyaluronan in lymphatic endothelium. *Journal of Biological Chemistry*, *276*(22), 19420-19430.

Pruksanusak, N., Suntharasaj, T., Suwanrath, C., Phukaoloun, M., & Kanjanapradit, K. (2012). Fetal cardiac rhabdomyoma with hydrops fetalis: report of 2 cases and literature review. *Journal of Ultrasound in Medicine*, *31*(11), 1821-1824.

Pujol, F., Hodgson, T., Martinez-Corral, I., Prats, A. C., Devenport, D., Takeichi, M., ... & Tatin, F. (2017). Dachsous1–Fat4 signaling controls endothelial cell polarization during lymphatic valve morphogenesis—brief report. *Arteriosclerosis, thrombosis, and vascular biology*, *37*(9), 1732-1735.

Rakhmanov, Y., Maltese, P. E., Bruson, A., Beccari, T., & Bertelli, M. (2018). Genetic testing for Hennekam syndrome. *The EuroBiotech Journal*, *2*(s1), 16-18.

Ramsing, M., Gillessen-Kaesbach, G., Holzgreve, W., Fritz, B., & Rehder, H. (2000). Variability in the phenotypic expression of Fryns syndrome: A report of two sibships. *American journal of medical genetics*, *95*(5), 415-424.

Randolph, G. J., Ivanov, S., Zinselmeyer, B. H., & Scallan, J. P. (2017). The lymphatic system: integral roles in immunity. *Annual review of immunology*, *35*, 31-52.

Randolph, G. J., Sanchez-Schmitz, G., & Angeli, V. (2005, January). Factors and signals that govern the migration of dendritic cells via lymphatics: recent advances. In *Springer seminars in immunopathology* (Vol. 26, pp. 273-287). Springer-Verlag.

Ratajska, A., Gula, G., Flaht-Zabost, A., Czarnowska, E., Ciszek, B., Jankowska-Steifer, E., ... & Radomska-Lesniewska, D. (2014). Comparative and developmental anatomy of cardiac lymphatics. *The Scientific World Journal*, *2014*.

Rauniyar, K., Jha, S. K., & Jeltsch, M. (2018). Biology of vascular endothelial growth factor C in the morphogenesis of lymphatic vessels. *Frontiers in bioengineering and biotechnology*, *6*, 7.

Ravenhill, B. J., Kanjee, U., Ahouidi, A., Nobre, L., Williamson, J., Goldberg, J. M., ... & Weekes, M. P. (2019). Quantitative comparative analysis of human erythrocyte

surface proteins between individuals from two genetically distinct populations. *Communications biology*, *2*(1), 350.

Ray, A., & Cohn, L. (1999). Th2 cells and GATA-3 in asthma: new insights into the regulation of airway inflammation. *The Journal of clinical investigation*, *104*(8), 985-993.

Reddy, U. M., Goldenberg, R., Silver, R., Smith, G. C., Pauli, R. M., Wapner, R. J., ... & Willinger, M. (2009). Stillbirth classification—developing an international consensus for research: executive summary of a National Institute of Child Health and Human Development workshop. *Obstetrics and gynecology*, *114*(4), 901.

Reed, H. O., Wang, L., Sonett, J., Chen, M., Yang, J., Li, L., ... & Kahn, M. L. (2019). Lymphatic impairment leads to pulmonary tertiary lymphoid organ formation and alveolar damage. *The Journal of Clinical Investigation*, *129*(6), 2514-2526.

Reichert, S. L., McKay, E. M., & Moldenhauer, J. S. (2016). Identification of a novel nonsense mutation in the FOXP3 gene in a fetus with hydrops—expanding the phenotype of IPEX syndrome. *American Journal of Medical Genetics Part A*, *170*(1), 226-232.

Reiss-Sklan, E., Levitzki, A., & Naveh-Many, T. (2009). The complex regulation of HIC (Human I-mfa domain containing protein) expression. *PLoS One*, *4*(7), e6152.

Remark, R., Becker, C., Gomez, J. E., Damotte, D., Dieu-Nosjean, M. C., Sautès-Fridman, C., ... & Gnjatic, S. (2015). The non–small cell lung cancer immune contexture. A major determinant of tumor characteristics and patient outcome. *American journal of respiratory and critical care medicine*, *191*(4), 377-390.

Revencu, N., Fastre, E., Ravoet, M., Helaers, R., Brouillard, P., Bisdorff-Bresson, A., ... & Vikkula, M. (2020). RASA1 mosaic mutations in patients with capillary malformation-arteriovenous malformation. *Journal of medical genetics*, *57*(1), 48-52.

Robinson, M., & McCarthy, D. J. Smyth (2009). EdgeR: A Bioconductor package for differential expression analysis of digital gene expression data. *Bioinformatics*, *26*(1).

Romani, N., Tripp, C. H., & Stoitzner, P. (2012). Langerhans cells come in waves. *Immunity*, *37*(5), 766-768.

Rudolph, A. M. (2010). Congenital cardiovascular malformations and the fetal circulation. *Archives of Disease in Childhood-Fetal and Neonatal Edition*, *95*(2), F132-F136.

Sabin, F. R. (1902). On the origin of the lymphatic system from the veins and the development of the lymph hearts and thoracic duct in the pig. *American Journal of Anatomy*, *1*(3), 367-389.

Sabin, F. R. (1904). On the development of the superficial lymphatics in the skin of the pig. *American Journal of Anatomy*, *3*(2), 183-195.

Sabine, A., & Petrova, T. V. (2013). Interplay of mechanotransduction, FOXC2, connexins, and calcineurin signaling in lymphatic valve formation. *Developmental Aspects of the Lymphatic Vascular System*, 67-80.

Sabine, A., Agalarov, Y., Maby-El Hajjami, H., & Jaquet, M. (2012). Haä gerling R, Pollmann C, Bebber D, Pfenniger A, Miura N, Dormond O, et al. *Dev Cell*, *22*, 430-445.

Sabine, A., Saygili Demir, C., & Petrova, T. V. (2016). Endothelial cell responses to biomechanical forces in lymphatic vessels. *Antioxidants & redox signaling*, *25*(7), 451-465.

Saif, M. W., Knost, J. A., Chiorean, E. G., Kambhampati, S. R. P., Yu, D., Pytowski, B., ... & O'Neil, B. H. (2016). Phase 1 study of the anti-vascular endothelial growth factor receptor 3 monoclonal antibody LY3022856/IMC-3C5 in patients with advanced and refractory solid tumors and advanced colorectal cancer. *Cancer chemotherapy and pharmacology*, *78*, 815-824.

Schneider, S., Köllges, R., Stegmann, J. D., Thieme, F., Hilger, A. C., Waffenschmidt, L., ... & Müller, A. (2022). Resequencing of VEGFR3 pathway genes implicate GJC2 and FLT4 in the formation of primary congenital chylothorax. *American Journal of Medical Genetics Part A*, *188*(5), 1607-1611.

Schulz, R. A., & Yutzey, K. E. (2004). Calcineurin signaling and NFAT activation in cardiovascular and skeletal muscle development. *Developmental biology*, *266*(1), 1-16.

Schunkert, H., König, I. R., Kathiresan, S., Reilly, M. P., Assimes, T. L., Holm, H., ... & Ziegler, A. (2011). Large-scale association analysis identifies 13 new susceptibility loci for coronary artery disease. *Nature genetics*, *43*(4), 333-338.

Secker, G. A., & Harvey, N. L. (2015). VEGFR signaling during lymphatic vascular development: From progenitor cells to functional vessels. *Developmental Dynamics*, *244*(3), 323-331.

Seeger, H., Bonani, M., & Segerer, S. (2012). The role of lymphatics in renal inflammation. *Nephrology Dialysis Transplantation*, *27*(7), 2634-2641.

Sekar, R. (2019). Hydrops fetalis. In *Complications of Pregnancy*. London, UK: IntechOpen.

Senti, G., Prinz Vavricka, B. M., Erdmann, I., Diaz, M. I., Markus, R., McCormack, S. J., ... & Kündig, T. M. (2008). Intralymphatic allergen administration renders specific immunotherapy faster and safer: a randomized controlled trial. *Proceedings of the National Academy of Sciences*, *105*(46), 17908-17912.

Sequeira-Lopez, M. L. S., Lin, E. E., Li, M., Hu, Y., Sigmund, C. D., & Gomez, R. A. (2015). The earliest metanephric arteriolar progenitors and their role in kidney vascular development. *American Journal of Physiology-Regulatory, Integrative and Comparative Physiology*, *308*(2), R138-R149.

Sever, R., & Brugge, J. S. (2015). Signal transduction in cancer. *Cold Spring Harbor perspectives in medicine*, *5*(4).

Sevick-Muraca, E. M., & King, P. D. (2014). Lymphatic vessel abnormalities arising from disorders of Ras signal transduction. *Trends in cardiovascular medicine*, *24*(3), 121-127.

Shah, S., Conlin, L. K., Gomez, L., Aagenaes, Ø., Eiklid, K., Knisely, A. S., ... & Bull, L. N. (2013). CCBE1 mutation in two siblings, one manifesting lymphedema-cholestasis syndrome, and the other, fetal hydrops. *PloS one*, *8*(9), e75770.

Sharma, S., & Sicinski, P. (2020). A kinase of many talents: non-neuronal functions of CDK5 in development and disease. *Open biology*, *10*(1), 190287.

Shawber, C. J., Funahashi, Y., Francisco, E., Vorontchikhina, M., Kitamura, Y., Stowell, S. A., ... & Kitajewski, J. (2007). Notch alters VEGF responsiveness in human and murine endothelial cells by direct regulation of VEGFR-3 expression. *The Journal of clinical investigation*, *117*(11), 3369-3382.

Shehab, O., Tester, D. J., Ackerman, N. C., Cowchock, F. S., & Ackerman, M. J. (2017). Whole genome sequencing identifies etiology of recurrent male intrauterine fetal death. *Prenatal Diagnosis*, *37*(10), 1040-1045.

Shen, O., Michaelson-Cohen, R., Gross-Tsur, V., Eilat, A., Yanai, N., Green, T., ... & Meiner, V. (2016). Prenatal observation of nystagmus, cataracts, and brain abnormalities in a case of Zellweger spectrum disorder syndrome. *Prenatal Diagnosis*, *36*(9), 894-895.

Shiffman, D., Pare, G., Oberbauer, R., Louie, J. Z., Rowland, C. M., Devlin, J. J., ... & McQueen, M. J. (2014). A gene variant in CERS2 is associated with rate of increase in albuminuria in patients with diabetes from ONTARGET and TRANSCEND. *PLoS One*, *9*(9), e106631.

Sibler, E., He, Y., Ducoli, L., Keller, N., Fujimoto, N., Dieterich, L. C., & Detmar, M. (2021). Single-cell transcriptional heterogeneity of lymphatic endothelial cells in normal and inflamed murine lymph nodes. *Cells*, *10*(6), 1371.

Silveira, K. C., Moreno, C. A., & Cavalcanti, D. P. (2017). Beemer–Langer syndrome is a ciliopathy due to biallelic mutations in IFT122. *American Journal of Medical Genetics Part A*, *173*(5), 1186-1189.

SimonsM, G. (2016). Claesson-WelshL. *Mechanisms and regulation of endothelial VEGF receptor signalling*, *17*(10), 611-625.

Skobe, M., & Detmar, M. (2000, December). Structure, function, and molecular control of the skin lymphatic system. In *Journal of Investigative Dermatology Symposium Proceedings* (Vol. 5, No. 1, pp. 14-19). Elsevier.

Smith, T., Heger, A., & Sudbery, I. (2017). UMI-tools: modeling sequencing errors in Unique Molecular Identifiers to improve quantification accuracy. *Genome research*, *27*(3), 491-499.

Smith-Bindman, R., Hosmer, W., Feldstein, V. A., Deeks, J. J., & Goldberg, J. D. (2001). Second-trimester ultrasound to detect fetuses with Down syndrome: a meta-analysis. *Jama*, *285*(8), 1044-1055.

Snider, L., & Tapscott, S. J. (2005). XIC is required for Siamois activity and dorsoanterior development. *Molecular and cellular biology*, *25*(12), 5061-5072.

Snider, L., Thirlwell, H., Miller, J. R., Moon, R. T., Groudine, M., & Tapscott, S. J. (2001). Inhibition of Tcf3 binding by I-mfa domain proteins. *Molecular and Cellular Biology*, *21*(5), 1866-1873.

Song, Y., Bi, Z., Liu, Y., Qin, F., Wei, Y., & Wei, X. (2023). Targeting RAS–RAF–MEK–ERK signaling pathway in human cancer: Current status in clinical trials. *Genes & Diseases*, *10*(1), 76-88.

Sosnik, A., Chiappetta, D. A., & Carcaboso, Á. M. (2009). Drug delivery systems in HIV pharmacotherapy: what has been done and the challenges standing ahead. *Journal of Controlled release*, *138*(1), 2-15.

Sparks, T. N., Thao, K., Lianoglou, B. R., Boe, N. M., Bruce, K. G., Datkhaeva, I., ... & University of California Fetal–Maternal Consortium (UCfC). (2019). Nonimmune hydrops fetalis: identifying the underlying genetic etiology. *Genetics in Medicine*, *21*(6), 1339-1344.

Spektor, A. (2007). *Identification and characterization of CP110-interacting proteins in centrosome function* (Doctoral dissertation, New York University).

Spong, C. Y. (Ed.). (2011). *Stillbirth: prediction, prevention and management*. John Wiley & Sons.

Spyropoulos, D. D., Pharr, P. N., Lavenburg, K. R., Jackers, P., Papas, T. S., Ogawa, M., & Watson, D. K. (2000). Hemorrhage, impaired hematopoiesis, and lethality in mouse embryos carrying a targeted disruption of the Fli1 transcription factor. *Molecular and cellular biology*, *20*(15), 5643-5652.

Srichai, M. B., & Zent, R. (2010). Integrin structure and function. *Cell-extracellular matrix interactions in cancer*, 19-41.

Srinivasan, R. S., Dillard, M. E., Lagutin, O. V., Lin, F. J., Tsai, S., Tsai, M. J., ... & Oliver, G. (2007). Lineage tracing demonstrates the venous origin of the mammalian lymphatic vasculature. *Genes & development*, *21*(19), 2422-2432.

Srinivasan, R. S., Escobedo, N., Yang, Y., Interiano, A., Dillard, M. E., Finkelstein, D., ... & Oliver, G. (2014). The Prox1–Vegfr3 feedback loop maintains the identity and the number of lymphatic endothelial cell progenitors. *Genes & development*, *28*(19), 2175-2187.

Srinivasan, R. S., Geng, X., Yang, Y., Wang, Y., Mukatira, S., Studer, M., ... & Oliver, G. (2010). The nuclear hormone receptor Coup-TFII is required for the initiation and early maintenance of Prox1 expression in lymphatic endothelial cells. *Genes & development*, *24*(7), 696-707.

Stacker, S. A., & Achen, M. G. (2018). Emerging roles for VEGF-D in human disease. *Biomolecules*, *8*(1), 1.

Stanczuk, L., Martinez-Corral, I., Ulvmar, M. H., Zhang, Y., Laviña, B., Fruttiger, M., ... & Mäkinen, T. (2015). cKit lineage hemogenic endothelium-derived cells contribute to mesenteric lymphatic vessels. *Cell reports*, *10*(10), 1708-1721.

Steiner, R. D., & Basel, D. (2021). COL1A1/2 osteogenesis imperfecta.

Steward, C. G., Newbury-Ecob, R. A., Hastings, R., Smithson, S. F., Tsai-Goodman, B., Quarrell, O. W., ... & Brennan, P. (2010). Barth syndrome: an X-linked cause of fetal cardiomyopathy and stillbirth. *Prenatal diagnosis*, *30*(10), 970-976.

Stillbirths and neonatal deaths in Australia. (2017). www.aihw.gov.au/

Stolarczyk, J., & Carone, F. A. (1975). Effects of renal lymphatic occlusion and venous constriction on renal function. *The American journal of pathology*, *78*(2), 285.

Stone, O. A., & Stainier, D. Y. (2019). Paraxial mesoderm is the major source of lymphatic endothelium. *Developmental cell*, *50*(2), 247-255.

Stratton, R. F., & Patterson, R. M. (1993). DNA confirmation of congenital myotonic dystrophy in non-immune hydrops fetalis. *Prenatal diagnosis*, *13*(11), 1027-1030.

Su, F., Viros, A., Milagre, C., Trunzer, K., Bollag, G., Spleiss, O., ... & Marais, R. (2012). RAS mutations in cutaneous squamous-cell carcinomas in patients treated with BRAF inhibitors. *New England Journal of Medicine*, *366*(3), 207-215.

Summers, B. D., Kim, K., Clement, C. C., Khan, Z., Thangaswamy, S., McCright, J., ... & Reed, H. O. (2022). Lung lymphatic thrombosis and dysfunction caused by cigarette smoke exposure precedes emphysema in mice. *Scientific Reports*, *12*(1), 5012.

Supek, F., Lehner, B., & Lindeboom, R. G. (2021). To NMD or not to NMD: nonsense-mediated mRNA decay in cancer and other genetic diseases. *Trends in genetics*, *37*(7), 657-668.

Szigeti, Z., Csapó, Z., Joó, J. G., Pete, B., Papp, Z., & Papp, C. (2006). Correlation of prenatal ultrasound diagnosis and pathologic findings in fetuses with trisomy 13. *Prenatal Diagnosis: Published in Affiliation With the International Society for Prenatal Diagnosis*, *26*(13), 1262-1266.

Takeda, A., Hollmén, M., Dermadi, D., Pan, J., Brulois, K. F., Kaukonen, R., ... & Jalkanen, S. (2019). Single-cell survey of human lymphatics unveils marked endothelial cell heterogeneity and mechanisms of homing for neutrophils. *Immunity*, *51*(3), 561-572.

Tamary, H., Shalev, H., Luria, D., Shaft, D., Zoldan, M., Shalmon, L., ... & Zaizov, R. (1996). Clinical features and studies of erythropoiesis in Israeli Bedouins with congenital dyserythropoietic anemia type I.

Tammela, T., & Alitalo, K. (2010). Lymphangiogenesis: molecular mechanisms and future promise. *Cell*, *140*(4), 460-476.

Tanaka, K., Miyazaki, N., Matsushima, M., Yagishita, R., Izawa, T., Tanigaki, S., ... & Iwashita, M. (2015). Prenatal diagnosis of Klippel–Trenaunay–Weber syndrome with Kasabach–Merritt syndrome in utero. *Journal of Medical Ultrasonics*, *42*, 109-112.

Tanaka, M., & Iwakiri, Y. (2016). The hepatic lymphatic vascular system: structure, function, markers, and lymphangiogenesis. *Cellular and molecular gastroenterology and hepatology*, *2*(6), 733-749.

Tayebi, N. (2008). Cornelia de Lange syndrome. *Indian journal of human genetics*, *14*(1), 23.

Teasdale, F., & Jean-Jacques, G. (1985). Morphometric evaluation of the microvillous surface enlargement factor in the human placenta from mid-gestation to term. *Placenta*, *6*(5), 375-381.

Tessier, A., Sarreau, M., Pelluard, F., André, G., Blesson, S., Bucourt, M., ... & Guerrot, A. M. (2016). Fraser syndrome: features suggestive of prenatal diagnosis in a review of 38 cases. *Prenatal Diagnosis*, *36*(13), 1270-1275.

Tonni, G., Panteghini, M., Bonasoni, M., Pattacini, P., & Ventura, A. (2013). Prenatal ultrasound and MRI diagnosis of Jeune syndrome type I (asphyxiating thoracic dystrophy) with histology and post-mortem three-dimensional CT confirmation. *Fetal and Pediatric Pathology*, *32*(2), 123-132.

Trevaskis, N. L., Kaminskas, L. M., & Porter, C. J. (2015). From sewer to saviour—targeting the lymphatic system to promote drug exposure and activity. *Nature reviews Drug discovery*, *14*(11), 781-803.

Trutmann, M., & Sasse, D. (1994). The lymphatics of the liver. *Anatomy and embryology*, *190*, 201-209.

Tsai, H. F., Wu, M. H., Cheng, Y. C., Chang, C. H., & Chang, F. M. (2014). Prenatal ultrasonography and postnatal follow-up of a case of McKusick-Kaufman syndrome. *Taiwanese Journal of Obstetrics and Gynecology*, *53*(2), 241-244.

Tümer, Z., & Bach-Holm, D. (2009). Axenfeld–Rieger syndrome and spectrum of PITX2 and FOXC1 mutations. *European Journal of Human Genetics*, *17*(12), 1527-1539.

Ugorski, M., Dziegiel, P., & Suchanski, J. (2016). Podoplanin-a small glycoprotein with many faces. *American journal of cancer research*, *6*(2), 370.

Ulvmar, M. H., & Mäkinen, T. (2016). Heterogeneity in the lymphatic vascular system and its origin. *Cardiovascular research*, *111*(4), 310-321.

Vaahtomeri, K., Karaman, S., Mäkinen, T., & Alitalo, K. (2017). Lymphangiogenesis guidance by paracrine and pericellular factors. *Genes & development*, *31*(16), 1615-1634.

Van Maldergem, L., Verloes, A., Lejeune, L., & Gillerot, Y. (1992). The Baller-Gerold syndrome. *Journal of medical genetics*, *29*(4), 266-268.

Vandamme, D., Herrero, A., Al-Mulla, F., & Kolch, W. (2014). Regulation of the MAPK pathway by raf kinase inhibitory protein. *Critical Reviews™ in Oncogenesis*, *19*(6).

Vittet, D. (2014). Lymphatic collecting vessel maturation and valve morphogenesis. *Microvascular research*, *96*, 31-37.

Von der Weid, P. Y., & Zawieja, D. C. (2004). Lymphatic smooth muscle: the motor unit of lymph drainage. *The international journal of biochemistry & cell biology*, *36*(7), 1147-1153.

Vuorio, T., Tirronen, A., & Ylä-Herttuala, S. (2017). Cardiac lymphatics–a new avenue for therapeutics?. *Trends in Endocrinology & Metabolism*, *28*(4), 285-296.

Wan, T., Yin, H., Yang, Y., Wu, F., Wu, Z., & Yang, Y. (2019). Comparative study of anterior segment measurements using 3 different instruments in myopic patients after ICL implantation. *BMC ophthalmology*, *19*(1), 1-8.

Wang, Y., Baeyens, N., Corti, F., Tanaka, K., Fang, J. S., Zhang, J., ... & Simons, M. (2016). Syndecan 4 controls lymphatic vasculature remodeling during mouse embryonic development. *Development*, *143*(23), 4441-4451.

Wennerberg, K., Rossman, K. L., & Der, C. J. (2005). The Ras superfamily at a glance. *Journal of cell science*, *118*(5), 843-846.

Wigle, J. T., & Oliver, G. (1999). Prox1 function is required for the development of the murine lymphatic system. *Cell*, *98*(6), 769-778.

Wilting, J., Aref, Y., Huang, R., Tomarev, S. I., Schweigerer, L., Christ, B., ... & Papoutsi, M. (2006). Dual origin of avian lymphatics. *Developmental biology*, *292*(1), 165-173.

Witte, C. L., Chung, Y. C., Witte, M. H., Sterile, O. F., & Cole, W. R. (1969). Observations on the origin of ascites from experimental extrahepatic portal congestion. *Annals of Surgery*, *170*(6), 1002.

Witte, M. H., Bernas, M. J., Martin, C. P., & Witte, C. L. (2001). Lymphangiogenesis and lymphangiodysplasia: from molecular to clinical lymphology. *Microscopy Research and Technique*, *55*(2), 122-145.

Wong, B. W., Zecchin, A., García-Caballero, M., & Carmeliet, P. (2018). Emerging concepts in organ-specific lymphatic vessels and metabolic regulation of lymphatic development. *Developmental cell*, *45*(3), 289-301.

Wood, K. C., Durgin, B. G., Schmidt, H. M., Hahn, S. A., Baust, J. J., Bachman, T., ... & Straub, A. C. (2019). Smooth muscle cytochrome b5 reductase 3 deficiency accelerates pulmonary hypertension development in sickle cell mice. *Blood advances*, *3*(23), 4104-4116.

Wu, Y., Seong, Y. J., Li, K., Choi, D., Park, E., Daghlian, G. H., ... & Hong, Y. K. (2020). Organogenesis and distribution of the ocular lymphatic vessels in the anterior eye. *JCI insight*, *5*(13).

Yamada, M., Clark, J., & Iulianella, A. (2014). MLLT11/AF1q is differentially expressed in maturing neurons during development. *Gene Expression Patterns*, *15*(2), 80-87.

Yang, F., Jin, C., Yang, D., Jiang, Y., Li, J., Di, Y., ... & Fu, D. (2011). Magnetic functionalised carbon nanotubes as drug vehicles for cancer lymph node metastasis treatment. *European journal of cancer*, *47*(12), 1873-1882.

Yang, Y. S., Ma, G. C., Shih, J. C., Chen, C. P., Chou, C. H., Yeh, K. T., ... & Chen, M. (2012). Experimental treatment of bilateral fetal chylothorax using in-utero pleurodesis. *Ultrasound in obstetrics & gynecology*, *39*(1), 56-62.

Yang, Y., & Oliver, G. (2014). Development of the mammalian lymphatic vasculature. *The Journal of clinical investigation*, *124*(3), 888-897.

Yang, Y., Cha, B., Motawe, Z. Y., Srinivasan, R. S., & Scallan, J. P. (2019). VE-cadherin is required for lymphatic valve formation and maintenance. *Cell reports*, *28*(9), 2397-2412.

Yang, Y., García-Verdugo, J. M., Soriano-Navarro, M., Srinivasan, R. S., Scallan, J. P., Singh, M. K., ... & Oliver, G. (2012). Lymphatic endothelial progenitors bud from the cardinal vein and intersomitic vessels in mammalian embryos. *Blood, The Journal of the American Society of Hematology*, *120*(11), 2340-2348.

Yao, L. C., Testini, C., Tvorogov, D., Anisimov, A., Vargas, S. O., Baluk, P., ... & McDonald, D. M. (2014). Pulmonary lymphangiectasia resulting from vascular endothelial growth factor-C overexpression during a critical period. *Circulation research*, *114*(5), 806-822.

Yeang, C. H., Ma, G. C., Shih, J. C., Yang, Y. S., Chen, C. P., Chang, S. P., ... & Chen, M. (2012). Genome-wide gene expression analysis implicates the immune response and lymphangiogenesis in the pathogenesis of fetal chylothorax. *PLoS One*, *7*(4), e34901.

Yu, X., & Li, S. (2017). Non-metabolic functions of glycolytic enzymes in tumorigenesis. *Oncogene*, *36*(19), 2629-2636.

Yuan, L., Moyon, D., Pardanaud, L., Bréant, C., Karkkainen, M. J., Alitalo, K., & Eichmann, A. (2002). Abnormal lymphatic vessel development in neuropilin 2 mutant mice.

Yücel, Y. H., Johnston, M. G., Ly, T., Patel, M., Drake, B., Gümüş, E., ... & Gupta, N. (2009). Identification of lymphatics in the ciliary body of the human eye: a novel "uveolymphatic" outflow pathway. *Experimental eye research*, *89*(5), 810-819.

Zenker, M., Aigner, T., Wendler, O., Tralau, T., Müntefering, H., Fenski, R., ... & Reis, A. (2004). Human laminin β2 deficiency causes congenital nephrosis with mesangial sclerosis and distinct eye abnormalities. *Human molecular genetics*, *13*(21), 2625-2632.

Zhang, G., Brady, J., Liang, W. C., Wu, Y., Henkemeyer, M., & Yan, M. (2015). EphB4 forward signalling regulates lymphatic valve development. *Nature communications*, *6*(1), 6625.

Zhang, S. Q., Yang, W., Kontaridis, M. I., Bivona, T. G., Wen, G., Araki, T., ... & Neel, B. G. (2004). Shp2 regulates SRC family kinase activity and Ras/Erk activation by controlling Csk recruitment. *Molecular cell*, *13*(3), 341-355.

Zhang, Z., Lu, Y., Qi, J., & Wu, W. (2021). An update on oral drug delivery via intestinal lymphatic transport. *Acta Pharmaceutica Sinica B*, *11*(8), 2449-2468.

Zheng, W., Aspelund, A., & Alitalo, K. (2014). Lymphangiogenic factors, mechanisms, and applications. *The Journal of clinical investigation*, *124*(3), 878-887.

Zhong, Y., Chen, L., Cheng, Y., & Huang, P. (2009). Correlation between blue-on-yellow perimetry and scanning laser polarimetry with variable corneal compensation measurements in primary open-angle glaucoma. *Japanese journal of ophthalmology*, *53*, 574-579.